Processing and characterization of PEI/PBT and PEI/PBT/PTFE high-performance polymer blends

A THESIS SUBMITTED TO THE DOCTORAL PROGRAM OF ENGINEERING SCHOOL AT UNIVERSIDAD EAFIT
FOR THE DEGREE OF DOCTOR OF PHILOSOPHY

BY
Mauricio VÁSQUEZ RENDÓN

ADVISOR
Ph.D. Mónica Lucía Álvarez-Láinez

Medellín – Colombia
2018

Acceptation grade

_____

_____

JURY

_____

_____

_____

Medellín – Colombia
2018

Dedicated

To my mother.

"*My mother is the making of me*" (Thomas Edison)

Acknowledgements

First, thanks to my mother. Your love and unconditional support are invaluable. Of course, thanks to all my family: Lu, Junior, Naty, and Willy. You all walked with me this long road.

Thanks to my supervisor Mónica Álvarez, who shared her experience and encouraged me to finish “alive" this experience. She was my guide along this whole process.

Thanks to Dr. Dieter Lehman for receiving me at the Leibniz Institute for Polymer Research – IPF. He taught me so much about polymers processing and technology during the time I was there. Also, thanks to Professor Hoffman for the interesting discussion of my research results.

That amazing experience at IPF came together with amazing people. Thanks to Alejo, Roberto, Michela, Donato, Jan, Guido, and Fei. I still miss our coffee breaks at “my office”.

Thanks a lot to Professor Demarquette at ETS. You helped me solve my “spider-web” during almost one year. I really enjoyed the long conversations with you, and learn a lot from your vast experience in polymers and polymer blending.

From Universidad EAFIT, thanks to Alex Ossa who first interviewed me and open to me what I call the “EAFIT door”. Thanks to Ángela Sanchez from the research direction for all your support. Also special thanks to Jorge Tabares. You are a truly Godfather.

Thanks to my friends Ángela, Lina Paola, Susana, Juliana, William, and Andrés for their supporting words, advices, and discussions of my reasearch results. Also to my colleagues at EAFIT: Juliana, Carolina, Natalia, and Andrés for your comments, feedback, and support.

Thanks to the technicians and collaborator partners. You were indispensable during my research work. Thanks a lot to Juan and Javier at EAFIT, Konnie at IPF, and Nabil at ETS.

Finally, thanks to Colciencias for the scholarship and to Universidad EAFIT for the financial support.

Abstract

Polymer blending emerged as an attractive strategy to obtain new materials with tailored properties from already existing ones. It has focused mainly on the development of blends from commercial polymers. Fewer works have studied in depth the fabrication of blends from high-performance polymers, since fundamental studies in polymer-polymer interactions are not usually performed with these challenging materials. This work aim to study blends obtained from three high-performance polymers with good flammability characteristics: poly(ether imide) (PEI), poly(butylene terephthalate) (PBT) filled with a flame retardant compound, and poly(tetrafluoroethylene) (PTFE); and presents for the first time, the relationship between processing conditions, viscoelastic properties, interfacial tension, and composition with the morphology and final performance for this kind of systems.

Two sets of blends, binary PEI/PBT and ternary (PEI/PBT)/PTFE blend, are prepared by melt processing in an internal mixer. A complete miscibility study is performed from thermal analysis using MDSC and DMA, accompanied by a theoretical approach of the interfacial tension by using the harmonic mean equation. In relation to ternary blends, phase's interaction is predicted from the Harkin's spreading coefficient model. Morphological study is contrasted to miscibility results and the distribution of blends constituents is evaluated by SEM and TEM analyses. As blends resulted being partially miscible, the use of selective extraction technique allows us to better evidence the PEI and PBT distribution in binary blends. To evaluate the mechanical performance, tensile tests are performed to Type V samples obtained by injection molding. The thermal stability is studied by TGA and DTG techniques, and flammability tests from a horizontal burning tests according to the UL-94 standard.

The first set of blends is obtained between PEI and PBT, which have notable differences in their processing characteristics. Previous works were found on PEI/PBT blends that mix simultaneously PEI and PBT phases by different solution and melt processing methods. In this work a novel *two-step melt processing method* to fabricate binary PEI/PBT blends in an internal

mixer is proposed. The main processing parameters are defined after the thermal and rheological characterization of pure materials, to obtain binary PEI/PBT blends within the entire composition range using the same processing conditions. The second set of blends is obtained with the aim of modify the mechanical properties of PEI/PBT blends by adding PTFE concentrations of 5 wt%, 10 wt%, and 15 wt%. The same two-step melt processing method proposed for binary PEI/PBT blends is used for (PEI/PBT)/PTFE blends fabrication. It is found that PTFE must be added during step 1 in order to enhance phases' integration during mixing. Ternary blends are obtained for PEI concentrations higher than 50 wt% for the same reason.

A complete miscibility study provided information about the phases' heterogeneity in both, binary and ternary blends. The binary PEI/PBT blends resulted being partially miscible depending on PEI composition, and two groups of blends are identified: PBT-rich blends and PEI-rich blends. Miscibility evaluation by MDSC and DMA reveals that PBT-rich blends are immiscible, since it is no noticed any shift in the glass transition temperatures (Tg) of the pure components. PEI-rich blends on the other hand, exhibit a significant displacements of Tg to higher temperatures suggesting miscibility between PEI and PBT. The study of miscibility in ternary blends, reveals that PTFE does not interfere with the miscibility behavior of PEI and PBT, since there are noticed the same thermal transitions as those for binary blends. Interfacial tension values reveal that all phases are highly immiscible for all possible polymer pairs, due to the notable differences between their polar components. Prediction of phase's distribution in ternary blends by the spreading coefficient model, reveals there is favored the encapsulation of PTFE phase by PEI when PBT is the matrix.

Morphological evaluation of binary PEI/PBT blends is in good agreement to blends microrheology theory proposed by Taylor and Grace. PBT-rich blends exhibit coarse droplets distribution of highly viscous PEI phase, with sub-inclusions of small droplets of low viscous PBT phase. By using the Soxhlet selective extraction technique together with SEM and TEM, it is presented new evidence on the morphological evolution of PBT-rich blends, and we noticed that PBT-rich and PEI-rich blends are separated by an intermediate cocontinuous morphology at even PEI and PBT compositions. PEI-rich blends on the other hand, exhibited tiny droplets of PBT (as small as 120 nm) bonded to PEI matrix through a fibrillar interface, and a new morphology denominated *spore-like* morphology is presented. In order to validate the addition of PTFE to the PEI phase during step 1 in ternary blends fabrication, we evaluate the

morphology formed between PEI/PTFE blends. It is noticed that under these conditions it is favored the distribution of PTFE phase in two major fashions: well-embedded PTFE nano-sized droplets, and debonded PTFE spheres of 1.5 μm of average diameter. SEM and TEM analysis of ternary blends confirm the miscibility study results, and encapsulation of PTFE droplets by PEI phase in ternary blends when PBT is the matrix, is predicted by the spreading coefficient model.

Mechanical, thermal, and flame resistance performance is strongly influenced by miscibility and the morphologies obtained in both, binary and ternary blends. The experimental results are discussed in terms of theoretical additivity approaches. In binary bends, the tensile modulus reveal a positive deviation from additivity, and even a synergic contribution is obtained for blends containing 50 wt% and 80 wt% of PEI. The yield strength on the other hand, is strongly affected by phase's immiscibility and the interfacial adherence between constituents, and a combinatorial deviation from additivity is obtained: negative for PBT rich-blends and positive for PEI-rich blends. In addition, the elongation at break for all blends is compromised by the morphology of PBT-rich blends, and by the densification of PEI-rich blends. The blend with 50 wt% of PEI exhibits the best elongational at break result due to its co-continuous morphology. PTFE phase does not affect PEI/PBT stiffness since any significant variation in tensile modulus values is observed. On the other hand, a progressive decrease in tensile strength with increasing PTFE concentration caused by the low yielding strength characteristic of PTFE is noticed. The results of elongation at break show that PTFE addition decreases even more the ductility of binary PEI/PBT blends. However, surprising results are found when only 5 wt% of PTFE phase is added to the blends containing 80 wt% of PEI. It is noticed a considerable improvement of blends ductility due to the highly crystalline PTFE phase inhibits the densification of PEI/PBT blends. On the contrary, PTFE improves substantially PEI/PBT blends thermal stability and flammability, since it enhances blends charring formation.

Table of contents

List of figures

List of tables

List of abbreviations

ASA	acrylonitrile styrene acrylate
BR	poly(butadiene)
CUT	continuous use temperature
DMA	dynamic mechanical analysis
DSC	differential scanning calorimetry
DTG	derivative thermogravimetric analysis
FEP	perfluoro ethylene propylene
FTIR	Fourier transform infrared spectroscopy
HBCD	hexabromocyclododecane
HDPE	high-density poly(ethylene)
HIPS	high-impact poly(styrene)
HPP	high-performance polymer
HPPB	high-performance polymer blend
LCP	liquid crystal polymer
LDPE	low-density poly(ethylene)
LOI	limiting oxygen index
LVR	linear viscoelastic region
MDSC	modulated differential scanning calorimetry
mPEO	m-Poly(ethylene) oxide
MWCNT	multi-wall carbon nanotubes
NDB	negatively deviating blend

PA	poly(amide)
PA-6	poly(amide) 6
PA-66	poly(amide) 66
PAEK	poly(aryl ether ketone)
PAI	poly(amide imide)
PAr	poly(arylate)
PBI	poly(benzimidazole)
PBT	poly(butylene terephthalate)
PC	poly(carbonate)
PDB	positively deviating blend
PEEK	poly(ether ether ketone)
PEI	poly(ether imide)
PES	poly(ether sulfone)
PEST	polyesters
PET	poly(ethylene terephthalate)
PHBA	poly(p-hydroxybenzoic acid)
PI	poly(imide)
PNDB	positively and negatively deviating blend
POM	poly(acetal) or poly(oximethylene)
PP	poly(propylene)
PPE	poly(phenyl ether)
PPS	poly(phenylene sulfide)

PS	poly(styrene)
PSF	bisphenol-A poly(sulfone)
PSU	poly(sulfone)
PTFE	poly(tetrafluoroethylene)
PU	poly(urethane)
PVC	poly(vinyl chloride)
Py-GCMS	pyrolysis-gas chromatograph-mass spectrometry
SAN	poly(styrene-*co*-acrylonitrile)
SAOS	small-amplitude oscillatory shear
SBM	poly(styrene)-*block*-poly(butadiene)-*block*-poly(methyl methacrylate)
SEM	scanning electron microscopy
TBBPA	tetrabromo bisphenol A
TEM	transmission electron microscopy
TGA	thermogravimetric analysis
TPEE	thermoplastic elastomer
TPU	thermoplastic poly(urethane)
XPS	X-ray photoelectron spectroscopy
XRD	X-ray diffraction

Chapter 1 Introduction, objectives and organization of the thesis

1.1 Introduction

Polymer blending is a versatile way of obtaining new materials by combining existing ones. From the very first blend patented in 1846 between natural rubber and gutta percha, several polymer-polymer combinations were developed from either solution or melt processing methods,[1] being melt-blending of greater technological importance because it is possible to develop new materials from using industrial processing approaches.

Blending polymers is comparable to a stepwise process that involves *formulation* and *performance evaluation*. During formulation, there are considered either polymers viscoelasticity, interfacial interaction, processing conditions, composition, or all;[2] whereas in performance there are evaluated thermal, mechanical, electrical, or chemical resistance. Blend's formulations have to be repeated as many times as necessary until they match the performance pursued for a specific application. The understanding of all possible parameters involved in a blending process leads to developing tailored *structures* in miscible blends, or *morphologies* in immiscible blends. As a rule of thumb, miscibility is the first parameter to be evaluated in polymer blends studies. Depending on the physicochemical properties of the individual components —that is the molecular weight, crystallinity, glass transition, chemical composition, etc.—, polymer blends are classified as miscible, partially miscible, or immiscible.[2]

Two polymers are *miscible* when they interact intimately at molecular scale and form a single-phase structure; they are considered *partially miscible* if they are miscible within a certain composition range; and they are called *immiscible* polymers if well-separated phases are noticed, consisting of a dispersed phase and a matrix. When polymer pairs are immiscible, the kinetic and thermodynamic conditions will lead blends components to be distributed in different fashions giving rise to multiple morphologies, some conventional such as droplets, fibers,

and laminar; or some more complexes such as core-shell and co-continuous. The control of these morphologies is of great importance since they will define the final properties of blends.

Even though several studies are found on the development of new materials from polymers blending technology,[3–22] the greatest attention has being placed on blends obtained from commercial or commodity polymers. These polymers are mass-produced, their processing conditions are very well understood, and they represent the 71% of the world's plastic consumption in the market.[23] Nevertheless, this scenario discloses an opportunity for studying the development of new blends by using industrial processing methods from the remaining 29% of polymers: the high performance polymers (HPP) family.

Polymers families are classified from either their structure, molecular nature, origin source, or performance under thermal conditions. The continuous use temperature (CUT) classification is commonly applied in the automotive and aerospace industries to evaluate which polymers meet their demanding requirements. It points to four major groups: commodity, engineering, specialty, and ultra polymers.[1] The last three comprise the HPP family, and similarly to commodity polymers, their properties are commonly modified by using additives, fillers, or by blending them with other polymers. However, blends between HPP are barely studied due to fundamental studies in polymer-polymer interactions are not performed with HPP, since they are challenging materials to work with. They are more expensive than commodity polymers and they usually need processing temperatures higher than 300 °C.

However, from a technological point of view, combining the outstanding properties of HPP into a single material is highly attractive for applications that require extreme mechanical, thermal, fire, or electrical performance such as aerospace, military and defense industries, fabrication of medical devices, gas and liquid separation membranes, solar cells, and fire protection.[1,24,25] The mentioned industries make great efforts developing new materials for human safety against fire events. This is linked to the increasingly demanding applications that force users to wear extra protection for the hazardous conditions they are exposed.[26–28] In 2015, Kahn and coworkers reported 2775 fatality cases of firefighters between 1990 and 2012, only in the United States. During that period, the deaths caused by burns decreased by 3.8% to a certain extent, due to the improvement of thermal, fire, and mechanical resistance of materials.[29]

According to Horrocks, polymers exposed to flames (convective heat), contact heat, radiant heat, sparks, molten metals, or hot gases and vapors[26] must fulfil both, heat and flame re-

sistance.[30] However, it is difficult for polymers alone to meet these requirements and sometimes it is necessary using thermal stabilization and flame retardant additives, although these commonly lead to detriment of mechanical properties. The development of high-performance polymer blends (HPPB) appears as an engaging manner to develop novel materials for fire protection applications without compromising the mechanical properties.

As reported by Utracki,[1] the HPPB technology must pursue two main objectives: i) to improve the processability of one blend component and ii) to improve the performance of the other. One strategy used to accomplish these objectives is by combining pairs of high-performance polymers with low and high glass transition temperatures (Tg).[1,23] Low Tg engineering polymers such as PET, PA, PBT are easily processed during extrusion and injection molding; while high Tg specialty and ultra polymers such as PEEK, PI, PPS, PEI, LCP are difficultly processed, but they provide thermal and fire resistance, stiffness, and dimensional stability over broader temperature and humidity ranges.[23] However, not too many publications are found on the development of HPPB, and even fewer on the study of the morphology control from melt-blending processing.

To address the present study, we focused on two main issues still existing in HPPB development. The first involves the fabrication of these blends from melt processing methods. The elevated temperatures required during blending process (above 300 °C) lead to polymers decomposition to become a competitive process with melting, particularly if the blend is based in commodity or engineering polymers. The second issue, is linked to the lack of studies on the control of the structure or morphology of HPPB obtained from melt processing. Since specific applications may pursue immiscible phases in the blend, it must be understood how is the interfacial interaction between the polymers in order to obtain the desired physical and mechanical properties. For these reasons, we selected the blends components based on to their individual structure, mechanical performance, thermal properties, and flame resistance.

We obtain binary blends between poly(ether imide) (PEI), and poly(butylene terephthalate) (PBT), and ternary blends between PEI, PBT, and poly(tetrafluoroethylene) (PTFE) by means of a melt-processing method. The results obtained from the experimental evaluation of blends miscibility and performance, are contrasted and explained from using classical blends theories. We take as starting points questions as: *how to handle the great Tg values differences between amorphous and semicrystalline HPP in order to obtain a homogeneous blend?; can the compo-*

nent with lower Tg make easier the processing of that with higher Tg?; will there be miscibility between blends components?; how will be affected the blends structure or morphology by the physicochemical differences between components and by the processing conditions?

In terms of the morphology and interfacial analysis: *can we control blend's morphology evolution from varying processing conditions like temperature, rotation rate, and mixing time?; do high-temperature processing conditions (above 300 °C) affect the study of interfacial interaction between polymers?; the existing theoretical models used to calculate interfacial tension values, can be applied to HPPB systems?*

In the light of above questions, the main objectives of this work are following mentioned.

1.2 Objectives

1.2.1 General objective

To develop high-performance polymer blends (HPPB) between PEI, PBT, and PTFE for fire protection applications by using a melt processing method, and to control their structure or morphology from understanding the kinetic parameters involved in the blending process, in order to tailor blends performance.

1.2.2 Specific objectives

To understand the relationship between viscoelasticity, interfacial tension, composition, and processing conditions with phase morphology; as well as their effect on the mechanical, thermal, and flame resistance properties of blends.

To develop a melt processing method to produce binary and ternary blends between engineering and specialty polymers, from setting the major processing parameters based on individual thermal and rheological characteristics of materials.

To evaluate blends miscibility and the effect of individual characteristics of materials and processing conditions on the evolution of HPPB structure or morphology.

To propose new HPPB with lower processing temperatures and outstanding performance, and make a comparison to conventional materials used in fire protection applications.

1.3 Organization of the thesis

The following chapters of this thesis will show the development of the experimental work. In Chapter 3, it is discussed the methodology to fabricate binary blends with flame retardant characteristics between two HPP with notable differences in their processing characteristics: poly(ether imide) (PEI) and flame retardant poly(butylene terephthalate) (PBT), and it is proposes a novel *two-step processing method*. It is presented the miscibility study by thermal analysis (MDSC and DMA), and it is discussed for the first time, the effect of the viscoelastic properties, interfacial tension, processing conditions, and composition on PEI/PBT blends morphology. New evidence is revealed on the morphological evolution of PEI/PBT blends in the entire compositional range after SEM and TEM analyses, and we present a morphology we called *spore-like* morphology. The mechanical, thermal stability, and flame resistance properties are also discussed in terms of morphology, and thermal stability and flame resistance analyses on PEI/PBT blends are reported for the first time.

In Chapter 4, it is presented the modification of the mechanical and thermal properties of PEI/PBT blends by adding PTFE. For that, it is used the same two-step melt processing method. It is found that PTFE must be added during step 1 to PEI compositions greater than 50 wt%, to ensure phases integration during mixing. Evaluation of blends morphology by SEM and TEM reveals that step 1 favors PTFE phase spheroidization. The morphology of ternary (PEI/PBT)/PTFE blends is discussed from the interfacial tension differences between blends components, and prediction from the spreading coefficient model is made. The effect of PTFE addition on mechanical, thermal, and flammability properties of PEI/PBT blends, is also studied.

The final section of the thesis, Chapter 5, is focused on presenting the concluding remarks, the main implications of the research and further work recommendations.

Chapter 2 Literature Review

2.1 High-performance polymers (HPP)

2.1.1 Overview

Based on the high-temperature tests performed to polymers for aerospace applications, high-performance polymers (HPP) —also called high-temperature polymers— are defined as materials that can stand service temperatures of at least 175 °C. Most HPP are amorphous polymers with glass transitions temperatures (Tg) of about 200 °C. Contrary to amorphous HPP, the service temperature of semicrystalline HPP is defined by their melting temperatures (Tm),[33] where Tm values below 400 °C are desirable to avoid the melting point starts to compete with decomposition during melt-processing.[31,32]

Utracki stated a similar classification for polymers based on the CUT which include both, amorphous and semicrystalline polymers, and it is defined as the temperature at which the mechanical properties of materials decrease by 50% within a certain period of time. The CUT classification points to four major groups: commodity polymers (CUT ≤ 75 °C), engineering polymers (100 °C < CUT ≤ 140 °C), specialty polymers (CUT 140 °C – 240 °C), and ultra-high performance polymers (CUT > 240 °C), as presented in Table 2.1.[31] For ease of interpretation, we include the last three categories in the high-performance polymers (HPP) family.

Table 2.1 Polymers classification based on the CUT.[31]

Category	Amorphous	Semicrystalline
Commodity	PVC, PS, PMMA, SAN	PP, HDPE, LDPE
Engineering	PC, PPE	PBT, PET, PA, TPU
Specialty	PEI, PES, PSU	PPS, PTFE, LCP
Ultra	PI, PAI, PBI	PEEK, PAEK

In Figure 2.1, it is presented a global evaluation of the production of plastics carried out by Pardos Marketing.[31] It is evidenced that the production of commodity plastics was approximately 100 million tons (Mtons) at the end of the 90s, and the projection indicates that it will grow five times for the year 2020. Although the production of engineering polymers will also increase fivefold, it will reach only 25 million tons for the same period.[31] In addition, it is noticed that the production of specialty polymers is very low compared to other polymers, and has remained stable for the last 60 years.

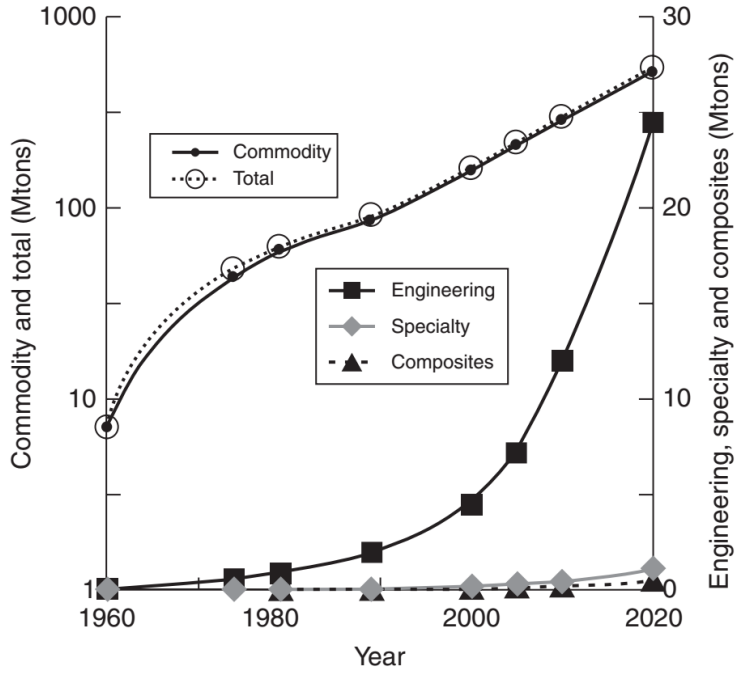

Figure 2.1 Plastics production worldwide in million tons, extrapolated to 2020. (Source: "*High Temperature Polymer Blends*" by DeMeuse).[31]

The low production of specialty polymers is related to the high requirements that high-performance polymers must accomplish, and their niche markets usually require low volumes. This situation leads to exponential increases in their prices compared to commercial polymers.[33] In Figure 2.2, we contrasted the prices of different groups of resins, finding that some HPP cost up to 20 times more than any commodity polymer, e.g. poly(imide). Nevertheless, these materials are still necessary in multiple applications that require high mechanical, chemical, electrical, thermal, or flame resistance performance, which cannot be substituted by any commodity polymer.

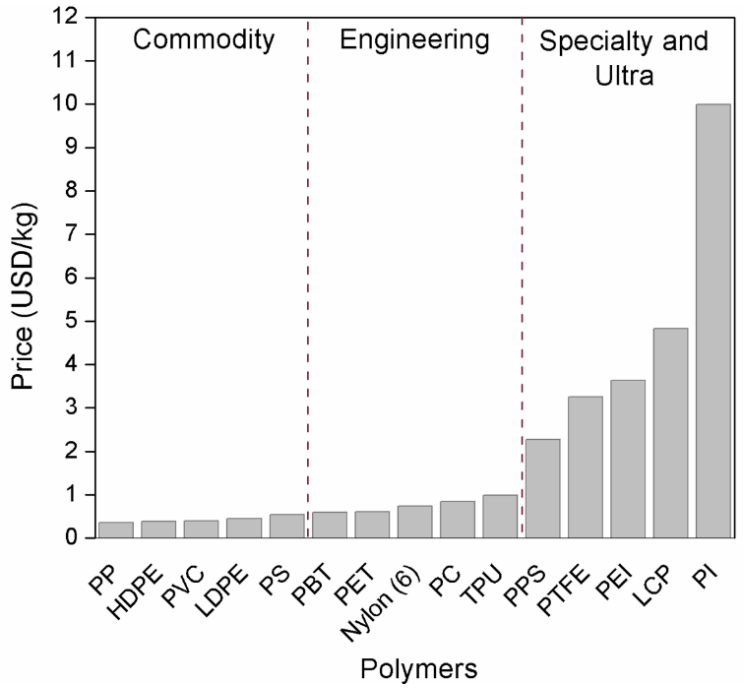

Figure 2.2 Prices of representative commodity, engineering, specialty, and ultra polymers. (Data obtained from http://www.plasticsnews.com/resin, updated to 2017).

2.1.2 Properties of HPP

The outstanding properties of HPP lead to aerospace, automotive, military, and firefighters industries to use them for applications such as fuel tank sealants, coatings, adhesives, composite matrices, separation/barrier materials, high-strength fibers, fire barriers, protective clothes, etc.[33] Most of these mechanical and thermal properties are associated to the physicochemical properties of HPP, and factors such as: primary bond strength, molecular structure, secondary bonding forces, molecular weight and distribution, molecular symmetry, purity, etc.; being the primary bond strength the most relevant.[33]

Depending on the energy needed to break the primary bond of the backbone, the polymer will exhibit certain mechanical or thermal resistance. The chemical bonds with higher dissociation energies are C=C, C=N, and C–F, as it is listed in Table 2.2. These polymers chain structural features produce stiffer macromolecules in high-performance polymers than those of commodity polymers; even more, aromatic rings provide highly thermal stabilization.[33] Polymers with aromatic rings in their backbone structure usually have Tg values higher than 200 °C.

Table 2.2 Typical primary bond dissociation energy for polymers.[33]

Chemical bond	Dissociation energy (kcal/mol)
C–C	83
C=C	145
C–H	99
C–N	70
C=N	147
C=O	84
C–F	123

2.1.3 HPP used in this work

In order to fulfill the two main objectives stated by Utracki in the development of high-performance polymer blends technology: *i) to improve the processability of one component and ii) to improve the performance of the other*;[1] different alternatives of low Tg semicrystalline and high Tg amorphous HPP were considered for our studies. Low Tg engineering polymers such as PET, PA, PBT have good chemical resistance and are easily processed during extrusion and injection molding; while high Tg specialty and ultra polymers such as PEEK, PI, PPS, PEI, PTFE have thermal and fire resistance, stiffness, and dimensional stability over broader temperature and humidity ranges.

As the most popular HPP consist of polyimides, polyesters, and fluoropolymers families, three different polymers are selected based on the technological importance and the characteristics of the individual components: PEI, PBT, and PTFE.

Poly(ether imide) (PEI)

In 1982 General Electric introduced the first poly(ether imide) (PEI) under the trade name Ultem. PEI is an amorphous, amber-to-transparent thermoplastic with high thermal stability, high Tg value (around 215 °C), exceptional elastic modulus, and toughness. This material is categorized as a specialty and sometimes as an ultra polymer due to its outstanding temperature and

inherent flame resistance. It combines low smoke evolution and high oxygen index. Its properties are related to its robust backbone structure comprised by aromatic rings, Figure 2.3.

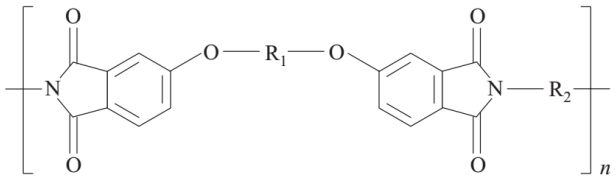

Figure 2.3 Repeating unit of poly(ether imide) (PEI).

PEI applications

PEI is commonly used in printed circuit boards and hard disks for computers, under the-hood automotive uses, and reinforced composites for aerospace applications.[34] It is also hydrolysis resistant and tolerates repeated autoclaving cycles, which makes it suitable to be used in reusable medical devices that require steam sterilization. Other characteristic uses include analytical instrumentation and structural components that require high strength and rigidity at elevated temperatures.[35–38] Due to its inherent flame resistance, it is also used in flame-resistant garment fabric for firemen and race car drivers.[39] It needs high processing temperatures around 340 °C – 425 °C, even though it is processed by most conventional thermoplastics techniques.[37] Besides, its amorphous nature makes it susceptible to dissolution in organic solvents.[40,41]

Poly(butylene terephthalate) (PBT)

PBT is a semicrystalline engineering polymer that belongs to thermoplastic polyesters families, like PET. PBT molecule has flexible segments (four methylene group) and a hard segment (a terephthalate group) in its repeating unit, as presented in Figure 2.4. It has outstanding resilience and toughness due to the chain flexibility derived from the four methylene units. Its semicrystalline nature makes it highly resistant to organic solvents and it has low melt-viscosity attributed to its Tg value (close to 50 °C). It melts at 220 °C and is easy to process from almost all the thermoplastic conventional techniques.[34,41–43]

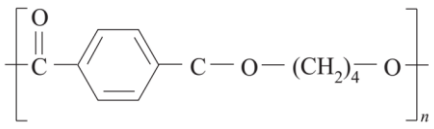

Figure 2.4 Repeating unit of poly(butylene terephthalate) (PBT).

PBT applications

PBT is used in everyday applications including switches and relays to motor housings, key caps for computer key boards, valves and valve bodies, timing screws, gears, bushings and bearings, wear strips, fuel pump components, and fuel system connectors and rotors. As PBT is approved by the FDA for direct food contact, it is used for food processing equipment and food piston pumps.[34,44] Although PBT is one of the best resins to use for injection molding, it has some limitations. PBT is sensitive to hot water, strong bases, oxidizing acids and ketones. PBT with no glass reinforcement is notch sensitive, and it is susceptible to direct flame contact.[44] To improve its flame resistance, it is commonly filled with flame retardant additives such as antimony trioxide and brominated compounds. Even though this approach enhances flammability properties, the mechanical properties are usually compromised.[33]

Poly(tetrafluoroethylene) (PTFE)

PTFE is a semicrystalline specialty polymer with a melting temperature around 342 °C and melt-viscosity of 10 GPas. It has the lowest coefficient of friction from all polymers and due to its simple molecular structure shown in Figure 2.5, it reaches high crystallinity degrees (until 98%). The last gives it outstanding organic solvents resistance.[23] The bond energy of C–F bonds is significantly high, what makes it highly thermal stable[23] with excellent flame resistant.[33]

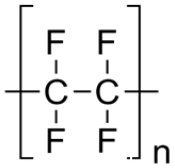

Figure 2.5 Repeating units of poly(tetrafluoroethylene) (PTFE).

PTFE applications

There exist three major presentations of PTFE: granular, fine powder, and micropowders. Granular and fine powder forms are commonly used in electrical wire insulation, seals, valves, pipe fittings and linings for aggressive chemical applications. Fine powders are also prepared in fiber, filament, and porous fabric forms. PTFE dispersions are used in glass cloth coatings to provide weather protection, mechanical strength, and chemical resistance. PTFE micropowders on the other hand, are used as additives to inks, lubricants, and plastics to provide lubricity, antiburning, and nonstick properties.[34]

2.2 Melt blending of high-performance polymers

2.2.1 Overview

Whether polymer blends are processed by melt or solution, the aim is to highlight the positive attributes of both materials while attempting to eliminate the negative ones.[31,45] That is why several studies are found on this topic, driven by both, academic and industrial sectors.[4,34,46–53] However, most of the efforts are focused in the production of blends from commodity polymers,[4,12,14,54–56] and blends between HPP are barely studied. The last is caused by the high cost of raw materials, the difficulty to control their processing conditions —particularly for those blends obtained from melt processing— and because fundamental studies in polymer-polymer interactions are not performed with these complicated systems. Nevertheless, from a technological point of view, it is of great interest to obtain high-performance materials and study the interaction between the constituents in order to tailor their final properties.[1,34]

Blends properties will depend on whether there is molecular interaction between polymers or not. This leads to three main categories: miscible, partially miscible, or immiscible blends. A miscible polymer blend is a homogeneous single-phase structure, where blends components interact intimately at molecular level and behave as a single polymer. If two polymers are miscible only within a certain composition range, the blend is defined as partially miscible. Finally, an immiscible blend is formed by two separate phases usually consisting of a dispersed phase and a matrix.

2.2.2 Thermodynamics of polymer blends

The most commonly criterion used to define if blends components are miscible or immiscible is the glass transition temperature. One Tg detected e.g. by differential scanning calorimetry (DSC), it is considered there is interaction between polymers at molecular level and they form a single-phase structure. From a thermodynamic approach, miscibility in polymer blends is commonly explained from the Gibbs free energy of mixing, ΔG_{mix}, defined by Equation 2.1 as:[57]

$$\Delta G_{mix} = \Delta H_{mix} - T\Delta S_{mix} \qquad \text{Equation 2.1}$$

where ΔH_{mix} is the enthalpy of mixing and ΔS_{mix} is the entropy of mixing at a given temperature T. The condition for two polymers to form a miscible blend is that Gibbs free energy of mixing should be negative ($\Delta G_{mix} < 0$). In low molecular weight materials, the entropy of mix-

ing is the most important parameter leading miscibility. However, due to the macromolecular nature of polymers the term $T\Delta S_{mix}$ is positive, but quite small, and the free energy of mixing is entirely leaded by the enthalpic term. In such case, ΔH_{mix} —which is the heat consumed as a result of the mixing of components at a constant pressure— must be negative to promote miscibility. That means, if heat is liberated the enthalpy of mixing is negative.

Exothermic mixing thus gives a negative contribution to the Gibbs free energy of mixing leading to polymers miscibility. The enthalpy of mixing is normally positive unless the two materials have attractive forces to each other through specific interactions, such as dipole-dipole and hydrogen bonding.[58,59]

However, merely having a negative free energy does not guarantee miscibility. The second derivative of the free energy in a composition x at fixed temperature and pressure must be greater than zero to guarantee a thermodynamic equilibrium state, Equation 2.2:

$$\left(\frac{\partial^2 \Delta G_{mix}}{\partial x^2}\right)_{T,P} > 0 \qquad \text{Equation 2.2}$$

In his work, DeMeuse[45] found numerous miscible blends between HPP. Many of these polymer pairs are miscible when cast from solution techniques, but immiscible when are obtained from melt processing. The author concluded that phases separate when are heated above their glass transition temperature indicating that kinetic factors more than thermodynamic are controlling misciblity.

Due to all the necessary parameters to achieve miscible blends, immiscibility predominates in polymer blending technology.

2.2.3 Immiscible polymer blends

Commonly, during morphology study of two immiscible polymers (A and B) are found three phases distributions, as presented in Figure 2.6. In i), the phase A is the matrix and B is the dispersive phase; in ii), an intermediate region of dual-phase inversion appears, where A and B are continuous phases; and finally in iii), phase B is the matrix and A the dispersive phase.

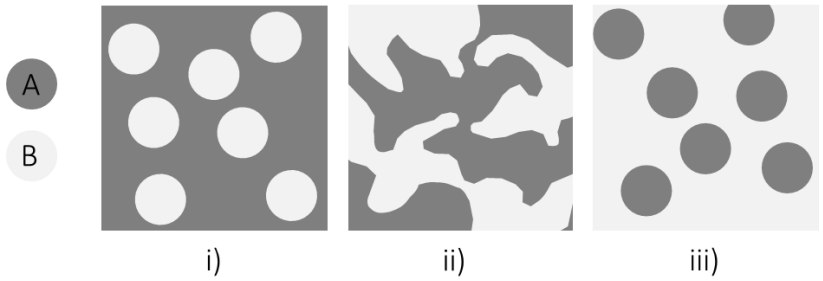

Figure 2.6 Scheme of the generalized morphologies in immiscible polymer blends.

Several works study the phase morphology of immiscible blends obtained from melt processing.[3–6,8–10,12–17,19–21,60] The results reveal that morphology is influenced by a combination of some or all of the following causes: materials characteristics (physicochemical, viscoelastic, thermodynamic, etc.), processing conditions (solution or melt processing, steps processing, temperature, mixing time, etc.), and finally, blends composition. If blends composition is the only variable during a morphological study, it is expected the dispersive phase distribution and particle size to be controlled by viscoelastic properties of individual components, as well as by the coalescence phenomena (interfacial tension).

Interfacial tension

In general, polymer blends result in an immiscible system with two differentiable phases. The morphologies obtained will strongly depend on composition, viscoelastic properties, processing conditions, and the most important, interfacial tension. The direct measurement of interfacial tension between all polymer pairs is a challenge, due to difficulties related to the intrinsic properties of components or experimental difficulties.[61]

Interfacial tension calculation

Some theoretical approaches are useful to estimate the interfacial tension based on the surface characteristics of each component. The surface tension of each component (γ) is the amount of energy required to build an unit area of a given material, Equation 2.3:[62]

$$\gamma = \left(\frac{\partial G}{\partial A}\right)_{T,P,n} \qquad \text{Equation 2.3}$$

where G is the Gibbs free energy and A is the interfacial area, T is the temperature, P is the pressure, and n is the total number of moles in the system.

The mentioned theoretical approaches include Antonoff's rule, Good and Girifalco theory, and harmonic mean equation.[62] Antanoff proposed the first theoretical method to calculate the interfacial tension between components i and j, by using Equation 2.4:

$$\gamma_{ij} = \gamma_j - \gamma_i \quad (\gamma_j \geq \gamma_i) \qquad \text{Equation 2.4}$$

Above equation is valid only if: i) there is zero contact angle between phase i and phase j, and ii) both phases are in vapor equilibrium. Since polymers have negligible vapor pressure, the second condition is not accomplished, then Equation 2.4 is not valid for polymer blends.

Later was proposed an expression based on the work of adhesion W^a —required energy to separate the interface of two materials— Equation 2.5:

$$W^a = \gamma_i + \gamma_j - \gamma_{ij} \qquad \text{Equation 2.5}$$

where γ_i and γ_j are the surface tensions of components i and j, and γ_{ij} is the interfacial tension. Good and Girifalco introduced an interaction parameter $\emptyset$ related to the molar volume, polarizability, ionization potential, and dipole moment of the polymers, and defined the interfacial tension as follows:

$$\gamma_{ij} = \gamma_i + \gamma_j - W^a \qquad \text{Equation 2.6}$$

where $W^a = 2\emptyset(\gamma_i\gamma_j)^{1/2}$, leading to the interfacial tension expression shown in Equation 2.7:

$$\gamma_{ij} = \gamma_i + \gamma_j - 2\emptyset(\gamma_i\gamma_j)^{1/2} \qquad \text{Equation 2.7}$$

However, Equation 2.7 gives good predictions on the interfacial tension for small-molecule organic liquids.

Later, Wu proposed the harmonic mean equation,[62] where it is considered the theory of fractional polarity in which molecular forces such as dispersive ${\gamma_i}^d$ and polar ${\gamma_i}^p$ (being d and p the superscripts corresponding to dispersive and polar components, respectively), are linearly additive, Equation 2.8:

$$\gamma_i = {\gamma_i}^d + {\gamma_i}^p \qquad \text{Equation 2.8}$$

This expression is valid for low energy materials and polymers, and represents the combination of the polar and the dispersion components of the work of adhesion, Equation 2.9:

$$\gamma_{ij} = \gamma_i + \gamma_j - \frac{4\gamma_i{}^d\gamma_j{}^d}{\gamma_i{}^d + \gamma_j{}^d} - \frac{4\gamma_i{}^p\gamma_j{}^p}{\gamma_i{}^p + \gamma_j{}^p} \quad \text{Equation 2.9}$$

Moving to experimental methods to calculate interfacial tension between polymer blends, Demarquette and coworkers compared five methods to obtain interfacial tension in molten polymer blends: pendant drop, Neumann triangle, breaking thread, embedded fiber, and rheological measurements.[63]

The pendant drop method consists of the study of a drop profile of one denser liquid suspended in a led dense liquid at mechanical equilibrium. The interfacial tension is inferred from an expression that relates the surface tension to the difference of density between both liquids and the geometrical profile of the droplet. Similarly to pendant drop, the Neumann triangle or sessile drop method consists of studying the profile of a drop of one liquid resting on a flat plate surrounded by another liquid of smaller density. It suggests interfacial tension can be calculated from the shape of the drop at mechanical equilibrium.[63]

The breaking thread method relates the evolution of a long fluid thread embedded in another. Due to Brownian motion, small distortions are generated on the thread surface. The pressure differences between the inside and the outside of the thread, induce deformation effects caused by the interfacial tension that tends to reduce the interfacial area. Similar to breaking thread method, is the embedded fiber, but in this one the fiber is shorter.[63]

The rheological method used to calculate interfacial tension is an effective approximation when it is not possible to use the mentioned experimental methods. Valera and coworkers tried to determine experimentally interfacial tension values for PMMA/PS/PP ternary blend, with PMMA as the matrix.[64] The highly viscous matrix did not allow to determine the interfacial tension values between the discrete components and the matrix of PMMA by conventional methods. They fit experimental rheological values to a theoretical rheological model: Palierne model. This model is based on the emulsion model developed to predict the linear viscoelastic behavior of polymer blends,[65] and correlates rheological measurement with the study of phase morphology from image analysis, Equation 2.10:

$$G_B{}^*(\omega) = \frac{1 + 3\sum_i \varphi_i H_i{}^*(\omega)}{1 - 2\sum_i \varphi_i H_i{}^*(\omega)} G_M{}^*(\omega) \quad \text{Equation 2.10}$$

where G_B^* and G_M^* are the complex dynamic modulus of the blend B and the matrix M, respectively; φ_i is the volume fraction of the dispersed phase, and $H_i^*(\omega)$ is expressed as:

$$H_i^*(\omega) = \frac{4\left(\frac{\gamma}{R_i}\right)[2G_M^*(\omega) + 5G_d^*(\omega)] + [G_d^*(\omega) - G_M^*(\omega)][16G_M^*(\omega) + 19G_d^*(\omega)]}{40\left(\frac{\gamma}{R_i}\right)[G_M^*(\omega) + G_d^*(\omega)] + [2G_d^*(\omega) - 3G_M^*(\omega)][16G_M^*(\omega) + 19G_d^*(\omega)]}$$

G_d^* corresponds to the complex dynamic modulus of the dispersed phase d, γ refers to the interfacial tension of the binary blend, and R_v is the volume average radius of the particles of the dispersed phase:

$$R_v = \frac{\sum_i (R_i \varphi_i)}{\sum_i \varphi_i}$$

where R_i is the average radius of the dispersed phase.

Palierne model correlates the dynamic response of blends to their morphology, composition, and interfacial tension. This model assumes that polymer blends can be treated as emulsions in both, diluted and molten state; and can be used only for spherical morphologies, viscoelastic and incompressible fluids, and fluids under linear viscoelastic regime.[66] The analysis is made from very low frequencies of small amplitude oscillatory shear measurements, to determine the relaxation times corresponding to the interfacial response of the blend.

Whether it is calculated by theoretical approaches or by experimental methods, the interfacial tension value allows predicting the morphology of polymer blends.

Morphologies of immiscible blends

During the mixing process of two polymers, the applied flow field deforms the domains of each component leading to combinatorial breakup and coalescence phenomena. Taylor studied the deformation and breakup of one diluted Newtonian liquid suspended into other Newtonian liquid, and observed that whether the size of drops or deformation rate is high enough, it will lead to drops break up.[47,50] He derived an expression based on the "competition" between deformation or viscous force (shear stress, $\eta_m \dot{\gamma}$) and recovery force (interfacial force, γ_{ij}/R), and defined the capillary number (Ca), Equation 2.11:

$$Ca = \frac{\eta_m \dot{\gamma} R}{\gamma_{ij}} \qquad \text{Equation 2.11}$$

where η_m is the matrix viscosity, $\dot{\gamma}$ is the shear rate, R is the radius of the drop, and γ_{ij} is the interfacial tension. When a critical value Ca_{crit} is reached, the stress destabilizes the elongated particles and break up occurs.

Grace[67] found that Ca_{crit} is a function of the viscosity ratio p —that is the relation between viscosity of the dispersive phase η_d, and viscosity of matrix η_m—, Equation 2.12:

$$p = \frac{\eta_d}{\eta_m} \qquad \text{Equation 2.12}$$

The relation between Ca_{crit} and p suggests that droplets will be stable when their Ca number is lower than the critical value, and break up will be easiest when p is between $0.25 - 1$ for shear flow. The Ca_{crit} values are reached under elongational flow in a wider viscosity ratio range.

Regarding the coalescence between blend components, Everaert and coworkers explained that from all variables involved in the coalescence of droplets, interfacial tension is the most important. They describe coalescence as a four-step process: first, droplets will approach to each other as a results of flow field or Brownian motions; second, collision and deformation of droplets will take place, removing the matrix phase between them; third, the remainder concentration of matrix between droplets will break up; and finally, the coalescing drops will form a single and coarser one.[3]

Usually, coalescence leads to a phenomena called “dual-phase transition”, as described in Figure 2.6. Several models have been proposed to either explain or predict the critical point of occurrence of the dual-phase inversion.[68–71]

Theoretical models for predicting dual-phase transition point on polymer blends

The first model was proposed by Paul and Barlow,[72] and later Jordhamo and coworkers defined the Equation 2.13.[69] This empirical model is based on the volume fraction (φ) of each component and the viscosity ratio. According to this model, phase inversion should occur when

$$\frac{\varphi_1}{\varphi_2} = \frac{\eta_1}{\eta_2} \qquad \text{Equation 2.13}$$

Later, Miles & Zurek[70] used the same Equation 2.13 in their experiments, but found that viscosity ratios values have to correspond to specific dynamic viscosities under melt-mixing conditions, and proposed a variation on Jordhamo's expression, Equation 2.14:

$$\frac{\varphi_1}{\varphi_2} = \frac{\eta(\dot{\gamma})_1}{\eta(\dot{\gamma})_2} \qquad \text{Equation 2.14}$$

However, this model was designed for low shear rates conditions and favors the phase inversion when viscosity ratio is close to one ($p \approx 1$). Jordhamo's model is not accurate to predict the phase inversion point on blends between materials with large differences in their melt-viscosity values.

A similar approach made by Ho and coworkers[68] on plastic/rubber blends systems, and later applied by Chen and Su[73] on poly(phenylene sulfide) (PPS), and poly(ethylene) (PE), considers large differences in melt-viscosities between blend components, Equation 2.15:

$$\frac{\varphi_{hv}}{\varphi_{lv}} = 1.2\left(\frac{\eta_{hv}}{\eta_{lv}}\right)^{0.3} \qquad \text{Equation 2.15}$$

where hv and lv denote the high and the low viscous phases, respectively. These authors claim that Equation 2.13 overestimates the volume fraction of the highly viscous phase.

Equation 2.15 was obtained empirically from the least squares fitting of experimental data variation of volume ratio with viscosity ratio. The fractional exponent indicates that the effect of viscosity ratio is weaker than the suggested in Jordhamo's model. Chen and Su explained Equation 2.15 results from the disperse phase coarsening after melt-blending, which depends more heavily on the matrix viscosity: lower matrix viscosity favors coalescence, and hence, dispersed phase coarsening.

A second model was proposed later by Metelkin & Blekht.[74] Authors considered the capillary instabilities during the blending process, Equation 2.16:

$$\varphi_2 = \left[1 + \frac{\eta_1}{\eta_2}\left[1 + 2.25log\left(\frac{\eta_1}{\eta_2}\right) + 1.81\left(log\left(\frac{\eta_1}{\eta_2}\right)\right)^2\right]\right]^{-1} \qquad \text{Equation 2.16}$$

All models described above are based on the effect of viscosity ratio, and their predictions lead to less viscous phase will tend to form the matrix.[50] Besides, these models give a single composition point for the phase inversion rather than a composition range.[75]

The final morphology in a polymer blend is a result of dispersion and coalescence processes that depend on the viscoelastic character of the components, the interfacial tension, and the stress history. However, when there are more than two blend constituents things can change substantially.

Morphologies of multicomponent blends

Interfacial studies in multiphase polymers systems have been mainly focus in binary blends. Near the 90's, bigger efforts began to be made in studying combinations of more than two polymers,[64,76–80] finding different and complexes morphologies than those obtained in binary blends. Some ternary blends exhibit core-shell morphology (encapsulation of one phase by other), which behavior is attributed to the *wettability* phenomena, that is consider as *the driving force of encapsulation*. Wettability can be compared to the "droplet sandwich analysis" presented in Figure 2.7, for three different polymers 1, 2, and 3.[81] Depending on the interfacial tension interaction between the polymers, three possible interaction cases may occur:

I. A thin layer of polymer 2 spreads between polymers 1 and 3. This is the most thermodynamically undesirable situation, since it occurs when the interfacial tension value between the three phases is too high.
II. A droplet of polymer 2 embeds in polymer 3. This will occur when the matrix is polymer 1, and the interfacial contact between polymers 1 and 2 is the most unstable.
III. A droplet of polymer 2 locates between polymers 1 and 3. In this situation, the three polymers can be directly in contact with each other since there is not much difference between phases stability.

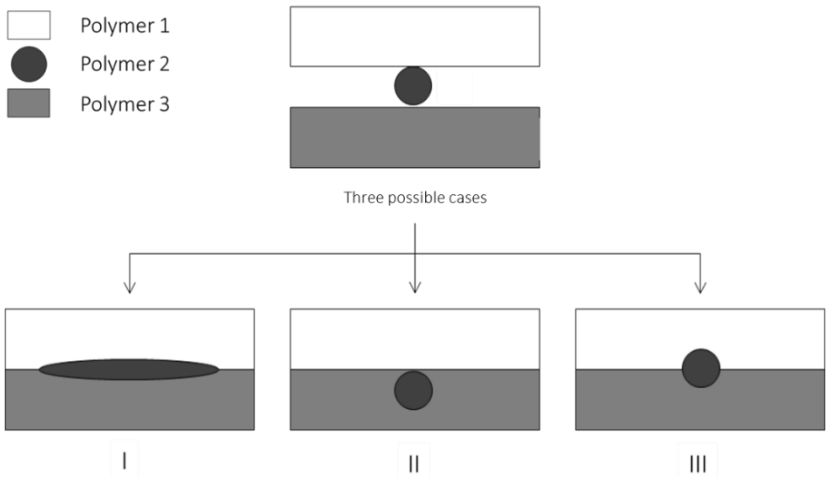

Figure 2.7 Droplet sandwich scheme to describe encapsulation in ternary blends.[81]

Based on the mentioned analysis, some theoretical approaches are proposed to predict the distribution of the constituents in a ternary blend. The most popular are: the spreading coefficient model proposed by Hobbs et al.,[76] the minimum free energy model proposed by Guo et al.,[82] and the interfacial energy dynamic model proposed by Reignier et al.;[80] being the spreading coefficient model the most used due to the accurate prediction results contrasted to experimental observations.[81,83–85]

Spreading coefficient model

In their work, Hobbs and coworkers[76] studied the morphologies of blends consisting of three phases by applying Harkin's principle, which describes the tendency of a liquid to spontaneously spread across a solid or liquid subtract, by means of the relation between their surface energies values, Equation 2.17:

$$\lambda_{ij} = \gamma_j - \gamma_i - \gamma_{ij} \qquad \text{Equation 2.17}$$

where γ_i and γ_j are the surface tensions of phases i and j, and γ_{ij} is the interfacial tension between the two phases. λ_{ij} is defined as the spreading coefficient, and it predicts spreading of phase i over j only if positive values of λ_{ij} are obtained, Figure 2.8.

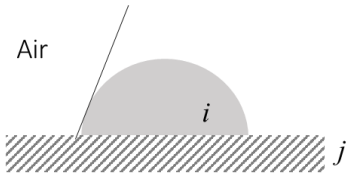

Figure 2.8 Schematic diagram showing spreading of phase i over j.

A first modified version of Harkins's theory was reported by Torza and Mason for three immiscible liquids.[86] Later, Hobbs[76] rewrote Harkins' equation for polymeric systems comprise by three immiscible phases where two of them are dispersed in the other. Considering three components 1, 2, and 3 where 2 is the matrix, and by substituting the surface tensions by the appropriate interfacial tensions, the spreading coefficient of phase 3 over the phase 1, is given by Equation 2.18:

$$\lambda_{31} = \gamma_{12} - \gamma_{32} - \gamma_{13} \qquad \text{Equation 2.18}$$

where γ_{12}, γ_{32}, and γ_{13} are the interfacial tensions for each components pair, and λ_{31} is the spreading coefficient for component 3 on component 1, and describes the physical situation in which component 3 is capable to displace the matrix 2 from component 1 to encapsulate it. This situation is valid if λ_{31} is positive.

Calculation of spreading coefficient allows predicting the morphology that will be formed in multiphase systems. In Figure 2.9 is presented the schematic representation of different cases that may occur according to spreading coefficient values.

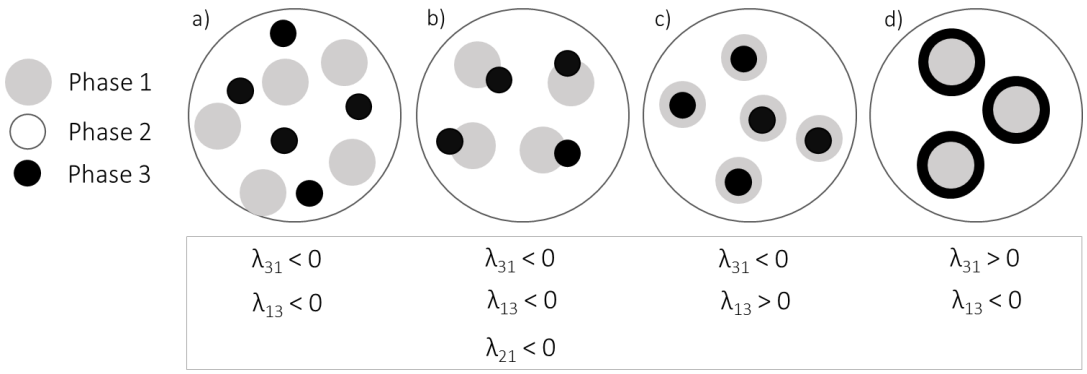

Figure 2.9 Schematic representation of the morphologies in a ternary 1/2/3 system: a) separate dispersions, b) partial encapsulation, c) complete encapsulation of phase 1 to phase 3, and d) complete encapsulation of phase 3 to phase 1.[87–90]

If λ_{31} and λ_{13} are negative, phases 1 and 3 will be dispersed separately in the matrix of 2. In the case λ_{21} is also negative, there will be partial encapsulation of phases 1 and 3. Finally, the spreading coefficient must be positive for any of the dispersive phases to encapsulate the other. This equation represents the tendency for the phase that forms the highest interfacial tension with the matrix to enter inside the other.

Minimum free energy model

This model relates the surface areas of the interfacial regions between blend components with the interfacial tension values, Equation 2.19:[64,81,91,92]

$$G = \sum_i n_i \mu_i + \sum_{i \neq j} A_i \gamma_{ij} \qquad \text{Equation 2.19}$$

where G is the free energy; μ_i and n_i are the chemical potential and the number of moles of specie i, respectively; and A_{ij} and γ_{ij} are the interfacial area and interfacial tension between components i and j, respectively.

For a morphological prediction analysis from this model, it must be considered only the second term, because the first one is the same for all types of morphologies.[65] If we come back to the example in Figure 2.9d), where phase 1 is encapsulated by 3, the model is written in the form:

$$\left(\sum_{i \neq j} A_i \Gamma_{ij}\right)_{3/1} = (4\pi)^{1/3}\left[{n_1}^{1/3} x^{2/3} \gamma_{13} + {n_3}^{1/3}(1-x)^{2/3}\gamma_{23}\right](3V_3)^{2/3} \qquad \text{Equation 2.20}$$

where $= V_1/V_3$, being V_i the volume fraction of phase i; n_1 and n_3 are the number of particles of phases 1 and 3, respectively; and γ_{ij} is the interfacial tension between the components i and j.

This model works under the assumption that all surfaces tend to minimize their free energy. Thus, the lower free energy value corresponds to the phase structure of the multicomponent system more stable, and this will be the morphology preferably formed.

Dynamic interfacial energy model

Reignier and Favis[80] proposed a model that considers the effect of the flow rate during the blending process on the interfacial tension values. This model is based on the assumption of Vanoene: "the elastic contribution to interfacial tension can lead to encapsulation of the less elastic component by the more elastic one". Thus, substituting Vanoene's postulate in Guo's equation, the minimum free energy required for phase 3 to encapsulate phase 1 is written as:

$$\left(\sum_{i \neq j} A_i \gamma_{ij}\right)_{3/1} = 4\pi {R_e}^2 \left[\gamma_{32} + \frac{Re}{6}(N_{1,3} - N_{1,2})\right] + 4\pi {R_i}^2 \left[\gamma_{13} + \frac{Re}{6}(N_{1,1} - N_{1,3})\right] \qquad \text{Equation 2.21}$$

where $N_{1,i}$ refers to the first normal stress of each phase, and R_e and R_i are the external and internal radii for a core-shell morphology (Figure 2.9c) and Figure 2.9d)). Again, the lowest free energy value will correspond to the more stable phase morphology, and that will be the morphology of the blend.

2.2.4 Morphology evolution by melt processing of polymer blends in an internal mixer

From all the melt processing equipment that exist on the market (single or twin screw extruders, injection molders, etc.), the internal mixer is a very useful tool for preparing small quantities of compounds and thermoplastic polymer blends, including the HPP. After the materials are processed in an internal mixer, they are characterized so that the product and process development can be scaled later to a continuous industrial process, such as extrusion.[93] During materials homogenization in an internal mixer, the torque is monitored while the processing parameters such as temperature, residence time, and intensity of mixing (rotors speed) are being controlled.[13,61] In polymer blends studies performed in an internal mixer, it is possible to track the morphology evolution of immiscible blends at different compositions, as presented in Figure 2.10.

In their work, Lee and Han[13] obtain blends in an internal mixer between five different semicrystalline and amorphous polymer pairs (nylon 6/HDPE, PMMA/PS, PC/PS, PS/HDPE, and PS/PP), and studied the morphological evolution of blends as a function of mixing time and polymers composition. They proposed a schematic representation to describe what happens to the morphology when two immiscible polymers with different glass transition or melting temperatures are mixed. They observed that depending on viscosity ratio and composition differences, the morphology evolves from dispersed droplets to either dual-phase transition or droplets breakup.

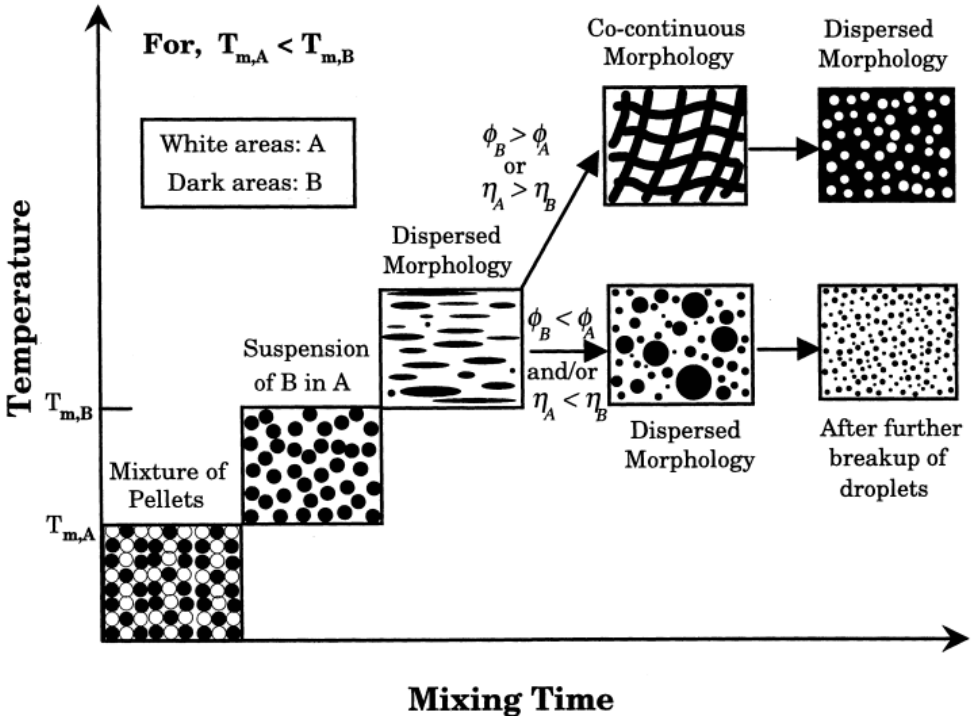

Figure 2.10 Schematic representation of the evolution of blends morphology of two immiscible polymers (A and B) in an internal mixer as a function of temperature and mixing time. In the figure, T_m is the melting temperature, ϕ is the volume fraction, and η is the viscosity.[13]

2.3 High-performance polymer blends (HPPB)

2.3.1 Overview

High-performance polymer blends consist of at least one HPP in its formulation. Similarly to the previous description of HPP, the service temperature of high-performance blends is around 175 °C.[31,45] Even though their commercial activity is limited somehow to military and aerospace applications, a great number of technological advances and commercial opportunities were achieved in the past decade from blending high-performance polymers.[24,25,33,45,94–104]

HPPB technology still deals with some issues related to polymers degradation caused by the high temperatures needed to process HPP —particularly for those blends obtained from melt processing—, and the lack of control of phase's distribution in the blends.[31,45] In this work, it is apply the compensation principle proposed by Utracky, which claims: "*the advantage of one component should compensate for the deficiencies of the other*".[23]

Different combinations between PEI, PBT, and PTFE were melt processed, and it is expected the new materials obtained to be thermally and mechanically improved, as well as with excellent melt processability.

2.3.2 PEI and PBT high-performance polymer blends

Two decades ago, an increasing amount of works were focused on the study of blends between two major HPP families: specialty poly(imides) and engineering poly(esters) blends.[40–43,94,95,97,99–101,104,105] In those groups, were found blends based on PEI and polyesters like PET and PBT, due to the interest on developing new polymeric materials with outstanding combination of performance and processing characteristics.

PEI is a specialty polymer from the poly(imide) family, used in blends fabrication with PAr, PPS, PSO, PEEK, PA, PEST, PC, PPE, PSF, LCP. On the other hand, PBT is an engineering polyester commonly used to obtain blends with PET, PC, PA-6, and PA-66. In Table 2.3 are summarized some HPPB that use PEI or PBT in their formulation, as well as the processing method used. In these works, authors improved the electrical, thermal, and mechanical resistance of engineering polymers, and enhanced the processability of poly(imides).

Table 2.3 High-performance polymer blends using either specialty PEI or engineering PBT in their formulation.

High-performance polymer blends	Acronym	Processing method	References
Nylon 66/Poly(ether imide)	PA66/PEI	Melt-blending in an internal mixer. Improved PEI processability.	101
Poly(ether ether ketone)/poly(ether imide)	PEEK/PEI	Melt-mixing by extrusion. Thermal-induced phase separation.	103,104
Poly(ether imide)/Polyarylate	PEI/PAr	Melt-mixing in a Brabender Pasticoder.	99
Poly(ether imide)/poly(ethylene terephthalate)	PEI/PET	Melt-mixing in a Brabender Pasticoder and direct blending by injection.	102
Poly(ether imide)/poly(trimethylene terephthalate	PEI/PTT	Melt-mixing twin screw extruder.	94
Poly(phenilene sulfide)/poly(ether imide)	PPS/PEI	Melt-mixing in a Brabender Pasticoder.	95
Sulfonated poly(ether ether ketone)/poly(ether imide)	SPEEK/PEI	Solution blending in DMAC.	97
Poly(ethylene terephthalate)/poly(trimethylene terephthalate)/poly(butylene terephthalate)/poly(ether imide)	PET/PTT/PBT/PEI	Solution blending in dichloroacetic-acid.	106

High-performance polymer blends	Acronym	Processing method	References
Poly(butylene terephthalate)/Polyarylate	PBT/PAr	Solution precipitation in methanol from a TCE/Ph solution.	[100]
Poly(ether imide)/poly(ethylene terephthalate); poly(ether imide)/poly(butylene terephthalate); poly(ether imide)/poly(ether ether ketone)	PEI/PET; PEI/PBT; PEI/PEEK	Ball milling.	[107]

2.3.3 PEI/PBT blends

With blending PEI and PBT it is expected a unique combination of properties, due to PEI possesses mechanical and thermal stability, and PBT offers crystallinity and good flow property at processing temperatures.[40,41] However, not too many studies are found about binary PEI/PBT polymer blends, all of them reported miscibility between PEI and PBT in the whole composition range evaluated,[40–43,96,105] and only one evaluates an industrial melt processing method for blends fabrication.

In 1997 Woo and Yau[40,105] obtained PEI/PBT blends by direct melt mixing by using an aluminum plate with 2 g capacity and hand stirring. After blending, they performed heat treatment of quenching to PEI/PBT samples before miscibility evaluation by DSC and DMA. They observed a single Tg in the entire composition range as a sign of miscibility between PEI and PBT phases. Besides, they noticed PBT exhibited cold crystallization temperature (Tc) that shifted to higher temperatures while PEI concentration increased.

The same year, Chen and coworkers[42] fabricated PEI/PBT blends by solution precipitation in dichloroacetic acid at room temperature. They used different annealing times to study the blends crystallinity evolution at 250 °C. Although they observed a strong PEI phase segregation due to PBT crystallization, they conclude that PEI and PBT are miscible. Additionally to Woo and Yau work, they stated that PBT crystallization rate decreased with increasing PEI content. In other words, PEI hindered PBT crystallization by raising the whole blend's Tg.

One year later, Jang and Sim[43] also used precipitation technique codissolving PEI and PBT in 1,1,2,2-tetrachloroethane and phenol mixture at 100 °C. Thin films were obtained by press molding at 250 °C, and miscibility of PEI/PBT blends by FT-IR ATR (Fourier Transform Infrared Spectroscopy with Attenuated Total Reflectance) was studied. They found that C=O stretching

peak of PEI/PBT blend shifted to lower wavenumber as the crystallization of PBT took place, as a sign of miscibility between PEI and PBT in the entire compositional range.

Later in 2001, Vallejo and contributors[41] prepared PEI/PBT blends by using a co-rotating double screw extruder. They established the processing temperature depending on the major components in the blends. For PEI-rich blends, processing temperature was 290 °C, while for PBT-rich blends it was 270 °C. They tested the solid state behavior of blends by DSC, DMTA, and specific volume measurements. Results showed again that PEI and PBT were completely miscible. They also detected an increase on Tc with PEI addition by DSC scanning and an important decrease in crystallinity of PBT attributable to a PEI hindering effect on PBT crystallinity, which is in good agreement with previous PEI/PBT works. Additionally, they found that PBT improved PEI processability, and a synergism in elasticity modulus and yield stress for 90/10 and 80/20 PEI/PBT blends.

2.3.4 HPPB containing PTFE

It is well known that PTFE has the lowest coefficient of friction from all polymers, it is highly thermal stable, fire resistant, and also has an outstanding solvent resistance due to its highly crystalline structure.[108–113] However, it has poor wear resistance due to that crystalline structure which is easily cut or pulled out during the process of friction and wear.[109,110]

Some studies on high-performance blends show that PTFE is mostly used in improving friction resistance of polymers.[109–116] It is added either as a filler in the solid state to form polymer composites or as a new phase to produce polymer blends, depending on the processing method used (solution or melt processing). In their work, Anbinder and coworkers[115] obtained blends of PU with different compositions of PTFE, from 2 wt% to 50 wt%. Blends were prepared by using an aqueous dispersion technique to later fabricate films by casting dispersion, evaporating the water content at 30 °C. The resulting hydrophobic materials exhibited much higher contact angles than pure PU, and enhanced thermal stability due to PTFE addition.

Other reports show strategies to improve wear resistance of PTFE by mixing it with other HPP. Chen and collaborators[110] used compression molding to fabricate binary PTFE based blends. They obtained four blends by reinforcing PTFE with 20% of either PI, PEEK, poly(phenyl *p*-hydroxybenzoate) (PHBA), or perfluoro ethylene propylene (FEP). Blends were prepared by pressing powders into sheets at room temperature, and sintering them at 380 °C. Authors

found that wear resistance of PTFE was improved by adding some of the mentioned resins, due to variations in the PTFE structure.

PTFE has also being added to high-performance polymers such as PI, PPS, and poly(hydroxy benzoic acid), and to commodity polymers such as PP, which exhibited enhanced tribological and mechanical properties.[112,117–119] It is found that adding up to 20 wt% of PTFE is enough to obtain the desire modification of properties of blends.

2.3.4.1 PEI and PTFE blends

PTFE has been added to poly(imides) e.g. PAI, PEI, PI, to improve their friction resistance.[109,112] Bijwe and coworkers[112] studied the effect of PTFE in a commercial wear-resistance PEI resin (ULTEM 4001). This resin originally from General Electric Company, is found to be filled with 13 wt% to 15 wt% of PTFE, amount enough to make PTFE as the dominant material in the friction resistance.

In their work, Ma and coworkers[120] combined PEI with 5 wt% to 15 wt% of two solid lubricants, PTFE and graphite. They compared the effect of both lubricants in PEI friction resistance, and found that friction coefficient for PEI reduced from 0.41 to 0.3 when was filled with PTFE. Additionally, they found that both, tribological and mechanical properties (tensile strength, bending strength, impact strength, and Rockwell hardness) of PEI filled with PTFE were higher than those filled with graphite. Similar results are reported by Ren in his work.[108] They filled different HPP such as PEEK, PPS, PI, and PEI with PTFE powders. All materials exhibited interesting properties such as excellent strength at high temperatures, low coefficient of friction, remarkable chemical resistance, and tribological properties.

2.3.4.2 PBT and PTFE blends

PTFE is also used as a solid lubricant in blends with PBT for under-the-hood applications in automotive industry. HPPB are very attractive in this industry since they may save costs and weight by replacing the commonly used metallic materials.[121]

In their work, Danila and coworkers[122] added 10 wt% of PTFE to PBT and studied their tribological characteristics. Even though friction resistance was improved, the wear resistance of PBT/PTFE blends was lower than that of single PBT.

In 2016, Hussain and coworkers[114] fabricated blends between thermoplastic elastomer (TPEE) with poly(butylene terephthalate) (PBT) via melt processing, and added small quantities of PTFE. They studied the mechanical and thermal properties of TPEE/PBT blends. Results revealed that TPEE improves PBT mechanical properties, but the thermal resistance is compromised. Authors found out that adding 0.5 wt% of PTFE to TPEE/PBT blends was enough to significantly improve their mechanical and thermal properties. It was the first time it was studied the effect of PTFE on the mechanical and thermal properties of a blend, since major works on blends based on PTFE are related to abrasion resistance assessment. The resultant material was proposed as a baffle plate for use under-the-hood of an automobile.

Later the same year, it was published a study of the effect of PTFE on the mechanical properties of PBT. Musteata and collaborators[123] varied PTFE content (10 wt%, 15 wt% and 20 wt% of PTFE) on PBT/PTFE blends, and contrary to Hussain findings, authors do not recommend PTFE for improving PBT mechanical properties since elongation at break is highly affected. However, interesting improvement in modulus and yield strength of PBT/PTFE blends was noticed, getting values significantly higher than those for pure PBT. The yield strength of pure PBT is 40.58 MPa, and increased to 46 MPa with 10 wt% of PTFE.

2.4 HPPB in fire protection applications

2.4.1 Overview

The increasingly demanding applications of today's world, force users to wear extra protection in their garments, uniforms, architectonical structures, protective housing of electronic devices, etc., to face the hazardous conditions they are exposed.[26–28] In this scenario, materials play a crucial role in human and goods protection. In 2015, Kahn and coworkers reported in their study "*Line of duty firefighter fatalities: An evolving trend over time*", 2775 fatality cases of firefighters between 1990 and 2012, only in the United States. During that period the deaths caused by burns decreased by 3.8%, to some extent, thanks to the improvement of thermal, flame, chemical, and mechanical resistance of materials.[29]

In this matter, polymers are not the exception. Industries such as firefighters, military, public buildings, maritime transportation, medical, metal casting, automotive, aerospace, etc.[27,124,125] have driven the development of new polymeric materials with better resistant to heat and flame conditions. However, it is necessary to make great efforts to avoid the loss of other prop-

erties, such as mechanical resistance. The industry of technical fibers for instance, is always looking forward for developing new protective fabrics that are flame retardant, non-toxic, and environmentally friendly, but at the same time comfortable to wear (soft, light, aesthetic, etc.).[124,126,127]

According to Horrocks, materials for human protective garments should fulfil both, heat and flame resistance.[30] These materials are usually exposed to contact heat, radiant heat, sparks, molten metals, flames (convective heat), and hot gases and vapors. As these materials are used for human protection, it should also be avoided the production of smokes and toxic gases evolution.

Human tissue is very sensitive to temperature. The degree of injury depends on the heat transfer to the skin (0.64 cal/cm^2 causes pain sensation, and 1.2 cal/cm^2 secondary burns).[26] In the electric power industry for instance, workers are constantly exposed to arc flash events. The protective garments for these situations must withstand at least 4 cal/cm^2 according to the standard IEC 61482-2:2009. Because of that, protective clothing should provide enough time to interact, escape, and avoid and minimize burns. Materials used in this field must accomplished three main principles: i) *flame resistance* (materials do not burn after flame contact); ii) *integrity* (materials wont shrink or melt, and they will form brittle charring); and iii) *insulation* (retard heat transfer and avoid liquids production).[30]

2.4.2 Principles of heat and flame resistance for polymers

When solid polymers are heated or exposed to direct flame contact, they undergo both physical and chemical changes. As a consequence, they may experience undesirable changes in their properties that lead them to decomposition, degradation, or both.[32]

It should be stated the difference between decomposition and degradation. During decomposition polymers experience changes at a chemical level (break-up of their molecular structure, e.g. chain scission). Degradation on the other hand, is related to loss of physical, mechanical, or electrical properties when they are heated. In terms of fire, the most relevant change in polymers is the thermal decomposition.[32]

2.4.2.1 Thermal decomposition of polymers

During thermal decomposition, polymers go through four main steps: heating > decomposition (gasification and fuel generation) > ignition (flame) > flame propagation, Figure 2.11.[124] During the combustion process, polymers generate a gaseous fuel —also called volatiles– that can burn above the solid material surface. The flame propagation takes place if the combustion process is self-sustaining, which means it is necessary that burning gases have to feed sufficient heat back to the material to continue the production of fuel vapors. These volatiles react with the oxygen in the air and part of this is transferred back to the polymer to continue the process.[32]

Solid polymers go through several transformations while heating. Their decomposition is commonly lead by changes in their chemical structure. However, physical changes such as melting and charring may also take place during polymers combustion before passing to the gaseous phase, and may change the decomposition and burning characteristics of the material.[32] If carbonaceous layers are formed —also called charring products or intumescent layer— the polymer is protected against direct fire exposition, and if they are appropriately formed, they slow down further thermal decomposition.

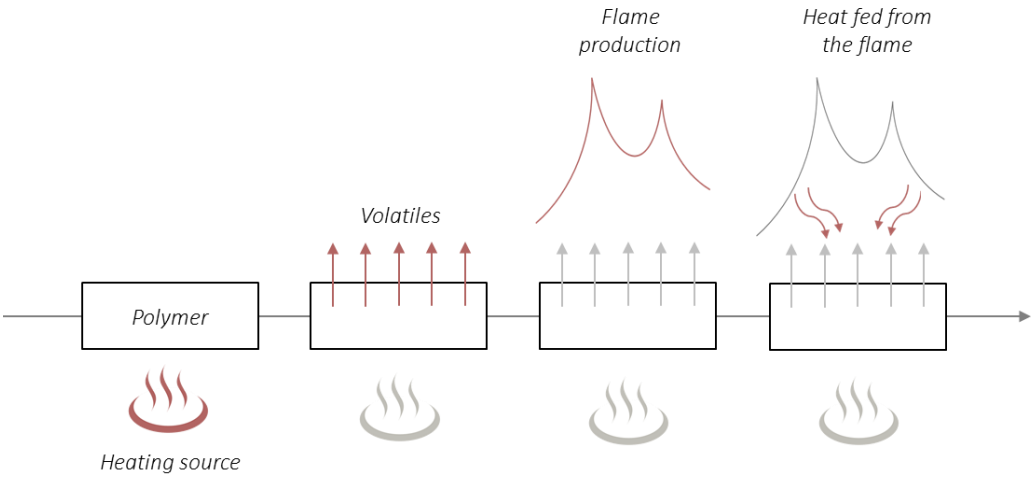

Figure 2.11 Combustion process of solid polymers.

2.4.3 Study of flammability in polymers

The thermal stability and flame resistance of polymers is commonly measured by techniques that relates the kinetics and thermodynamics of the decomposition process such as thermogravimetric analysis (TGA) and derivative thermal analysis (DTA). Also, by techniques that con-

cern with the nature of the decomposition from the point of view of combustion and toxicity, such as pyrolysis-gas chromatograph-mass spectrometry (Py-GCMS).[32] However, thermal decomposition studies are not always the best indicators of polymers fire performance. One first approach to study the flammability of polymers is by measuring the limiting oxygen index (LOI).

The LOI is the minimum oxygen content necessary for the polymer ignite or burn. Its measurement is based on the oxygen concentration in air, which contains 21% of O_2, and it is expected to be higher in polymeric materials used in direct fire contact applications. If the LOI < 21% the polymer is considered flammable. When LOI = 25% it is classified as a material of low flammability. Materials with LOI > 21% will not burn in normal air conditions.

Table 2.4 lists some polymers commonly used in the technical textiles industry (in Table A- 1 are listed the main trade names and main applications of some of these polymers). The HPP used in this work and presented in italics. Polymers are organized from the lowest to the highest LOI values. As mentioned, thermal stability is not an indicator of polymers flammability. The decomposition temperature of PA for instance, is much higher than PPS temperature. However, PPS has better flame resistance than PA, as indicate its LOI values.

Table 2.4 Thermal events in materials commonly used in textile industry and the HPP used in this work (shown in italics). Materials are organized from the lowest to the highest LOI value.

Polymer	**Physical changes**		**Chemical change**	**LOI (%)**	**References**
	Tg (°C)	*Tm (°C)*	*Td (°C)*		
Cotton			105	19.9	[124]
PA	50	215	431	20 – 21	[32,33]
PBT pure	*60*	*225*	*397*	*21*	[34]
Wool			245	25	[124]
PBT + flame retardant filler	*60*	*225*	*342*	*30*	[a]
Modacrylic	<80	>240	273	29 – 30	[124]
PPS	85	285	300	34 – 35	[34,124]
PI	315		500	36 – 38	[32,34]
PBI	426		600	41	[34,124]
PEI	*217*		*527*	*47*	[35, a]

Polymer	Physical changes		Chemical change	LOI (%)	References
	Tg (°C)	*Tm (°C)*	*Td (°C)*		
PTFE	*130*	*325*	*472*	*95*	[32,34,a]

[a] Data obtained from supplier material's data sheet

Some authors have related the LOI with polymers charring measured by TGA as the residual material after polymer pyrolysis at 850 °C.[27,32] The formation of char is one of the most effective attributes that a material has against fire propagation.

2.4.3.1 Heat and fire burns prevention

For a polymer combustion to take place, there must coincide three factors: oxygen (air), heat (fire source), and fuel (polymer). These are known as the "fire triangle", and depends on all three factors. If one of them is removed, fire will be prevented or extinguished.[128,129]

The prevention of structural damages, and specially, burns in humans are the major motivations to improve materials fire resistance. Some strategies used in this matter include: i) dilution of combustible gases (oxygen) with non-combustible gas in order to eliminate oxygen from combustion zone, ii) trapping of the active radicals by using halogenated compounds, iii) use materials with inherent charring formation or induce it with additives to reduce the amount of flammable fuel formed by polymers, and iv) use heat-absorbent additives that decompose endothermically to reduce the heat generation.[27,30,125,127,130,131]

Even though the most effective flame retardants are those which promote the transformation of a polymer backbone to carbonaceous char —because char does not burn in normally air conditions (LOI > 50%)[27]—, one of the most common technique includes the use of compounds based on antimony: antimony trisulphide, triphenyl stibine, sodium antimony, antimony trioxide (the most popular) to name a few.[129,132] These are normally combined with halogenated compounds to reach synergetic effects. However, one of the principal issue is related to the toxicity during the processing and combustion stages. To avoid this problem, some authors tried adding aluminum and magnesium hydroxides. However, they have to be added in greater amounts in order to the polymer reaches fire retardancy properties (>40%), affecting tremendously the mechanical properties of the materials.[133]

Conclusions – Chapter 2

It is highlighted the attractive thermal and mechanical properties of HPP family, as well as their applications in industries with particularly demanding high performance. The implementation of the blending technology to HPP is a striking manner of obtaining new materials, especially if the fabrication of the HPPB is made from melt processing methods. In addition, the high costs of HPP linked to their low production volumes compared to commodity polymers, can be whether reduced or justify by doing a performance/cost analysis.

Some authors developed new materials between engineering polymers such as PBT, in combination with specialty amorphous or semicrystalline polymers with elevated Tg. This is a suitable approach for combining remarkable performance and processability into a single material since PBT is a low Tg semicrystalline polymer, which enhances the melt processability of highly viscous polymers.

Blends between PBT and PEI are also found. Most authors obtained blends from casting solution techniques, resulting in miscible blends along the entire composition range. Only one work uses an industrial melt processing approach to fabricate these blends. As expected, low viscosity PBT enhances PEI processability. However, authors changed processing temperature based on PEI content (290 °C for PEI-rich blends, and 270 °C for PBT-rich blends). Surprisingly, they also obtained miscible blends despite the melt processing method used, which leads to suppose that temperature ranges from blends' Tg and the phase separation temperature is wide enough to process miscible PEI/PBT blends in the melt state.

There are still some gaps left on the study of blends between PEI and PBT, particularly from melt processing methods:

- The effect of constant processing parameters on the entire composition range on blends miscibility;
- An interfacial interaction analysis as well as a micrographic study of phases, to better understand the miscibility phenomena and phases distribution;
- The relationship between the rheology, interfacial tension, composition, and processing conditions and the mechanical, thermal stability and flame resistance performance of blends.

Industry sectors such as technical textiles may be interested in using these materials. Combining these two polymers may result in a new material with remarkable thermal stability and flame resistance with excellent processability. Since it is difficult to obtain high-performance and comfort in a single material, blends between PEI and PBT appear as an attractive solution for this purpose.

Even though some authors found synergism on modulus and yield strength for PEI-rich blends, blends revealed poor ductility. Some authors tried adding rubbery polymers to a blend containing 80 wt% of PEI and 20 wt% of PBT. They improved the impact strength, but results revealed that ductility was even lower due to poor interfacial interaction between blends components. There is still missing a study of adding a third component to enhance the mechanical properties without affecting the thermal and flame performance, and analyses the phases' interaction at interfacial scale. In this scenario, PTFE enters as an attractive option to modify binary PEI/PBT blends.

Chapter 3 Fabrication of binary high-performance polymer blends (HPPB) between PEI and PBT obtained by melt processing

3.1 PART I – Development of a *two-step melt processing method* to fabricate binary blends between high-performance polymers with notable processing conditions differences: PEI and PBT

3.1.1 Introduction

Blending high-performance polymers (engineering, specialty, and ultra-high performance) rises as an opportunity to obtain materials with outstanding mechanical, thermal, and chemical properties, with good processability from melt processing techniques. Engineering polymers combine high-performance (100 °C < CUT ≤ 140 °C, and tensile strength > 40 MPa) with good processability. This group comprises poly(amides) (PA), poly(carbonates) (PC), poly(esters) (PBT, PET, PTT), poly(acetal) (POM), and poly(p-phenylene ether) (PPE). On the other hand, specialty and ultra-high performance polymers have remarkable mechanical properties, thermal stability, some of them display inherent flame resistance, and poor processability. They include polymers such as poly(fluoro carbons) (PTFE, PVDF), poly(siloxanes), sulfur-containing polymers (PPS), poly(imides) (PI, PEI), poly(ether ketones) (PEEK), among others.[1,23,24]

In this section, it is discussed the methodology we use to fabricate blends with flame retardant characteristics between two HPP with notable differences in their processing characteristics: poly(ether imide) (PEI) and flame retarded poly(butylene terephthalate) (PBT). In this thesis, we propose a novel *two-step melt processing method* to fabricate PEI/PBT blends using an internal

mixer. We settled the processing temperature (Tp), mixing rate (n), and mixing time (t) after a complete thermal and rheological characterization of pure materials. Conversely to Vallejo and coworkers,[41] we prepare PEI/PBT blends within the entire compositional range at the same processing conditions, varying only blends composition.

3.1.2 Experimental

Materials

Blends between PEI and flame retardant PBT were obtained. Both commercial grade polymers were purchased from Sabic Innovative Plastics: poly(ether imide) (PEI) Ultem 1000, and poly(butylene terephthalate) (PBT) filled with a flame retardant compound (brominated and antimony trioxide compound) Valox 310SE0.

Unfilled PBT (Uf-PBT) Valox 325 was also characterized to contrast its thermal and rheological properties to those of the flame retardant PBT. Some relevant raw materials characteristics obtained from suppliers' data sheet are listed in Table 3.1.

Table 3.1 Characteristics of raw materials. Values were obtained from suppliers' data sheet.

Polymers	Acronym	Density (g/cm^3)	Melt flow index (g/10 min)	Color
Poly(ether imide)	PEI	1.27	9[a]	Ambar transparent
Flame retardant poly(butylene terephthalate)	PBT	1.4	8[b]	White opaque
Unfilled poly(butylene terephthalate)	Uf-PBT	1.31	18[b]	White translucent

[a] *Obtained at 337 °C and 6.6 kg*
[b] *Obtained at 250 °C and 2.16 kg*

Blending process

Before blending, PEI and PBT were vacuum dried at 110 °C for 16 hours to prevent PBT hydrolysis. Materials were taken out of the oven just before the mixing process in a Haake Rheomix 3000 OS internal mixer fitted with roller type rotors. Blends were prepared under standard atmosphere within the entire compositional range. For each blend composition, it was calculated the amount of PEI and PBT by using Equation 3.1:

$$m = \rho_B \, V \, f \qquad \text{Equation 3.1}$$

where ρ_B is the density of the blend calculated from the weight fractions of both polymers ($\rho_B = w_1\rho_1 + w_2\rho_2$), V is the free volume inside the mixing chamber ($V = 310\ cm^3$ for roller type rotors), and f is the filling factor ($f = 0.9$).

The major processing parameters involved during mixing are the processing temperature (Tp), the rotors speed (n), and the mixing time (t). All these parameters were defined from thermal analysis and the viscosities of both, PEI and PBT.

Thermal analysis

The processing temperature (Tp) was defined after DSC and TGA analyses under a nitrogen atmosphere.

DSC was performed in a Q200 model from TA Instruments on 20±1 mg samples. The thermal program started with heating from 0 °C to 290 °C at 20 °C/min, and held on for one minute; followed by cooling down to -90 °C at 20 °C min^{-1}. The second heating was performed in modulated mode up to 300 °C at 2 °C/min.

The thermal stability study was carried out in a TGA Q500 model from TA Instruments on 40±2 mg samples, within a temperature range from 25 °C to 900 °C at 10 °C/min.

Polymers viscosities

The rotors speed (n) was defined from studying the viscosities of PEI and PBT in a Haake MARS III rotational rheometer from Thermo Scientific. It was used a cone/plate configuration of 20 mm diameter with a cone angle of 1°. The analysis was made in a shear strain sweep from 0.01 s^{-1} to 60 s^{-1} at 300 °C for PEI, and 280 °C for PBT. Tests were carried out under standard atmosphere. As the cone angle used is less than 3°, it was possible to associate the shear rate values with the rotors speed in the internal mixer according to standard BS 2782 – Part 7,[134] using the equivalence equation, Equation 3.2:

$$\dot{\gamma} = \frac{\omega}{\beta} = kn \qquad \text{Equation 3.2}$$

where $\dot{\gamma}$ is the shear rate, ω is the angular speed, β is the cone angle, k is a non-dimensional number that depends on the cone angle (at a cone angle of 1°, $k = 6$; at an angle of 2°, $k = 3$; and at an angle of 4° $k = 0.75$), and n is the rotational speed.

Molten polymers evolution in the mixer

The time needed to prepare the blends (t) was defined by means of torque stability, viscous dissipation, and decomposition of PEI and PBT. For this, it was tracked the evolution of torque and temperature for pure materials inside the mixing chamber as a function of time. Materials decomposition was identified by visual inspection taking off samples from the mixer at different times.

3.1.3 Results and discussion

Defining processing conditions

Processing temperature (Tp)

The differential scanning calorimetry (DSC) of pure materials is presented in Figure 3.1. PEI exhibits a single variation in the baseline at 215.7 °C indicating its glass transition temperature (Tg). PBT, on the other hand, shows a change in the baseline at 58 °C during the first heating corresponding to its Tg, followed by an exothermic reaction close to 110 °C attributable to thermal reactions between brominated and antimony trioxide compounds (flame retardant fillers). This exothermic response was not evidenced for unfilled PBT samples, as presented in Figure A- 5.1. A major endothermic peak shows its melt transition temperature at 222 °C (Tm). The Tg of amorphous PEI and Tm of semicrystalline PBT overlap in the temperature range between 213 °C and 225 °C. During the cooling program, the PBT reveals its crystallization temperature (Tc) at 196 °C.

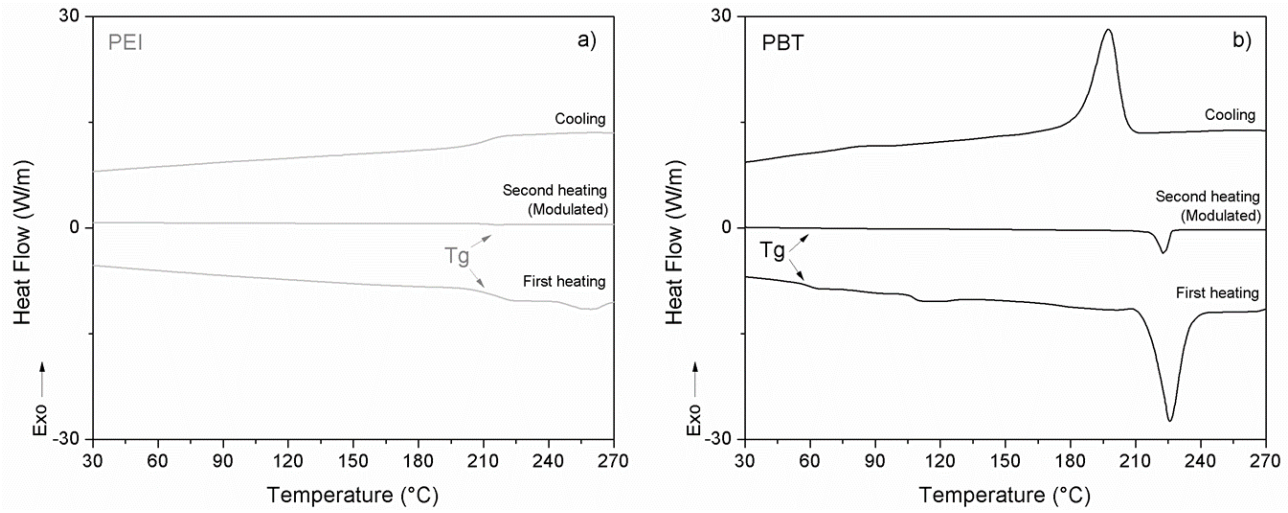

Figure 3.1 Thermal characterization from DSC for pure materials: a) PEI, and b) PBT.

In Figure 3.2, the thermogravimetric analysis (TGA) for both materials display a single step decomposition reaction where the initial (Ti) and the final (Tf) decomposition temperatures are well defined. For PEI, Ti is around 497 °C, while for PBT decomposition starts at 300 °C, which suggest that PBT should not be processed above 300 °C to avoid degradation of its backbone structure.[38] At the end of the tests, the residue of PEI is more than half its initial weight, 53.56%, and it is much higher than that of PBT, 15.28%. This corroborates that the thermal decomposition of PEI is leaded by charring formation phenomena. As it is observed in the derivative thermogravimetric curves (dashed lines), PBT displays a second decomposition event at 500 °C that overlaps with PEI decomposition temperature. This signal corresponds to the oxidation of antimony trioxide filler, that takes place at temperatures close to 500 °C.[135,136]

According to DSC and TGA analysis, the processing temperature of PEI/PBT blends should be within a range between 260 °C and 290 °C to keep the structural integrity of PBT during the blending process.

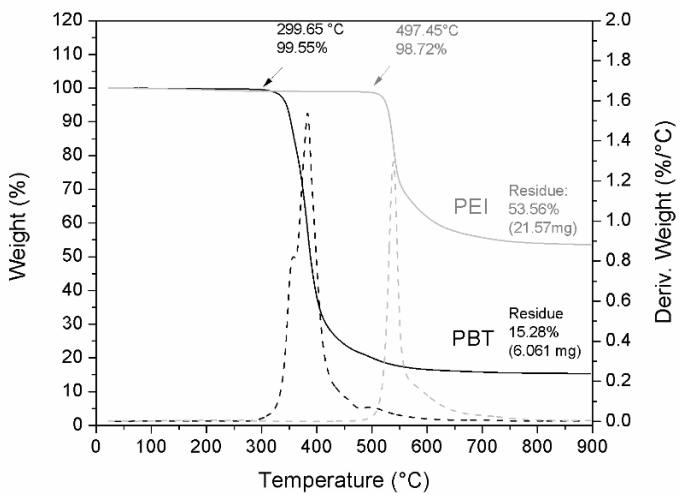

Figure 3.2 Thermogravimetric analyses (solid lines) and their derivatives (dash lines) for pure PEI (gray), and pure PBT (black).

Mixing rate (n)

PEI and PBT viscosity curves are shown in Figure 3.3a). PEI viscosity is higher than PBT in the entire shear rate range evaluated. PEI exhibits a Newtonian plateau at a low shear rate that evolves to shear-thinning behavior while deformation increases. In comparison to PEI, PBT does not display plateau as a consequence of the inorganic fillers content which inhibits viscosity stability of the molten polymer at low shear rates, resulting in a continuous decreasing of viscosity with increasing shearing. This is a common rheological response of molten polymers filled with inorganic particles, where a gel-like behavior predominates at low shear rates be-

cause the collision between particles limits chains mobility and avoids viscosity to stabilize.[137–139]

Mixing rate (n) is settled by using the shear rate/rotors speed equivalence equation, Equation 3.2, together with the viscosity curves of pure materials. We calculate the rotational speed at the end of the shear thinning region of PEI curve between 20 s^{-1} and 50 s^{-1}, which is equivalent to 30 rpm to 80 rpm. As 30 rpm is a very slow speed to process highly viscous PEI, we choose an intermediate value of 45 s^{-1} —just before the test finishes— that is equivalent to a rotors speed of 70 rpm.

Mixing time (t)

Mixing time (t) is defined by tracking torque and temperature evolution of pure materials inside the mixer. In Figure 3.3b), it is observed that PEI reaches torque values of 250 Nm within the first minute, and after nine minutes, torque stabilizes and temperature reaches values close to 350 °C as a consequence of PEI high viscous dissipation. PEI does not suffer decomposition at these experimental conditions, which suggests it can be processed at temperatures as high as 350 °C during 10 minutes. On the other hand, PBT reaches torque values close to 200 Nm within the first minute and decreases just after putting it in the mixer. Within the first three minutes, torque reaches 1 Nm and stabilizes. The temperature remains constant at approximately 280 °C. After four minutes, PBT starts to change its white color to a light yellow as a sign of decomposition. This change of color indicates that PBT must be homogenized at times lower than 4 minutes.

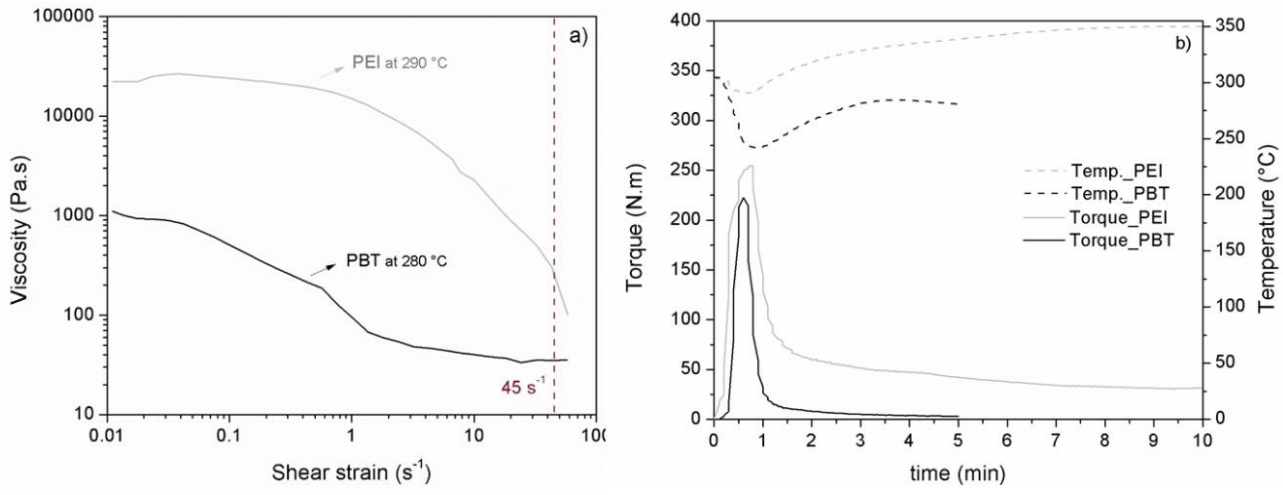

Figure 3.3 Melt flow behavior of pure PEI and PBT: a) viscosity as a function of shear rate for PEI at 290 °C ± 10 °C and PBT at 280 °C ± 5 °C; and b) torque and temperature as a function of time for pure PEI at 330 °C and pure PBT at 280 °C.

PEI and PBT show clear differences in their thermal and viscoelastic properties. PEI exhibits a higher Tg, thermal stability, and shear viscosity contrasted to PBT, that exhibits a lower Tg, thermal sensibility, and shear viscosity. These characteristics suggest that PEI/PBT blends need to be processed by steps. Thus, we proposed a *two-step melt processing method* using temperatures and mixing times according to the characteristics of individual materials, and keeping the rotational speed constant.

Figure 3.4 exemplifies the blending process in the case of 70 wt% of PEI and 30 wt% of PBT. During *step 1*, PEI is added at a temperature of 330 ± 10 °C. At this temperature PEI pellets flow and homogenize properly inside the mixer. Six minutes later, the mixing chamber is cooled down to incorporate the PBT at a lower temperature to avoid its thermal decomposition. When time reaches ten minutes, *step 2* takes place with the addition of the PBT phase. The temperature is kept constant at a lower temperature of 280 ± 5 °C. This temperature is kept during the remaining mixing process that takes 3 more minutes, until the torque values reach an equilibrium state. The entire mixing is settled to maximum 13 minutes for all blends.

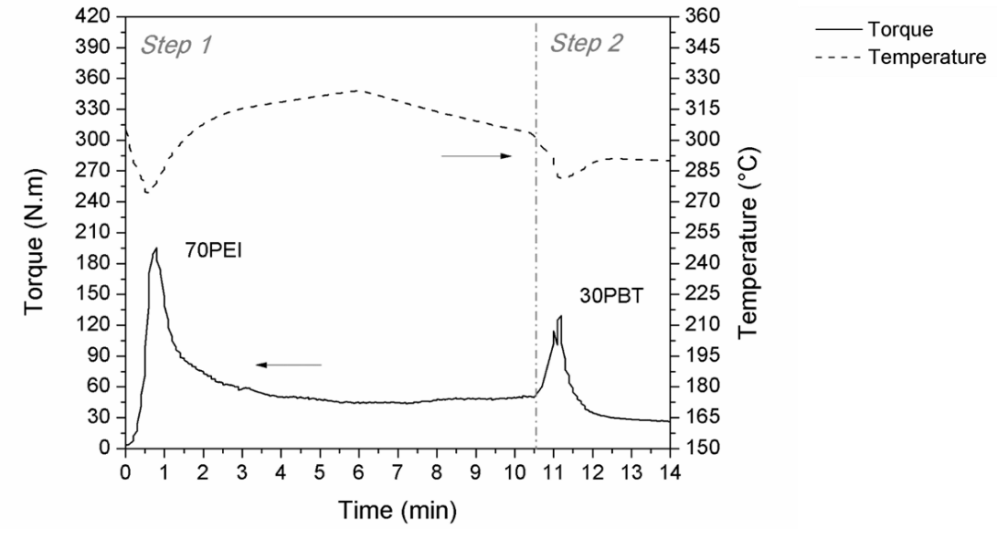

Figure 3.4 Two-step melt processing method for a blend containing 70 wt% of PEI and 30 wt% of PBT.

Conversely to our work, other authors processed PEI/PBT blends using a non-industrial melt mixing methods[40] or a solution blending techniques,[42,43,105] which are expensive for the post-processing required to remove the solvent traces, and hence are difficult to scale to industrial level. In their work, Vallejo and coworkers, used an industrial melt processing technique mixing simultaneously PEI and PBT in a corotating double-screw extruder.[41] However, they used different temperatures depending on PEI concentrations: for PEI-rich blends the Tp = 290 °C; and for

PBT-rich blends the Tp = 270 °C. In our work, we obtained PEI/PBT blends in the entire composition range using a melt processing method at the same processing conditions (Tp, n, and t).

In Table 3.2 are summarized the characteristics measured of individual materials, as well as the parameters settled to fabricate PEI/PBT blends using the two-step melt processing method. We obtain blends within the entire compositional range with PEI compositions of 10, 30, 40, 50, 60, 70, and 80 in weight percent (wt%).

Table 3.2 Summary of thermal and rheological characterization results of pure materials, and processing parameters to obtain PEI/PBT blends using the two-step melt processing method proposed in this work.

Material	Thermal events (°C)				Viscosities (Pa.s)	Processing parameters		
	Tg[a]	*Tm*[a]	*Tc*[a]	*Ti*[b]	*At a shear rate of 45 s^{-1}*	*Tp (°C)*	*t (min)*	*n (rpm)*
PEI	215.72	--	--	497.45	300	330 °C	10	70
PBT	58	222.58	196	299.65	35	280	3	70

[a] *Values obtained from the MDSC analysis.*
[b] *Values obtained from TGA analysis.*

Processability of PEI/PBT blends

It is known that torque obtained in an internal mixer is associated to the viscosity at constant shear strain,[69,140] and hence to the melt flow tendency of blends at a constant shear strain. Keeping this in mind, we study the relation between blends composition and processability. There were analyzed the torque values obtained after 13 minutes of mixing —when all blends reach an equilibrium state— as a function of PEI concentration.

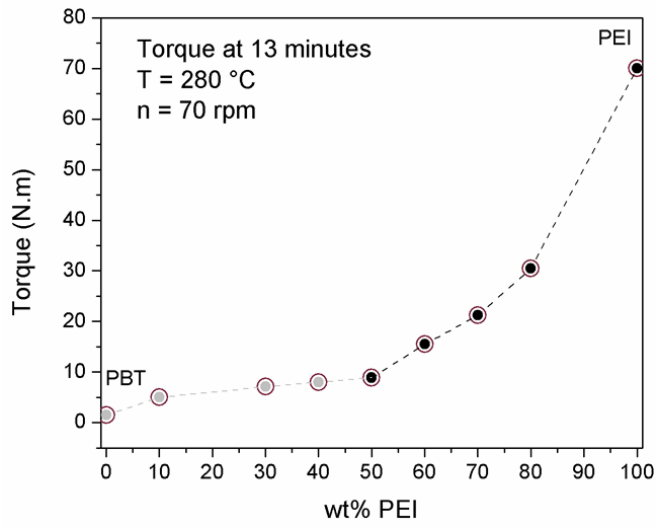

Figure 3.5 Effect of composition on processability of blends.

In Figure 3.5 it is evidenced that higher amounts of PBT (gray markers: PBT-rich blends) reduce the torque needed to homogenize the blends. Even 20 wt% of PBT (black markers: PEI-rich blends) reduce torque values by 40% compared to pure PEI. These results suggest that addition of PBT during step 2 contributes to improving blends processability. Previous works have reported similar results when PEI is blended with lower viscosity polymers (PBT, PAr, PET, PA).[41,99,101,102] In their work, Vallejo and coworkers found that relative processability of PEI/PBT blends was improved by PBT addition.[41] They attributed this effect to the increasing PBT concentration and its low viscosity contribution.

Nevertheless, melt flow of polymer blends depends also on phases interaction —if polymers are miscible or not—, as well as on the processing steps.[101] This explains the change of the slope observed in Figure 3.5 around 50 wt% of PEI, which suggest there is a transition strongly dependent on blends composition.

3.2 PART II – Miscibility and morphological study of PEI/PBT blends obtained by two-step melt processing method in an internal mixer

3.2.1 Introduction

The importance of miscibility level and its relationship with blends properties is well known,[2,72] and it is commonly the first parameter evaluated when polymer blends are studied. A single glass transition temperature is the most widely accepted criteria for miscibility, since it is assumed that blends display a single Tg when are mixed at molecular level,[47,72,141] while multiple Tg's indicate phase separation or partial miscibility.[142] Transitional and rotational characteristic motions in polymers are associated with glass-rubber relaxation. Thermal analyses such as DSC and DMA allow detecting relaxation on the chain segments in a polymer blend, and hence, the interaction, miscibility, and phase separation of each blend component.[142,143]

Nevertheless, polymers miscibility depends on several kinetic (processing conditions and rheology) and thermodynamic parameters. One approach widely used to study the correlation between these parameters and the miscibility level, is the deviation from additivity rule, Equation 3.3:[144,145]

$$logF = \sum w_i logF_i \qquad \text{Equation 3.3}$$

where F and F_i.are the rheological functions, e.g. shear viscosity, torque, shear storage (G') or loss (G'') moduli; and w_i is the weight fraction of polymer i. This rule allows understanding the melt flow tendency of blends, when contrasted with the experimental rheological results.

The structure and morphology of polymer blends is strongly linked to the fundamental rheological properties of blends components.[144–148] According to Utracki, it is possible to predict if a pair of polymers is miscible or not during melt mixing process by means of the log-additivity rule, Equation 3.3. He proposed the use of this semi-empirical equation to identify the three types of polymer blends: i) positive deviating blends (PDB), ii) negative deviating blends (NDB), and iii) positive and negative deviating blends (PNDB) with a sigmoidal dependence.[144–146] A higher viscosity than the predicted by the log-additivity rule (PDB), is characteristic of miscible and immiscible blends with strong interfacial interaction. A lower viscosity than the log-additivity rule (NDB), is typical of incompatible blends where interaction of phases is weak, leading to slip effect or delamination at the interface. When both behaviors are observed, it is a sign of a strong composition-dependence transition that leads to changes in structure or morphology of blends.[148,149] The additivity rule application yields to interesting information about phases' interaction. However, this method should be based on the zero shear viscosity or the viscosity at a constant shear stress.[135]

As the characterization of blends viscoelastic properties should be performed under conditions that guarantee minimum modification of their structure,[145] small amplitude oscillatory shear (SAOS) tests may provide an accurate response of phases under flow since experimental conditions are made within the linear viscoelastic region (LVR).

Miscibility of PEI/PBT blends

In previous studies of blends between PEI and PBT,[40–43,105] authors described complete miscibility within the entire compositional range after DSC, DMA, or FTIR analyses, regardless the blending method used.[40–43,105] In their works, Chen,[42] Woo,[40] and Vallejo[41] evaluated miscibility by thermal analysis. They found that PBT's Tg and cold crystallization temperature (Tcc) shifted to higher temperatures as a consequence of the increase in chains stiffness caused by PEI addition. Woo and Yau[40] complement their thermal results with optical microscopy and SEM. They observed in optical microscopies a transparent and homogeneous phase, and from SEM results

no heterogeneous phase domains were identified. However, the morphological evaluation presented in some of those studies lacks clear evidence of phase differences between PEI and PBT blends,[42] and it is not possible to conclude if PEI and PBT are truly miscible since images have very poor resolution.

In a different work, Jang and Sim[43] also evidenced a single Tg on PEI/PBT blends by thermal analysis. Additionally, they performed FTIR measurements and found that $C = O$ stretching peak of PEI/PBT blends shifted to lower wavenumber as PBT crystallization proceeded as an indicator of miscible phases.

Previous works on PEI/PBT blends do not present viscoelastic behavior studies that supports miscibility analysis. In Vallejo et al,[41] the only approximation to rheological properties was made from evaluation of processability by relating torque as a function of PBT addition. In this work, it is discussed for the first time for PEI/PBT blends, the relationship between viscoelastic properties, interfacial tension, processing conditions, and composition with blends morphology. Since all blends in this work are obtained under the same processing conditions, we are able to evaluate the effect of melt processing on the interfacial interaction between PEI and PBT, and perform a complete analysis on blends structure or morphological evolution.

We approach the miscibility study from thermal analysis and tracking structure and morphological evolution for the entire compositional range. In thermal analysis, it is used modulated differential scanning calorimetry (MDSC) and dynamic mechanical analysis (DMA). For morphological evolution we use the Soxhlet selective extraction technique together with SEM and TEM analyses. In this work, it is presented new evidence on the morphological evolution of PEI/PBT blends.

For PBT-rich blends, we found miscibility study is in good agreement with morphological analyses. Thermal analyses show Tg corresponding to each phase signal, and from SEM and TEM there are noticed PEI droplets dispersed in the PBT matrix. On the contrary, thermal analysis on PEI-rich blends displays a noticeable shift of PBT Tg to higher temperatures, while SEM and TEM micrographs show small droplets of PBT bonded to the PEI matrix through a fibrillary interface, giving the appearance of what we called *spore-like* morphology. We also demonstrate that PEI/PBT blends experience dual-phase transition at even PEI and PBT concentrations. Experimental observation of phase inversion phenomena is contrasted to exist-

ent prediction models, and it is proposed a phase transition scheme of Dn and Dv as a function of PEI concentration.

3.2.2 Experimental

PEI/PBT blends

PEI/PBT blends within the entire compositional range were prepared in an internal mixer using the processing conditions described in Table 3.2. Blends designation, weight fraction, and volume fraction are listed in Table 3.3.

Table 3.3 Compositions for PEI/PBT blends in weight fraction and volume fraction.

PEI/PBT blends designation	Weight fraction (w)		Volume fraction (φ)[a]	
	PEI	PBT	PEI	PBT
0/100	0	1	0	1
10/90	0.1	0.9	0.11	0.89
30/70	0.3	0.7	0.32	0.68
40/60	0.4	0.6	0.42	0.58
50/50	0.5	0.5	0.52	0.48
60/40	0.6	0.4	0.62	0.38
70/30	0.7	0.3	0.72	0.28
80/20	0.8	0.2	0.81	0.19
100/0	1	0	1	0

[a] *Calculated from the solid densities of PEI and PBT list in Table 3.1.*

Rheological characterization

Viscoelastic properties of all materials were measured by means of a Physica MCR 501 rheometer from Anton Paar. Discs of 20 mm diameter and 2 mm width were obtained by injection molding in a HAAKE MiniJet Pro Injection System from Thermo Scientific, using the conditions listed in Table A- 2. It was used a parallel-plate geometry with a gap of 1 mm under a nitrogen atmosphere at a constant temperature of 280 °C. Strain sweeps were performed at different angular frequencies to define the linear viscoelastic region (LVR). SAOS experiments were per-

formed to pure materials and PEI/PBT blends at 0.1 % of amplitude in a scanning range from 300 rad/s to 0.1 rad/s. All specimens were vacuum dried at 110 °C during 16 hours before LVR and SAOS tests to avoid the prompt hydrolytic degradation of the PBT phase.

Miscibility study

Miscibility between PEI and PBT was studied by tracking the Tg of both components using modulated differential scanning calorimetry (MDSC), and dynamic mechanical analysis (DMA).

Modulated differential scanning calorimetry (MDSC)

Glass transition of pure materials and their blends were examined using a DSC Q200 from TA Instruments. Samples of 20 ± 1 mg were heated from 0 °C to 290 °C at 20 °C/min, and held on at this temperature for 1 minute, followed by cooling to -30 °C at 20 °C min^{-1}, and heated again in modulated mode from 0°C to 300 °C at 2 °C/min with a modulation amplitude of ±1.27 and a period of 60 seconds.

Dynamic mechanical analysis (DMA)

DMA measurements were completed under torsional mode using solid clamps assembly of a HAAKE MARS III rheometer from Thermo Scientific. Injected molded samples of 8 ± 0.2 mm length, 10 ± 0.2 mm width, and 4 ± 0.2 mm thickness were heated from 30 °C to 250 °C, at 5 °C/min, at 1 Hz frequency, and 0.5% strain to ensure the linear viscoelastic region. Samples were preconditioned before testing within a strain program from 0.1% to 1.2% at 30°C.

Morphological analysis

Morphological evolution was studied using a scanning electron microscope SEM JOEL JSM-7100. All samples were immersed in liquid nitrogen for 20 minutes, mechanically cryofracture, and later coated with a gold layer.

Selective dissolution of PEI phase was made with chloroform by using the Soxhlet extraction technique. It was only performed on PBT-rich blends because it was impossible to find a solvent that selectively dissolved PBT phase without affecting PEI. Each sample was summited to a certain number of cycles according to PEI concentration, as it is shown in Figure A- 5.4. Samples were vacuum dry at 100 °C during 8 hours to remove the excess of solvent.

For a better morphology evolution assessment, we used a transmission electron microscope TEM Tecnai G2 F20 from FEI. Thin sections of approximately 60 nm thickness were cut with a diamond knife at 25 °C using a Leica ultramicrotome.

3.2.3 Results and discussion

Viscoelastic properties of PEI, PBT, and PEI/PBT blends

In Figure 3.6a) and Figure 3.6b), are plotted the complex viscosity (η*) and storage modulus (G') as a function of angular frequency, respectively. PEI exhibits much higher η* and G' values than PBT within the entire frequency range. PEI concentration display similar results in SAOS and torque. A higher amount of PEI leads to a higher viscous and elastic blends. Conversely, small PBT amounts improve the flow behavior of blends. For PBT-rich blends, in both η* and G' plots, the disturbance observed at low frequencies (<0.5 rad/s), corresponds to the hydrolytic degradation of PBT phase due to long exposition times at 280 °C during the SAOS tests.

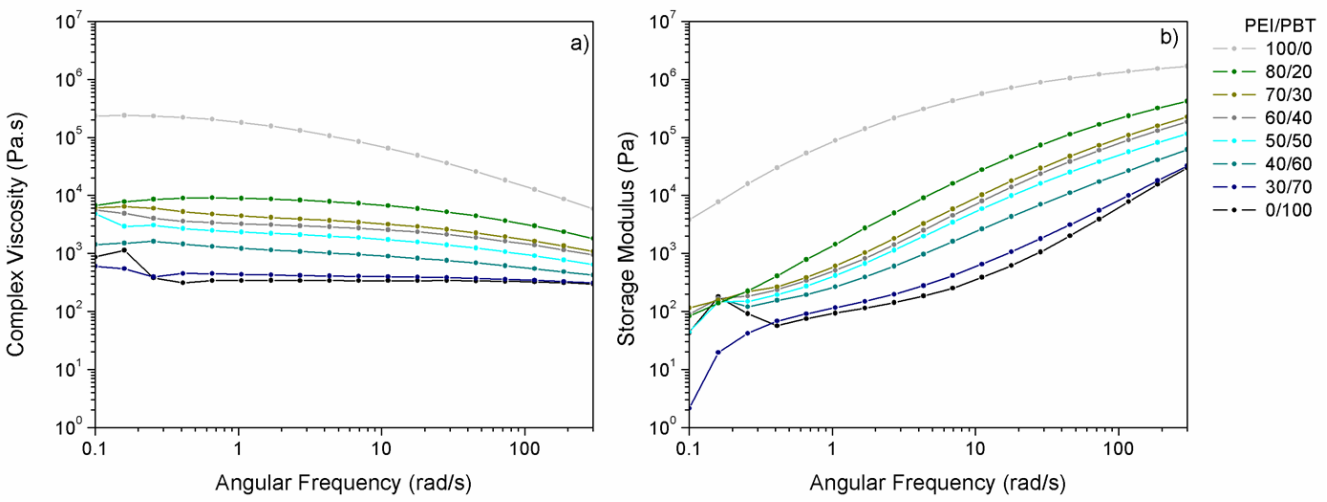

Figure 3.6 Viscoelastic properties of PEI, PBT, and PEI/PBT blends: a) complex viscosity, and b) storage modulus.

In order to evaluate the effect of PEI composition on the morphology of blends under the linear viscoelastic regime, we compare experimental η* and G' results obtained at 300 rad/s to those calculated from the log-additivity rule (see Figure 3.7). Both, η* and G' exhibit experimental values lower than the calculated from the log-additivity rule obeying to a NBD behavior that extends along the entire PEI compositional range. These results suggest that PEI/PBT blends tend to be immiscible in the molten state at 280 °C. Several authors have attributed the NBD to lack of interaction between components and the formation of an interlayer slip phenomenon which gives rise to a reduction in the viscosity of the blend.[101,147,148] In the present study, the

occurrence of the slip layer may be originated by the low viscosity of PBT that enables the lubricating effect between the two phases. The interlayer slip is also attributable to dilatation at the interface in immiscible blends that causes a discontinuity in both, shear strain and shear stress.[146]

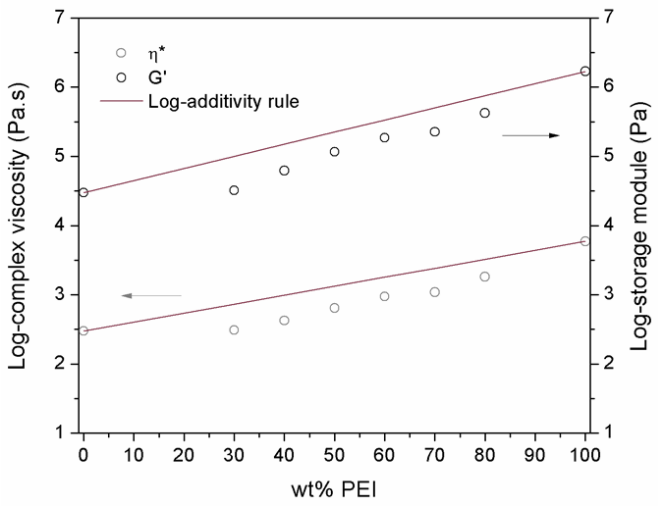

Figure 3.7 Comparison of PEI/PBT blends experimental viscoelastic values with those calculated using the log-additivity rule.

It should be pointed out that classification of polymer blends using the deviatory behavior from the log-additivity rule is pertinent for blends' flow behavior, but not for chemical nature of the blends. Changes in molecular weight or in test temperature may vary significantly the deviation from the rule.[146] Besides, miscibility in the molten state does not necessarily mean miscibility on solid state, e.g. if one component is semicrystalline, the crystallization usually leads to phases separation.[101,144]

Miscibility study by means of thermal analysis

Modulated differential scanning calorimetry (MDSC)

In Figure 3.8 are presented MDSC results for pure PEI, PBT, and their blends. It is noticed that Tg of PEI appears at 215.72 °C, and Tm of PBT at 222.5 °C. Both, transitions overlap in the range between 213 °C and 225 °C, hiding the variation of PEI Tg in the blends and making impossible to study miscibility by tracking Tg shifts of PEI and PBT. Therefore, the following discussion will be focus on variations of PBT Tg.

Figure 3.8a) presents the cooling program results after erase the thermal history of PEI/PBT samples. PBT crystallization temperature (Tc) appears at 196 °C as a sharp peak, and its intensi-

ty decreases with increasing PEI concentration. Tc is almost completely inhibited in 70/30 and 80/20 blends. The crystallinity of PBT phase —calculated from the melting peaks in Figure 3.8b) using a 100 % crystalline PBT with heat of fusion of 145 J/g[150]— varies from 18% for pure PBT to 6% for 70/30 blend and 0.8% for 80/20 blend. The decrease in PBT crystallinity is caused by the segregation of PEI into the amorphous domain of PBT phase, which enriches the amorphous domain of blends. Similar results were found in previous works on PEI/PBT blends.[43] However, authors reported Tc shifts to lower temperatures when PEI concentration increases. In our results, the dashed vertical line shows that Tc remains invariable for all PBT-rich blends.

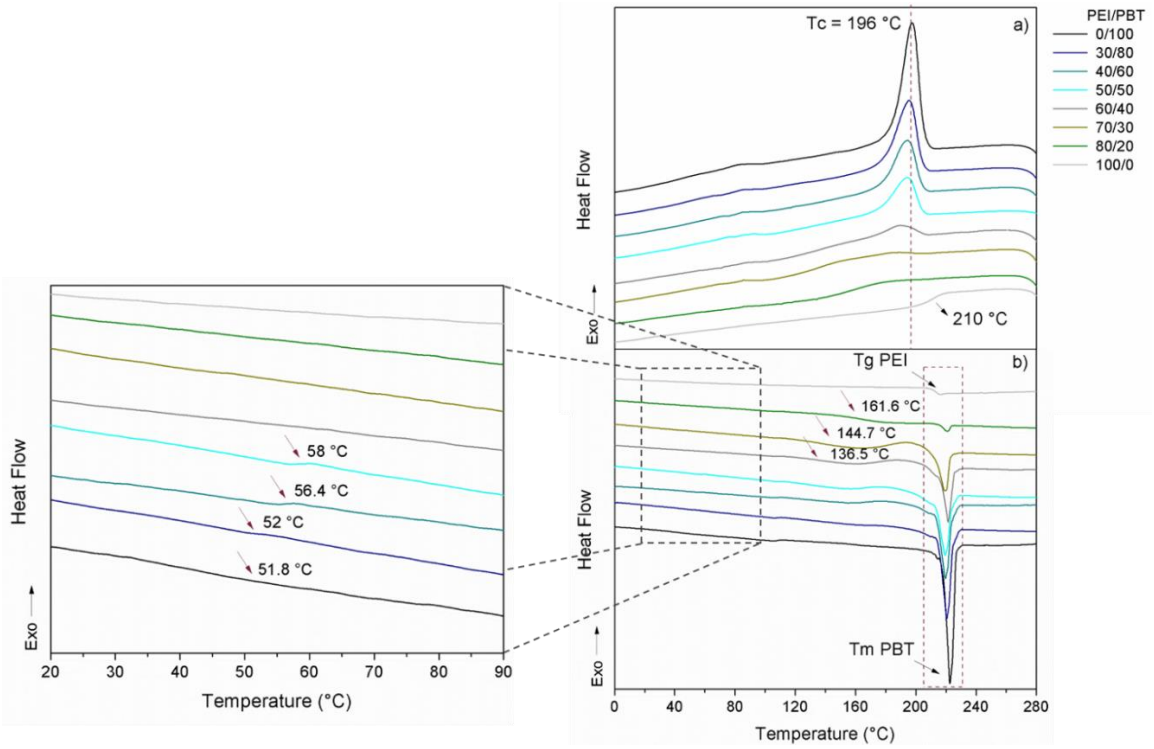

Figure 3.8 Miscibility study of PEI/PBT blends from DSC thermal analysis. The thermal transitions are presented during: a) cooling, and b) second heating on modulated mode (MDSC). The data was reorganized on the y-axis.

A magnification in Figure 3.8b) within the temperature range from 20 °C to 90 °C, shows the thermal events of PBT-rich blends. It is observed a smooth shift of PBT Tg between 51.8 °C and 58 °C, indicating PEI and PBT are partially miscible at high PBT concentrations. Within the magnification region, PEI-rich blends no longer exhibit PBT thermal transition, suggesting PBT Tg shifts to higher temperatures. It is noticed a smooth variation in PEI-rich blends (60/40, 70/30, and 80/20) between 136 °C and 161 °C that may correspond to PBT Tg shift to higher temperatures. However, as DSC is not a technique sensitive enough to detect small thermal relaxation events, these results will need to be corroborated with a different highly sensitive technique such as DMA.

The smooth exothermic signal observed between PBT Tg and Tm in blends with 40, 50, 60, and 70 wt% of PEI, corresponds to PBT cold crystallization temperature (Tcc). Tcc is characteristic of polymers that have passed through a quenching thermal treatment during cooling and appears at temperatures higher than Tg.[151] When the quenched-in amorphous structure becomes mobile enough, crystallization occurs during heating giving rise to an exothermic response before Tm. In our work, in spite of PEI/PBT blends are cooled in air after the mixing process, and no thermal treatment is performed, PEI solidification takes place before PBT, avoiding PBT mobile phase crystallization. The differences in solidification between both phases produce an "in-situ" quenching on PBT structure. Tcc is not observed in 80/20 blends, as a sign of strong molecular interaction between amorphous phases of components, leading to miscibility.

In previous results on PEI/PBT blends, authors performed heating treatments of quenching just after the blending process,[40,43] and annealing at different times and temperatures conditions.[42] Chen and coworkers[42] obtained PEI/PBT blends by solution precipitation and performed melt annealing at 250 °C to study PEI and PBT compatibility. They observed cold crystallization signals of PBT phase and found that higher annealing times lead to higher Tcc and also, that Tg shifts to higher temperatures. They reported PEI and PBT are completely miscible in the entire compositional range.

In contrast to other author's findings,[40–43,96,105] PEI/PBT blends obtained under the experimental conditions used in this work are partially miscible depending on PEI composition.

Dynamic mechanical thermal analysis (DMA)

Figure 3.9 displays DMA results for pure PEI, PBT, and their blends. Tg values are calculated from the onset of the storage modulus G', and are contrasted to those from DSC. Intermediate transitions are analyzed from both, storage modulus onsets and tan (δ). Generally, intermediate thermal events are easy to visualize from tan (δ) results.

Thermal transitions of pure materials obtained by DMA are in good agreement with those from DSC results. In Figure 3.9a), the G' plot of PEI exhibits a sharp drop at 213 °C revealing its Tg. On the other hand, PBT displays a G' decline near 50 °C corresponding to its Tg. In Figure 3.9b), the tan (δ) plot reveals that PEI Tg and PBT Tm overlap at 235 °C. Therefore, miscibility analyses from DMA results will be made according to PBT Tg behavior.

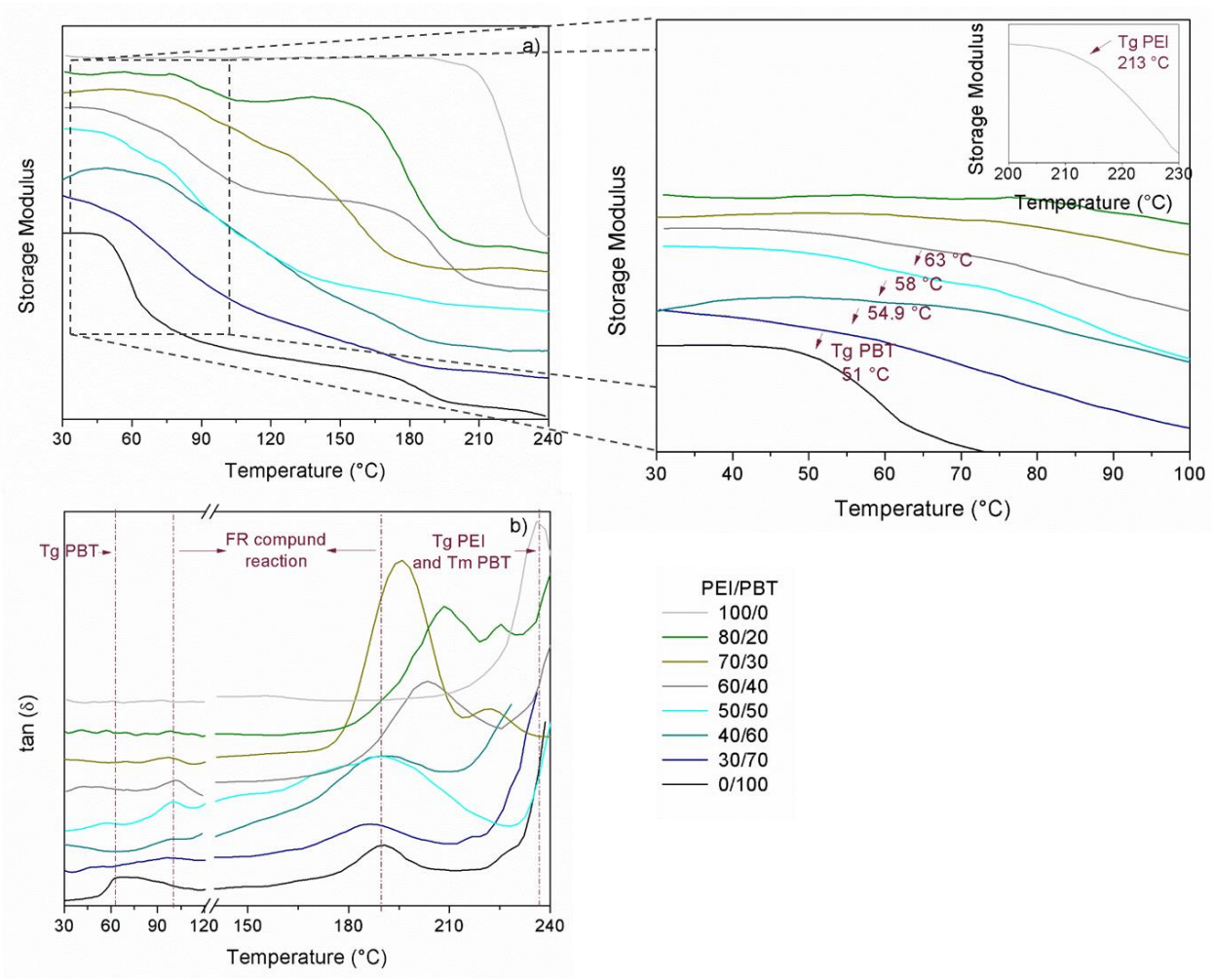

Figure 3.9 Miscibility study of PEI/PBT blends from DMA analysis performed under torsional mode. It is presented: a) the storage modulus and b) tan (δ). The data was reorganized on the y-axis for ease of analysis.

Magnification on G' plot shows the Tg values of PBT, PBT-rich blends, and PEI. It is noticed that Tg values are close to those obtained from DSC tests. However, PEI-rich blends do not exhibit PBT Tg within the range between 51 °C and 63 °C. This is caused by the "rejection" of the non-crystallizable segments on PBT from the emerging crystals, acting as a diluent phase that enriches the amorphous phase of the blends.[142] As a result, blends with high PEI concentrations tend to be miscible. Similar results are reported on blends between PBT and bisphenol A poly(arylate) (PAr);[98,100] and between poly(ether ether ketone) (PEEK) and PEI.[103,104]

In G' plot, PBT exhibits a second thermal transition at 180 °C undetected by MDSC analysis. According to EDS, XRD, Raman, and XPS results showed in Figure A- 5.2, the flame retardant (FR) compound present in PBT sample, is a combination of antimony trioxide and bromides. Bromides are susceptible to state changes in the range between 170 °C and 190 °C, as reported by Rzyman and coworkers in their work.[152] They studied the thermal behavior of tetrabromo

bisphenol A (TBBPA) by DSC —a flame retardant additive commonly used in unsaturated polyesters flame retardancy[153]—, finding that its melting temperature appears around 180 °C.[152] In order to verify if this transition is originated by bromide compounds, we contrasted the DMA results of flame retardant PBT to unfilled PBT (Uf-PBT). Results presented in Figure A- 5.3 show no evidence of thermal transitions around 180 °C for PBT.

The thermal transitions corresponding to flame retardant compounds are evidenced as a smooth peak at 100 °C and a peak at 188 °C in tan (δ) plots. It is observed that both transitions remain constant for all PBT-rich blends. Conversely, PEI-rich blends exhibit marked differences in their signals at temperatures higher than 180 °C. 60/40 blend shows a Tg shift caused by the partial miscibility between PEI and PBT; 70/30 blend reveals a sharp signal produced by the overlapping of PBT cold crystallization, flame retardant compounds, and PEI thermal events; and finally, 80/20 blend shows a Tg shift together with a double-peak signal due to PEI phase is in higher proportion and the enrichment of blends amorphous phase is more notable.

Morphology evolution of PEI/PBT blends

When two immiscible or partially miscible polymers are mixed, they distribute in different manners according to their individual properties and processing conditions. As stated by Favis: "if the minor component has a lower viscosity than the major one (as in the case of PEI-rich blends), then the minor component will be finely and uniformly dispersed. Conversely, the minor component will be coarsely dispersed if its viscosity is higher than that of the major component (as in the case of PBT-rich blends)".[50] This claim as simple as it sounds, involves several factors such as: the weight or volume fractions, the structural paramenters of the constituents (viscosity ratio, elasticity ratio, and interfacial tension), and the processing conditions (shear or elongational deformation); that will affect phases' distribution and the morphologies formed.[154]

Viscoelastic properties and interfacial tension of PEI/PBT blends

The following morphological analysis will be made based on pure PEI and PBT viscoelastic characteristics and surface tensions, as well as on PEI/PBT interfacial tension.

PEI/PBT blends viscoelastic ratios

The viscosity ratio when PEI or PBT is the matrix, is calculated from the measured viscosities of blends components shown in Figure 3.6a) and by using Equation 3.4:

$$p_{(PBT\ matrix)} = \frac{\eta_{PEI}}{\eta_{PBT}} \quad or \quad p_{(PEI\ matrix)} = \frac{\eta_{PBT}}{\eta_{PEI}} \qquad \text{Equation 3.4}$$

where p is the viscosity ratio when either PBT or PEI is the matrix, η_{PEI} is the viscosity of PEI, and η_{PBT} is the viscosity of PBT.[50]

The elasticity ratio can be evaluated in analogy to the viscosity ratio by calculating the storage moduli for PEI and PBT from the SAOS tests presented in Figure 3.6b) by using Equation 3.5:

$$\psi_{(PBT\ matrix)} = \frac{G'_{PEI}}{G'_{PBT}} \quad or \quad \psi_{(PEI\ matrix)} = \frac{G'_{PBT}}{G'_{PEI}} \qquad \text{Equation 3.5}$$

where ψ is the elasticity ratio when either PBT or PEI is the matrix, G'_{PEI} is the storage modulus of PEI, and G'_{PBT} is the storage modulus of PBT.[50]

As both, viscosity and storage modulus are temperature and frequency dependent, and the frequency should correspond to shear rates similar to those in the processing equipment,[154] p and ψ ratios are calculated at the same blends' processing temperature of 280 °C and at a constant frequency of 300 rad/s. The values are listed in Table 3.4.

Table 3.4 Viscosity ratios and storage modulus ratios for PBT-rich blends (PEI dispersed) and PEI-rich blends (PBT dispersed), calculated at 280 °C and 300 rad/s.

Material	Complex viscosity (Pa.s)	Storage modulus (Pa)	Viscosity ratio $-$ p		Storage modulus ratio	
			$p_{(PBT\ matrix)}$	$p_{(PEI\ matrix)}$	$\psi_{(PBT\ matrix)}$	$\psi_{(PEI\ matrix)}$
PEI	5910	1690000	19.77	0.05	56.52	0.02
PBT	299	29900				

Since PEI is much more viscous and elastic than PBT, both p and ψ ratios show a wide difference between values when PEI or PBT is the matrix. Looking back at Figure 3.6, it is observed that this behavior is kept for the entire frequency range studied. These differences on viscoelastic properties have a direct effect on blends morphology, and will be discussed later on.

PEI/PBT blends interfacial tension

As mentioned, interfacial tension values between polymers pairs give relevant information about blends interaction and phase's miscibility. Several theoretical and experimental approaches are used for calculating this parameter. In this work, the direct measurement of interfacial tension between experimental methods was a challenge due to difficulties related to in-

trinsic properties of components, such as: high temperatures needed for PEI and PTFE, and the thermal sensitivity of PBT.

Due to the last issue, it was not possible to use the rheological approach to calculate interfacial tension by means of the Palierne model, since PBT could not reach the low frequencies needed for this model to be applied (0.01 rad/s – 0.001 rad/s) without affecting its molecular structure. Hence, the interfacial tension between PEI and PBT is calculated from a theoretical approach using the harmonic mean equation shown in Equation 2.9.

According to Wu,[62] the interfacial tension between two polymers can be calculated from harmonic method measuring the contact angles of two liquids —one polar and one dispersive— on the surfaces of the two polymers. If the polar and dispersive components, and thus the surface tension of the liquids are known, the total surface tension of each polymer ($\gamma_L = \gamma^d + \gamma^p$) can be obtained by using Equation 3.6:

$$(1 + \cos\theta)\gamma_L = \frac{4{\gamma_s}^d{\gamma_L}^d}{{\gamma_s}^d + {\gamma_L}^d} + \frac{4{\gamma_s}^p{\gamma_L}^p}{{\gamma_s}^p + {\gamma_L}^p} \qquad \text{Equation 3.6}$$

where θ is the contact angle between the liquid and the polymer.

Some polar and dispersive liquids combinations used in the calculation of polymers surface tension include water/α-bromonaphthalene, glycerol/diiodomethane, water/diiodomethane, and formamide/diiodomethane due to their high polarity differences.[155] We calculate the theoretical surface tension values of PEI and PBT from using literature reports of contact angles obtained with water and diiodomethane. In Table 3.5, are listed the results of PEI and PBT surface tensions, as well as the calculated PEI/PBT interfacial tension.

A first look into the total surface energies (γ_T), reveals that both PEI and PBT values are very close. However, the polar component of PBT is much higher than that for PEI, which favors polymers immiscibility to some extent. The polarity difference between both polymers is highlighted in PEI/PBT interfacial tension value.

In thermodynamics terms, if the interfacial tension between two polymers is zero, or close to zero, they will tend to be miscible. In their work, Guerrica-Echavarria and coworkers[158] evaluated the interfacial tension between some commodity, engineering and specialty polymer pairs using the harmonic method. Their results revealed that interfacial tension values lower than 2

dyn/cm lead to phases' miscibility, while values greater than 2 dyn/cm caused phases' segregation. According to those results, the calculated interfacial tension for PEI/PBT blends ($\gamma_{PEI/PBT}$ = 3.14 dyn/cm) indicates that PEI and PBT will tend to form separate phases. This results are in good agreement with those of the viscoelastic and thermal characterization previously described, which state that both phases tend to form separated domains during melt blending.

Table 3.5 Theoretical PEI and PBT surface tension values, and PEI/PBT interfacial tension values calculated from the harmonic mean equation.

Material	Contact angle (°)		Surface tension (dyn/cm)[c]			Interfacial tension (dyn/cm)[d]
	Water	Diiodomethane	γ^d	γ^p	γ_T	$\gamma_{PEI/PBT}$
PEI	75[a]	27[a]	41.12	4.94	46.06	
						3.14
PBT	63[b]	30[b]	36.65	11.92	48.57	

[a] Values obtained from reference[156]

[b] Values obtained from reference[157]

[c] Values calculated from Equation 3.6 using liquids surface tension values obtained from reference[155] [(water $\gamma_T = 72.8\ dyn/cm$; $\gamma^d = 22.1\ dyn/cm$; $\gamma^p = 50.7\ dyn/cm$); (Diiodomethane: $\gamma_T = 50.8\ dyn/cm$; $\gamma^d = 48.5\ dyn/cm$; $\gamma^p = 2.3\ dyn/cm$)]

[d] Values calculated from the harmonic mean equation, Equation 2.9

Morphology of PEI/PBT blends

In Figure 3.10, there are presented PEI/PBT blends morphologies in the entire compositional range. Figure 3.10a) and Figure 3.10h), display the cryofracture surfaces of pure materials after being processed in the internal mixer at the same processing conditions as for blends.

In Figure 3.10a), it is observed that PBT fractured surface has an uneven appearance. The white particles correspond to the flame retardant compound. Contrary to PBT, PEI fracture looks like a smooth surface characteristic of amorphous polymers, Figure 3.10h). Regarding blends samples shown from Figure 3.10b) to Figure 3.10g), it is noticed a considerably variation of morphology when PEI concentration is increased. PBT-rich blends (30/70 and 40/60) exhibit PEI domains with grouped drops poorly bonded to the matrix. Figure 3.10d) shows the morphology changes at even PEI and PBT concentrations, where PEI phase is no longer distributed as droplets, and both phases are bonded through a fibrillary interface, as exemplify in Figure 3.11.

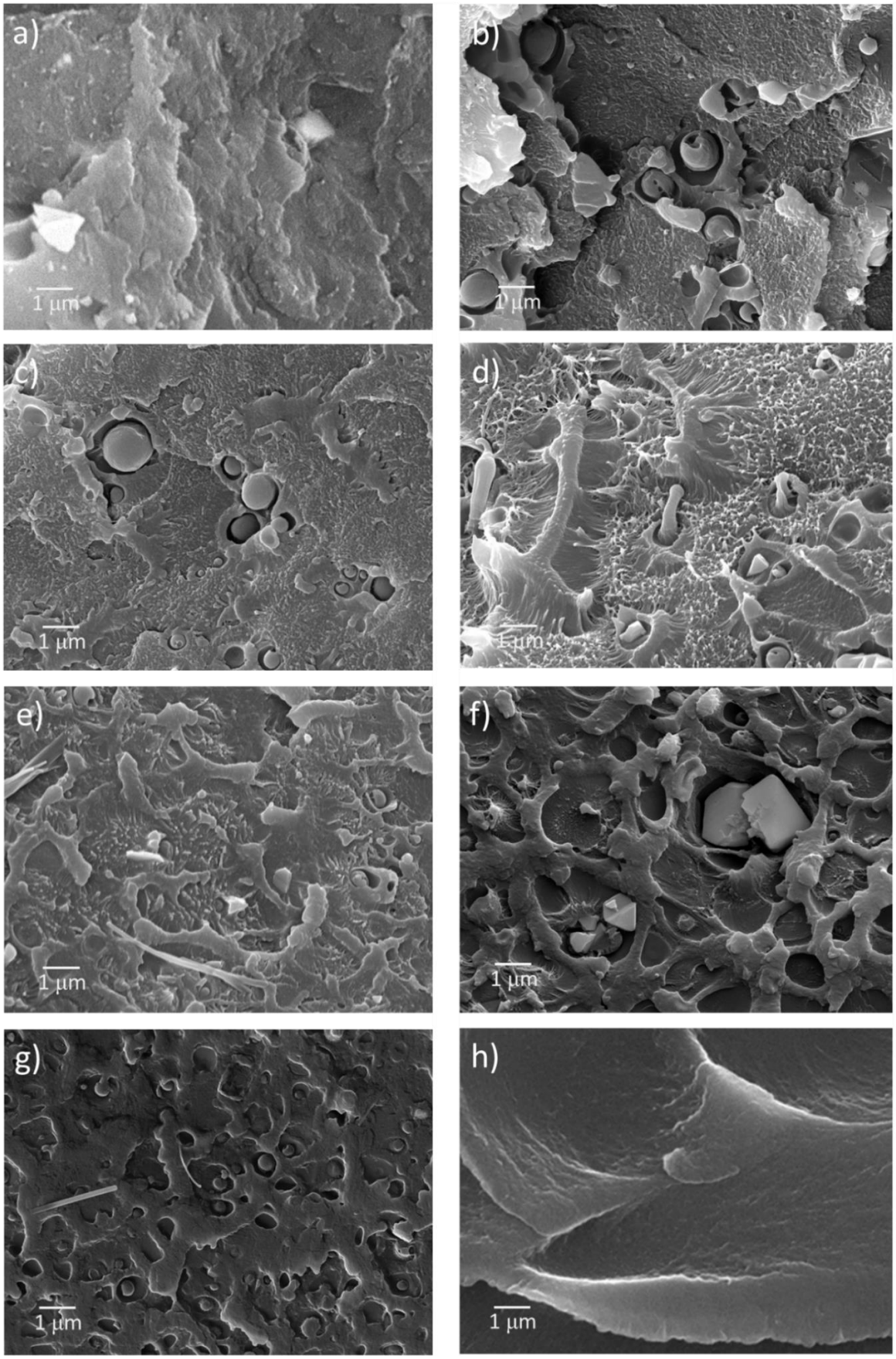

Figure 3.10 SEM micrographs of PEI/PBT blends within the entire compositional range: a) 0/100, b) 30/70, c) 40/60, d) 50/50, e) 60/40, f) 70/30, g) 80/20, and h) 100/0. All images were taken at a magnification of 10kX.

On the other hand, PEI-rich blends (70/30 and 80/20) show the matrix entirely dominated by the smoother PEI phase, which is covering fire retardant particles as well as tiny PBT droplets. There are noticed some PBT droplets attached to the PEI matrix through the fibrillary interface, just as observed for the other blends compositions.

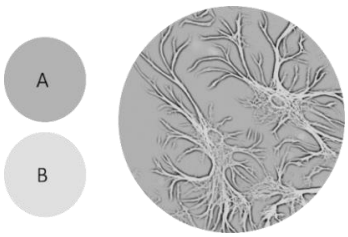

Figure 3.11 Scheme of the proposed fibrillary interface between a matrix A and a dispersive phase B.

Having in mind only SEM results, it is difficult to differentiate the phase shape and to measure the size of the dispersed phases along the different compositions. In order to better understand PEI/PBT blends morphology, we addressed the morphological study from two complementary approaches: Soxhlet extraction technique and TEM analysis and the detailed study of the morphology for PBT-rich blends and PEI-rich blends.

PBT-rich blends morphology

In Figure 3.12, it is displayed the morphology of three PBT-rich blends after PEI selectively extraction (images on the left) contrasted with TEM results (images on the right).

10/90 blend

Figure 3.12a) shows the morphology of the 10/90 blend.[1] It is noticed that extraction of PEI phase let well-defined droplets of different sizes along the PBT matrix, together with small spheres inside PEI domains that did not dissolve. The inserted image in SEM micrograph of Figure 3.12a), displays a single PEI droplet completely covered by PBT matrix before selective extraction. PEI phase is adhered to the matrix by the fibrillary interface that is characteristic of PBT phase. The TEM micrograph for the same blend shows the PBT matrix as a cloudy region

[1] It should be clarified this blend will be included only in this part of the document to illustrate the distribution of highly diluted PEI concentration. When PEI concentration as low as 10 wt% is added to the internal mixer during step 1, it is not properly homogenized when PBT phase is added during step 2 due to a lack of shear deformation of the dispersive phase. Hence, PEI concentration in this blend is surely less than 10 wt%.

because of its semicrystalline nature. The black spots correspond to antimony trioxide crystals, and the PEI droplets are revealed as the smoother and transparent regions, with smaller cloudy-droplets inside corresponding to PBT phase, which gives the idea of composite droplets formation.

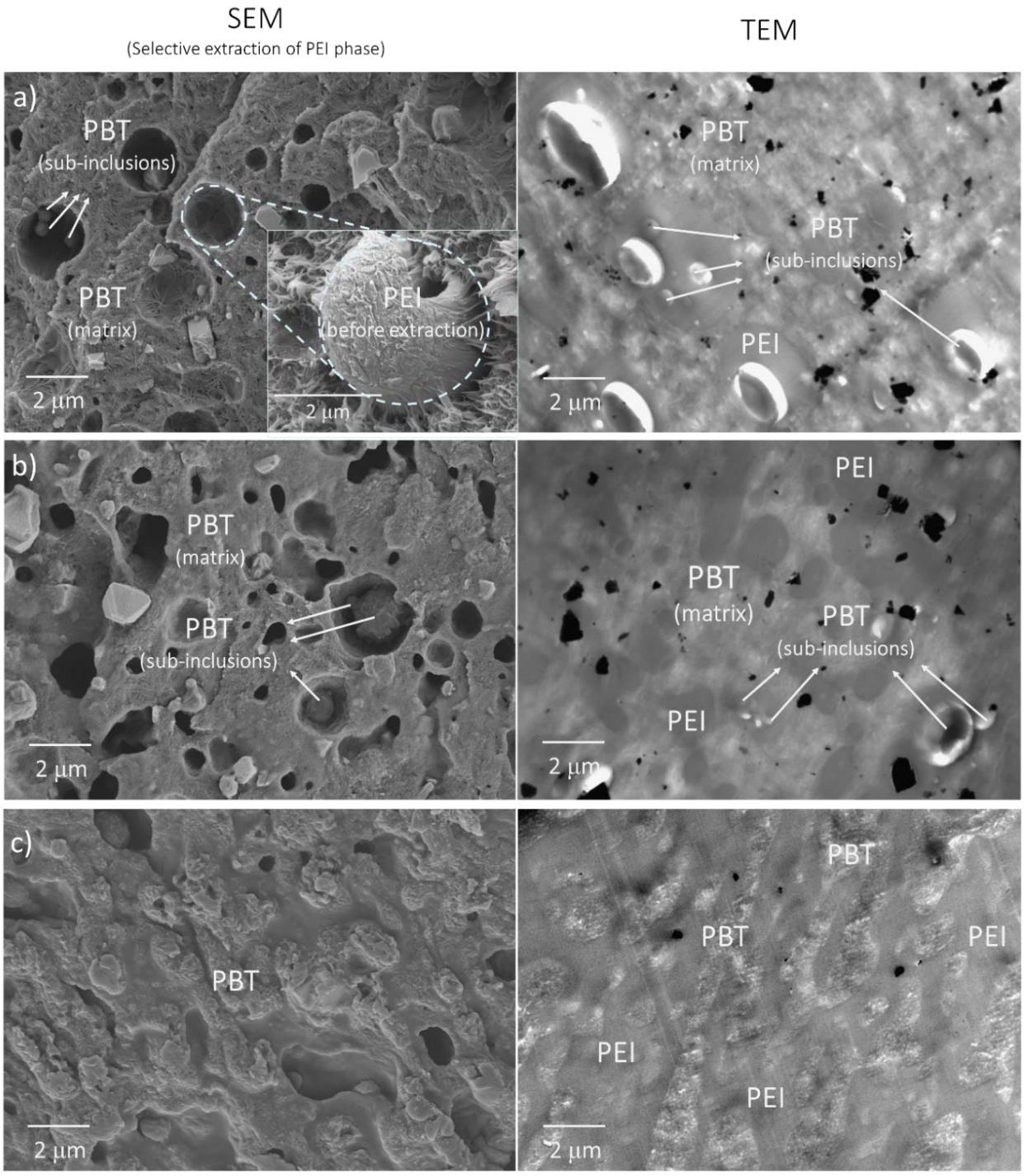

Figure 3.12 Contrast of the morphology of PBT-rich blends observed by SEM (left) and TEM (right), for PEI/PBT blends with: a) 10/90, b) 30/70, and c) 50/50. SEM micrographs show specimens with the extraction of PEI phase, and TEM micrographs show samples without PEI extraction.

In binary systems, the formation of composite droplet morphology is well known for blends between brittle polymers and rubbery particles when it is necessary to improve the impact resistance and toughness of the matrix.[159–161] According to Favis, this morphology is hard to obtain, and even more difficult to control, from melt processing methods.[7] In this work, we observed a well-defined morphology of composite droplets on PBT-rich blends that comprise three main parts: PBT matrix, PEI dispersive phase, and PBT sub-inclusions within PEI droplets. This morphology is caused by a combination of two main effects: the steps processing method we used to fabricate the blends, and the significant differences in the viscoelastic properties between PEI and PBT previously described.

During step 2 of processing, three minutes is the maximum mixing time for simultaneous mixing of PEI and PBT phases. Within this time, the highly elastic PEI droplets encapsulate the low elastic PBT phase forming the core-shell morphology. Besides, the viscosity of PEI at 280 °C is too high compared to that of PBT, causing high retention of PBT in PEI droplets. This phenomenon is described by Vanoene[162] and it was observed by Berger and coworkers in their experiments with PET/PA blends.[163] In the PC/PP system studied by Favis and coworkers, they found that increasing the mixing time will diminished droplets retention. In our experiments, mixing times longer than three minutes will result in PBT thermal decomposition.

30/70 blend

So far, phase distribution observed in PBT-rich blends seems to fit more to the classical theory of Taylor and Grace, which explains the effect of the viscosity ratio on blends morphology. When highly viscous PEI is the dispersive phase, the viscosity ratio is greater than one ($p >> 1$), exceeding the breakup limit established by Taylor and Grace under shear deformation field ($p > 3.7$)[47,50] and preventing PEI droplets to deform and breakup into smaller particles. However, when the dispersive phase concentration increases the morphology formation is more influenced by the processing conditions. For instance, PEI particles in 30/70 blends have smaller size contrasted to those in 10/90 blends. This is due to PEI higher concentrations are better homogenized by the kneaders during the mixing process, and hence, PEI particles in the 30/70 blends are elongated and broke up into finer particles.

Additionally, as it is expected, higher concentrations of the dispersive phase enhance the number of particle-particle collisions and as a consequence, they coalesce. Figure 3.12b) shows that

PEI droplets in 30/70 blend are not as even and spherical as those observed in 10/90 blend. From TEM micrograph, it is confirmed that PEI particles coalesce when the concentration increases, giving as a result an uneven dispersive phase, with some droplets connected to each other. Several authors have studied the coalescence effect on the development of blends morphology,[3,5,9,10,14–18,22,60] and they defined the basic influencing parameters during coalescence as: weight or volume fraction of dispersive phase, particle radius, phase's viscosity, and interfacial tension. Since the calculated interfacial tension between PEI and PBT (3.14 dyn/cm) points to immiscibility between both phases, coalescence between PEI particles will be enhanced during processing.

However, in TEM image shown in Figure 3.13 we performed a close up of one PEI droplet in the 30/70 blend. The semicrystalline PBT matrix is composed by well-defined spherulites formation that surrounds some antimony trioxide crystals (black spots), and the PEI droplet. The magnification reveals that spherulites around PEI droplet interpenetrate the PEI/PBT interface. This phenomenon is known as inter-spherulitic interaction and is common in blends between rigid amorphous and flexible semicrystalline polymers.[142,164,165] When PEI and PBT are mixed, PEI acts as an amorphous diluent of PBT amorphous phase, and some miscibility degree is achieved. Once again, this explains the small Tg shifts observed for PBT-rich blends in the DSC and DMA results, which are attributable to partial miscibility between PEI and PBT phases.

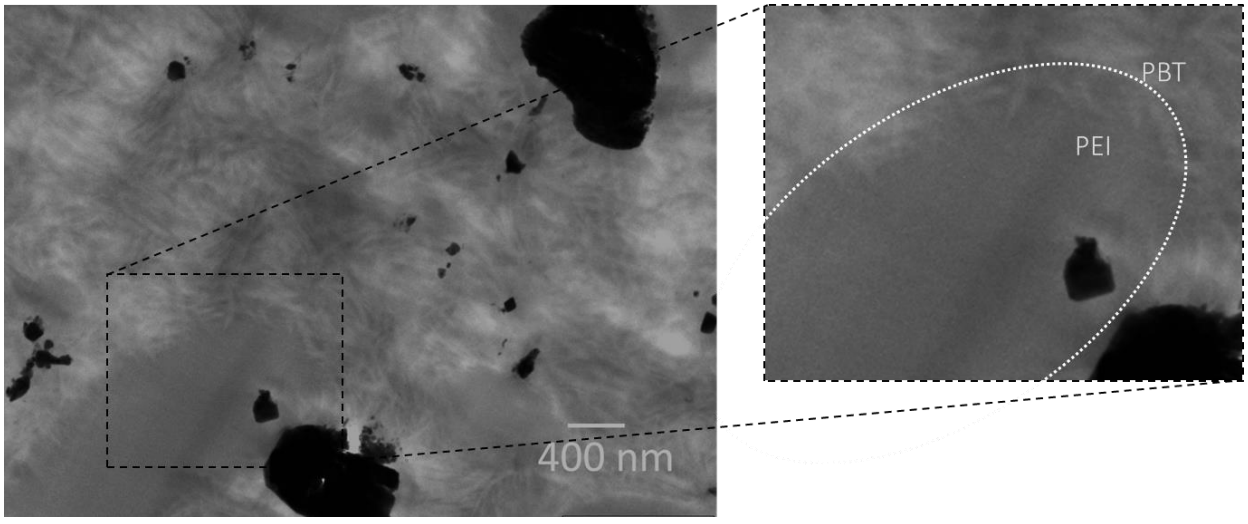

Figure 3.13 30PEI/70PBT TEM micrograph showing PBT phase crystals and one PEI droplet. The magnification displays the interface between the two phases (dashed line).

50/50 blend

In both, SEM and TEM micrographs shown in Figure 3.12c), it is revealed that when even PEI and PBT concentrations are mixed it takes place a dual-phase transition event. In a complete compositional range study of immiscible polymers blend, it is expected a phase inversion point where the two phases are fully co-continuous and it is impossible to differentiate the matrix from the dispersive phase.[75,166] If the composition continues increasing the former matrix becomes the dispersed phase and the former dispersed phase becomes the matrix.

The mentioned morphological transformation will lead to considerable changes in blends' properties. For this reason, it is of great interest to determinate the composition where the phase inversion takes place.[154]

Dual-phase transition of PEI/PBT blends

Earlier in this chapter, it was made a discussion on the effect of PEI concentration on rheological properties and phases' interaction of PEI/PBT blends by means of the log-additivity rule by using Equation 3.3. The analysis performed to PEI/PBT samples in the linear viscoelastic region during SAOS tests indicated that PEI/PBT blends are immiscible in the entire compositional range (Figure 3.7), which is somehow in a good agreement with SEM and TEM findings. However, from log-additivity rule it was not possible to identify, and even less to predict, the occurrence of the phase inversion.

In order to understand at which composition the dual-phase inversion takes place, a discussion from the qualitative understanding of the driving forces behind the formation of the phase inversion region from existent theoretical models will be made.

Experimental vs. calculated dual-phase transition point of PEI/PBT blends

In Chapter 2, there were described some theoretical models for predicting dual-phase transition point on polymer blends. In Table 3.6 are listed the volume fractions by using Jordhamo's, Chen's, Metelkin's, and Bourry's theoretical approaches to predict the dual-phase inversion point. For PEI/PBT blends, experimental volume fractions are based in the range where it is observed the dual-phase inversion in SEM and TEM images, which is approximately between 40 wt% and 60 wt% of PEI. These values converted to volume fraction are $\varphi_{PEI} = 0.42$ and $\varphi_{PEI} = 0.62$, respectively.

Table 3.6 Prediction of dual phase-inversion point of PEI/PBT blends, and experimental values observed from SEM and TEM micrographs.

Volume fraction	Jordhamo model (Equation 2.13)	Chen & Su model (Equation 2.15)	Metelkin & Blekht model (Equation 2.16)
φPEI	0.95	0.75	0.95
Volume fraction obtained experimentally from TEM φ PEI = 0.42 – 0.62			

The phase inversion point from Jordhamo's and Metelkin's models predict that phase inversion will take place at $\varphi_{PEI} = 0.95$, suggesting that low viscosity PBT phase will tend to be the continuous phase in almost the entire compositional range. These discrepancies between the observed and the calculated phase inversion points are attributable to the hypothesis of both, Equation 2.13 and Equation 2.16, which is based in the idea that less viscous phase will tend to be the matrix. Previous viscoelastic characterization of pure components revealed that PBT is notoriously lesser viscous than PEI, and hence, these models overestimate the viscosities differences in PEI/PBT system.

The model proposed by Chen and Su, on the other hand, was estimated for polymer systems with large viscosities differences. Although the predicted results from Equation 2.15 are closer to our experimental observations, it is still far from the phase inversion point observed in SEM and TEM micrographs for PEI/PBT blends.

Some authors modified Chen and Su's model to better fit their experimental results to a theoretical approach.[3,167] In their study on phase morphology of PA66/PS blends obtained by melt-blending in a corotating twin-screw extruder, Sobha and coworkers[167] varied Equation 2.15 to obtain phase inversion point values closer to their experimental observations. A similar strategy was applied by Everaert and coworkers[3] by removing the term 1.2 from the same equation. This arbitrary modification resulted in a better fitting of their experimental results on the phase inversion evaluation of PP/(PS/PPE) blends.

Following the same approach of the aforementioned authors, we found that replacing the coefficient 1.2 by 0.45 we obtained an expression that fit better to our experimental phase inversion point values, Equation 3.7. Contrasted results of original and modified Chen and Su's model are listed in Table 3.7.

$$\frac{\varphi_{hv}}{\varphi_{lv}} = 0.45\left(\frac{\eta_{hv}}{\eta_{lv}}\right)^{0.3} \qquad \text{Equation 3.7}$$

Table 3.7 Modified Chen and Su equation for phase inversion point prediction.

Volume fraction	Chen and Su model		
	Equation 2.15	Modified by Everaert[a]	Modified in this work
φPEI	0.75	0.71	0.52

It is a fact that this model has to be modified to fit some particular experimental results, which is a clear evidence there is a lack of parameters to be considered, and they do not predict the behavior of all polymer blends pairs. Similar discrepancies in predicting phase inversion values are found in several works with different polymer blends systems.[3,75,168–170] All authors agree these models lack considerations such as materials characteristics —interfacial tension and materials elasticity— and processing conditions —mixing time and mixing sequence—. In this work, it is noticed that high PEI/PBT interfacial tension together with steps-blending process, highly influences PEI distribution in PBT matrix, and hence, dual phase inversion transition.

Even though the values obtained with Chen and Su's model, with and without modifications, SEM and TEM evidences shown in this work point out to the occurrence of phase inversion in PEI/PBT blends with 50 wt% of PEI and 50 wt% of PBT.

PEI-rich blends morphology

When we applied the Soxhlet extraction to PEI-rich blends, it washed away almost the whole sample, and the remained material did not support itself to be observed by SEM. Therefore, the morphology study of these blends will be discussed from the cryofractured samples by SEM and the microtomed samples by TEM, without selective phase extraction.

60/40 blend

Figure 3.14 displays the morphology of blends after the dual phase transition. In Figure 3.14a), it is noticed that the smooth PEI phase covers more area along the sample surface and that both phases are adhered through the characteristic fibrillary structure described previously. The TEM micrograph shown in Figure 3.14b), reveals that PBT phase is distributed along the PEI matrix as droplets with irregular sizes and shapes —not as well defined as PEI droplets in PBT-rich blends—. This is caused by the increase of PEI concentration above the dual-phase inversion point, where PEI becomes the matrix and PBT the dispersive phase. These results are in good agreement with the predicted phase inversion point Equation 3.7, where the phase inver-

sion point takes place at even PEI and PBT concentrations, for PEI volume fractions greater than 0.42 and lower than 0.62, as indicated in Table 3.6.

A magnification presented in Figure 3.14c), shows more in detail the fibrillary interface between PBT droplets adhered to the PEI matrix, which is found to be similar to the inter-spherulitic interaction described previously in Figure 3.13, suggesting this that the fibrillary interface is rich in PBT phase.

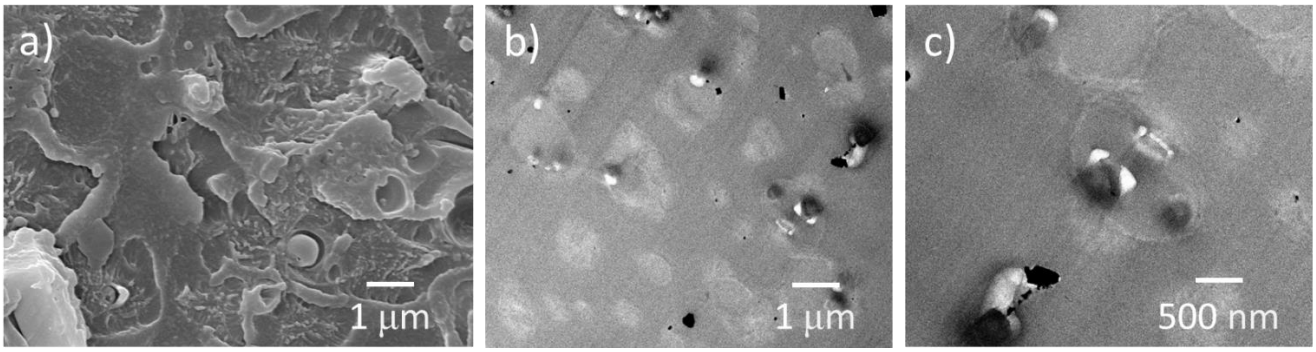

Figure 3.14 Morphology of PEI/PBT blends containing 60 wt% of PEI: a) SEM micrograph, b) and c) TEM micrographs.

70/30 and 80/20 blends

The increasing in PEI concentration leads to significant changes in PEI/PBT blends morphology. A close up of the morphology of blends containing 70 wt% of PEI and 80 wt% of PEI is presented in Figure 3.15. There is noticed that small PBT droplets are attached to the PEI matrix with a fibrillary interface, giving the appearance of what we called a *spore-like* morphology. In a recent work, Bahrami and coworkers found that binary PPE/SAN blends compatibilized with SBM triblock terpolymer exhibit a similar morphology. They attributed the fibrillary linkage between PPE and SAN to the effect of the chemical compatibilization.[171] In our work, no compatibilizer agents were used, and the interaction between PEI and PBT phases is a sign of good physical compatibilization between both phases. This singular morphology in PEI-rich blends is attributable to the partial miscibility caused by the inter-spherulitic interaction between both phases, and mainly, to the differences of shrinkage between the two materials. PBT is a semicrystalline polymer with fast crystallization rate and as a consequence, a small shrinkage feature has been reported.[172]

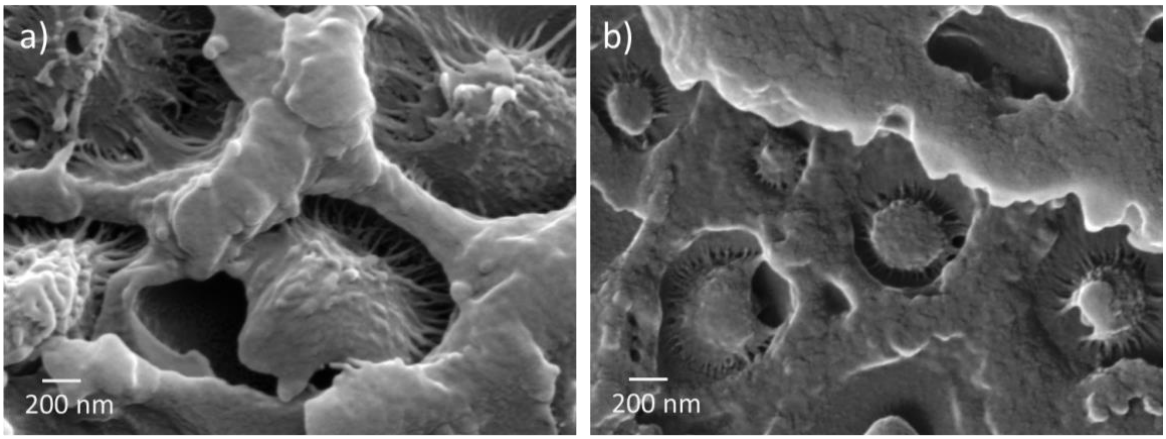

Figure 3.15 *Spore-like* morphology of PEI-rich blends: a) 70 wt% of PEI, and b) 80 wt% of PEI.

In their work in HDPE/PC blends, Leclair and Favis[173] explain that when an immiscible polymer blend is composed by a highly semicrystalline and a highly amorphous phase, a voiding mechanism takes place at the interface when the amorphous phase is the matrix. Immiscibility between HDPE and PC is attributed to their molecular structure differences, and to their transitions temperatures during cooling. In Figure 3.16 it is presented a schematic representation of what happens to both PEI and PBT phases during the mixing process, as well as during the cooling stage after PEI-rich blends are removed from the mixer. When PBT is added to the fluid PEI in step 2, PBT pellets melt, deform, and split into tiny droplets as a consequence of the shearing and elongation forces caused by the rotors speed and the highly viscous PEI phase. The cooling stage starts with both materials at 280 °C, with both, PEI and PBT in fluid and molten state, respectively. At 210 °C, PEI phase is below its Tg and the matrix becomes rigid, hosting inside the still molten portion of immiscible PBT phase. When temperature reaches 196 °C, PBT starts to crystallize, and due to its semicrystalline nature, PBT droplets experience a significant shrinkage which leads voids generation between PEI and PBT phases. However, due to the partial miscibility between both phases, the voids are combined with a fibrillary attachment between PBT droplets and the PEI matrix.

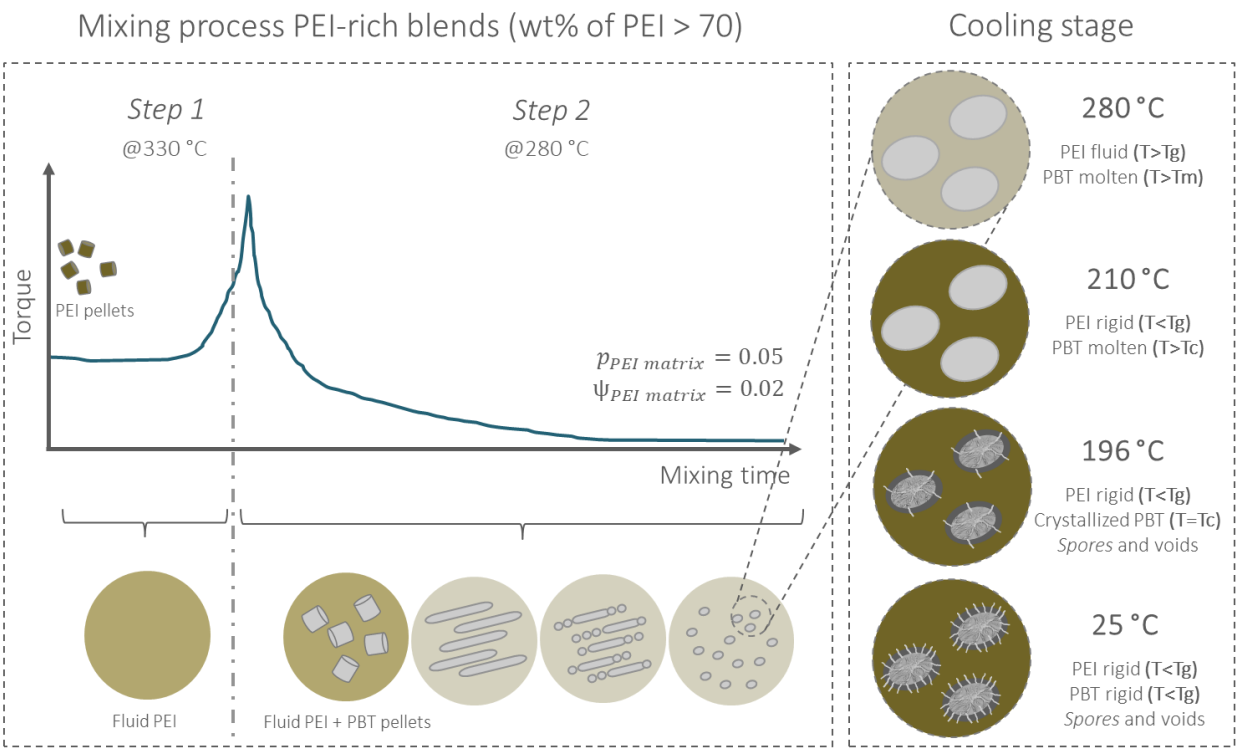

Figure 3.16 Schematic representation of spore-like morphology formation in PEI-rich blends regarding its cooling stages.

In Figure 3.17 it is displayed the evolution of the irregular and coarse particles in 60/40 blends to small and well defined droplets distributed along the PEI matrix in 70/30 and 80/20 blends. Two hypotheses came to light to explain this behavior: the first, claims that finer particles size of PBT phase when PEI is the matrix is in good agreement with the theory of Taylor and Grace. As PEI is much viscous than PBT —as evidenced in the viscous and modulus ratios in Table 3.4— at the time the torque stabilizes PBT phase is distributed in the PEI matrix as fine droplets. The second hypothesis comprises capillary instabilities in the blend in the steady state after mixing process. However, this hypothesis was discarded since PEI's viscosity is high enough to stabilize PBT droplets to avoid capillary instabilities after the shear flow ceased.[50]

As expected, PBT particles on TEM micrographs are the same size of those spore-like morphologies observed by SEM. In 80/20 blend, we measured spores close to nanoscale sizes —until 120 nm—. Some authors reported that the use of surfactants or compatibilizer agents improve the interfacial adhesion between components,[11,15,133,160,174,175] but they may also lead to the reduction in the size of the dispersive phase to nanoscale.[176,177] According to Sundararaj and Macosko,[178] the main effect of the interfacial modificators is to reduce the particle size to even a third of its original size, and to narrow the particle size distribution. In this work, the reduc-

tion reached in PBT particle size results from processing conditions, and it is sensed by DSC and DMA as a single Tg for PEI-rich blends (Figure 3.8 and Figure 3.9), suggesting there exists miscibility between PEI and PBT. Although some miscibility between PEI and PBT may make a lot of sense —because the amorphous PEI phase acts as a diluent of the amorphous structure of PBT (as observed in Figure 3.13 for 30/70 blend)—, the evidences observed by SEM and TEM show that PEI and PBT tend to be immiscible in the entire composition range, which is in good agreement to the log-additivity rule analysis performed from PEI and PBT viscoelastic properties in Figure 3.7.

The reduction of the dispersive particle size is also promoted by processing sequences. In their work, Cimmino and coworkers studied the interfacial adhesion of PA-6/EPM/EPM-g-SA blends by changing the mixing sequence of the graft copolymer. They found that one-step mixing resulted in coarse particles, while two-step mixing gave as a result finely dispersed morphology and excellent mechanical properties.[179] Even though in our work we did not use compatibilizer agents, we obtained very small PBT particles sizes after adding during step 2, where the highly viscous PEI deform the PBT phase into small particles.

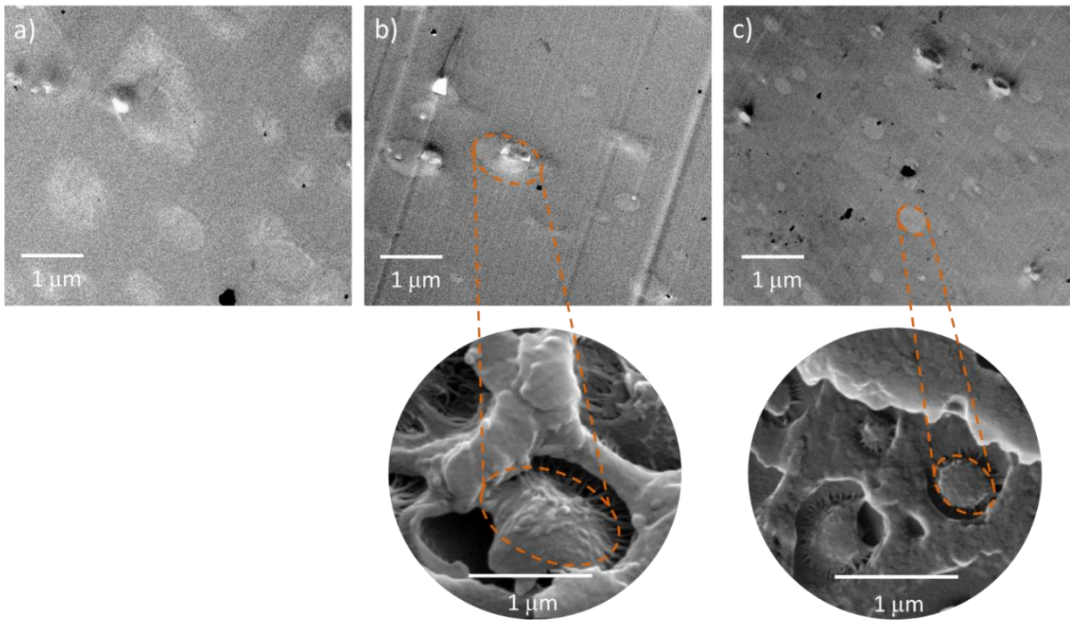

Figure 3.17 TEM micrographs of PEI-rich blends for: a) 60 wt% of PEI, b) 70 wt% of PEI, and c) 80 wt% of PEI; and comparison with the spore-like morphology observed by SEM for blends with 70 wt% of PEI and 80 wt% of PEI.

Effect of PEI concentration on blends particle size

The previous morphological study reveals that the morphology of PEI/PBT blends strongly depends on the processing conditions, the viscoelastic differences between pure components,

and PEI composition. Figure 3.18 shows the effect of blends composition on the particle size of the dispersive phase. In Figure 3.18a), the dashed lines in Dn and Dv vs. wt % of PEI plot represent the generalized behavior of particles size before and after the dual-phase inversion. The results for PEI/PBT blends are presented in Figure 3.18b), where is shown a plot of dispersive phase diameters as a function of PEI concentration. The number-average diameter (Dn) and volume-average diameter (Dv) are calculated by using Equation 3.8 and Equation 3.9, for at least 100 particles.

$$Dn = \frac{\sum_i d_i}{n} \qquad \text{Equation 3.8}$$

$$Dv = \left(\frac{\sum_i {d_i}^3}{n}\right)^{1/3} \qquad \text{Equation 3.9}$$

Some authors reported that particle size increases gradually with increasing composition as a consequence of coalescence, and just after phase inversion, the minor phase is deformed and breaks up into smaller particles.[167–169] Contrary to these reports, we found that PEI droplets have coarser size at lower concentrations. This unexpected behavior is explained by the processing conditions proposed in this work and the enormous differences between the viscoelastic properties of pure materials. When small amounts of PEI (10 wt%) are added to the mixer during step 1, the kneaders soften and smoothly deform the PEI phase. At the time high concentration of PBT phase is added during step 2, it melts and surrounds PEI phase. As PBT phase is much less viscous, it do not exert significant shear over PEI phase which distributes freely in the PBT matrix without suffering major deformation adopting a coarse size droplets. While increasing PEI concentration to 30 wt% and 40 wt%, a combination of shear and elongational flows takes place inside the mixer and PEI particles deform and break up into finer sizes. PEI-rich blends on the other hand, follow the generalized behavior. The increasing concentration of the highly viscous matrix leads to obtaining finer particles sizes of the less viscous dispersive phase.

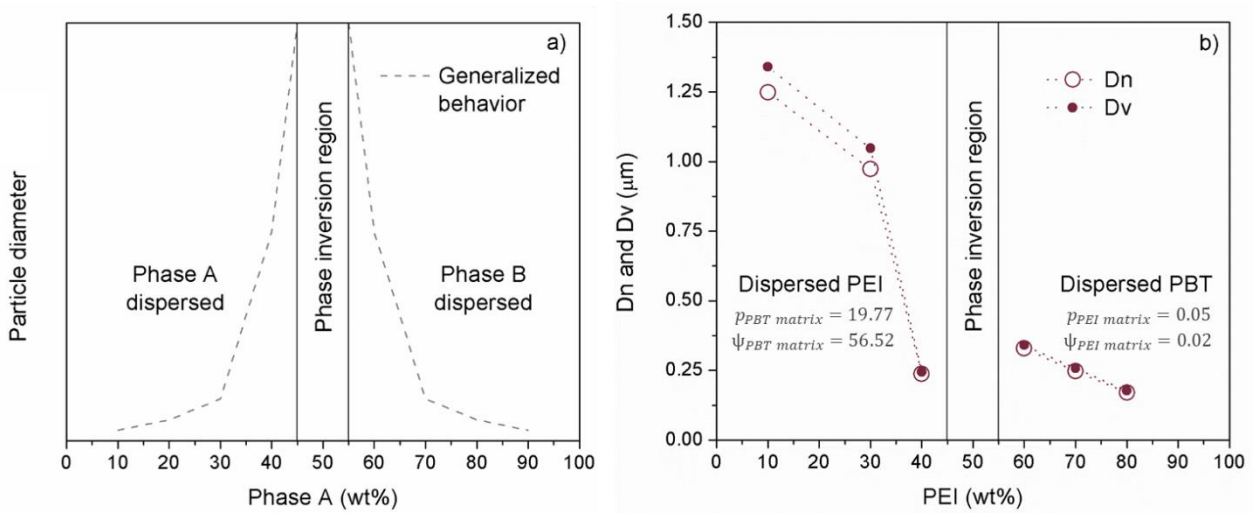

Figure 3.18 Effect of blends composition on the size of the dispersive phase: a) Generalized behavior for blends with dual-phase inversion, and b) effect of PEI composition on the dispersed particle size of PEI/PBT blends.

In order to better observe not only the size but also the shape of the dispersive phase morphology when whether PBT or PEI is the matrix, Figure 3.19 shows a schematic representation of PEI/PBT blends' morphology evolution as a function of PEI composition. The scale of the TEM micrograph for each blend is kept in its original size, and the drawn morphology is modified to take all particles to a common scale of 2 μm. The differences observed for each composition are entirely attributable to the processing parameters and the mixing sequence used in this work. Important parameter such as interfacial tension —which strongly influences the morphology of immiscible blends— is considered to be constant for all blends compositions.

According to Wu,[62] interfacial tension between two substances will vary when there are changes in components polarities, temperature, and molecular weight of components. As blending conditions in this work were kept constant for all PEI/PBT blends in the entire compositional range, there are no changes in the interfacial tension that affect blends morphology. What does change for each blend while increasing PEI concentration is the morphology shape, and hence, the contact surface area between PEI and PBT.

Contrary to other works on PEI/PBT blends, our results reveal that PEI and PBT phases are well differentiated from each other in the entire compositional range. The main differences with those reports are the characteristics of the commercial resins —we use flame retarded PBT—, the processing methods, and the step processing conditions.

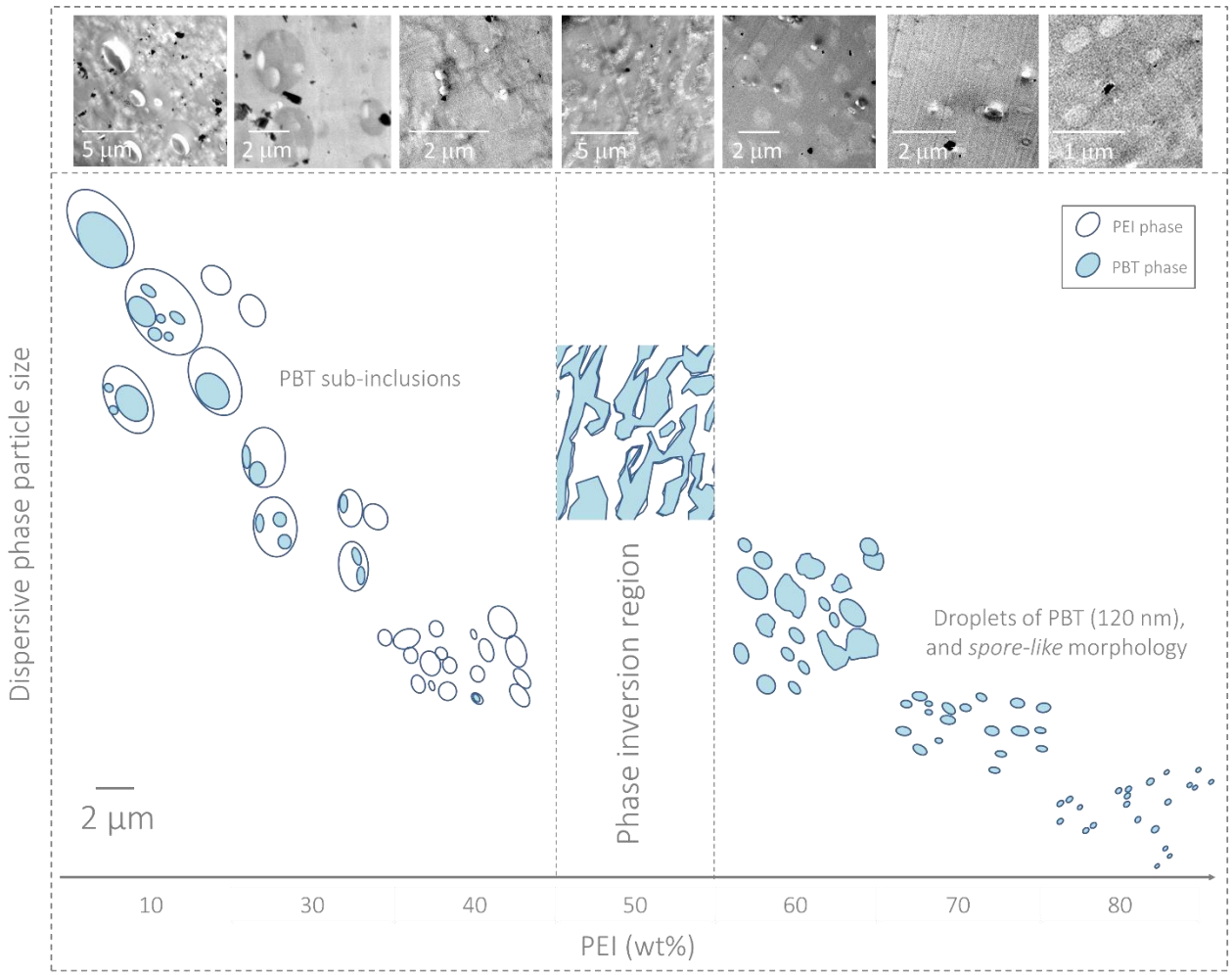

Figure 3.19 Schematic representation of the morphological evolution of PEI/PBT blends in the entire compositional range.

With the aim of verifying if raw materials influences on blend's miscibility, we fabricate binary blends between PEI and unfilled PBT (Uf-PBT), using 30 wt% and 50 wt% of PEI. In Figure 3.20a), the 30/70 blend exhibits dispersed droplets of PEI phase attached to the PBT matrix through the characteristic fibrillary interface, similarly to observations on SEM results in blends with flame retarded PBT. In Figure 3.20b), the 50/50 blend displays the co-continuous morphology as blends with filled PBT, with both phases bonded through the fibrillary interface. These results confirm that immiscibility found between PEI and PBT in this work, it is mainly favored by the step processing conditions we used, and that morphology is completely influenced by blends composition.

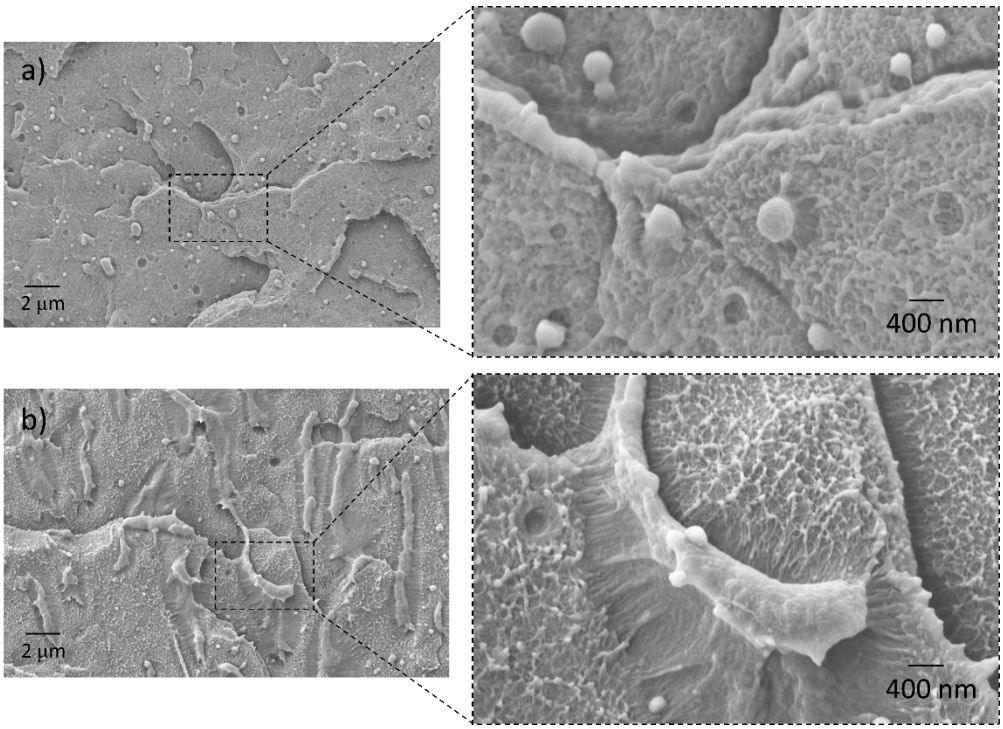

Figure 3.20 Morphology of blends between PEI and Uf-PBT: a) 30/70, and b) 50/50.

3.3 PART III – Effect of morphology on the mechanical properties, thermal stability, and flammability resistance of PEI/PBT blends

3.3.1 Introduction

Mechanical and thermal performance on polymer blends, will be strongly affected by the miscibility level between the individual constituents. For instance, miscible polymer pairs may exhibit superior properties to those of the individual constituents, leading to synergetic behaviors.[180,181] On the other hand, properties of immiscible blends will depend on the composition and the type of morphology obtained.[2,3,46,182–187] Conversely to miscible polymer mixtures, immiscible polymer blends generally exhibit poor mechanical properties due to the components may lack of enough interfacial interaction, and hence, synergetic behavior is not commonly obtained in these systems. To counter this issue, there are commonly used chemical compatibilizing agents that induce some sort of interaction between blends components at interfacial level. However, as mentioned in previous sections in this work we avoided the use of any chemical compatibilizer, and the fibrillary interaction bond observed by SEM and TEM is reached by the proper physical compatibilization during the mechanical mixing process, together with the partial miscibility between PEI and PBT.

In this section, it is studied the effect of blends composition on the mechanical, thermal, and fire resistance properties of PEI/PBT blends by using known experimental techniques together with semi-empirical additivity approaches. It is known that blending technology is based on the principle of additivity, and it is a suitable way to relate physical, chemical, mechanical, thermal and electrical properties with blend's composition.[72,180] The additivity rule allows to evaluate the effect of components interaction in both, miscible and immiscible blends, and several properties such as modulus, impact strength, heat resistance, color, hardness, flame retardancy, thermal conductivity, etc. obey this rule described in Equation 3.10:

$$P_b = w_1 P_1 + w_2 P_2 \qquad \text{Equation 3.10}$$

where w_i and P_i are the weight fraction and the property of interest of polymer i, respectively. For instance, when predicting the mechanical properties in immiscible blends, the negative deviation from the additivity rule is linked to poor interfacial interaction between blend components that promote the early failure. In this situation, blends are said to be non-synergetic or incompatible. If there exists positive deviation, the blends exhibit a synergetic behavior as a consequence of strong interfacial interaction or partial miscibility.

A first look into the tensile results for PEI/PBT blends, reveals an intermediate behavior respect pure materials. When there are plotted the mechanical properties as a function of PEI composition, the elastic moduli deviate positively from additivity rule and tensile strength values exhibit both positive and negative deviation. Even a synergetic contribution of moduli values for 50/50 and 80/20 blends phases is observed. This synergic behavior is attributed to strong phase adhesion between PEI and PBT, and to blends' embrittlement promoted by the PEI addition. Results from elongation to break, revealed a negative deviation from additivity rule for all compositions, and that the blend with 50 wt% of PEI exhibits the best elongational at break capacity due to its co-continuous morphology.

Miscibility also plays a crucial role in thermal stability and flame resistance of polymer blends. Besides, the interactions between the constituents and their products during thermal decomposition is also of highly importance. In immiscible blends, for example, these interactions involve diffusion of a small mobile product species (molecule or radical) from one phase to other.[182,188] In their work, McNeill and Gorman reported there are four main possible interaction in heterogeneous blends: i) small molecule + macromolecule; ii) small molecule + macro-

radical; iii) small radical + macromolecule; and iv) small radical + macroradical.[188] Since these interactions may stabilize or destabilize the thermal behavior of polymers, the degree of dispersion of the phases in immiscible blends is a crucial factor. For example, an immiscible PS/BR blend is more thermally stable than its pure components because the products from the polyolefin degradation diffuses into the polystyrene phase and acts as a scavenger for polystyryl radicals.[188] Conversely, Naffakh and coworkers noticed that the degradation of PEEK/LCP blends is accelerated by blending process, and that the thermal stability is strongly influenced by the level of interaction between the two components.[184]

The study of thermal stability in polymer blends is commonly performed by TGA. From this technique, it is possible to predict the decomposition behavior of blends and to detect the mentioned interactions between constituents or their decomposition products.[183] When accompanied with FTIR, it is possible exploring the reactions that are taking place and provide a degradation mechanism. Nevertheless, study of these mechanisms is not the aim of this study.

Thermal stability results show that PEI addition improves considerably PBT's thermal properties, even at low PEI concentrations. Moreover, the flammability tests reveal that the charring ability of PEI remains in all blends compositions as the main flame protection barrier. It is known that flame retardancy property is usually desirable to mitigate flame propagation on consumer goods, protect the integrity of human body, and in extreme cases, save lives.[132] In protective textiles applications, for example, the thermoplastic fibers that are commonly used such as polyesters, PP, and PA —even with flame retardant additives—, exhibit melt dripping and form holes when are directly exposed to flame. These polymers cannot be used in applications such as protective clothing and barrier textiles, since char formation is an essential requirement for protection.[27,125,127]

For the best of our knowledge, this is the first time there are reported the mechanical behavior together with thermal stability and flammability study on PEI/PBT blends, and that such properties are related to phases interaction in the entire compositional range.

3.3.2 Experimental

Tensile tests

Tensile tests were made according to standard ASTM D638 – 14. Type V samples were injected molded in a HAAKE MiniJet Pro Injection System from Thermo Scientific. Conditions for injection molding are listed in Table A- 3. Samples were tested in an Instron 3366 at a crosshead speed of 1 mm/min using an extensometer with a gauge length of 10 mm. At least five specimens of each blend were measured and the average values were reported.

Thermal stability and flammability tests

Thermal stability of PEI, PBT, and PEI/PBT blends was studied by means of TGA. The flammability tests were settled according to the UL94 standard.

Thermogravimetric analysis (TGA)

Thermal stability study was carried out in a TGA Q500 model from TA Instruments on samples of 40±2 mg, within a temperature range from 25 °C to 900 °C at a heating rate of 10 °C/min. All thermal evaluation tests were performed under nitrogen atmosphere.

Flame resistance analysis

For flammability tests, samples of 125 mm length, 10 mm width, and 3 mm thickness were obtained by injection molding in a HAAKE™ MiniJet Pro Injection System from Thermo Scientific. The injection molding conditions are the same as the ones described in Table A- 3. An assembly was fabricated to perform horizontal burning (HB) tests according to the standard UL 94, Figure 3.21. The lab-made assembly consisted of a laboratory burner positioned at 45°, a supply of natural gas, a sample holder, and a universal laboratory support. According to the UL94 standard, two marks were made in the specimens at 25 mm and 100 mm length from the tip that is exposed to direct flame contact, in order to measure the burning rate in mm/s. Three specimens were tested for each blend. The flame traces in the samples were video and photographically recorded.

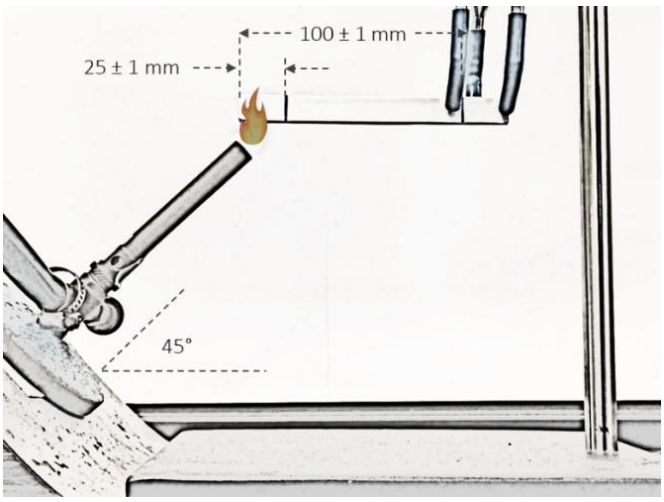

Figure 3.21 Lab-made assembly for the horizontal burning test according to standard UL 94 – Section 7.

3.3.3 Results and discussion

Mechanical properties of PEI/PBT blends

Figure 3.22 displays the stress vs. strain curves for pure materials and their blends. Pure PEI and PBT show the characteristic behavior of ductile polymers. PEI goes through a cold-drawing process with a maximum value of the yield stress, σ_y (or tensile strength) at 103.6 MPa, followed by a stress drop as a sign of necking. The stress stabilizes until PEI breaks at 20% deformation. PBT on the other hand, reaches its σ_y at 56.9 MPa and deforms gradually until it breaks after 40% deformation.

Regarding PEI/PBT blends, they exhibit intermediate tensile strength with respect to pure components, which increases with PEI phase addition. However, there are clear differences in the elongational break performance of blends. Most blends exhibit cold-drawing behavior, but only 50/50 blend, and to some extent 40/60 and 60/40 blends, exhibit deformation similar to pure components. Two brittle blends are observed: 30/70 blend, and surprisingly 80/20 blend —with spore-like morphology— that break just after they reach the yield stress.

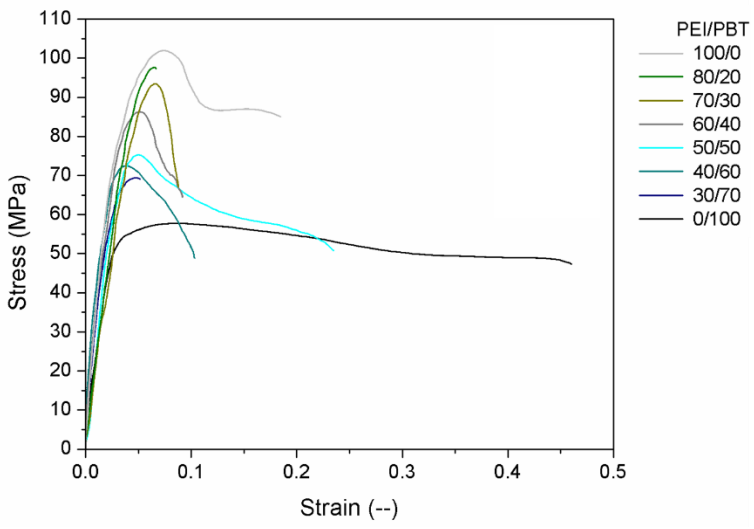

Figure 3.22 Tensile stress-strain curves for PEI, PBT, and PEI/PBT blends.

In Figure 3.23 are displayed the tensile moduli for PEI/PBT blends as a function of PEI concentration. The moduli values are calculated from the slope of the elastic region of stress-strain curves at early deformations where no interfacial debonding takes place.[189,190] The solid line corresponds to the moduli values calculated from the additivity rule by using Equation 3.10, and the dashed horizontal line delimits the modulus of pure PEI. It is noticed that all blends whether comply or deviate positively from additivity rule, which suggests that PEI and PBT phases are not incompatible in any composition. This is in good agreement with blends' partial miscibility attributed to the inter-spherulitic interaction, and with the interfacial bonding through the fibrillary structure observed by SEM and TEM results. The monotonic increase of moduli values is attributed to the increase in the PEI phase that enhances blends' rigidity due to its robust chemical structure composed of aromatic rings and imide functional groups.

Despite 30/70 and 70/30 blends show a brittle behavior, their tensile moduli values comply with the additivity rule. The brittleness is attributed to these blends have the poorest interfacial interaction between PEI and PBT phases compared to the rest of PEI compositions. The SEM and TEM micrographs of the blend with 30 wt% of PEI, show a coarse size of the PEI particles together with PBT sub-inclusions that lead to low mechanical performance. On the other hand, although the 70/30 mixture exhibits a spore-like morphology, at this composition there are large spaces between the PBT domains and the PEI matrix from which early fracture is promoted, as observed in Figure 3.15a). The blends containing 40 wt% and 60 wt% of PEI display moduli values above additivity, due to the proximity of these compositions to the dual-phase inversion (co-continuous morphology).

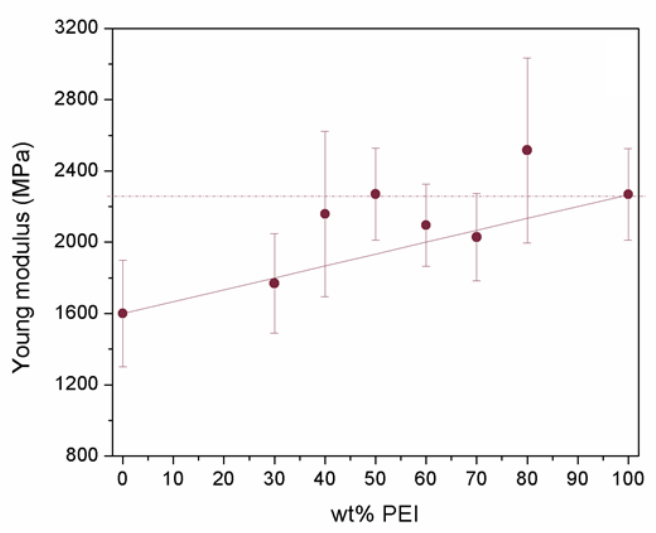

Figure 3.23 Young modulus of PEI, PBT, and PEI/PBT blends as a function of PEI concentration. The standard deviation was calculated for n = 5.

The blends with 50 wt% and 80 wt% of PEI, exhibit a synergetic contribution —values above those of PEI— associated with the fashion in which phases are distributed. PEI and PBT phases in 50/50 blends have a co-continuous structure and the contribution of the highly rigid PEI phase is noticed as a substantial increase in modulus values. The synergic behavior observed in the blend containing 80 wt% of PEI is a combination of the higher concentration of PEI in the blend, the distribution of the tiny crystalline PBT phase in the shape of spore-like structure, and the rigidity gained by the densification caused by the inter-spherulitic interaction.

Vallejo and coworkers reported similar synergic results for PEI-rich blends.[41] They attributed it to the reduction in the specific volume of blends when high PEI concentrations are mixed with PBT. Barlow and Paul explained the effect of free volume on the mechanical properties of polymer blends from a thermodynamic approach.[2,191] They said that when an exothermic reaction occurs during blends' components interaction, Gibbs free energy of mixing is negative and the blend will be miscible. What should be expected then, is a volume contraction in the blend known as densification. This phenomena known as "thermal embrittlement" explains the embrittlement occurs when miscible blends with high Tg polymers —such as PEI— experiences free volume loss. As discussed in the previous section, PEI/PBT blends exhibit partial miscibility that favors the free volume loss —particularly PEI-rich blends because of the high amount of amorphous phase— and hence, densification of the blends. This behavior leads blends to exhibit higher moduli than those of pure materials, and as a consequence, synergism is observed.

Figure 3.24 exhibits the yield stress —calculated as the maximum stress in the elastic-to-plastic transition region— as a function of PEI concentration. Contrary to the elastic modulus, the yield stress in polymer blends is sensitive to adhesion of components, and generally indicates if the interface is strong enough to transmit the tensile stress up to break.[189,190] Similarly to moduli, it is observed that σ_y values increase monotonically with PEI addition, and despite they are close from fulfilling additivity, it is observed a smooth deviation in both, negative and positive directions. PBT-rich blends have negative deviation due to PEI and PBT at concentrations lower than 40 wt% are immiscible, and PEI is distributed as coarse droplets along PBT matrix. Interesting results are observed for tensile strength in 50/50 blends, which reveal a negative deviation from additivity. This suggests that the interfacial adhesion between PEI and PBT is not too stiff, and that PBT mechanical properties predominates over those of PEI when the tensile stress is close to the yield stress. This makes sense, since the fibrillary morphology observed in SEM and TEM micrographs is mainly composed by PBT crystallization during the cooling stage, which is the most ductile phase.

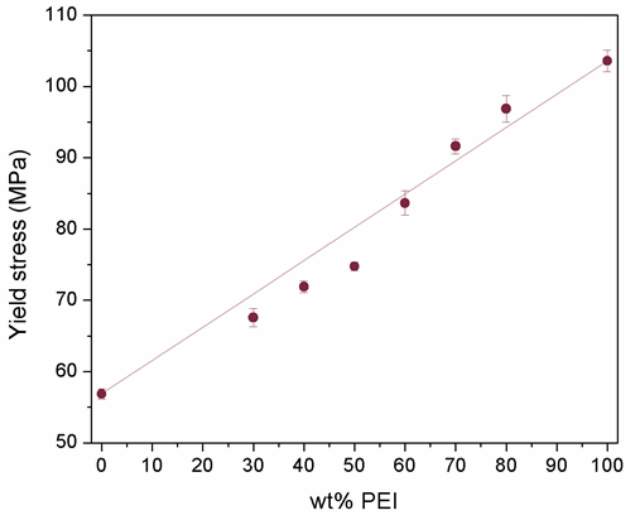

Figure 3.24 Yield stress of PEI, PBT, and PEI/PBT blends as a function of PEI concentration. The standard deviation was calculated for n = 5.

Regarding PEI-rich blends, it is noticed a positive deviation from additivity as a sign of PEI and PBT partial miscibility, which suggest amorphous PEI dilutes some amorphous domains of PBT. This is noticed as an increase in the tensile strength of blends. In their study, Leclair and Favis observed that when semicrystalline and amorphous polymers are blended, it is reached a reinforcement effect when the amorphous phase is added to the semicrystalline matrix. They obtained HDPE/PC blends in the entire compositional range, and noticed the mentioned effect

when PC is added to HDPE. Conversely, when HDPE is added to the PC matrix, no adhesion is observed at the interface and the mechanical performance decreased for PC-rich blends.[173] In our work, we obtained a mechanism to reinforce PEI-rich blends with the formation of the spore-like morphology, and although PBT-rich blends are not incompatible the coarse size inclusions of PEI domains, the sub-inclusions of PBT in PEI droplets, and to some extent the inorganic fillers (flame retardant additives), do not favor mechanical performance of these blends. The discrepancies found between both works are due to the coarse size obtained in PBT-rich blends, and the high crystallization kinetics of PBT that enhances the spore-like formation that acts as the bond between both phases.

Different results are observed in PEI/PBT blends ductility. In Figure 3.25a), it is observed how ductility of blends experiences a negative deviation from additivity. This behavior is directly related to PEI/PBT blends morphological structure and partial miscibility. PBT-rich blends have immiscible PEI coarse particles that reduce the ductility of blends. Additionally, PBT sub-inclusions inside PEI droplets are completely disconnected from PEI phase, which causes stresses concentration and promotes early fracture (Figure 3.10b)). On the other hand, PEI-rich blends are partially miscible, and their poor elongation at break is attributable to the thermal embrittlement, resulting in a considerable increase in modulus or strength together with a dramatic reduction in ductility.[2,192]

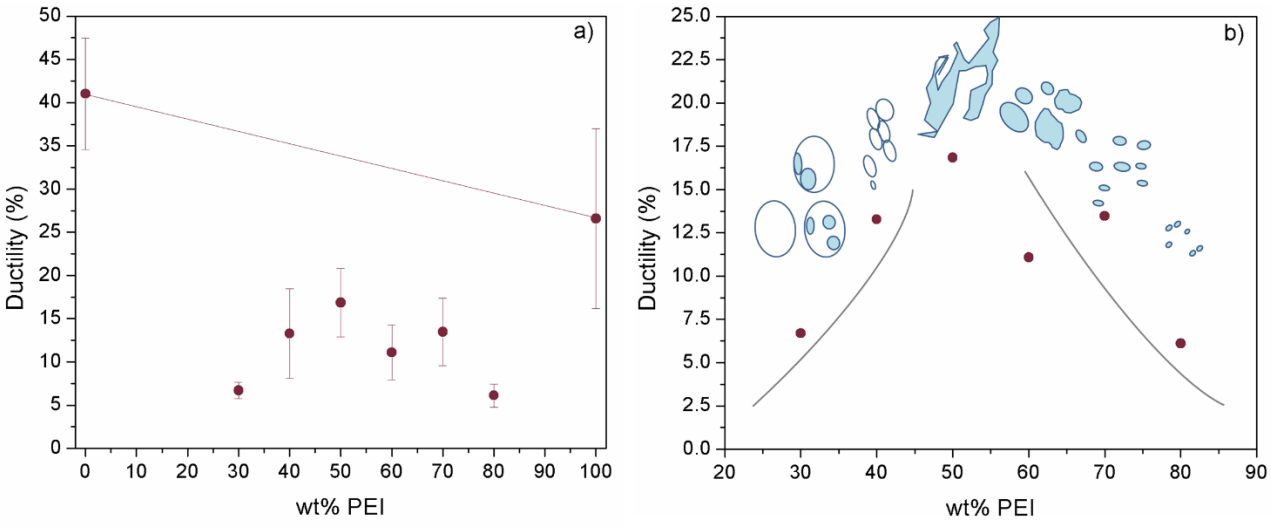

Figure 3.25 Ductility of PEI, PBT, and PEI/PBT blends: a) Ductility as a function of PEI concentration (standard deviation was calculated for n = 5), and b) schematic representation of the effect of morphology on PEI/PBT blends ductility.

The effect of morphology evolution on PEI/PBT blends ductility is represented in Figure 3.25b). Elongation at break is higher close to the vicinity where dual phase transition region takes place. In their work, Murff and coworkers observed a similar behavior for immiscible PC/PET blends when PC composition was close to phase inversion point.[193] This suggests that both, PEI and PBT phases contribute to the ductility of blends.

Thermal stability and flammability of PEI/PBT blends

As presented in the thermogravimetric analysis for pure components (Figure 3.2), PEI exhibited higher thermal stability than flame retarded PBT. In addition, PEI has an inherent charring ability,[38] which is noticed by the mass loss lower than 50%.

Thermogravimetric analysis (TGA)

In Figure 3.26a), there are presented the TGA results for PEI, PBT, and their blends. Their respective derivative curves are presented for a temperature range between 270 °C and 630 °C —delimited by the dashed square— as shown in Figure 3.26b). The decomposition of pure materials takes place in a single step, which is retained in the corresponding blends leading to an intermediate two-step decomposition behavior. The small signal observed at 500 °C in pure PBT —enclosed in the orange dashed circle— corresponds to the oxidation of one of the components of the flame retardant additive: Sb_2O_3.[135,136,194] When Sb_2O_3 starts to oxidize, it reacts with the bromide compound to produce an antimony-bromide complex that acts with a synergistic effect delaying the flame propagation —in case the polymer undergoes a combustion process—, as described by Sallet and coworkers in their work.[195]

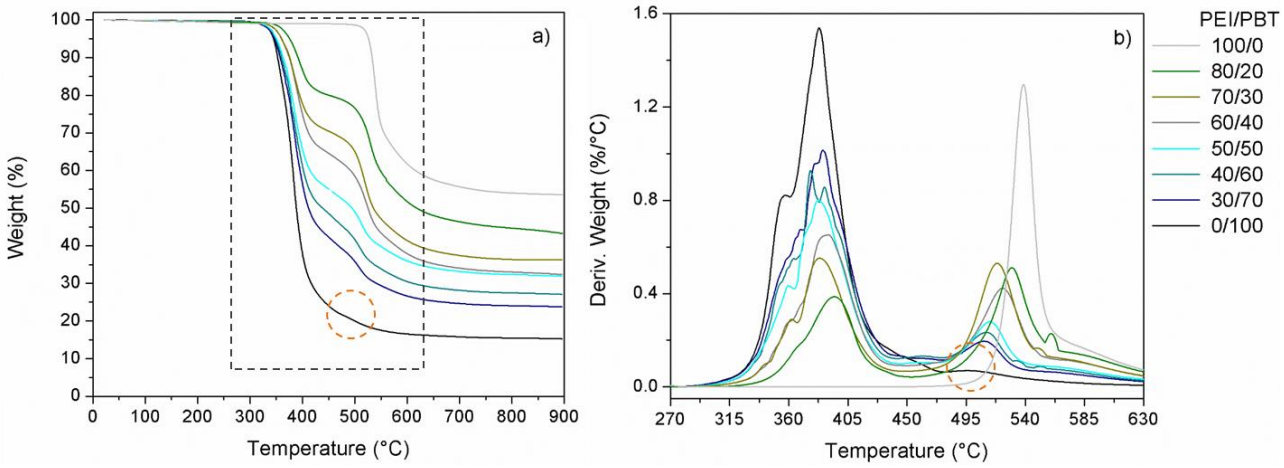

Figure 3.26 Thermal stability of PEI, PBT, and PEI/PBT blends: a) TGA, and b) DTGA.

In Table 3.8 are summarized the results for the initial decomposition temperature Ti —which is the temperature measured just before the initial decomposition event— and the residual weight at 900 °C, as well as the maximum decomposition rate temperature Tmax —measured at the maximum value of the decomposition peaks— obtained from DTG curves. As PEI/PBT blends exhibit two peaks corresponding to the thermal event of each phase, they are called T1max for PBT and T2max for PEI. It is noticed that the increase of PEI concentration results in a notorious improvement of Ti, as well as in the maximum decomposition rate temperatures T1max and T2max. These results suggest that PEI acts as a thermo-protective phase for PBT, delaying its thermal decomposition and improving its thermal stability. More remarkable results are observed in the increasing residues percentage with PEI addition, demonstrating that PEI/PBT blends exhibit charring formation, and hence, the thermal stability of blends is increased with PEI addition.

The last row in Table 3.8, presented in italics, shows the results of the thermal stability analysis for PBT sample without flame retardant (Uf-PBT). Curiously, Ti for unfilled PBT sample is higher than that of the flame retarded PBT. The difference in the Ti values for both PBT samples is explained from the self-extinguish effect of the flame retardant compound (Sb_2O_3 + bromide), which causes an early decomposition of the filled PBT sample. Similar results were observed by Sato and collaborators in their study on blends between a flame retardant PBT and bromide-poly(carbonate) (Br-PC) blends.[130] They noticed these blends exhibit an initial decomposition temperature lower than that of pure PBT, caused by the flame-retarding effect of the additives. Generally, it is understood that the effect of halogenated additives reaches a synergetic effect when they are blended with antimony oxide, forming a volatile antimony halides that act as free radical traps and anticipates to the polymer decomposition to prevent flame propagation.

Table 3.8 Results of thermal decomposition analysis of PEI, PBT, and their blends.

PEI/PBT blend (wt%)	Ti (°C)[a]	Weight residue at 900 °C (%)[a]	T1max (°C)[b]	T2max (°C)[b]
0/100	299.65	15.28	383.15	--
30/70	322.29	23.80	388.42	509.12
40/60	328.63	27.11	377.45	511.14
50/50	336.25	31.93	385.66	513.17

PEI/PBT blend (wt%)	Ti (°C)[a]	Weight residue at 900 °C (%)[a]	T1max (°C)[b]	T2max (°C)[b]
60/40	345.28	32.48	390.52	525.32
70/30	341.23	36.31	383.48	518.65
80/20	353.92	43.40	394.53	529.85
100/0	497.45	53.56	--	538.64
Uf-PBT[c]	*356.90*	*0.1146*	*434.07*	--

[a] Data obtained from TGA curves.

[b] Data obtained from DTGA curves.

[c] Data obtained from TGA and DTGA curves in Figure A- 5.1b).

TGA results reveal that PEI/PBT blends decomposition is strongly influenced by each polymer thermal behavior. However, it is not clear the existence of possible interactions between blends' constituents or their decomposition products. Several authors have reported that depending on the nature of these interactions blends may exhibit positive or negative effects on thermal stability.[182–184,188,196] Although it is not the aim of this work to study the mechanisms of decomposition of PEI/PBT blends, we calculated the theoretical TGA and DTG curves by using the additivity relation that allows studying the interaction between PEI, PBT, and their decomposition products. If the experimental data of the individual components is multiplied by a factor corresponding to the wt% of each component in the blend, the resulting data will represent the thermal behavior expected for each composition in the absence of any kind of interaction between phases or their decomposition products.[182–184,188,196] The differences found between both, the experimental and calculated data, yields information about the existence of some kind of interaction (molecule-molecule, molecule-radical, radical-radical) during thermal decomposition.

In Figure 3.27 there are presented the experimental and calculated results of three PEI/PBT blends containing 30 wt%, 50 wt% and 80 wt% of PEI. The curves for pure polymers are also shown for comparative purposes. The solid lines represent the behavior observed experimentally and the dashed lines the calculated weight loss curves in the absence of any interaction. For all compositions, it is noticed that both curves have a similar tendency, with two step decomposition behavior corresponding to each phase response. During the first decomposition step, the experimental and predicted curves are in good agreement, it corroborated that PEI delays the initial degradation of PBT phase improving its thermal stability. In their work on

PVC/PS blends, Dodson and coworkers[183] found that the TGA signal for blends containing 1:1 by weight of each component exhibited a notorious delay in the weight loss curve within the range between 250 °C and 350 °C. In this region, the initial decomposition of PVC takes place; hence the delay is attributable to PS phase help to retard the dehydrochlorination reaction of PVC.

Nevertheless, our results reveal clear differences between experimental and calculated curves that appear just before the decomposition signal of the second step. It is noticed that the loss weight behavior of the experimental curves is lower than that of the theoretical curves, as a sign of some kind of interaction that is taking place, leading to the less stable polymer (PBT) destabilize the more stable one (PEI). Previously, it was mentioned that some interactions could involve diffusion of small species (molecules, radicals, or both) between phases.[182] Some PBT thermal decomposition products or byproducts (butadiene, tetrahydrofuran, or acetaldehyde)[197–199] may interact with the PEI molecule causing its prompt degradation during step two.

The presence of the flame retardant additive in the blends (antimony trioxide and bromide compounds) also affects the thermal stability of PEI. In the morphological analysis of blends, it is observed that Sb_2O_3 particles are well dispersed along the whole samples, even in the PEI phase of PEI-rich blends. The decomposition event observed at 500 °C —which correspond to antimony oxide signal— coincide with the early decomposition of the PEI phase in the blends, accelerating the presence of products such as phenol, benzonitrile, and isopropylene groups decomposition products that commonly appear at 550 °C.[200]

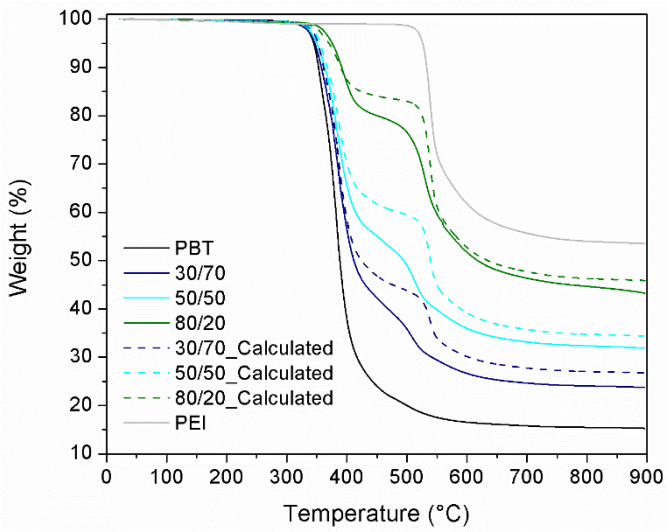

Figure 3.27 Experimental and calculated TGA curves for three representative PEI/PBT blends: 30/70, 50/50 and 80/20.

To better understand the effect of these interactions on the thermal stability of blends, we evaluate different characteristic decomposition temperatures. The corresponding plots of the initial decomposition temperature (Ti), and the temperatures at 10% (T10) and 40% (T40) of mass loss, are shown in Figure 3.28 as a function of PEI content. In general, the analysis is performed when the samples have lost 50% of the weight. However, PEI does not reach weight loss higher than 50 %, hence 40% will be used.

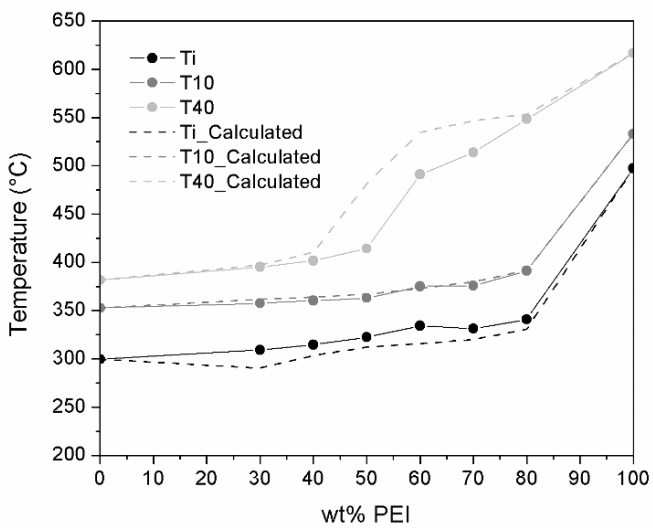

Figure 3.28 Experimental and calculated characteristic temperatures at different weight losses (Ti, T10, and T40).

It is noticed that the experimental data of Ti are slightly higher than the predicted, as a sign of a smooth improvement of PBT thermal stability caused by PEI addition. In the case of T10 experimental and calculated values, they are superposed for all PEI compositions. These results support the fact that there are neither interactions between blends constituents nor their degradation products during the first degradation step. At 40% weight loss (T40), the second degradation step has already appear, and it is observed that the experimental and calculated temperatures differ considerably in the composition region from 40 wt% to 80 wt% of PEI. Just before 40 wt%, the experimental values are similar to the calculated ones. However, when PEI concentrations is higher than 40 wt%, the characteristic temperature T40 increases abruptly as a sign of improvement in blends thermal stability. This is attributed to a combination of factors: the increase in PEI concentrations and the phase inversion phenomena that takes place at even compositions of PEI and PBT, where PEI phase starts being continuous. It is known that in immiscible blends, the change of continuous to discrete phases as the composition varied can also affect the thermal stability of blends. In their work, Sonnier and coworkers[201] evaluated the thermal and fire behavior of immiscible PC/PBT blends, finding that co-continuous morphology

improves considerably the thermal and fire resistance of PBT. They explained this behavior from PC charring characteristic, which forms a barrier that impedes decomposition rate of PBT when char covers the entire sample surface.

However, at difference of Sonnier and coworkers findings, when temperature reaches 450 °C PEI has not start to form the charring products. At this temperature, decomposition products of PEI such as phenol, benzonitrile, benzene, and aniline start to appear, just as reported by Perng in his work.[200] The effect of these products on the thermal stability of blends is noticed as a pronounced gap between the experimental and calculated characteristic temperatures, caused by the interaction between PBT and PEI degradation products.

Flame retardancy of PEI/PBT blends

As mentioned in Section 2.4.3.1, the most effective flame retardants are those which promote the transformation of a polymer backbone to carbonaceous products because char does not burn in normally air conditions (LOI > 50%).[27] From TGA results, it is noticed that PEI enhance the amount of residues produced by blends at 900 °C. In this part of the study, it is discussed the effect of composition on the limiting oxygen index (LOI) of blends, and on their flammability resistance.

Effect of blends composition on the limiting oxygen index (LOI) and charring formation

A first approach to study flammability of a polymer is by knowing its LOI. As oxygen concentration in the air is around 21%, measuring the limiting oxygen index will give key information on the minimum oxygen content necessary for the polymer to ignite. When the LOI < 21%, the polymer is considered flammable; when LOI > 21%, the polymer will not burn in normal air conditions; when LOI = 25%, the polymer is considered of low flammability; and when LOI > 50%, polymer does not ignite in air.[27]

In Table 3.9 are listed the LOI values of polymers used in this work, obtained from the supplier's data sheet. The PEI LOI value is close to the ignition limit (LOI > 50%), and it is much larger than that of the flame retardant PBT (LOI = 30). When compare the LOI values in both PBT samples, it is noticed that antimony and bromide compound increases by 60% the flammability of PBT, contrasted to that of unfilled PBT.

Table 3.9 Limiting oxygen index (LOI) values for pure materials. Data obtained from the supplier's data sheet.

Polymer	LOI (%)
PEI	47
PBT	30
Uf-PBT	20 – 21

We use the additivity rule to predict the LOI of PEI/PBT blends by using the LOI values of pure materials. Additionally, we compare these results with those of blends charring formation, obtained from the residues percentages values in TGA results. The LOI results are plotted as a function of PEI concentration in Figure 3.29a). We compare the predicted flammability results for blends fabricated between PEI and flame retarded PBT (PEI/PBT), and between PEI and unfilled PBT (PEI/Uf-PBT). The two horizontal dotted lines demarcate the low flammability limit and the limit of burning in air. All LOI values for PEI/PBT blends are situated between both limits, which means that in theory, none of the blends burn under normal air conditions or display low flammability. On the other hand, the combination of PEI with unfilled PBT leads to increase considerably the LOI value with only adding 30 wt% of PEI, overpassing the limit from flammable to low flammability. At higher PEI concentrations (PEI-rich blends), the effect of PEI on PEI/Uf-PBT blends LOI is quite similar to blends with flame retarded PBT.

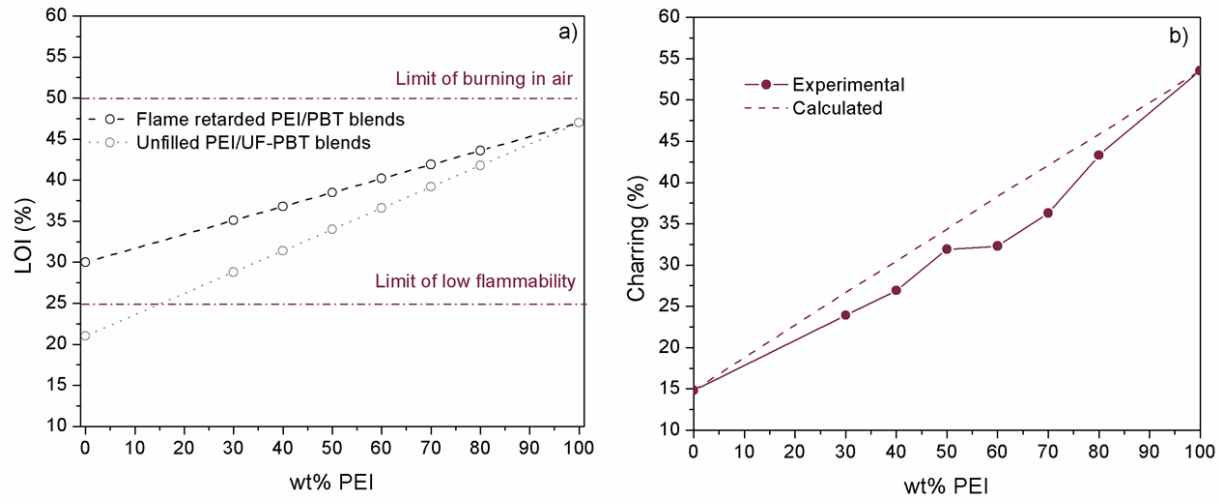

Figure 3.29 Flame behavior PEI/PBT blends: a) predicted LOI values for blends between PEI and flame retarded PBT, and unfilled PBT, and b) experimental and calculated charring percentage as a function of PEI concentration.

When char formation is measured in TGA results as the residual material after pyrolysis at 850 °C, it can be directly related to LOI.[27] According to TGA results showed previously, charring

formation of PEI/PBT blends is mainly attributed to PEI concentration. Figure 3.29b) shows the experimental and calculated charring amount of PEI/PBT blends as a function of PEI addition. Even though the experimental results are lower than the predicted ones in the entire compositional range —caused by the interaction between decomposition products of PBT with those of PEI—, it is noticed that charring products increase monotonically with PEI addition. These results confirm that even at low concentrations of PEI, its inherent charring ability is transferred to PEI/PBT blends, improving their resistance to flame propagation.

Above results confirm that PEI improves thermal stability and flame inhibition of PBT, even for unfilled PBT sample. These findings emerge as a striking option to replace conventional halogenated flame retardant compounds by blending engineering polymers with specialty polymers such as PEI. This assumption is clearly noticed in the results obtained after flammability tests.

Horizontal burning flammability test

Flammability experiments are performed in accordance with the Underwriters Laboratories standard UL94 for “Plastic Materials for Parts in Devices and Appliances”. This standard is commonly used for classifying polymeric materials (including polymer blends) used in electrical applications. We used the horizontal burning test similar to ASTM D635 tests, where bar specimens of 125 mm x 12 mm are directly exposed to flame, as shown in the assembly in Figure 3.21. Materials classified under this test should not have or exceed a burning rate of 75 mm/min over a 75 mm distance, for specimen’s thickness of 3 mm.

Figure 3.30 shows the qualitative results of flame resistance of PEI, PBT, and two representatives PEI/PBT blends, 40/60 and 70/30. Results are presented as a function of burning time from 0 to 120 seconds. It is noticed that in neither, the pure constituents nor their blends, the flame reach the first mark located at 25 mm from specimen’s tip after 60 s exposures. We expose the samples to flame more than 60 s, and no significant burning rate evolution was observed. These results indicate PEI/PBT blends classify as slow burning specimens (HB) according to UL94 standard for horizontal burning tests, since their burning rate is much lower than that stablished by the standard of 75 mm/min.

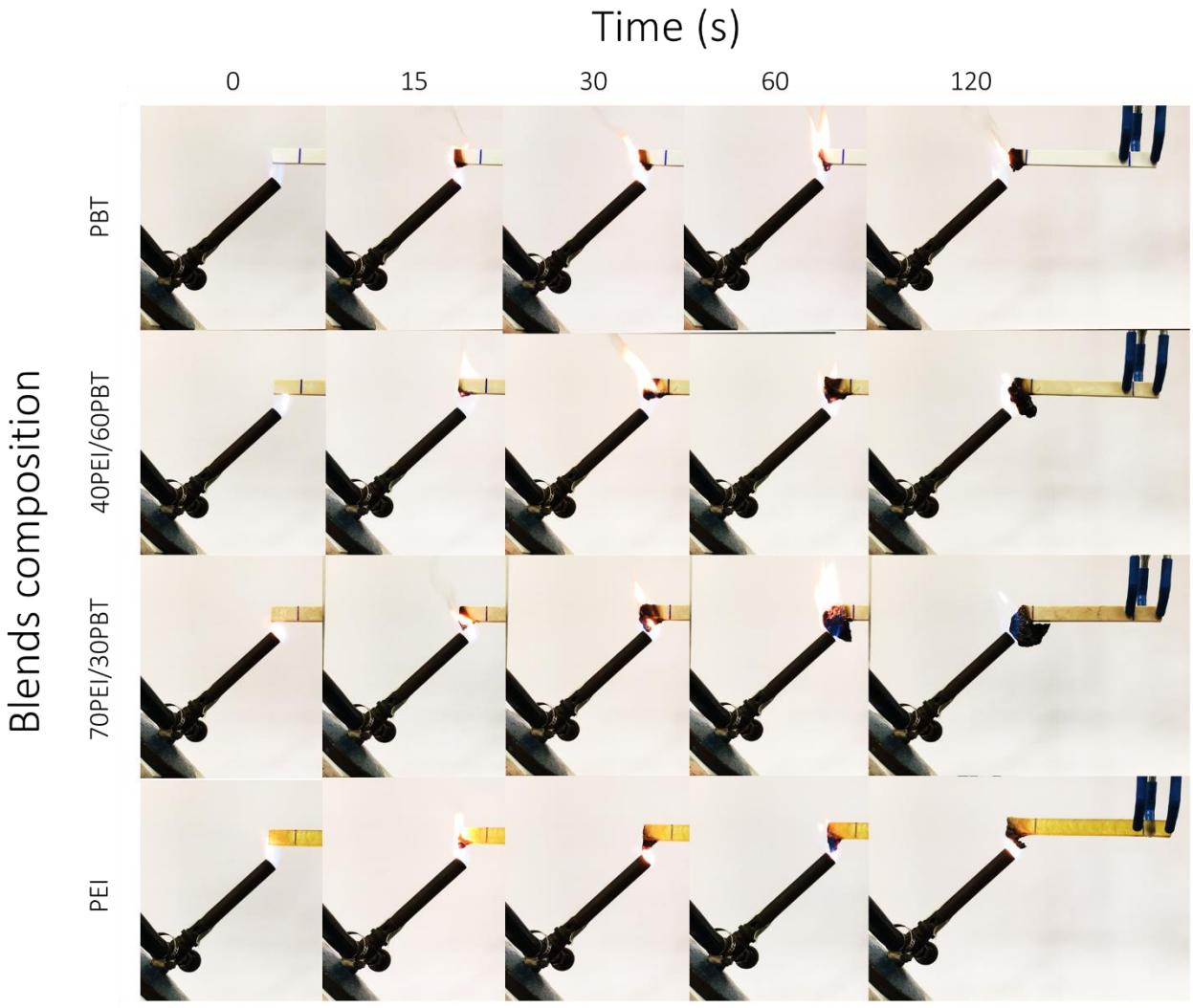

Figure 3.30 Time evolution during flammability tests for HB classification of pure PEI, pure PBT, and two PEI/PBT blends, containing 40 wt% and 70 wt% of PEI.

As observed in TGA results, the decomposition of PBT does not lead to high carbonaceous residues production (char formation). However, flammability results for PBT show that flame do not reach the 25 mm mark after 120 s of direct flame exposure, suggesting that PBT flame retardancy is controlled by the synergic self-extinguish effect caused by the antimony oxides and bromide compound reaction.[130,131,195,202] This assumption is made on the basis that the carbonaceous products formed over PBT surface are not large enough to avoid flame propagation and material consumption.

Conversely, results for 40/60 and 70/30 blends suggest that the flame retardancy is dominated by a combination of the self-extinguish effect of PBT additive with a strong influence of PEI charring formation. Large amounts of charring products are produced over the specimens avoiding flame to propagate through the inner sample. Finally, a remarkable flame resistance of

PEI sample is observed. The flame does not propagate along the PEI specimen because of the layer of charring products formed. Even after four minutes of direct flame contact, the PEI sample integrity is kept.

Figure 3.31 presents the results for all blends after 4 minutes of direct flame exposure. The upper dashed line delimits the maximum length of the specimens (125 mm), and the lower dashed line the first mark at a length of 25 mm from the specimen's tip. It is noticed that all blends exhibited charring products formations, and they are bigger than the initial specimen length for PEI-rich blends. This is caused by the higher amount of PEI phase in the blends.

As the flame did not overpass the first mark at 25 mm, it is possible to classify the pure materials and all their blends as HB, which according to the UL94 standard is the maximum flame retardant grade. This is due to the carbonaceous chars formed —also called intumescent layer— protected blends against direct fire exposition, and as they are appropriately form, they slow down their further thermal decomposition.

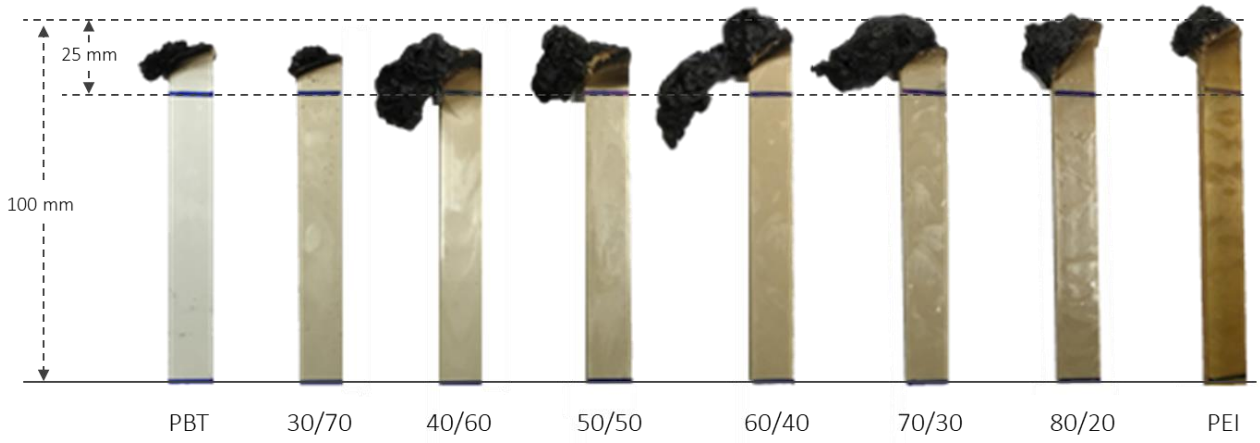

Figure 3.31 Photographs of the specimens of pure PEI, pure PBT, and PEI/PBT blends, after 4 minutes in direct contact with the flame in the HB test. PEI content increasing is shown from left to right.

Above results in LOI analysis and the horizontal burning test, indicate PEI/PBT blends have great potential to be applied in situations where flame resistance is required. In Table 3.10 are presented some examples of commercial polymer blends used in automotive, medical, sports, applications, to name a few. PEI/PBT blends LOI are higher than those presented in Table 3.10, suggesting that blends produced in this work stand more several conditions than those of commercial ones. Additionally, the horizontal burning flame is quite similar, particularly for PEI-rich blends where flame propagation is inhibited by charring formation promoted by the PEI phase.

Table 3.10 Commercial polymer blends used in flame retardant application.[23]

Polymer/Blend	Trade name	UL 94 flame classification – (Flame propagation in mm)	LOI (%)	Applications
PC/ABS	Cycoloy	HB – (1.54)	<21	Thin wall applications, cable channels, hospital cleaners, automotive interiors, etc.
ASA/PC	Geloy	HB – (1.60)	--	Outdoors and indoors applications for automotive industry
PC/PBT	Xenoy	HB – (1.55)	--	Interior pieces for automotive industry
PC/ABS	Bayblend	--	28	Automotive, electrical/electronic, sports, etc.

3.4 Conclusions – Chapter 3

We developed a new two-step melt processing method to obtain binary blends between two HPP, PEI and PBT, by means of a melt-processing method. The major processing parameters were settled in such a way that it is possible to obtain blends in the entire composition range without varying any parameter, except blends composition. In contrast to other works on PEI/PBT blends, this sequential melt processing method is easily scaled to industrial methods such as extrusion, injection molding, etc., since blends were obtain by means of an internal mixer, which is a technique commonly used in polymers industry to set the melt-processing parameters.

The results from miscibility study revealed that PEI/PBT blends are partially miscible, and the degree of miscibility is mostly affected by blends composition. To better understand phases' distribution within the entire composition range, we presented for the very first time the evaluation of morphological evolution of PEI/PBT blends. We identified two major groups of blends that obey to Taylor and Grace's theory: PBT-rich blends and PEI-rich blends. The former exhibits coarse particles of PEI that are distributed along the PBT matrix, together with little sub-inclusions of PBT retained by the highly viscous PEI phase. The second group on the other hand, shows tiny PBT droplets well dispersed along the PEI matrix, with the formation of a curious morphology —that we called spore-like morphology—. Additionally, it was found that at even

concentrations of PEI and PBT, blends experience a dual-phase transition where PEI and PBT phases are co-continuous.

The mechanical, thermal, and flammability performance of PEI/PBT blends is clearly influenced by blends' morphology. The tensile properties revealed that PBT-rich blends have poor tensile strength and ductility due to the coarse PEI droplets size; and that PEI-rich blends display a positive deviation from additivity in both, modulus and tensile strength, as well as a synergic effect in 80/20 blend. However, the ductility is also compromised by blends densification. On the other hand, 50/50 blend exhibits similar modulus value to that of pure PEI, together with higher ductility than other blends due to its cocontinous morphology. Regarding the thermal and flammability performance, the addition of PEI increases the thermal stability of PBT phase and reduces the flame propagation rate in PEI/PBT blends promoting charring formation. From the prediction of the limiting oxygen index, it was found that blends between PEI and Uf-PBT improves unfilled PBT flame resistance considerably, appearing this as a remarkable opportunity to obtain new flame retardant materials without using conventional halogenated compounds.

Chapter 4 Modification of the mechanical properties of binary PEI/PBT blends by adding a third component: PTFE

4.1 PART I – Development and phase behavior study of ternary (PEI/PBT)/PTFE blends by using a two-step melt processing method

4.1.1 Introduction

Improving the performance of existent materials is one of the major motivations on polymer blends development. Even in binary polymer blends, the addition of a third component is an attractive way to increase their mechanical, thermal, electrical or chemical resistance, or enhanced their processability. Nevertheless, to obtain a single material with the desired properties by mixing together three or more polymeric phases is a challenging task, since polymers tend to be thermodynamically immiscible, and it may result in incompatibility between the phases involved.

Elongation at breaks results observed for binary PEI/PBT blends encouraged us to add a third component to the binary blends. Even though the addition of PEI phase increases the stiffness of blends —even a synergic behavior is observed in Young modulus values for blends containing 50 wt% of PEI and 80 wt% of PEI—, the final result is an abrupt ductility decrease caused by densification of blends. In previous works, Zabaleta and collaborators[96] studied the improvement of impact strength of PEI/PBT blends by adding rubbery particles composed by a grafted poly(ethylene octene) copolymer (mPEO) and maleic anhydride. They found that impact strength was enhanced in tenfold respect the 80PEI/20PBT blend. However, they obtained highly debonded rubbery particles that decrease even more the ductility of blends.

In order to modify the formulations of PEI/PBT blends in our work, without altering other processing parameters than composition, we needed to find a polymer that stands the processing conditions established previously on the fabrication of binary PEI/PBT blends by melt processing. Conversely to Zabaleta and coworkers, we avoid the use of rubbery materials since the high processing temperatures used in this work could lead to their degradation. Besides, the third polymer has to contribute not only with mechanical but also with thermal and fire resistance performance. For this purpose, we selected poly(tetrafluoroethylene) (PTFE).

PTFE is mostly combined with other polymers to improve their tribological properties, since it has the lowest coefficient of friction from all polymers.[108–113,117] However, it has also excellent mechanical properties as well as high thermal stability and fire resistant.[109–116] PTFE is commonly added either as a filler in the solid state to form polymer composites or as a new phase to produce polymer blends, depending on the processing method used (solution or melt processing). Polymers such as PU, PI, PEEK, PHBA, and others, are found to be mixed with PTFE to improve their hydrophobic properties, thermal stability, friction and chemical resistance, etc.[110,112,115] PTFE has also been used in proportions from 5 wt% to 20 wt% as a solid lubricant in blends with PEI[120] and with PBT for under the hood applications in the automotive industry.[121]

In this section, it is described the fabrication of ternary (PEI/PBT)/PTFE blends using the two-step melt processing method proposed in Chapter 3. During experimentation we noticed PTFE phase must to be added during step 1 to enhance the integration of PEI and PTFE phases. The morphology achieved during step 1 reveals that PEI favors PTFE phase spheroidization and a later addition of PBT during step 2 enhances the integration of all phases together.

The interfacial tension study between all polymer pairs is calculated from the theoretical harmonic mean method by using Equation 3.6. From these results, it is inferred that due to the high interfacial tension between components ($\gamma_{PEI/PTFE}$ and $\gamma_{PBT/PTFE}$), PTFE phase does not interfere with PEI and PBT interaction, and the same morphologies as those obtained in binary PEI-rich blends will be formed. This is confirmed by the SEM and TEM observations, where there are noticed clear differences between the three immiscible phases. Additionally, we contrasted the morphological results with the spreading coefficient prediction described in Equation 2.18, and a complete wetting of PEI to both, PBT and PTFE phases was found. This behavior is attributed to the notable difference between the polar components of the interfacial ten-

sions between PBT and PTFE phases, which favor the encapsulation of PTFE by the PEI phase in the PBT-rich ternary blends.

4.1.2 Experimental

Materials

Ternary (PEI/PBT)/PTFE blends were fabricated by mixing commercial grade poly(ether imide) (PEI), and flame retarded poly(butylene terephthalate) from Sabic Innovative Plastics, and micronized powder of poly(tetrafluoroethylene) (PTFE), Lanco 1972 from Lubrizol. This commercial reference of PTFE has a maximum particle size of 4 μm, density of 2.2 g/cm^3. PEI and PBT characteristics are described in Table 3.1 in Chapter 3.

Blending process

Before blending all three materials together (PEI, PBT, and PTFE), we obtained binary PEI/PTFE and PBT/PTFE blends in order to study the phase distribution between all polymer pairs. We obtained blends using 20 wt% of PTFE that is the maximum concentration typically used in PTFE based blends. Ternary blends between PEI, PBT, and PTFE were prepared using PTFE concentrations of 5 wt%, 10 wt%, and 15 wt%. These PTFE concentrations are commonly used in industrial polymer blends and composites modifications, where it has been proven they are enough percentage for PTFE to provide the necessary mechanical or tribological properties.[109–116]

Materials were vacuum dried at 110 °C for 16 hours before blending process, and then mixed under a standard atmosphere in a Haake Rheomix 3000 OS internal mixer fitted with roller type rotors. The respective amounts of PEI, PBT, and PTFE for each blend formulation were calculated from each component density by using Equation 3.1.

Ternary blends were fabricated with PEI concentrations greater than 50 wt%, since mixing lower concentrations of PEI (wt% of PEI < 50 %) with PTFE during step 1 results in heterogeneous blends with poor phases integration. PTFE concentrations were calculated according to the binary PEI/PBT blends compositions 50/50, 60/40, 70/30, and 80/20. In Table 4.1 are listed the weight percentage and amount of each phase, as well as the nomenclature for each ternary blend obtained. The feeding sequence of PTFE was based on the results obtained from its thermal characterization.

Table 4.1 Formulation of PEI, PBT, and PTFE to fabricate ternary (PEI/PBT)/PTFE blends with 5 wt%, 10 wt%, and 15 wt% of PTFE.

PEI/PBT blend	PEI (wt%)	PBT (wt%)	PTFE (wt%)	PEI (g)	PBT (g)	PTFE (g)	Designation (PEI/PBT)/PTFE blends
50/50	47.5	47.5	5	168.3	185.5	30.7	50/50/5
	45	45	10	159.4	175.8	61.4	50/50/10
	42.5	42.5	15	150.6	166.0	92.1	50/50/15
60/40	57	38	5	202.0	148.4	30.7	60/40/5
	54	36	10	191.3	140.6	61.4	60/40/10
	51	34	15	180.7	132.8	92.1	60/40/15
70/30	66.5	28.5	5	235.6	111.3	30.7	70/30/5
	63	27	10	223.2	105.5	61.4	70/30/10
	59.5	25.5	15	210.8	99.6	92.1	70/30/15
80/20	76	19	5	269.3	74.2	30.7	80/20/5
	72	18	10	255.1	70.3	61.4	80/20/10
	68	17	15	240.9	66.4	92.1	80/20/15

This study is limited to the modification of PEI/PBT by adding a third component, without altering other parameters different than composition. For that reason, the major processing parameters (processing temperature (Tp), rotors speed (n), and mixing time (t)) are the same used in the two-step melt processing method for obtaining binary PEI/PBT blends.

Thermal characterization of PTFE powders

DSC was performed to PTFE powders in a Q200 model from TA Instruments on 20±1 mg samples. The thermal program started with heating from 0 °C to 380 °C at 20 °C/min, and held on at this temperature for one minute; followed by cooling down to -90 °C at 20 °C min^{-1}. The second heating was performed in modulated mode up to 380 °C at 2 °C/min.

The thermal stability study was carried out in a TGA Q500 model from TA Instruments under a nitrogen atmosphere. Samples of 40±2 mg samples were summited to a temperature range from 25 °C to 900 °C at 10 °C/min.

Ternary blends miscibility evaluation by MDSC

An approach to miscibility between PEI/PBT and PTFE phase was studied by tracking Tg of blends by means of modulated differential scanning calorimetry (MDSC) in a DSC Q200 from TA Instruments. For that, 20±1 mg samples were heated from 0 °C to 290 °C at 20 °C/min, and held on at this temperature for 1 minute, followed by cooling to -30 °C at 20 °C min^{-1}, and heated again in modulated mode from 0°C to 300 °C at 2 °C/min with a modulation amplitude of ±1.27 and period of 60 seconds.

Morphological analysis

Morphological evolution was studied using a scanning electron microscope SEM JOEL JSM-7100. All samples were mechanically cryofracture after immersion in liquid nitrogen for 20 minutes and coated with a gold layer.

To better identify the morphological evolution and to track PTFE dispersion, we used transmission electron microscope TEM Tecnai G2 F20 from FEI. Thin sections of approximately 60 nm thickness were cut with a diamond knife at 25 °C using a Leica ultramicrotome.

Interfacial tension and spreading coefficient analysis

The interfacial tension between all polymer pairs was calculated from a theoretical approach using the harmonic mean equation shown in Equation 2.9 described in section 0:

$$\gamma_{ij} = \gamma_i + \gamma_j - \frac{4{\gamma_i}^d{\gamma_j}^d}{{\gamma_i}^d + {\gamma_j}^d} - \frac{4{\gamma_i}^p{\gamma_j}^p}{{\gamma_i}^p + {\gamma_j}^p}$$

where γ_{ij} is the interfacial tension and γ_i and γ_j are the surface tensions of components i and j. The superscripts d and p correspond to the dispersive and polar components of the surface tensions of each component.

There were first calculated the theoretical surface tension values of PEI, PBT, and PTFE from using literature reports of contact angles obtained with water and diiodomethane by using the Equation 3.6 described previously in section 0:

$$(1 + \cos\theta)\gamma_L = \frac{4{\gamma_s}^d{\gamma_L}^d}{{\gamma_s}^d + {\gamma_L}^d} + \frac{4{\gamma_s}^p{\gamma_L}^p}{{\gamma_s}^p + {\gamma_L}^p}$$

where θ is the contact angle between the liquid and the polymer, γ_L is the total surface tension of the liquid calculated from its dispersive and polar components ($\gamma_L = \gamma^d + \gamma^p$), and ${\gamma_s}^d$ and ${\gamma_s}^p$ are the dispersive and polar components of the solid polymer.

From interfacial tension values, we predicted the morphology that will be formed in the ternary (PEI/PBT)/PTFE blend from using the spreading coefficient approach:

$$\lambda_{31} = \gamma_{12} - \gamma_{32} - \gamma_{13}$$

where γ_{12}, γ_{32}, and γ_{13} are the interfacial tensions for each components pair, and λ_{31} is the spreading coefficient for component 3 on component 1, and describes the physical situation in which component 3 is capable to displace the matrix 2 from component 1 to encapsulate it.

4.1.3 Results and discussion

Thermal analysis of PTFE

The results from thermal analysis of PTFE is presented in Figure 4.1a) (DSC) and Figure 4.1b) (TGA and DTA). A broad endothermic signal appears in the first heating close to 0 °C, which corresponds to crystallinity state changes of PTFE from a triclinic to a hexagonal structure.[203] At higher temperatures, a major endothermic event occurs at 321.08 °C, its melting point (Tm). During the cooling program, there are revealed crystallization temperature (Tc) at 303.68 °C and a minor exothermic peak at 5.84 °C caused by PTFE low-temperature crystallization transition.

The second heating shows an endothermic signal as a sharper peak at 14.08 °C, and the melting transition appears as a double peak close to 320 °C. This behavior is characteristic of PTFE when it is summited to low heating rates, i.e. 2 °C/min as in this case for MDSC mode. At high heating rates (10 °C/min or 20 °C/min) melting peak is sharp with a small shoulder at the low-temperature region. However, when heating rate is slowed down the shoulder evolves to a second peak.[118,204] Regarding glass transition temperature of PTFE, neither the first nor the second heating reveal a clear signal of this transition. According to McCrum, PTFE Tg should appear around 140 °C.[203] This is due to some authors have reported that PTFE reaches crystallinity values around 90% – 95%,[23,205] hence it is difficult to observe its Tg during DSC measurements.

The thermal stability results presented in Figure 4.1b) show that decomposition of PTFE takes place in a single step reaction starting at 485.36 °C. After 600 °C almost the entire PTFE sample has decompose letting only 0.14% of residue. The derivative curve of TGA (dashed line) shows that the maximum decomposition rate occurs at 574 °C.

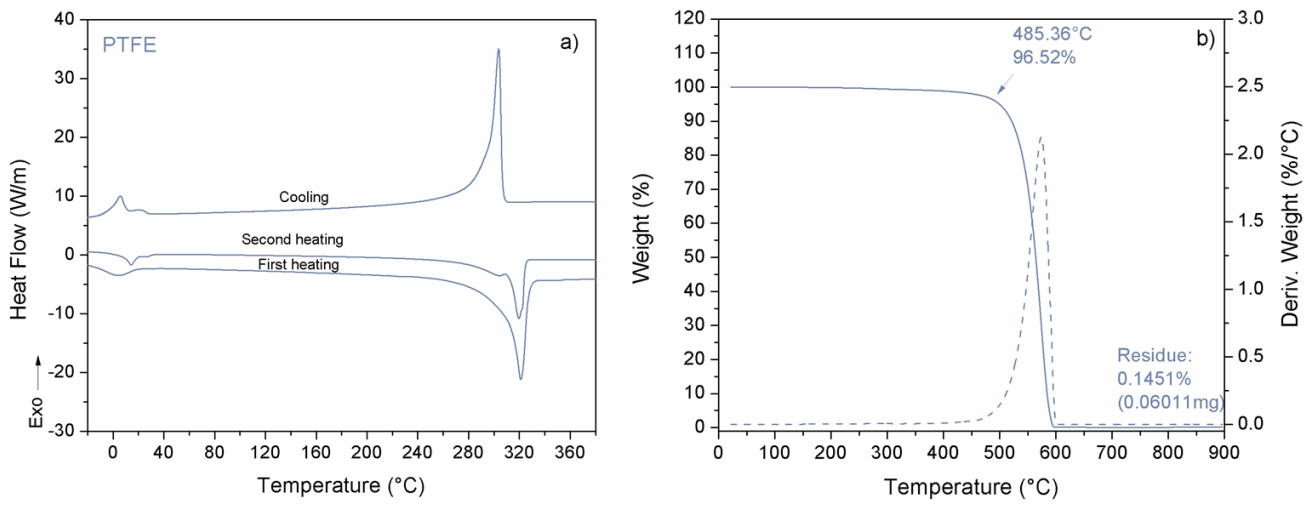

Figure 4.1 Thermal characterization results of PTFE: a) DSC, and b) TGA (solid line) and DTGA (dashed line).

Ternary blends preparation

In order to modify the properties of binary PEI/PBT blends, PTFE phase must be added in some of the steps of the two-step melt processing method proposed in this work. According to the thermal characterization results of PTFE, it can be fed to the mixer during any step in the blending process: at step 1 with PEI phase at 330 °C during ten minutes, or at step 2 with PBT addition at 280 °C during three minutes. Neither of the processing temperatures will lead to PTFE thermal decomposition. Additionally, due to the high crystallinity of PTFE —or in other words due to the lack of presence of amorphous domains in the PTFE phase— it is very unlikely that miscibility exists between the PTFE and the PEI or the PBT. Nevertheless, in order to evaluate the phase's distribution when the PTFE powders are mixed separately with PEI or PBT, we fabricate preliminary binary 80PEI/20PTFE blends and 80PBT/20PTFE blends by keeping the same processing conditions of each phase in Steps 1 and 2, and phase distribution was observed by SEM.

In Figure 4.2 are displayed the SEM micrographs for PTFE powders as received, as well as for binary 80PEI/20PTFE, and 80PBT/20PTFE blends. In Figure 4.2a) the PTFE powders show an irregular geometry and uneven particle size distribution. According to supplier's material data

sheet, particles size average is 4 μm. In Figure 4.2b) it is noticed that PTFE is distributed along the PEI matrix as spheres, apparently with non-interfacial bonding with the PEI matrix. Additionally, some PTFE domains are embedded in the PEI matrix that appear as the brightest white regions in the image. In spite of the porous/debonded appearance, the PEI/PTFE blend is quite compact once it is extracted from the mixer.

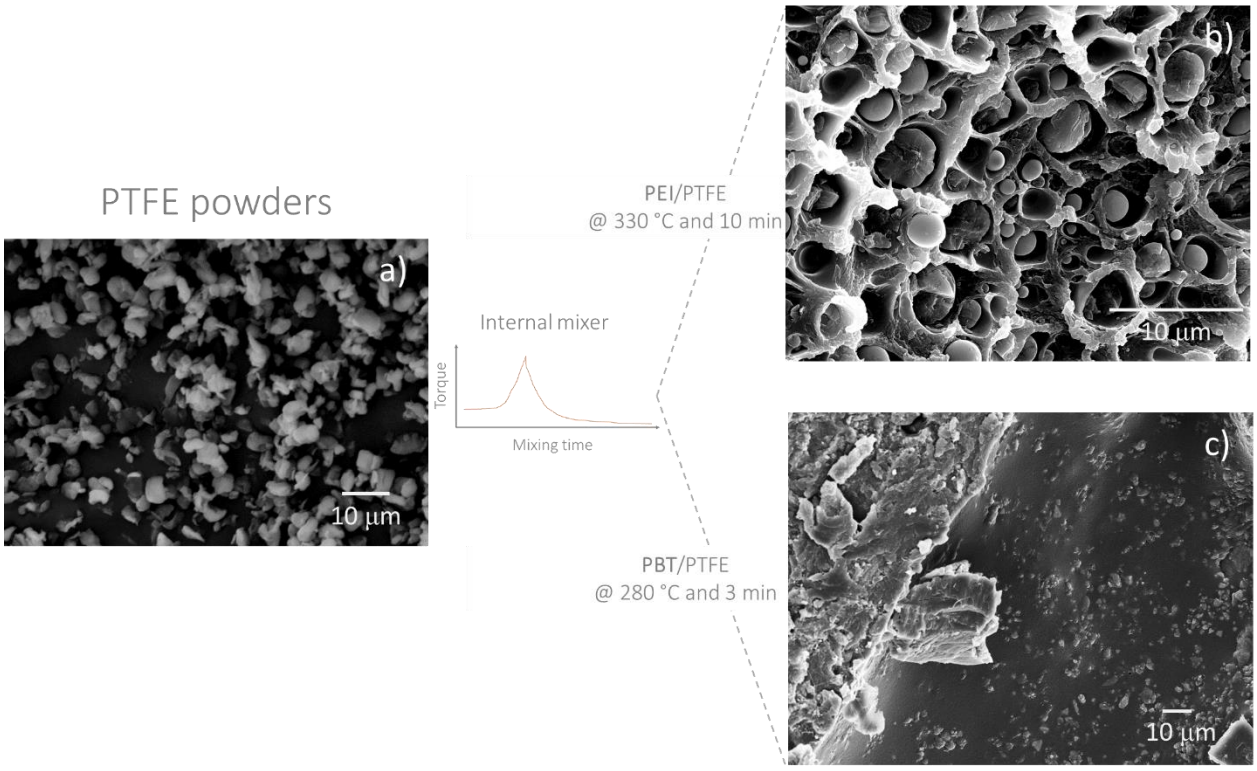

Figure 4.2 SEM micrographs of: a) PTFE powders (Lanco 1972), b) cryofracture surface of 80PEI/20PTFE blend, and c) cryofracture surface of 80PBT/20PTFE blend.

On the other hand, Figure 4.2c) shows the resultant morphology of the PBT/PTFE blend after it is processed at 280 °C during 3 minutes. The SEM results show that the irregular PTFE particles are distributed along the matrix and some agglomerations of PTFE particles are formed. This lack of homogenization between both phases suggests that the processing temperature for PTFE phase is not enough to get soften, hence it remains solid during the entire blending process. Besides, the mixing time is too short to achieve a proper homogenization with PBT phase. In addition, the texture of the blend once removed from the mixer is rough and fragile.

Above results lead us to fabricate the ternary blends feeding PTFE phase during step 1 together with PEI phase.

Two-step melt processing to produce ternary (PEI/PBT)/PTFE blends

After removing the dried PEI pellets from the oven, they are manually premixed with PTFE powders at room temperature and added to the preheated mixing chamber at 330 °C. In Figure 4.3 is displayed the blending process of a ternary 70/30/5 blend, represented by the torque and temperature evolution as a function of time. For comparative purposes, in the right side, it is also exhibited the blending process of a binary PEI/PBT blends for equal concentrations of PEI and PBT. It is noticed that adding 5 wt% of PTFE during step 1 reduces torque values by 75% approximately. This torque reduction is attributable to the low coefficient of friction of PTFE. When the temperature starts to decrease after three minutes, the torque reveals an increase to 13.5 Nm until step 1 is finished. This is a sign that both, PEI and PTFE phases are being properly homogenized during the mixing process.

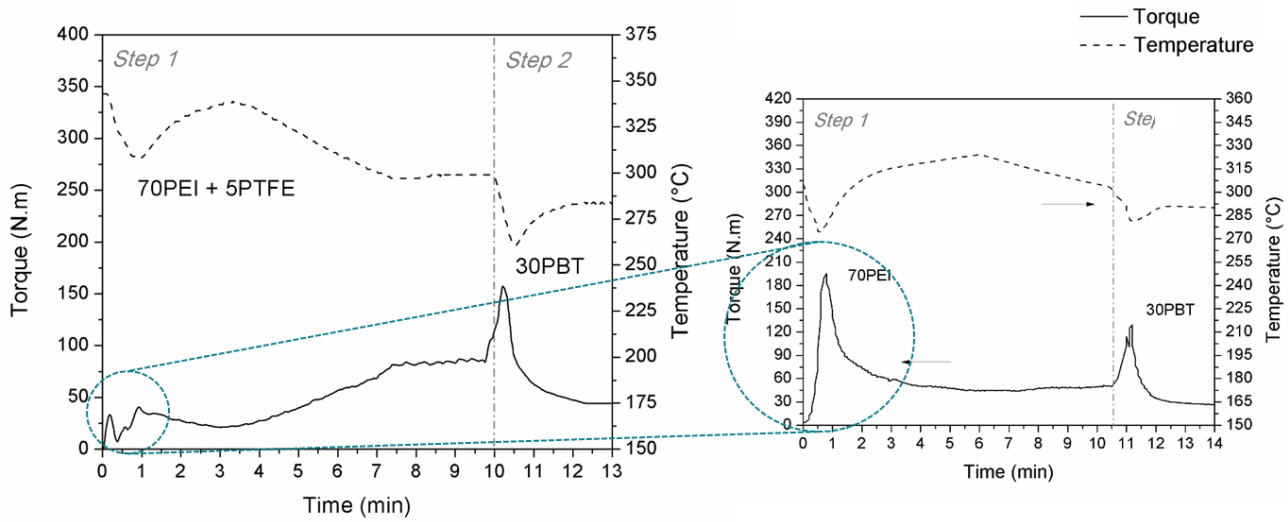

Figure 4.3 Torque and temperature as a function of time for a blend containing 70 wt% of PEI, 30 wt% of PBT, and 5 wt% of PTFE. For comparative purpose, in the right side, it is presented the blending process for equal concentrations of PEI and PBT

During feeding PBT phase in step 2, we observed a similar behavior in both binary and ternary blends. The torque increases to values close to 150 Nm, and temperature decreases to the processing temperature settled for step 2. Nevertheless, after 13 minutes of mixing it is noticed that the torque values for 70/30/5 blend are slightly higher than those of 70/30 blend, suggesting this that viscosity of ternary blends is greater than that of binary blends.

In Figure 4.4, it is exhibited the torque evolution as a function of PEI concentration for binary PEI/PBT blends and ternary (PEI/PBT)/PTFE blends with 15 wt% of PTFE. It is observed a similar PBT effect for both binary and ternary blends. Higher amounts of PBT reduce the torque needed to homogenize the blends, and hence processability is enhanced during step 2. Similarly to

binary blends, blends containing PTFE exhibit a similar behavior at PBT concentrations close to 50 wt%, which suggest this transition is also strongly dependent on blends composition. It is likely that PTFE does not interfere in the interaction between PEI and PBT and also, a cocontinuous morphology is formed.

The higher torque values evidenced for ternary blends are explained from PTFE viscoelastic properties. Even though one may think the torque has to be lower due to the lubricant characteristics of PTFE; these are noticed in the solid state as a considerable reduction in PEI torque values. However, in the molten state the viscosity of PTFE reaches values of around 10 GPas.[23,113,206] However, this increase does not have a major effect on the processability of blends, since the torque values are still between those of the pure components. Similar results were obtained for 5 wt% and 10 wt% PTFE concentrations.

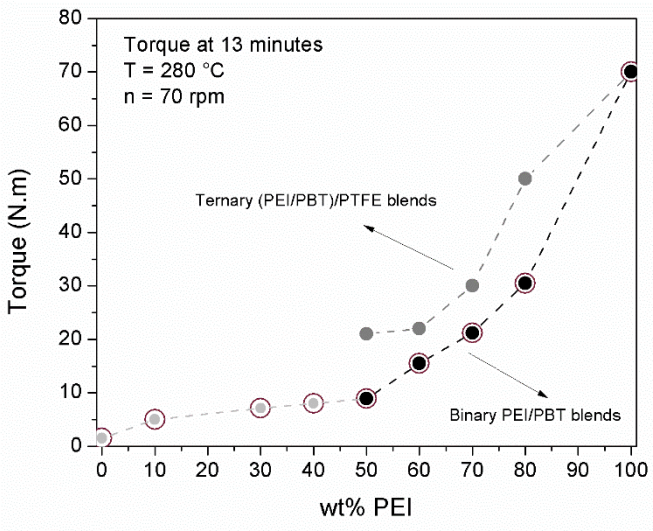

Figure 4.4 Effect of PBT and PTFE on the processability of binary and ternary blends with 15 wt% of PTFE.

Miscibility study of PEI, PBT, and PTFE phases by MDSC

The following discussion on miscibility study by MDSC is made for ternary blends with 5 wt% of PTFE, since the analyses for ternary blends with 10 wt% and 15 wt% of PTFE are quite similar and lead to the same results. In Figure 4.5a) and Figure 4.5b) are presented the MDSC results for cooling and second heating programs, respectively. Results of pure PEI, PBT, and PTFE are also shown for comparative purposes.

In Figure 4.5a), it is noticed that thermal transitions remain invariable to each phase in all blends. The crystallographic transition of PTFE —evidenced at 14.08 °C in the second heating— neither shifts to different temperatures nor is inhibited by the presence of PEI and PBT phases.

PBT Tg exhibits cold crystallization temperature close to its melting temperature, with a smooth displacement to lower temperatures. These results suggest that under the processing conditions used in this work, there is no molecular interaction between PTFE with neither PEI nor PBT, and there is immiscibility between all phases.

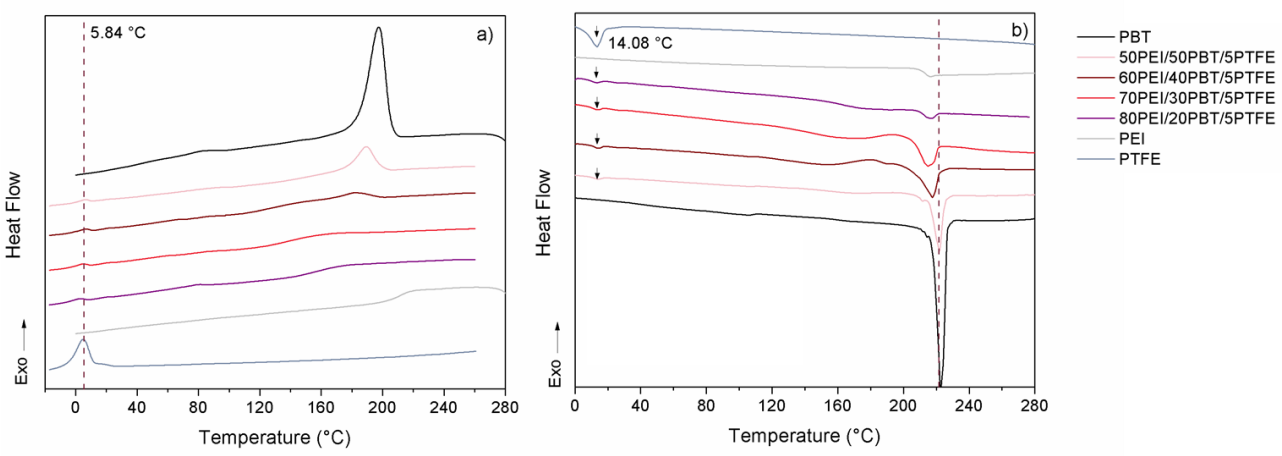

Figure 4.5 Tracking of ternary (PEI/PBT)/PTFE blends Tg from DSC analysis. The thermal transitions are presented during: a) cooling, and b) second heating on modulated mode (MDSC). The data was reorganized on the y-axis for ease of analysis.

To confirm above statement, we contrasted the thermal transitions between ternary blends with 5 wt% of PTFE and binary blends, as it is observed in Figure 4.6. Results displayed in Figure 4.6a) reveal that the small crystallization signal corresponding to PBT in the 50/50/5 blend disappears when PEI phase is increased, and PTFE does not seem to interfere in PBT cold crystallization event. Just as described in the miscibility study in Chapter 3, the inhibition in PBT crystallization when blending with PEI is a sign of partial miscibility between PEI and PBT on PEI-rich blends. These results suggest that the interaction between the thermal transitions of PEI and PBT predominates over those with PTFE with the blends, or even more, there is not interaction at all between the PTFE phase and the PEI/PBT blends. This can be corroborated with the low-cold crystallization thermal transition of PTFE at 5.84 °C, which remain invariable for all blends compositions. These results are attributable to complete immiscibility between PTFE and PEI and PBT phases, which may be linked to the differences between their chemical natures (surface tensions and interfacial energy differences).

In Figure 4.6b), it is noticed that PBT and PEI thermal transitions in both, binary and ternary blends, are the same. These results suggest that, despite having homogenized first PTFE and PEI phases during step 1, PTFE coexist as a separate phase from PEI and PBT phases, and it does not interfere with the interaction between PEI and PBT. This is explained from the poor amorphous

structure of PTFE (crystallinity around 90% – 95%[23,205]) that avoids miscibility with neither, PEI or PBT.

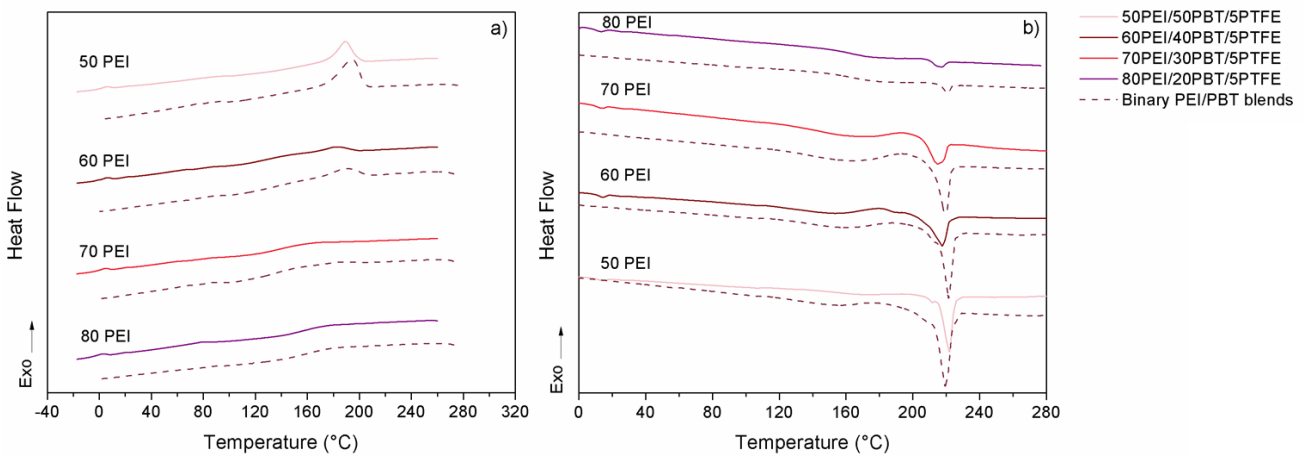

Figure 4.6 Thermal transitions of ternary (PEI/PBT)/PTFE blends with 5 wt% of PTFE contrasted to those of binary PEI/PBT blends: a) cooling, and b) second heating on modulated mode (MDSC). The data was reorganized on the y-axis for ease of analysis.

Morphology evolution of (PEI/PBT)/PTFE blends

It is known that blending immiscible polymers in ternary or multicomponent blends results in new and more complex morphologies. In Chapter 3, it was observed that processing conditions of PBT-rich blends favored a composite droplets morphology of PEI with PBT sub-inclusions. The mentioned morphology is commonly formed when brittle polymers are blended with rubbery particles, e.g. high-impact poly(styrene) (HIPS). Sub-inclusion formation takes place during PS polymerization and is favored by miscibility between the styrene and butadiene phases.

Favis and collaborators, found that PC/PP blends form sub-inclusions at compositions close to 50/50, but also at PC compositions as lower as 20 wt%.[7] They concluded that increasing the viscosity of the dispersed phase enhances the retention of PP sub-inclusions, just as it was observed in the binary PBT-rich blends. However, the occurrence of this particular morphology in ternary blends will strongly depend on the composition and interfacial interaction between components.[76,87,90,207,208]

In order to predict the possible morphologies that will be formed during the melt processing of ternary (PEI/PBT)/PTFE blends, we used a theoretical approach that involves the relationship between the interfacial tensions of all polymer pairs and blends composition.

Interfacial tension in ternary (PEI/PBT)/PTFE blends

When a ternary blend consists of one phase as a matrix with two different dispersive phases, it is possible to study the morphology prediction of ternary blends by some theoretical models such as spreading coefficient, minimum free energy and dynamic interfacial energy. These models include the interfacial values between the different polymer pairs. In this part of the work, we predicted the morphology of (PEI/PBT)/PTFE blends by using the spreading coefficient, since it is easily applied merely measuring or calculating the interfacial tension between blends components, and it has shown to be quite accurate for several polymer systems.[81,83–85]

First, we calculate the surface tension of PEI, PBT and PTFE from using the harmonic method approach described in Equation 3.6. Then, we obtain the interfacial tensions for all possible polymer pairs PEI/PBT, PEI/PTFE, and PBT/PTFE, by using the harmonic mean equation. In Table 4.2 are listed the surface tension values of pure components as well as the respective interfacial tensions for all polymer pairs.

It is noticed that surface tension values for PEI and PBT are very close to each other. In previous sections, the interfacial tension analysis for binary PEI/PBT blends lead to predict immiscibility between both polymers, yet the total surface tensions are quite similar. This is attributable to the marked differences between the polar components of the surface tensions of the constituents, which lead to surface tension values of 3.14 dyn/cm for PEI/PBT blends.

When evaluating the surface tension of PTFE, it is noticed that its value is less than half of that of PEI and PBT ($\gamma_{PTFE} = 19.5\ dyn/cm$). In addition, the polar component is too low letting no doubt that PTFE is completely immiscible with the other two phases in the ternary blends. The interfacial tension values for both PEI/PTFE and PBT/PTFE polymer pairs are greater than 10 dyn/min. According to other findings in the interfacial study of different polymer pairs,[158] if interfacial tension values are greater than 2 dyn/cm the phases are immiscible.

Nevertheless, when comparing the values of the polar components (γ^p) of the three polymers, it is noticed that the differences between PTFE and PEI are lower than that of PTFE and PBT, which suggest that during blending process PTFE will have higher interfacial affinity with PEI phase compared to PBT phase. This explains to some extent the lack of homogeneity during the preparation of binary PBT/PTFE blend as described previously, as well as the immiscibility results obtained in MDSC results.

Table 4.2 Theoretical PEI, PBT, and PTFE surface tension values, and PEI/PBT, PEI/PTFE, and PBT/PTFE interfacial tension values calculated from the harmonic mean equation.

Material	Contact angle (°)		Surface tension (dyn/cm)[d]			Interfacial tension (dyn/cm)[e]		
	Water	Diiodomethane	γ^d	γ^p	γ_T	$\gamma_{PEI/PBT}$	$\gamma_{PEI/PTFE}$	$\gamma_{PBT/PTFE}$
PEI	75[a]	27[a]	41.12	4.94	46.06			
PBT	63[b]	30[b]	36.65	11.92	48.57	3.14	11.84	15.29
PTFE	108[c]	88[c]	18.0	1.5	19.5			

[a] Values obtained from reference[156]

[b] Values obtained from reference[157]

[c] Values obtained from reference[209]

[d] Values calculated from Equation 2.12 using liquids surface tension values obtained from reference[155] [(water $\gamma_T = 72.8\ dyn/cm$; $\gamma^d = 22.1\ dyn/cm$; $\gamma^p = 50.7\ dyn/cm$); (Diiodomethane: $\gamma_T = 50.8\ dyn/cm$; $\gamma^d = 48.5\ dyn/cm$; $\gamma^p = 2.3\ dyn/cm$)].

[e] Values calculated from the harmonic mean equation, Equation 2.9.

The results for morphology prediction of ternary blends from the spreading coefficient model are presented in Table 4.3. The spreading coefficients were calculated for two cases: when PBT is the matrix (for blends containing 50 wt% of PEI and 50 wt% of PBT), and when PEI is the matrix (for PEI-rich blends). Negative values of spreading coefficient, suggest that PEI, PBT, and PTFE phases are distributed as independent phases and no encapsulation will occur. This situation is the more likely to happen in the blends when PEI is the matrix. Conversely, positive values mean that there is encapsulation of one phase, and the core-shell morphology will be more probable to happen. This is observed in the situation where PBT is the matrix.

Table 4.3 Spreading coefficient values of ternary (PEI/PBT)/PTFE blends.

Spreading prediction where any, PEI or PBT is the matrix		λ (dyn/cm)
PEI matrix	$\lambda_{PBT/PTFE} = \gamma_{PEI/PTFE} - \gamma_{PEI/PBT} - \gamma_{PBT/PTFE}$	-6.6
	$\lambda_{PTFE/PBT} = \gamma_{PEI/PBT} - \gamma_{PEI/PTFE} - \gamma_{PBT/PTFE}$	-24.0
PBT matrix	$\lambda_{PEI/PTFE} = \gamma_{PBT/PTFE} - \gamma_{PEI/PBT} - \gamma_{PEI/PTFE}$	0.3
	$\lambda_{PTFE/PEI} = \gamma_{PEI/PBT} - \gamma_{PBT/PTFE} - \gamma_{PEI/PTFE}$	-24.0

The slightly positive spreading coefficient ($\lambda_{PEI/PTFE} = 0.3\ dyn/cm$) suggests that PEI will tend to encapsulate PTFE phase because the high interfacial energy between PBT and PTFE displace

the PTFE phase to PEI domains. In none of the previous situations described, the PTFE phase encapsulates the other component.

Morphology of binary PEI/PTFE blend

Interesting results are observed in PTFE distribution in PEI matrix. Both materials are completely immiscible, which is easily explained by the high interfacial tension values previously described ($\gamma_{PEI/PTFE} = 11.84\ dyn/cm$), and PTFE is distributed in two fashions inside the PEI matrix: as debonded spheres, and as a well-embedded phase in the matrix. In order to understand these distributions, we study more in detail the morphology by SEM and TEM.

In Figure 4.7, there are observed SEM and TEM micrographs at different magnifications. The SEM image (Figure 4.7a)), shows that PTFE spheres have an average number diameter of $Dn = 1.5\ \mu m$ (measured for at least 100 particles), which is lower than PTFE powders particle size received. The PTFE powders transformation into well-defined spheres occurs when it is processed together with PEI at 330 °C. At this temperature PTFE is slightly above its melting temperature (320 °C), and it can reach viscosity values as high as 10 GPas.[23,206] In this state, the material does not behave like a viscoelastic liquid but more like a gel, hence it is easily deformable by the PEI matrix during the shear processing conditions inside the mixer. In addition, the significantly low yield stress (20.7 MPa[210]) needed for PTFE plastic deformation, especially at high temperatures,[117–119] contributes to the spheres formation.

The PEI matrix on the other hand, does not look as the typical smooth surface presented for PEI in the previous chapter (Figure 3.10h)). Instead, it has a rough appearance caused by the well-embedded PTFE phase in the PEI matrix. The TEM image in Figure 4.7b), reveals that PTFE phase looks like the brightest phase in the micrograph surrounded by a black halo that seems to correspond to cavities between PTFE spheres and the PEI/PTFE matrix. The droplets sizes in the TEM image are in good agreement with those of PTFE spheres' diameters calculated from SEM images.

At greater magnifications, 20000x (Figure 4.7c)) and 30000x (Figure 4.7d)), it is revealed that PTFE is distributed in the PEI matrix in a droplets-like fashion, with particle sizes close to 50 nm. The black halo is also visible in most particles, as well as the differences in the color intensities characteristic of PTFE particles. The particle size reduction is attributable to fragmentation of PTFE powders caused by the interaction with PEI during the first minute inside the mixer. Be-

fore PEI gets softened, it acts similar to a “ball mill” grinder, reducing the former particle size of PTFE. This is supported by the low yield stress resistance of PTFE, and it is similarly to the fragmentation behavior observed in the droplet split in half in Figure 4.7a).

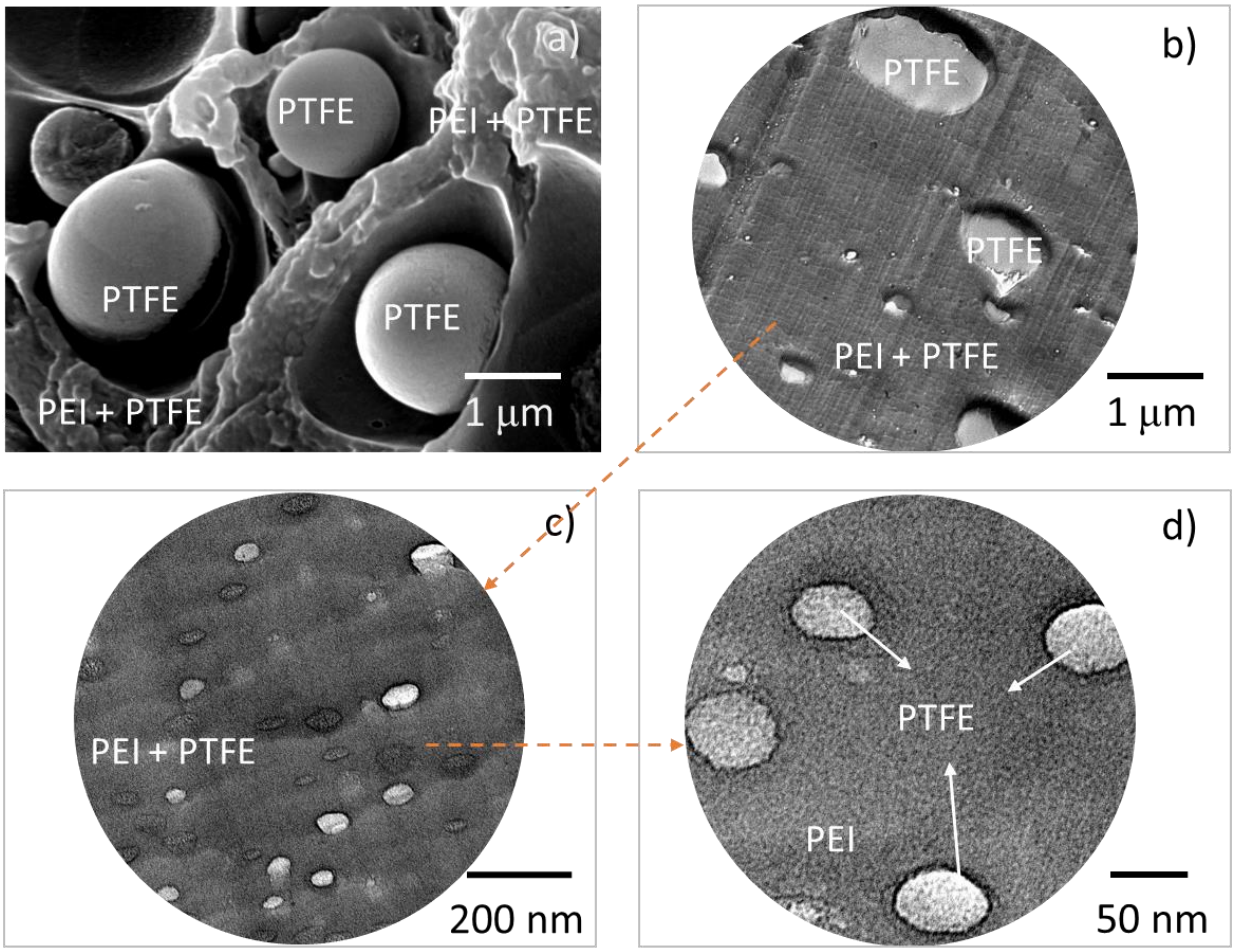

Figure 4.7 Binary 80PEI/20PTFE blend morphology: a) SEM micrograph of PTFE spheroidization, b) TEM micrograph of PEI and PTFE distribution, and c) and d) nano sized PTFE particles embedded in PEI matrix.

It is surprising that the highly crystalline PTFE phase look like white (brighter) particles in the TEM images. What is expected in crystalline phases is to observe darker domains compared to amorphous phases —such as PEI—. During the experimental measurements of TEM, there were observed notable changes in specific domains corresponding to PTFE particles. PTFE phase characterization in both, binary PEI/PTFE and ternary PEI/PBT/PTFE blends, resulted in a very challenging process, since it undergoes through chemical transformations when is exposed to the electron beam, even for short periods. In Figure 4.8 are revealed the changes in PTFE phase after one minute of electron beam exposure, for two blends containing 80PEI/20PTFE (white square), and 50PEI/50PBT/15PTFE (black arrows). It is notable how the darker spots corresponding to PTFE phase, rapidly change to brighter domains. In contrast, the black particle in

the 50PEI/50PBT/15PTFE sample (white circle) does not change after 1 second, since it corresponds to antimony trioxide filler that is not affected during TEM analysis. In their work, Kaushiva and coworkers[211] found similar results during TEM analysis of blends between PTFE and fluorocarbon copolymers. They attributed these changes to chain scission and PTFE degradation during electron beam exposure.

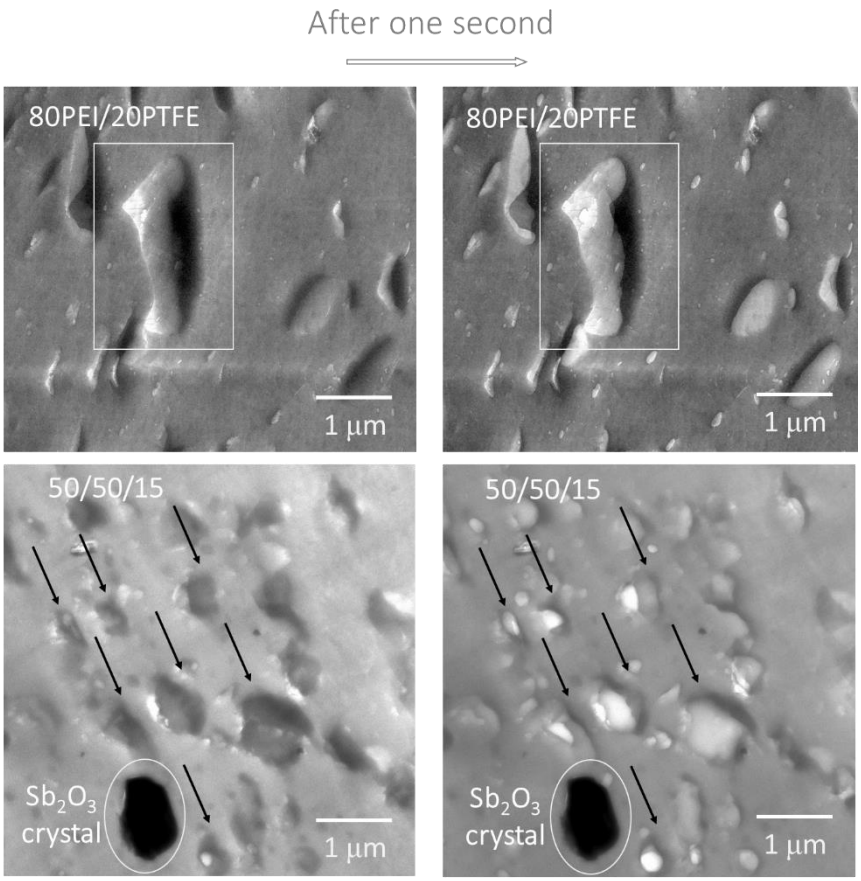

Figure 4.8 Chemical changes evidence in PTFE phase after one second electron beam exposure during TEM measurements for binary 80PEI/20PTFE blend and ternary 50/50/15 blend.

Morphology of binary PBT/PTFE blend

Regarding the distribution of PTFE in PBT matrix processed at 280 °C during three minutes, it is noticed that neither the temperature (below the melting point of PTFE) nor the mixing time are adequate to achieve a proper integration between both phases. Additionally, the calculated interfacial tension between PBT and PTFE is even higher than that between PEI and PTFE ($\gamma_{PBT/PTFE} = 15.29\ dyn/cm$). In Figure 4.9 it is observed the lack of integration between both phases, with the PTFE particles keeping their irregular shape. Additionally, several agglomeration of PTFE domains are observed, together with some fibers. This fibrillation of PTFE has been observed in other PTFE based blends processed at temperatures below the PTFE melting tem-

perature.[117–119] In a recent work, Huang and coworkers[117] studied the in-situ fibrillation of PTFE particles when blended with TPU by melt processing at temperatures range between 165 °C and 185 °C. They attributed this behavior to the low yielding strength of PTFE together with elevated temperatures and long mixing times, and also claimed that when PTFE is added as a filler, it has a tendency to deform into large aspect-ratio fibrillar structures and form interconnected physical entanglements within the matrix polymer. These results suggest that longer mixing periods between PBT and PTFE particles —and probably lower amounts of PTFE than 20 wt%— would result in in-situ PTFE fibers reinforcement to PBT matrix. In their works, Ali[120] and Huang[117] found that the mechanical properties of the respective polymer matrix used, improve substantially by the fibrillary PTFE reinforcement.

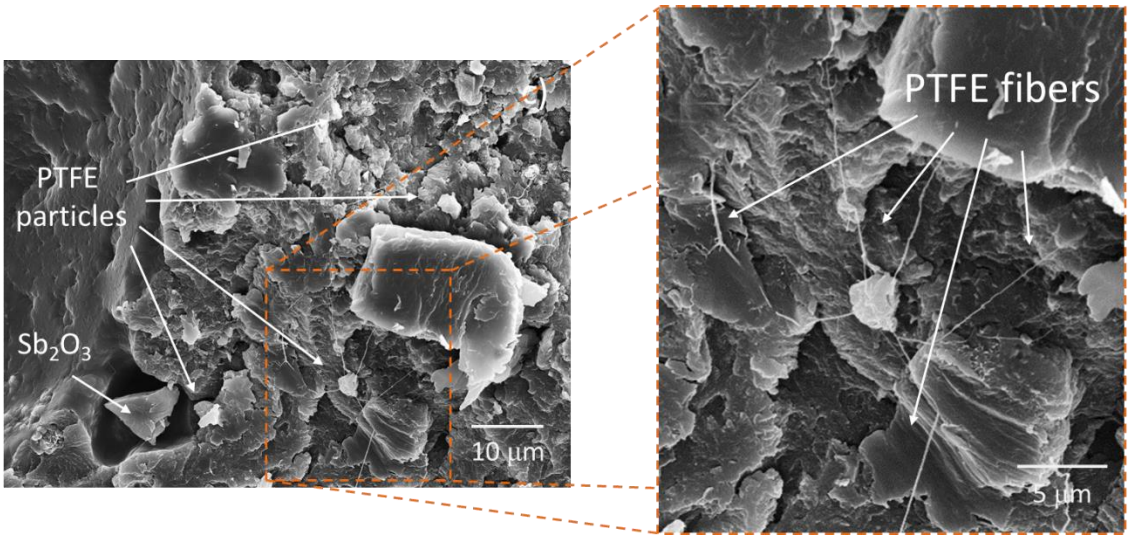

Figure 4.9 SEM micrographs of in situ fibrillation in binary 80PBT/20PTFE blend.

Morphology of ternary (PEI/PBT)/PTFE blends

In Figure 4.10, it is presented a general overview of the morphological evolution of ternary (PEI/PBT)/PTFE blends obtained with 5 wt%, 10 wt%, and 15 wt% of PTFE, and the comparison with the respective binary blends, named in the figure as 0 wt% of PTFE. It is noticed that the increase of PEI concentration leads to similar morphological variations as those observed for binary blends. These evidences suggest that PTFE phase has no influence in the ternary blends morphology that lead them to significant differences respect the binary blends with similar PEI and PBT compositions.

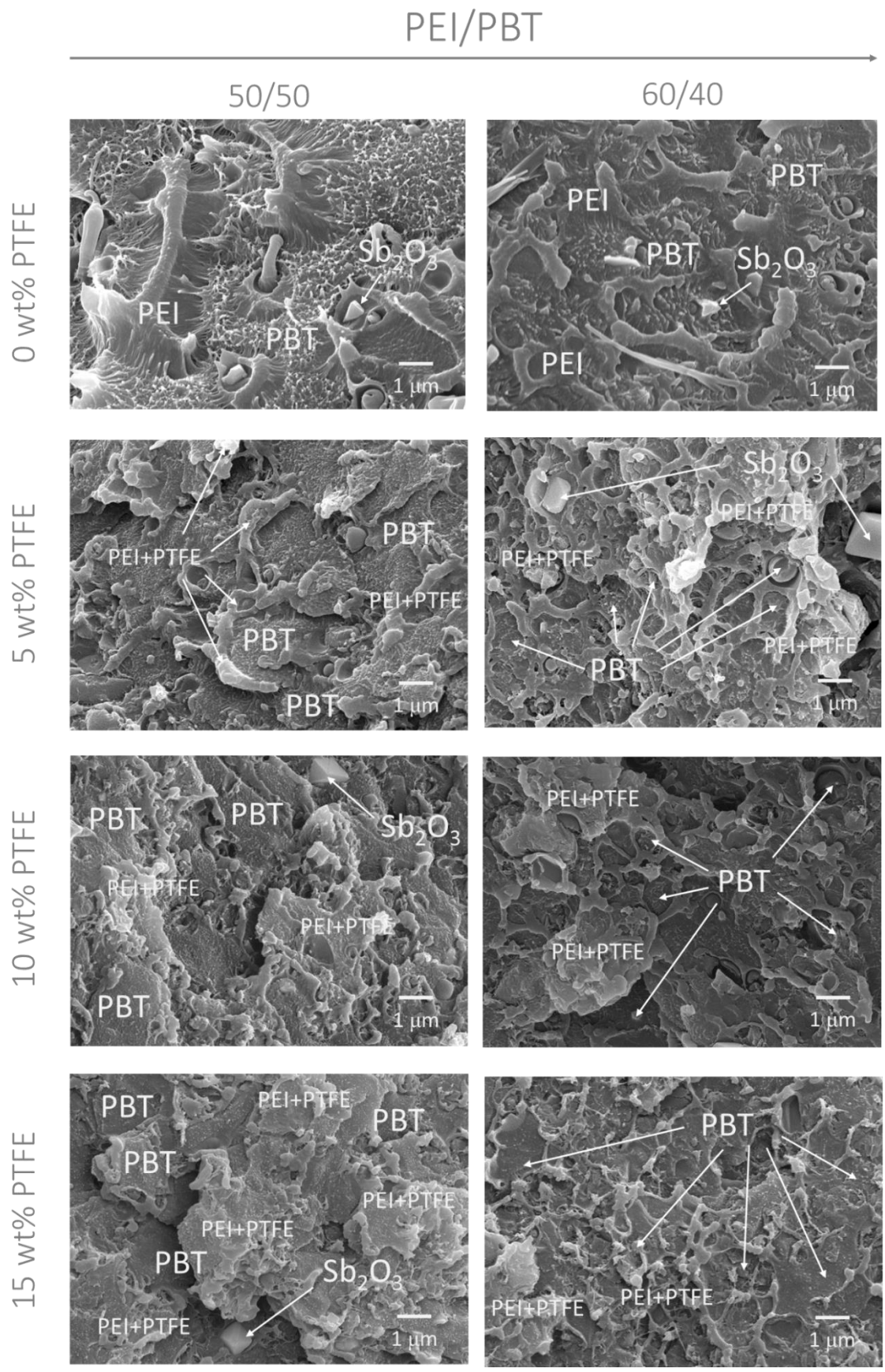

Figure 4.10 SEM micrographs of ternary (PEI/PBT)/PTFE blends. All images were taken at a magnification of 10kX.
(Continue next page)

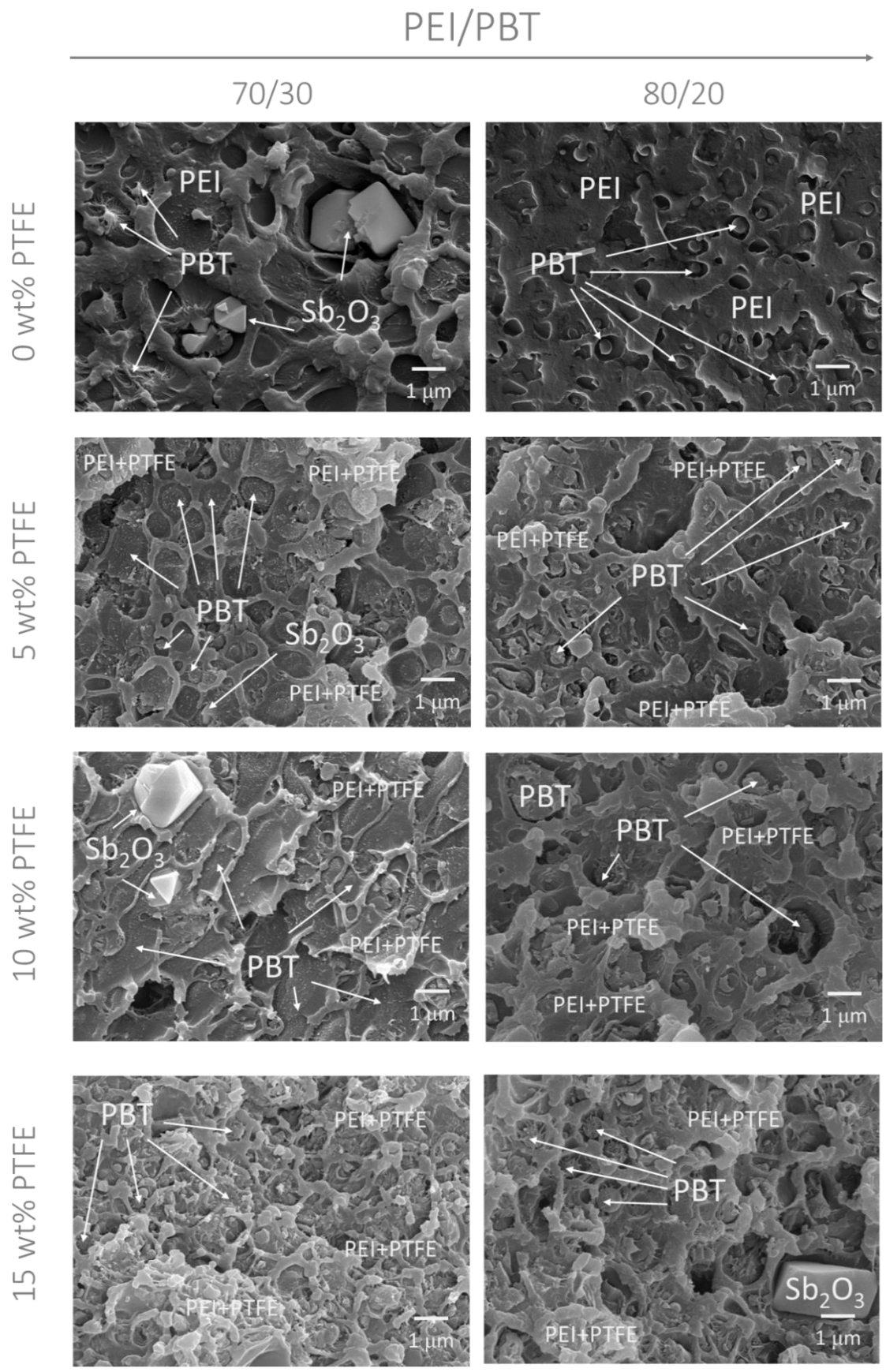

Continuation of Figure 4.10 SEM micrographs of ternary (PEI/PBT)/PTFE blends. All images were taken at a magnification of 10kX.

The mentioned behavior is explained from the high interfacial tension values between both, PEI and PBT phases, with the PTFE phase, and as it is observed in the morphology prediction by the spreading coefficient, in any case PTFE will not encapsulate the other two phases domains. Besides, all processing conditions are kept the same as those used in the two-step melt processing method of binary blends. Hence, the overall morphology of ternary blends will be leaded by the interaction between the PEI and PBT phases.

In Figure 4.11, it is presented a ternary diagram with all the PEI, PBT, and PTFE compositions used in this work, as well as the SEM magnifications of some representative ternary blends morphologies.

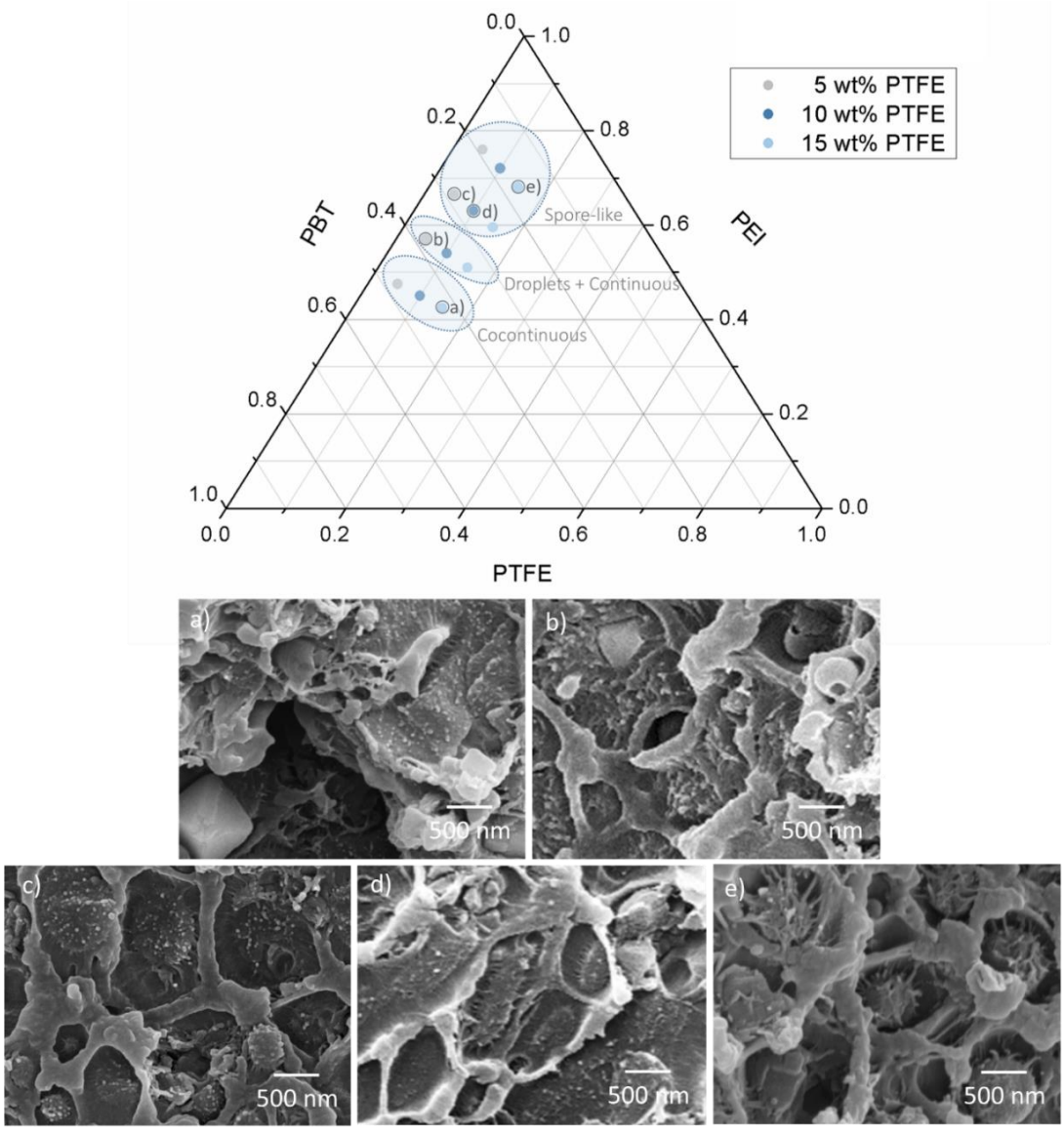

Figure 4.11 Ternary phase diagram of ternary (PEI/PBT)/PTFE blends, and morphology evolution observed by SEM: a) 50/50/15, b) 60/40/5, c) 70/30/5, d) 70/30/10, and e) 80/20/15.

These results confirm that the morphology evolution in the ternary (PEI/PBT)/PTFE blends obtained, starts with a co-continuous distribution (continuous PEI + PTFE, and continuous PBT), followed by PBT droplets and continuous PEI +PTFE morphology, and finaly with a spore like distribution of PBT phase in the PEI + PTFE matrix. This is the same evolution observed with the interaction between PEI and PBT in the binary PEI/PBT system. Besides, in all images in Figure 4.11, the fibrillary interface is formed as a sign of good physical compatibilization. However, the distribution of PTFE phase within the ternary blends is not clearly evidenced in SEM micrographs. To a certain extent, it is attributable to the nano size distribution of PTFE in the PEI matrix.

In order to study the PTFE distribution, we obtain TEM images of the ternary blends. In Figure 4.12, there are compared the binary PEI/PBT blends morphology with that of some representative ternary (PEI/PBT)/PTFE blends, and it is presented a schematic representation of phases distribution where there are overlapped the morphology of binary and ternary blends.

Since PTFE is found to be highly immiscible with both components —due to the high interfacial energy values calculated by the harmonic mean equation— there are three possible situations where PTFE will be preferably located. According to the droplet sandwich scheme described in Figure 2.7, when three immiscible polymers are mixed together three possible phases distribution can occur:[81] i) thin PTFE layers will be formed between PEI and PBT phases, ii) PTFE droplets will be embedded in the phase with which has the lowest interfacial energy, and iii) PTFE droplets will be located just between PEI and PBT phases forming stacked droplet morphology. Based on TEM results, neither of the situations i) or iii) occurs in the ternary blends presented in this work, and only the blend containing 50 wt% of PEI —with co-continuous distribution of PEI and PBT— complies the situation ii). The ternary 50/50/15 blend, exhibit some brighter domains —corresponding to 15 wt% of PTFE phase— that are preferably distributed along one of the continuous phase. As the interfacial tension between PEI and PTFE ($\gamma_{PEI/PTFE} = 11.84\ dyn/cm$) is lower than that of PBT and PTFE ($\gamma_{PBT/PTFE} = 15.29\ dyn/cm$), the PTFE phase is preferably located in the PEI matrix.

A similar analysis is made from the spreading coefficient values listed in Table 4.3. Two groups of blends are considered: PBT-rich blends and PEI-rich blends. In the first group, we consider the blends containing 50 wt% of PEI and 50 wt% of PBT, since at this compositions both phases are co-continuous. The positive spreading coefficient value ($\lambda_{PEI/PTFE} = 0.3\ dyn/cm$) suggests

that the PEI phase will encapsulate the PTFE phase when PBT is the matrix, favoring the complete wetting of PTFE by the PEI phase.

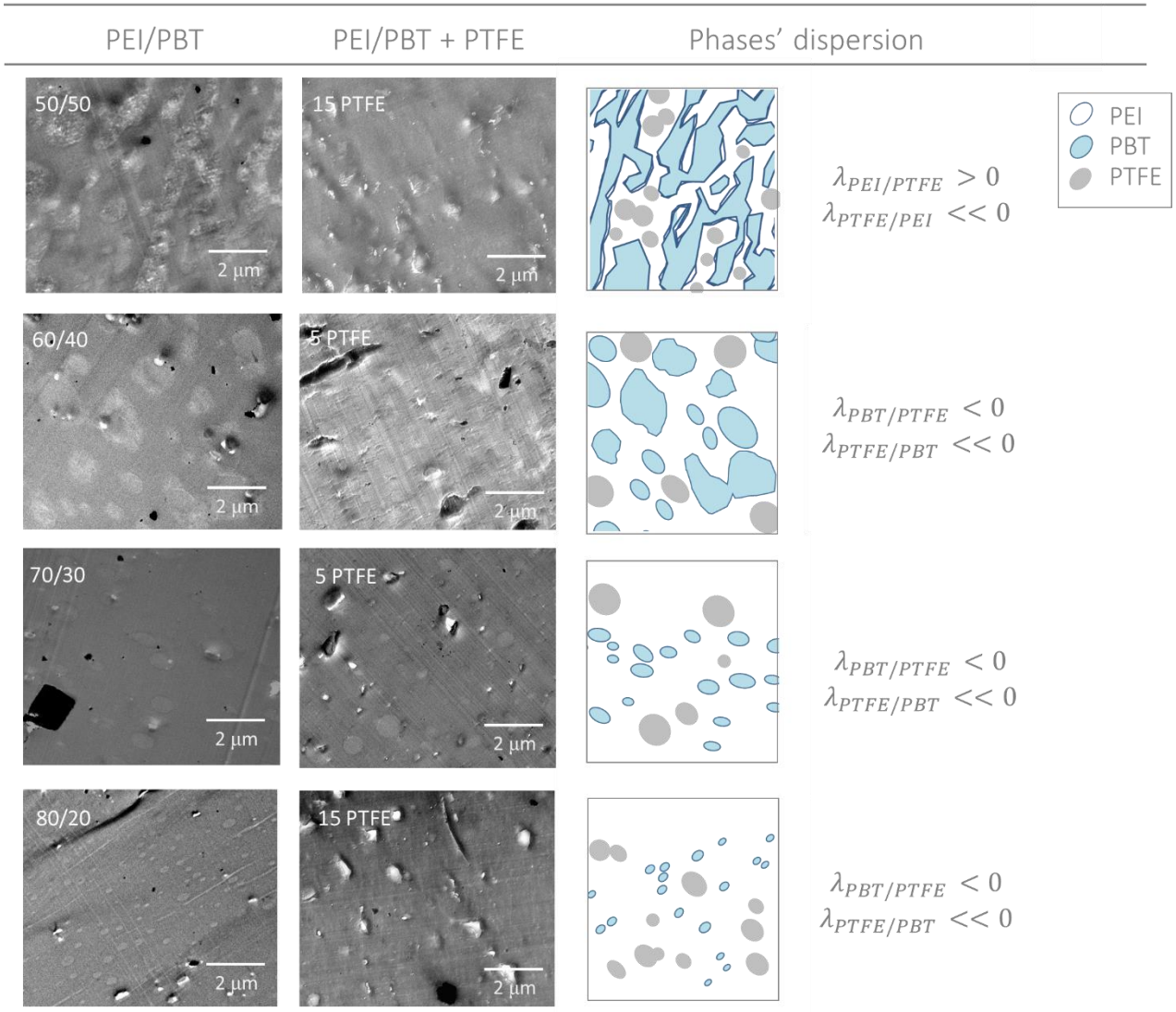

Figure 4.12 TEM results of morphology evolution of ternary (PEI/PBT)/PTFE blend: 50/50/15, 60/40/5, 70/30/5, and 80/20/15; and schematic representation of PTFE phase distribution according to spreading coefficient values.

Regarding the second group of blends, while PEI concentration increases, and the interfacial interaction between the three phases result in negative spreading coefficient values. This predicts the other case of complete wetting, where the PEI matrix hosts two separated dispersed PTFE and PBT phases, as it is observed in TEM images.

4.2 PART II – Effect of PTFE on the mechanical properties and thermal stability of (PEI/ PBT)/PTFE blends

4.2.1 Introduction

It is well known that PTFE is commonly used in the modification of mechanical, thermal, chemical resistance, and tribological properties of polymers.[109–119] It is mostly used as a solid lubricant due to it has the lowest coefficient of friction from all polymers. However, there are found some contradictory results regarding the PTFE effects on the mechanical properties of polymer blends.[109,113–118] To some extent, those results have shown that the processing method (solution or melt processing) and the processing conditions will strongly influence blends performance when PTFE is added.

There are few reports of the mechanical properties evaluation in PTFE based polymer blends produced from melt processing. In their work, Palabiyik and Bahadur[116] obtained binary PA/HDPE blends and modified their properties by adding PTFE. For PTFE incorporation, they used a processing temperature of 235 °C, hence it is dispersed in the blend in the solid state. It is found that PTFE significantly improves the friction resistance due to its self-lubricating behavior. However, it does not improve the mechanical performance of blends and slightly reduced their ductility. In other work performed by Bijwe and collaborators,[111] these authors evaluated the mechanical properties of PEEK/PTFE blends obtained in a twin-screw extruder at 350 °C. They found that increasing PTFE concentration from 0 wt% to 30 wt% improves the wear resistance of PEEK. However, all other properties are deteriorated (tensile strength from 87 MPa to 64.6 MPa, tensile modulus from 3.9 MPa to 1.23 MPa, and elongation at break from 21% to 8.87%), except one, the impact strength, which improves from 60 J/m to 126.42 J/m.

In a more recent work performed by Hussain and coworkers,[114] they mix thermoplastic elastomer (TPEE) with PBT, the blend was reinforced with PTFE nanoparticles. The process consisted of two separated steps: i) blending TPEE with PBT by extrusion at 265 °C, and ii) adding the PTFE powders in a second process using the same temperature conditions. Even though PTFE is not melted at the processing temperature used by the authors, they found by TEM evaluation a strong interface between PTFE and binary TPEE/PBT blend, and they attributed the high mechanical properties to this interaction.

In this part of the study, we evaluated the effect of PTFE addition on the mechanical, thermal, and flammability properties of (PEI/PBT)/PTFE blends. Since PEI, PBT, and PTFE are completely immiscible, once again we used additivity approaches and the results are contrasted with those obtained for binary PEI/PBT blends. The tensile tests results reveal that PTFE phase do not affect PEI/PBT stiffness since it is not observed any significant variation in the tensile modulus values. On the other hand, it is noticed a progressive decrease of blends tensile strength with increasing PTFE concentration. A similar response is observed on ductility values for ternary blends with 50 wt%, 60 wt%, and 70 wt% of PEI. However, ductility is improved adding only 5 wt% of PTFE in blends with 80 wt% of PEI. Even though the addition of higher PTFE concentration reduce progressively the ductility of blends with 80 wt% of PEI, in all the cases it is greater than that for binary 80PEI/20PBT blend.

Regarding thermal stability of blends measured by TGA, it is studied the interaction between components by calculating the theoretical decomposition behavior of blends when no interaction occurs.[182,188] Results reveal that PTFE addition did not compromise the thermal stability of blends. On the contrary, it is noticed a PTFE addition delays the thermal decomposition of blends when there are contrasted the values with those of binary PEI/PBT blends. Finally, the flammability results after the horizontal burning test reveal that the protection mechanism consisting of charring formation is enhanced by the addition of PTFE phase.

These results pave the way to promising applications of the high-performance (PEI/PBT)/PTFE ternary blends obtained in this work, due to the attractive combination of mechanical properties with enhanced thermal stability and flame resistance.

4.2.2 Experimental

Tensile tests

Tensile tests were made according to standard ASTM D638 – 14. Type V samples were injected molded in a HAAKE™ MiniJet Pro Injection System from Thermo Scientific. Conditions for injection molding are listed in Table A- 4. Samples were tested in an Instron 3366 at a crosshead speed of 1 mm/min using an extensometer with a gauge length of 10 mm. At least five specimens of each blend were measured and the average values were reported.

Thermal stability and flammability tests

Thermal stability of (PEI/PBT)/PTFE blends was studied by means of TGA and a flammability tests were settled according to the UL94 standard.

Thermogravimetric analysis (TGA)

Thermal stability study was carried out in a TGA Q500 model from TA Instruments on samples of 40±2 mg, within a temperature range from 25 °C to 900 °C at a heating rate of 10 °C/min. All thermal evaluation tests were performed under nitrogen atmosphere.

Flame resistance analysis

For flammability tests, samples of 125 mm length, 10 mm width, and 3 mm thickness were obtained by injection molding in a HAAKE™ MiniJet Pro Injection System from Thermo Scientific. The injection molding conditions are the same as the ones described in Table A- 4. An assembly was fabricated to perform horizontal burning (HB) tests according to the standard UL 94, Figure 3.21. The lab-made assembly consisted of a laboratory burner positioned at 45°, a supply of natural gas, a sample holder, and a universal laboratory support. According to the UL94 standard, two marks were made in the specimens at 25 mm and 100 mm length from the tip that is exposed to direct flame contact, in order to measure the burning rate in mm/s. Three specimens were tested for each blend. The flame traces in the samples were video and photographically recorded.

4.2.3 Results and discussion

Tensile properties of ternary (PEI/PBT)/PTFE blends

In Figure 4.13a) and Figure 4.13b), are presented the tensile moduli and tensile strength as a function of PEI concentration, respectively. The moduli values are calculated from the slope of the elastic region of stress-strain curves at early deformations where no interfacial debonding takes place.[189,190] The dashed horizontal line in Figure 4.13a) delimits the modulus of pure PEI, and the solid lines in both graphs correspond to the moduli and yield stress values calculated from the additivity rule by using Equation 3.10.

In Figure 4.13a) it is noticed a combined effect of PTFE addition on the blends stiffness. However, the general trend of the tensile moduli for ternary blends is close to that for binary blends,

and in all cases the moduli values whether equal or exceed those predicted by additivity. Additionally, the synergic effect observed in the binary blends with 50 wt% and 80 wt% of PEI is maintained by the ternary blends with the same PEI compositions. These results suggest that PEI and PBT phases exhibit partial miscibility due to the inter-spherulitic interaction described in Section 0, and that PTFE does not interfere in the interfacial bonding through the fibrillary structure, as observed by SEM and TEM results.

On the other hand, in the results presented in Figure 4.13b) for yield stress, it is noticed that increasing the concentration from 0 wt% to 15 wt% of PTFE decreases progressively the tensile strength of blends. Besides, it is noticed that blends with PTFE concentrations higher than 10 wt% exhibit a negative deviation from the additivity. Having in mind that contrary to the elastic modulus, the yield stress in polymer blends is sensitive to adhesion of components,[189,190] this behavior is attributable to two major effects: the first is linked to the high interfacial energy between phases that leads to blends' immiscibility, and hence, the interfacial adhesion between PEI and PBT with PTFE phase is not too strong; the second is related to the characteristic low yield strength of PTFE,[117–119] which is reflected in the performance of the blends.

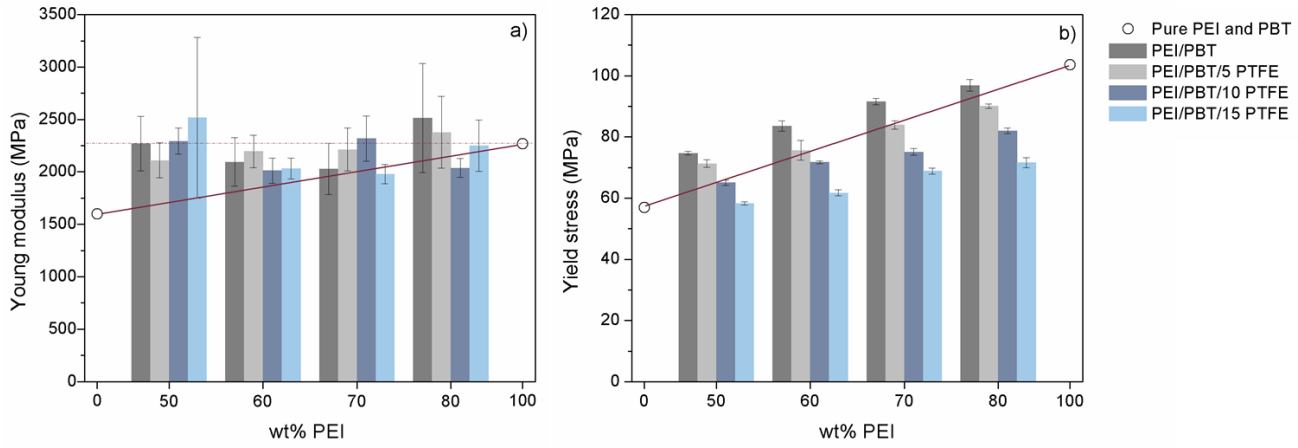

Figure 4.13 Tensile tests results of (PEI/PBT)/PTFE blends contrasted to tensile properties of binary PEI/PBT blends: a) Young modulus, and b) yield stress. Mechanical properties are plotted as a function PEI wt%. The standard deviation was calculated for n = 5. Values for pure PEI and pure PBT phases are shown in the open circles.

In Figure 4.14a) and Figure 4.14b), it is shown the effect of PTFE phase on blends elongation at break. The solid line in Figure 4.14a) delimits the ductility of blends calculated from the additivity rule. It is noticed that both, binary and ternary blends, exhibit a negative deviation from additivity, and that ternary (PEI/PBT)/PTFE blends containing 50 wt%, 60 wt%, and 70 wt% of PEI present even lower elongation at break performance than that of binary PEI/PBT blends. This behavior is similar to other results described in PTFE based polymer blends,[112,115] where the

increasing of PTFE particles in the blend results in a negative effect on blends ductility. Since the tensile modulus is not compromised with PTFE addition, this behavior may be due to the debonded PTFE portions that are not embedded in the PEI matrix during the spheroidization process in step 1, which may induce fails affecting the elongation of blends.

Nevertheless, the blends containing 80 wt% of PEI reveal a surprisingly increase in elongation at break resistance on ternary blends. The ductility values of 80/20/5 blends even reach values close to those of binary co-continuous 50/50 blends —which exhibit the highest elongation at break performance in binary PEI/PBT blends—. Two major effects explain this particular behavior: the first one includes the effective homogenization of PEI and PTFE during step 1. Under these conditions, the proper integration of both, PEI and PTFE phases, is enhaced by the shearing deformation inside the mixing chamber. Besides, the ternary blends are fabricated with lower PTFE concentrations than that presented in the example of the binary PEI/PTFE blend —80PEI/20PTFE blend developed for defining processing conditions purposes—, and the amount of PTFE debonded particles are likey to be lesser than those for bianry PEI/PTFE blends. On the contrary, the formation of PTFE nano droplets embedded in the PEI matrix will be promoted under these conditions, as observed in Figure 4.7c) and Figure 4.7d), together with the PBT phase distribution with particles sizes close to 120 nm.

The second effect is linked to the inhibition of blends densification by PTFE phase. In Chapter 3, it was described that the densification phenomena in 80PEI/20PBT blend causes the synergic behavior on the tensile modulus, which is also responsible of the low elongation at break performance of binary blends. Densification occurs by the volume contraction in the blend causing “thermal embrittlement”, which explains the embrittlement that occurs when miscible blends with high Tg polymers —such as PEI— experiences free volume loss. Since the PTFE phase is blended together with the amorphous PEI during step 1, it inhibits the free volume loss due to the highly crystalline domains of PTFE, which are well distributed along the PEI matrix, as observed by TEM evidences.

The progressively decrease in the elongation at break values for 80/20/PTFE blends is a negative effect on blends ductility when PTFE concentration is increased, similarly to the behavior observed in the ternary blends with 50 wt%, 60 wt%, and 70 wt% of PEI. Nevertheless, for ternary 80/20/PTFE blends ductility is higher than binary 80/20 PEI/PBT blend, suggesting that

densification of blends is also inhibited at these PTFE compositions. These results are shown for the first time in a ternary system comprised of high-performance polymers.

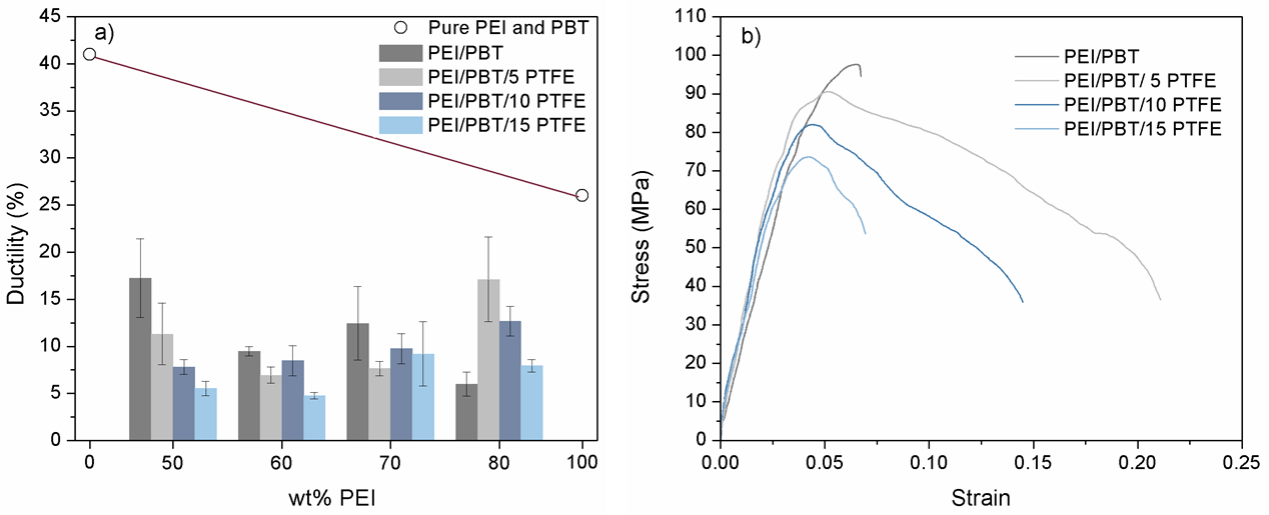

Figure 4.14 Elongation at break resistance for (PEI/PBT)/PTFE blends contrasted to binary PEI/PBT blends: a) ductility, and b) tensile stress-strain curves for binary and ternary blends containing 80 wt% of PEI. Mechanical properties are plotted as a function PEI wt%. The standard deviation was calculated for n = 5. Values for pure PEI and pure PBT phases are shown in the open circles.

In Figure 4.14b) it is clearly evidenced the PTFE phase effect in ternary blends. In ternary blends it is achieved a good combination between tensile strength and ductility for low concentrations of PTFE (lower than 10 wt% of PTFE). In his work, Ritchie reviewed the conflicts that commonly exist between strength and toughness in many classes of materials.[212] He says these two properties tend to be mutually exclusive, and the generation of toughness in a material is quite a challenge. When one material combines these two properties, it can be used in structural applications, as well as in safety applications where premature fractures are unacceptable.

Thermal stability and flammability of blends

Thermogravimetric analysis (TGA)

In Figure 4.15, there are shown the results for pure PEI, PBT, PTFE, and their blends. Since all ternary blends displayed the same tendency during thermal decomposition, only one concentration of PTFE (10 wt% of PTFE) is shown for demonstrative purposes.

In Figure 4.15a), decomposition of pure materials takes place in a single step, which is retained in the corresponding ternary blends leading to an intermediate three-step decomposition behavior. The respective DTG results are presented for a temperature range between 270 °C and 630 °C —delimited by the dashed square— as shown in Figure 4.15b). The derivative curves

show clearly the PTFE contribution as a peak that appears just after the PEI signal at 570 °C. The DTG signals do not show any temperature shifts, then they correspond to each phase in the blends, except for the 50/50/10 blend.

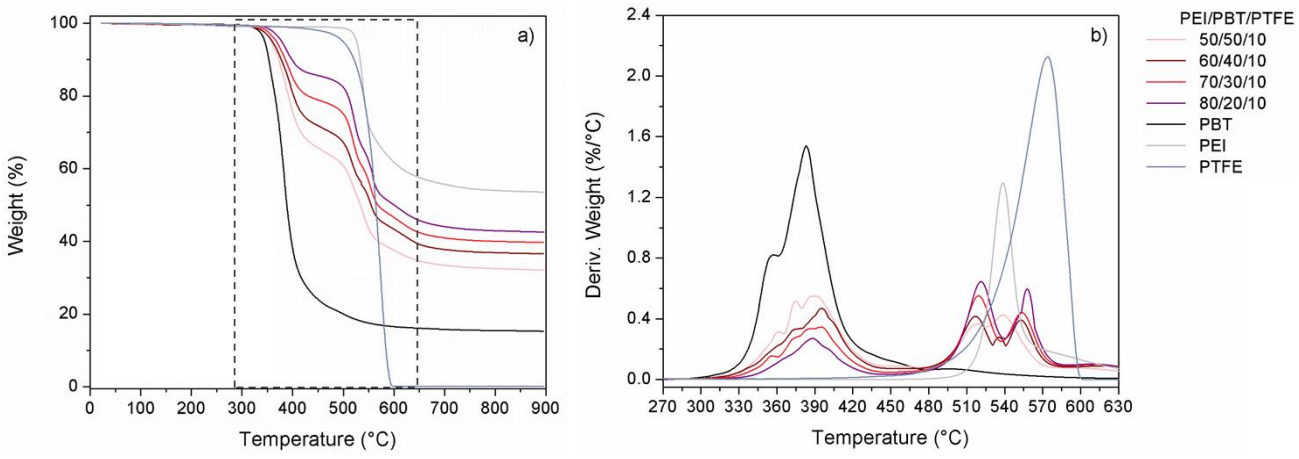

Figure 4.15 Thermal stability of PEI, PBT, PTFE and ternary (PEI/PBT)/PTFE with 10 wt% of PTFE: a) TGA, and b) DTGA.

TGA results reveal that the decomposition of ternary blends is strongly influenced by each polymer thermal behavior. In order to study the existence or not of interactions between PTFE or PTFE degradation products with PEI and PBT phases and their respective degradation products, we calculate the theoretical TGA curves by using an additivity relation, by multiplying the experimental data of the individual components by a factor corresponding to the wt% of each component in the ternary blend. The resulting data represents the thermal behavior expected for each composition in the absence of any kind of interaction between phases or their decomposition products.[182–184,188,196]

In Figure 4.16, there are compared the calculated and experimental TGA curves for ternary blends containing 5 wt% of PTFE. In Figure 4.16a), are also shown the curves for pure polymers for comparative purposes. The solid lines represent the behavior observed experimentally and the dashed lines the calculated weight loss curves in the absence of any interaction. For all compositions, it is noticed that both curves have a similar tendency, with three step decomposition behavior corresponding to each phase response. During the first decomposition step, the experimental and predicted curves are in good agreement, corroborating that PEI delays the initial degradation of PBT phase improving its thermal stability. However, clear differences between experimental and calculated curves start to appear just before the decomposition signal of the second step which corresponds to PEI decomposition. It is noticed that the loss weight

behavior of the experimental curves is lower than that of the theoretical curves, and just as in binary PEI/PBT blends, the less stable polymer (PBT) causes destabilization of the more stable one (PEI), suggesting that some kind of interaction is taking place (Section 0).

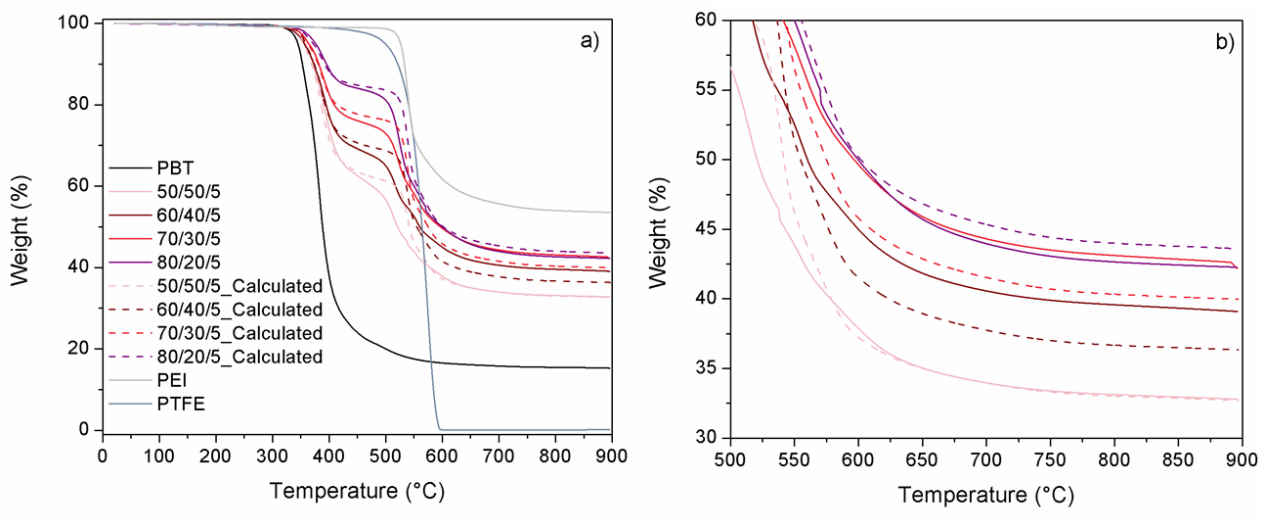

Figure 4.16 Experimental and calculated TGA curves ternary (PEI/PBT)/PTFE blends containing 5 wt% of PTFE.

During the final step corresponding to the PTFE phase, there is not noticed significantly difference between the experimental and calculated curves. Additionally, the magnification presented in Figure 4.16b) of the total weight loss, reveals the effect of adding 5 wt% of PTFE on the generation of carbonaceous residues —charring formation—. Theoretical and experimental curves for blends with 50 wt% and 80 wt% of PTFE, show no differences in the final residue formed. However, ternary blends with 60 wt% and 70 wt% of PEI, reveal that experimental carbonaceous residues (39.5% for blends with 60 wt% of PEI and 42.9% blends with 70 wt% of PEI) are higher than the theoretical ones (36.6% for blends with 60 wt% of PEI and 40.1% blends with 70 wt% of PEI). These results suggest that PTFE improves the thermal stability of PEI/PBT blends by enhancing the major mechanism against fire protection in polymers.

In order to understand the effect of these interactions, we obtain the characteristic decomposition temperatures at different weight loss percentages: initial decomposition temperature (Ti), and the temperatures at 10% (T10) and 40% (T40) of mass loss, as shown in Figure 4.17. Generally, the characteristic temperatures analysis is performed at 50% weight loss. However, the final PEI weight loss is higher than 50%, hence 40% will be used.

In previous thermal interaction analysis of binary PEI/PBT blends showed in Figure 3.28, it was noticed that PEI improves the thermal stability of PBT phase. This generalized behavior is still

noticed in the ternary blends characteristic temperatures. Similarly, PTFE addition also improves thermal stability of PEI/PBT blends. In all the thermal characteristic temperatures shown in Figure 4.17, PTFE causes a slightly delay in Ti and T10 temperatures, and the increasing amount of PTFE does not have any significant effect.

However, in Figure 4.17c), it is noticed that PTFE has a stronger effect on the temperature at 40% of sample decomposition, T40, particularly for ternary blends containing 50/50 of PEI and PBT phases (co-continuous morphology). The addition of only 5 wt% of PTFE to binary PEI/PBT blend, improves by 114% blends thermal stability. These results suggest that morphology of blends strongly influences their thermal performance. It is noticed that this effect is not as pronounced in blends containing 60 wt%, 70 wt%, and 80 wt% of PEI since in these cases high thermal stable PEI phase is the matrix and low thermal stable PBT is distributed as little droplets. Conversely to those blends, in 50/50 blends there is a bigger amount of PBT distributed as a continuous phase in the blend, hence the effect of the PTFE —which has an inherent thermal stability and flame retardancy— enhances 50/50/PTFE blends thermal performance.

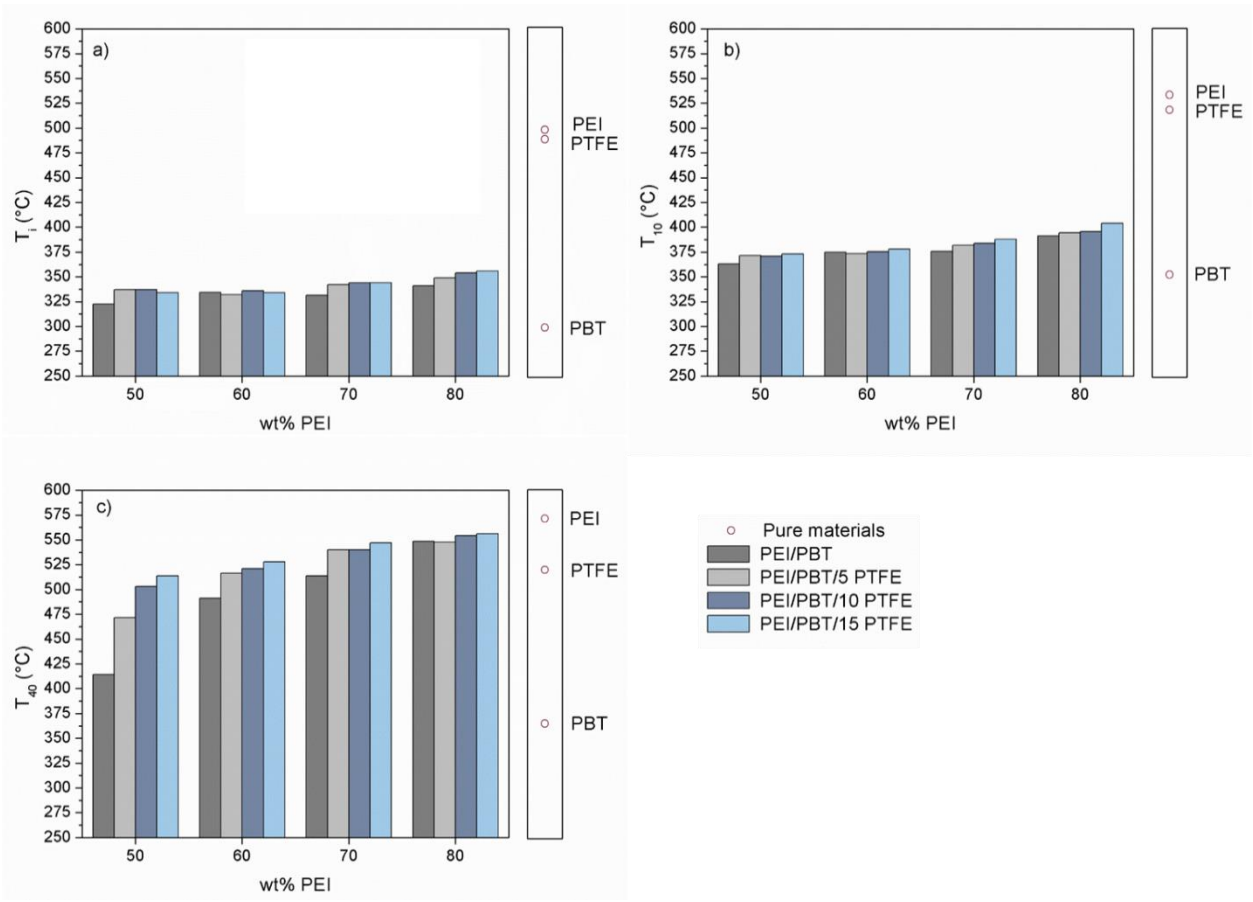

Figure 4.17 PTFE effect on thermal stability of ternary (PEI/PBT)/PTFE blends: a) Ti, b) T10, and c) T40.

Flame retardancy of (PEI/PBT)/PTFE blends

Limiting oxygen index (LOI) and charring formation on ternary (PEI/PBT)/PTFE blends

In Figure 4.1b), it is revealed that all PTFE sample degrades without any kind of residue. However, PTFE has an exceptionally high limiting oxygen limit, LOI = 95%,[34] because during flame exposure the defluorination of its backbone structure produce hydrogen fluoride HF,[205] which acts as a flame inhibitor. For that reason, PTFE is considered as an inherent flame retardant polymer.

Despite PTFE does not exhibit carbonaceous products after decomposition, it has the highest LOI value from all the polymers used in the ternary (PEI/PBT)/PTFE fabrication —as listed in Table 4.4—; hence, it should be expected lower charring ability in ternary blends than in binary PEI/PBT blends, and the protection mechanism against flame propagation should be different to that observed in binary PEI/PBT blends.

Table 4.4 Limiting oxygen index (LOI) values for pure materials used in ternary (PEI/PBT)/PTFE blends fabrication. Data obtained from the supplier's data sheet.

Polymer	LOI (%)
PEI	47
PBT	30
PTFE	95

Nevertheless, in Figure 4.16b) it was evidenced that PTFE enhances the charring formation of ternary blends with 60 wt% and 70 wt% of PEI. In order to study the effect of PTFE on the major fire protection mechanism of binary PEI/PBT blends, we evaluate the weight loss percentages (charring formation) for all PTFE concentrations used, and compare them with binary blends. In Figure 4.18, it is presented the charring percentage of binary and ternary blends as a function of PEI addition. It is noticed that for binary PEI/PBT blends (black curve), the charring products increase monotonically with PEI addition. Similar results are observed for ternary blends, which confirm that the inherent charring ability of PEI is transferred to both binary and ternary blends, improving their resistance to flame propagation.

Besides, it appears a surprisingly effect of PTFE addition on charring formation of ternary blends. Based on the weight percentage residue of pure PTFE observed in TGA results (Figure

4.15), the final residue values expected for ternary blends should be close to those of PTFE (very low), since the major fire protection mechanism of PTFE do not consist in charring formation. However, addition of PTFE to binary PEI/PBT blends, increases their charring production. The mentioned effect is mostly noticed in blends with 5 wt% of PTFE. Nevertheless, when it is added 10 wt% or 15 wt% of PTFE, the charring ability of PEI/PBT blends falls systemically while PTFE increases, and it is even compromised for blends with concentrations of 50 wt% and 80 wt% of PEI.

Above results suggest that low concentrations of PTFE enhance the interaction between the degradation products of PEI, PBT, and PTFE to react in a fashion that they improve the charring ability of the ternary (PEI/PBT)/PTFE blends. In addition, higher concentrations of PTFE in the ternary blends will lead to a protection mechanism characteristic of PTFE.

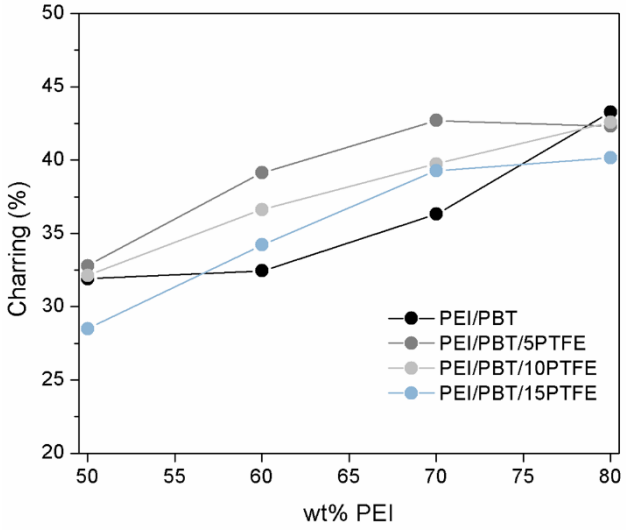

Figure 4.18 Experimental charring percentage of ternary (PEI/PBT)/PTFE blends as a function of PEI concentration.

Horizontal burning flammability test

In order to compare the charring formation of specimens after long exposure times, in Figure 4.19 are presented the results for all ternary (PEI/PBT)/PTFE blends after four minutes of direct flame exposure. The upper dashed line delimits the maximum length of the specimens (125 mm), and the lower dashed line the first mark at a length of 25 mm from the specimen's tip. All blends exhibited charring products formations, and that they are higher than the initial specimen length. Additionally, it is observed PTFE effect on enhancement charring formation, which leads to protective carbonaceous layers higher than those of binary PEI/PBT blends.

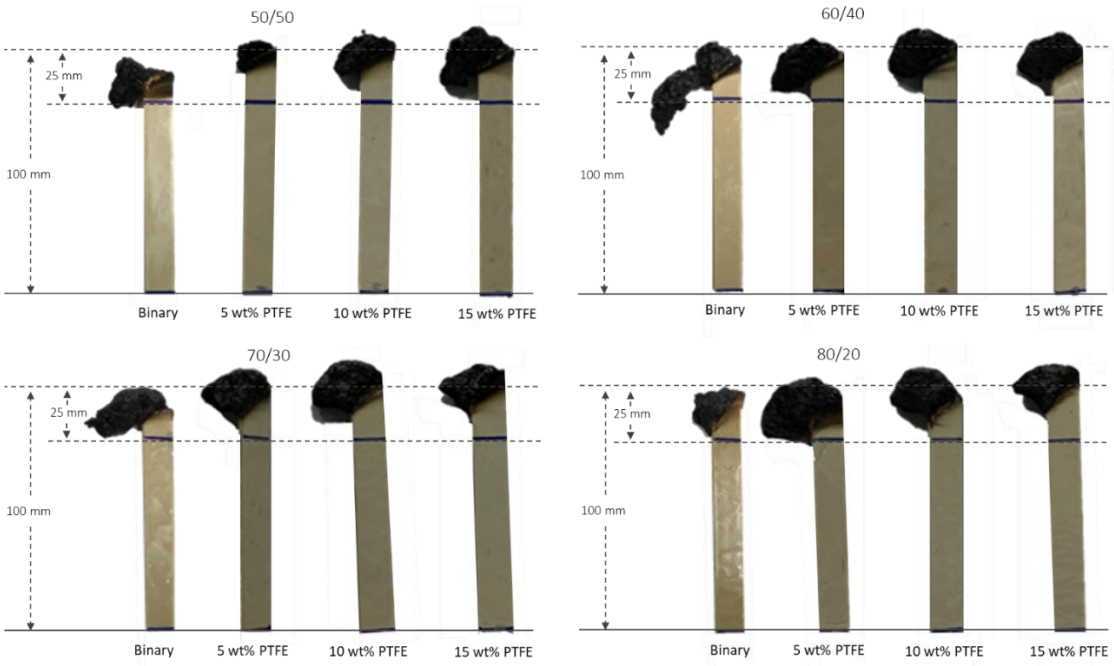

Figure 4.19 Photographs of the ternary blends specimens, after the HB test. PEI content increasing is shown from left to right, and PTFE increasing in shown from top to bottom.

Similarly to binary blends, as the flame did not overpass the first mark at 25 mm, it is possible to classify the ternary blends as HB, which according to the UL94 standard is the maximum flame retardant grade. This is caused by the combing effect between charring formation and self-flame inhibition characteristic of PTFE phase. All samples of ternary blends reveal that flame propagation in ternary blends is even lower than it was in PEI/PBT blends.

4.3 Conclusions – Chapter 4

The mechanical properties of binary PEI/PBT blends were successfully modified by adding 5 wt%, 10 wt%, and 15 wy% of PTFE. Ternary (PEI/PBT)/PTFE blends were obtained by using a two-step melt processing method, for PEI concentrations greater than 50 wt%. The integration sequence of the PTFE phase was defined in such a way that it is possible to obtain ternary blends without varying any processing parameter, except blends composition. Just as for binary PEI/PBT blends, ternary (PEI/PBT)/PTFE blends are easily scaled to industrial processing methods, since PTFE reduces significantly the torque needed to process the PEI in binary PEI/PBT blends. In addition, there are obtained homogeneous and compact materials after the mixing process for all PTFE concentrations used.

Interesting finidings on blends morphology were noticed on PEI/PTFE blends. During step 1, the processing conditions enhance PTFE distribution in PEI phase in two ways: nanosized droplets

embedded in the PEI matrix and debonded PTFE spheres of 1.5 μm of diameter. Nevertheless, from the miscibility study, PTFE is completely immiscible with both, PEI and PBT phases, and it does not interfere with the PEI and PBT interaction. As a consequence, when PBT is added in step 2, similar phase's distributions to those of binary PEI/PBT blends with PEI concentrations greater than 50 wt% are observed.

It is noticed that in both binary and ternary blends, the morphology evolves from co-continuous to matrix/droplet-like morphology. In contrast to binary blends, the matrix is not purely PEI, but a combination between immiscible PEI and PTFE phases. The PTFE phase is preferentially located in the PEI phase because the interfacial energy between PEI and PTFE is lower than that for PBT and PTFE. These results confirm PTFE addition during step 1 does not interfere with the interaction between PEI and PBT phases. Besides, there are not observed notorious cavities formed by PTFE spheres as it was observed in binary PEI/PTFE blend. Additionally, antimony trioxide crystals are observed in almost all samples, as well as the PBT phase enclosed in the PEI + PTFE matrix in the shape of droplets. The blends containing 70 wt% and 80 wt% PEI exhibit the spore-like morphology characteristic of PEI/PBT blends at these PEI compositions.

The results from the spreading coefficient analysis confirmed the observations on the morphological evaluation. Complete wetting of PEI over PBT and PTFE phases is observed in blends with 60 wt%, 70 wt%, and 80 wt% of PEI. On the contrary, blends containing even concentrations of PEI and PBT phases form co-continuous morphology, and PTFE phase is preferentially distributed in the PEI matrix, as predicted by the positive spreading coefficient value.

The influence of PTFE phase on the mechanical properties of binary PEI/PBT blends is noticed as a combined behavior. Tensile modulus is not significantly affected by PTFE addition, and there is not a notable adverse effect in the synergic behavior of tensile modulus for blends with 50 wt% and 80 wt% of PEI. The yield strength on the other hand, goes through a systematically reduction when PTFE concentration is increased. A stronger reduction is observed in blends ductility, particularly for blends containing 50 wt%, 60 wt% and 70 wt% of PEI. However, ductility increases considerably adding small concentrations of PTFE to the binary 80/20 blend, due to PTFE phase relieves the blends densification observed in the binary PEI/PBT blends, and hence, a rare combination between strength and ductility is obtained for ternary (PEI/PBT)/PTFE blends containing 80 wt% of PEI.

Additionally, PTFE phase improves thermal stability of PEI/PBT blends, in particular the co-continuous morphology region. Even though PTFE thermal decomposition is not leaded by charring formation, the interaction between decomposition products of the three phases results in an improvement on charring formation, even higher than the predicted theoretically. These results are corroborated by the horizontal burning tests, which revealed that flame propagation in ternary blends is more effective than that observed in the binary PEI/PBT blends.

Chapter 5 Conclusions, implications of the study and directions for future research

In order to address the two main issues still existing in HPPB development —i) polymers decomposition during melt-processing and ii) morphology control—, in this work it is successfully developed a methodology to obtain binary blends in an internal mixer, between two high-performance polymers with notable differences in their processing temperatures: PEI and PBT. The first challenge was overcome by developing the two-step melt processing method, from which it is avoided PBT thermal decomposition when is blended with PEI phase. The second challenge linked to the understanding of phase's morphology is fulfilled by applying the basis of materials science: evaluate viscoelastic properties of pure components, calculate interfacial tension between all polymer pairs, set the processing conditions, and change the phases' concentration. From these features, it is possible to control PEI/PBT phase morphology in the entire compositional range to tailor blends properties. For the first time, it is reported a complete morphological study in PEI/PBT blends together with their mechanical, thermal, and flammability performance evaluation. Regarding blends morphologies, we found interesting aspects: a co-continuous morphology is obtained at compositions near to 50 wt% of PEI and a new morphology is presented in the binary 70/30 and 80/20 blends, where PBT and PEI phases are bonded through a fibrillary interface. We call it spore-like morphology, and it is obtained without the need of using chemical compatibilizing agents. The mechanical, thermal, and flammability characteristics of blends result highly dependent on blends' morphology.

Certainly, binary 80/20 blend exhibited the most interesting behavior regarding mechanical and thermal properties. At this PEI composition, it is observed a synergic behavior in the tensile modulus. In addition, it is the blend with higher thermal and flame resistance properties. These properties are conferred by the interesting spore-like morphology. However, 50/50 blend with

cocontinous structure also reveals good mechanical and thermal properties, as well as the highest ductility of the binary blends obtained. Nevertheless, the highly stiffness of these blends leaded to reduce their elongation at break performance.

To modify binary PEI/PBT blends properties, the third blend component had to be accurately selected. The addition of PTFE to binary PEI/PBT blends allows obtaining ternary blends from melt processing using the same two-step melt processing method. It is found that PTFE phase improves PEI processability and does not interfere in the interaction between PEI and PBT. From Harkin's spreading coefficient model, it is predicted the encapsulation of PTFE particles by PEI phase when PBT is the matrix. The highly interfacial tension and the differences in the polar components of PTFE and PBT surface tensions, favors its immiscibility. It is observed an unusual morphology in binary PEI/PTFE blend. PTFE powders are spheroidized during step 1, and some PTFE nanoparticles are dispersed in the PEI matrix. This feature avoids blends densification during ternary 80/20/PTFE processing, resulting in a considerable improvement of the blends ductility. PTFE addition to PEI/PBT blends fulfilled the aim of improving PEI/PBT blends performance without decreasing binary PEI/PBT thermal and flammability properties. On the contrary, PTFE enhanced blends thermal stability.

From all ternary blends obtained, the addition of 5 wt% of PTFE to this blends with 80 wt% of PEI resulted in the highest ductility without affecting the synergic contribution in the tensile modulus. Another blend that exhibited interesting properties is the 50/50/5. The thermal stability of these blends is considerably increased by PTFE phase due to PTFE encapsulation in the PEI phase.

5.1 Implications of the study

The development of binary PEI/PBT blends and the modification of these blends to obtain ternary PEI/PBT/PTFE blends, have shown interesting implications that open the door to further interesting research works. Some of them are following highlighted.

The first is related to the results observed in the development of the two-step melt processing method —initially proposed for binary PEI/PBT blends fabrication— in an internal mixer. This method contributes to the development of new HPPB from melt processing methods, and points to be a great opportunity to produce blends from several HPP pairs with enhanced melt processability. We confirm this during the ternary blends fabrication, where all the processing

conditions were kept the same when adding the third component. As a consequence, processability of PEI/PBT blends is enhanced and due to the interfacial surface between blends components, the same morphology as that of binary blends is obtained. This finding is highly attractive from a technological point of view, since this two-step process can be easily scale up to an industrial process and produce binary and ternary —or multicomponent— blends from high-performance polymers. This scale up process could be a melt processing like extrusion.

Secondly, understanding PEI/PBT blends evolution in the entire compositional range evaluated, allows us to understand phases distribution and to control the morphology when ternary (PEI/PBT)/PTFE blends are obtained. Since, for binary and ternary blends, these tailored morphologies can be addressed to specific technological applications. In Table 5.1 are listed some of these blends with their mechanical, thermal, and flame resistance performance, and also the prices of each blend is calculated from the raw material commercial prices and the wt% used in each blend. The results are exhibited as a function of blends morphology evolution, and there are only presented the results for ternary blends with 5 wt% of PTFE.

We calculate the cost/performance index for ductility and charring formation in binary and ternary blends, and plotted them as a function of PEI wt%, Figure 5.1. The LOI was not used for this example because all blends obtained in this work can be used in protective clothes applications, since their LOI values are greater than 30%, which is the minimum value to be able to comply with flammability in protective applications. The best cost/ductility index is for binary blends with 50 wt% of PEI, and for ternary blends the compositions with 50 wt% and 80 wt% of PEI. In contrast to the binary blend, a remarkable improvement on ternary blend containing 80 wt% of PEI when it is added 5 wt% of PTFE is observed. Regarding charring formation, adding PTFE to the blend improves not only mechanical performance but flame resistance performance as well, and the cost/charring index for blend containing 80 wt% of PEI is the one with better performance. These results suggest that from blending PEI, PBT, and PTFE, can be obtained a high-performance polymer blend with enhanced mechanical and thermal performance, and additionally, very easy to process by industrial melt-processing methods.

Table 5.1 Summary of properties and potential applications of binary PEI/PBT and ternary (PEI/PBT)/PTFE blends.

Property	Binary PEI/PBT blends								Ternary (PEI/PBT)/PTFE blends				
	0	30	40	50	60	70	80	100	50	60	70	80	PTFE
Morphology	--	PBT matrix/Coarse PEI droplets + PBT sub-inclusions	PBT matrix/PEI droplets that starts to coalesce	PBT and PEI cocontinuous	PEI matrix/PBT irregular coarse drop-lets	PEI matrix/PBT spores	PEI matrix/PBT tiny spores	--	PBT and PEI cocontinuous + PTFE nano sized droplets and spherical particles	PEI matrix/PBT irregular coarse drop-lets +. PTFE nano sized droplets and spherical particles	PEI matrix/PBT spores + PTFE nano sized droplets and spherical particles	PEI matrix/PBT tiny spores + PTFE nano sized droplets and spherical particles	--
Processability													
Torque (Nm)	2	7	8	9	16	21	31	70	21	22	30	50	--
Mechanical													
Modulus (MPa)	1600	1769	2158	2270	2095	2029	2516	2268	2111	2196	2214	2378	--
Yield Strength (MPa)	57	68	72	75	84	92	97	104	71	76	84	90	21*
Ductility (%)	41	7	14	17	11	14	6	27	11	7	8	17	--
Thermal													
Ti (°C)	300	309	315	322	334	331	341	497	337	332	342	349	488
T10 (°C)	353	358	360	363	375	376	391	533	372	373	382	394	518

Property	Binary PEI/PBT blends								Ternary (PEI/PBT)/PTFE blends				
	0	30	40	50	60	70	80	100	50	60	70	80	PTFE
T40 (°C)	382	395	402	414	491	514	548	617	472	517	540	548	558
Flammability													
UL classification	HB	HB	HB	HB	HB	HB	HB	HB	HB	HB	HB	HB	--
Charring (%)	14.8	23.9	26.9	31.9	32.3	36.3	43.3	53.5	32.8	39.1	42.7	42.3	0.12
LOI (%)[a]	30.0	35.1	36.8	38.5	40.2	41.9	43.6	47.0	41.3	42.9	44.6	46.2	95
Price													
USD/kg[b]	0.6	1.5	1.8	2.1	2.4	2.7	3.0	3.6	2.2	2.5	2.7	3.0	3.3
Cost/performance index													
Cost/Yield Strength	0.011	0.022	0.025	0.028	0.029	0.029	0.031	0.035	0.031	0.033	0.032	0.033	0.157
Cost/Ductility	0.01	0.21	0.13	0.12	0.22	0.19	0.50	0.13	0.20	0.36	0.34	0.18	0.01
Cost/T40	0.002	0.004	0.004	0.005	0.005	0.005	0.005	0.006	0.005	0.005	0.005	0.005	0.006
Cost/LOI	0.020	0.043	0.049	0.055	0.060	0.064	0.069	0.077	0.053	0.058	0.061	0.065	0.035
Cost/Charring	0.041	0.063	0.067	0.066	0.074	0.074	0.069	0.067	0.067	0.064	0.063	0.071	27.500

[a] *Calculated from suppliers data using additivity rule.*

[b] *Calculated from data obtained from http://www.plasticsnews.com/resin, updated to 2017*

** Data obtained from reference* [210]

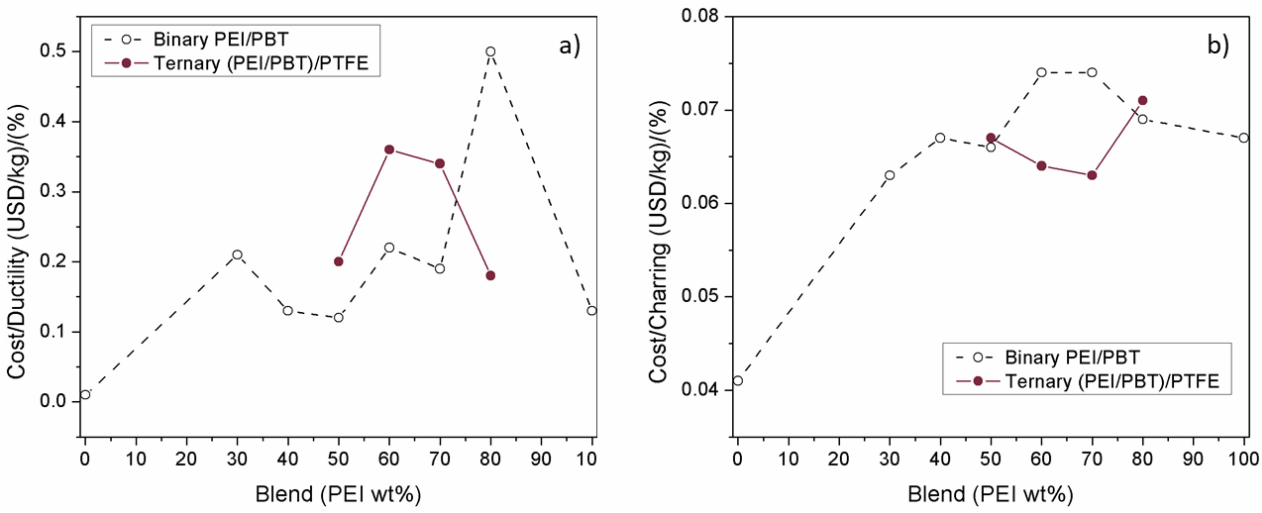

Figure 5.1 Cost/performance indexes for binary PEI/PBT and ternary (PEI/PBT)/PTFE blends:

The same exercise can be made for other properties, and the best cost/performance index will lead to address the blends to specific high-performance applications. In this work, both binary and ternary blends can be used in applications such as: firefighter suits, aircraft furnishing for aerospace industry, non-flammable curtains, athletic clothes, military personal protection, to name a few.

In the third place, it is highlighted that PBT flammability resistance is significantly enhanced by PEI addition in binary blends, which may lead to avoiding the use of halogenated compounds commonly used as flame retardant additives in polymers. These compounds are found to be highly toxic during combustion. In addition, the major flame protection mechanism of PEI is charring formation, which is the most attractive flame protection mechanism for applications such as textiles. Besides, the use of flame retardant additives reduces drastically blends mechanical properties, conversely to the results observed in the mechanical properties of binary PEI/PBT blends.

Finally, adding low PTFE concentrations to PEI/PBT blends with 80 wt% of PEI, it is obtained a material with an interesting combination of tensile strength and ductility, which is quite a challenge in materials science, since tensile strength is commonly linked to stiffness, and hence, to brittleness of materials. Additionally, PTFE increases the thermal and flame resistance of binary PEI/PBT blends.

5.2 Directions for future research

Data from the TGA evaluation in both, binary and ternary blends, needs to be deeply studied to understand the interaction mechanisms between the decomposition products of each phase in the blends, which cause the differences between the experimental and theoretical curves. For that, it is recommended to use Fourier transform infrared spectroscopy (FT-IR) and gas chromatography as fundamental tools to complement the analysis of the mechanisms involved in the degradation of polymers, and hence, evaluate the different decomposition mechanisms that occur during decomposition and combustion in both, binary and ternary blends.

Results from the morphological evaluation of PBT/PTFE blends revealed that PTFE particles formed in situ fibrillary reinforcement in the PBT matrix. This kind of behavior is commonly observed in PTFE based composites; when they are obtained from melt processing at lower temperatures than the melting temperature of PTFE. This appears as a striking possibility of increase the mechanical, tribological, thermal, and flame resistance properties of PBT from melt processing methods.

Appendix

Polymers commonly used in fire protection applications

In Table A- 1 are listed some engineering and specialty polymers commonly used in fire protection applications.

Table A- 1 Polymers and polymer fibers commonly used in fire protection applications.

Polymer/Fibers	Trade name	Properties	Comments	Applications
Poly(benzimidazole) (PBI)[26]		Organic fiber. LOI = 41%. Little smoke generation. Can withstand 600 °C for 3 – 5 s; and for longer periods up to 350 °C.[124]	Resistance to high temperature and chemicals. Comfortable to wear as cotton. Better than Aramid because remain flexible and keep their integrity. Don't exhibit afterglow.	Firefighter suits, escape suits for astronauts, and aircraft furnishing for aerospace industry. Replace asbestos.[124]
Phenolic fibers	Kynol (novoloid)	LOI = 30 – 35%. Ignition temperature above 250 °C.	Obtained by spinning and curing of phenol-formaldehyde. Carbonizes.	
	Philene	LOI = 39, and does not change its mechanical properties when heated for 24h@140°C or 6h@200°C.	High cross-linked phenolic resin, and aromatic glassy polymer with high carbon content (72 wt%).	
Poly(vinyl chloride) (PVC)	Chlorofiber		Relatively non-flammable. Do not emit flames nor release molten drops.	
Poly(vinylidene chloride) (VDC)	Rhoryl		Thermally comfortable to wear.	Non-flammable curtains and athletic clothes.
Poly(phenylene sulphide) (PPS)	Ryton	LOI = 34 – 35%.[124] Chemically resistant.	Produced by melt spinning.	Protective clothes.[124]
Poly(acrylate) fibers	Inidex	LOI = 43%	Does not burn or melt. Does not emit toxic smoke or gases. The durability is not too good.	Protection against chemicals as strong acids and alkalis. Useful in infiltration of liquids and hot gases.[124]
Semicarbon fibers	Firotex or As-		Obtained from viscose or PAN.	Protection against naked

Polymer/Fibers	Trade name	Properties	Comments	Applications
(Viscose fibers)	gard		Excellent resistance to molten metal splash.	flame.
	Panox		Stands 1000 °C. Resistant to acids and alkalis. Very durable. Breaths like wool and is comfortable.	
Modacrylic	Velicren FR SEF Kanecaron	LOI = 26 – 31%[124]	Generic class developed to improve behavior of acrylic fibers by copolymerization with 40% of chlorine monomers (Vinyl chloride or vinylidene chloride) along with sulphonated vinyl polymer.	
Poly(amide-imide)	Kermel	LOI = 31 – 32%	Resists 250 °C for long exposures (after 500 hours the mechanical properties loss is only 33%). Does not melt but carbonizes.	Used in France as firefighter and military personal protection.

Thermal characterization of Uf-PBT

The DSC and TGA characterization for Uf-PBT (without flame retardant compounds) are presented in Figure A- 5.1. DSC results show the glass transition temperature of unfilled PBT is close to 45 °C, and its melting temperature at 220 °C. Its thermal decomposition shown by TGA and DTG curves, display a single step reaction where the initial (Ti) and the final (Tf) decomposition temperatures are well defined. At 900 °C almost the entire sample has degraded, letting a residue of 0.1146% in the pan.

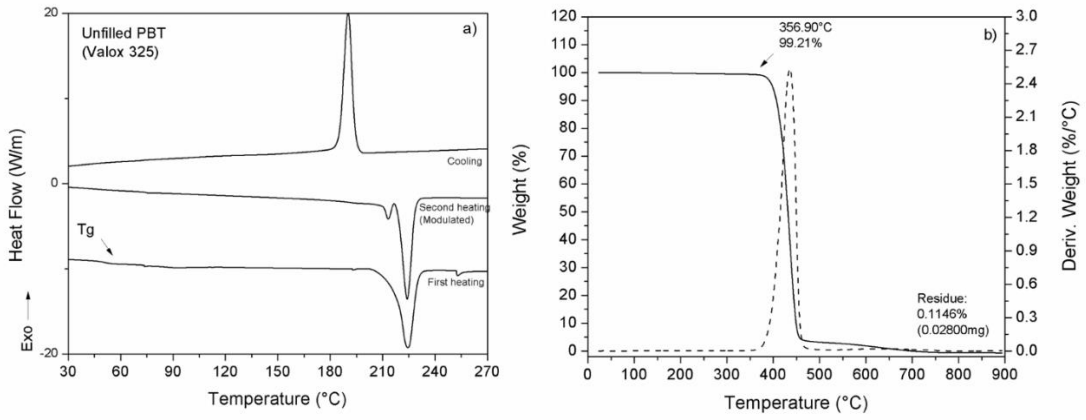

Figure A- 5.1 Thermal characterization of unfilled PBT (Uf-PBT): a) DSC, and b) TGA results.

Characterization of the flame retardant compound present in PBT sample

In Figure A- 5.2 are presented the characterization results of the flame retardant compunds present in the flame retarded PBT sample used in PEI/PBT blends fabrication. In Figure A- 5.2a) the EDS are presented the EDS results for a PEI/PBT blend containing 30 wt% of PEI. The orange (antimony, Sb) and yellow (bromine, Br) signals correspond to the flame retardant compounds. The X-ray diffraction (XRD) results shown in Figure A- 5.2b), reveal that antimony is present as antimony trioxide filler, and that the phase that prevails is senarmontite. Finally, Figure A- 5.2c) shows the X-ray photoelectron spectroscopy (XPS) results, which estimates that the amount of bromine compounds in the sample is of the order of 2.66%, which explains the great presence of this element exhibited in the EDS results.

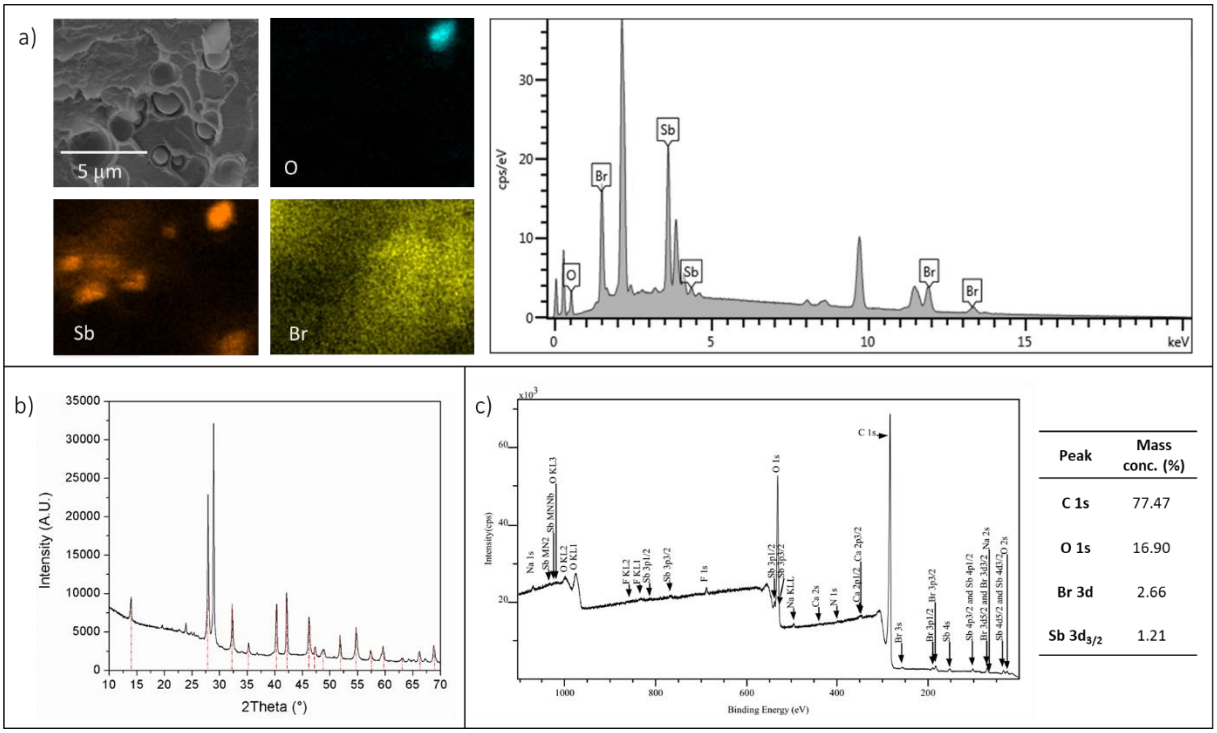

Figure A- 5.2 Flame retardant compound characterization: a) EDS, b) XRD, and c) XPS.

DMA characterization of PBT resin without flame retardant compound

Figure A- 5.3 shows the DMA results that compare both PBT samples, with and without antimony trioxide/bromide compounds. Clear differences are observed in the thermal transitions between both samples. The glass transition temperature for unfilled PBT starts at a temperature close to 45 °C —as observed in DSC characterization for the same sample—. The Tg for flame retarded PBT is shifted to higher temperatures due to the inorganic filler causes an stiffness effect on polymer chains, reducing their mobility when temperature is raised. When tem-

perature reaches 180 °C, it is noticed a second transition peak for the PBT sample with flame retardant fillers, which is attributable to the melting temperature of the bromide compound.

The Uf-PBT does not exhibit this transition. After its Tg, the following thermal transition corresponds to it melting temperature close 220 °C.

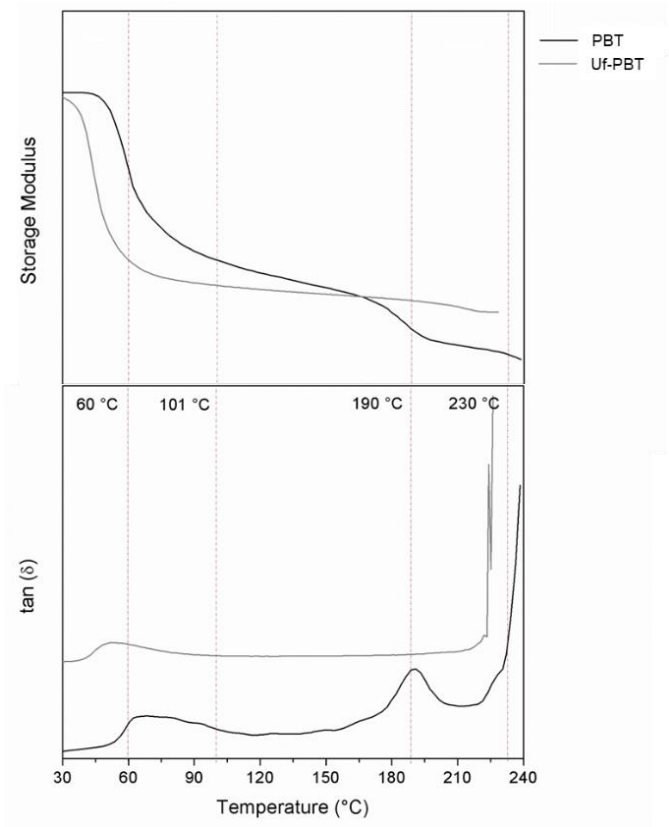

Figure A- 5.3 DMA results for both PBT references: flame retarded PBT, and unfilled PBT (Uf-PBT).

PEI selective dissolution from Soxhlet extraction technique

Soxhlet extraction technique is used to selectively remove the PEI phase from PBT-rich blends, in order to better observe the morphological distribution by SEM. The experiments were performed putting the specimens inside a stainless steel mesh, and summited to different washing cycles in chloroform at 100 °C. In the plot of the number of cycles as a function of PEI concentration, is noticed that the higher the concentration of PEI in the blends, the higher the cycles needed to remove it from blends.

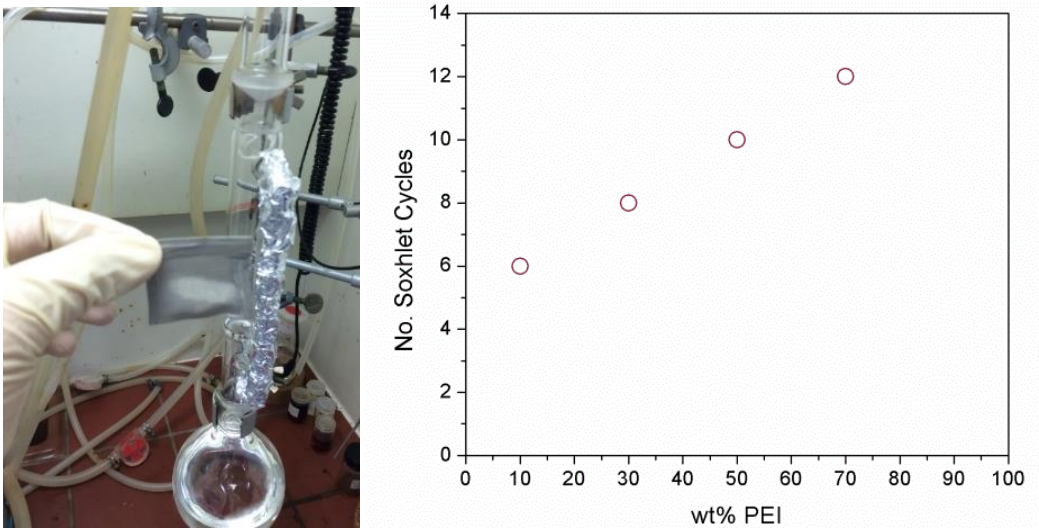

Figure A- 5.4 Assembly of Soxhlet extraction technique and sample preparation (left), and number of cycles used for each blend (right).

Injection molding parameters for binary and ternary blends

Injection of the different specimens for rheological, mechanical, and flammability tests is performed in a HAAKE MiniJet Pro Injection System from Thermo Scientific. In Table A- 2, there are presented the conditions used to prepare the specimens for rheological measurements of binary PEI/PBT blends, and Table A- 3 and Table A- 4 for the tensile tests of both, binary PEI/PBT and ternary (PEI/PBT)/PTFE blends.

Table A- 2 Injection molding conditions of discs for rheological measurements.

PEI/PBT blend (wt%)	Cylinder temperature (°C)	Mold temperature (°C)	Pressure (bar)	Holding time (s)	Post-pressure (bar)	Holding time (s)
0/100	270	120	400	6	300	2
30/70	270	120	400	6	300	2
40/60	270	120	400	6	300	2
50/50	270	120	400	6	400	2
60/40	270	120	400	6	400	2
70/30	280	120	500	6	500	2
80/20	280	120	500	6	500	2
100/0	350	210	500	6	500	2

Table A- 3 Injection molding conditions for Type V specimens for binary PEI/PBT blends tensile and flammability tests.

PEI/PBT blend (wt%)	Cylinder temperature (°C)	Mold temperature (°C)	Pressure (bar)	Holding time (s)	Post-pressure (bar)	Holding time (s)
0/100	270	120	400	6	300	2
30/70	270	120	400	6	300	2
40/60	270	120	400	6	300	2
50/50	270	120	500	6	400	2

PEI/PBT blend (wt%)	Cylinder temperature (°C)	Mold temperature (°C)	Pressure (bar)	Holding time (s)	Post-pressure (bar)	Holding time (s)
60/40	280	120	500	6	400	2
70/30	285	120	550	6	400	2
80/20	295	120	550	6	400	2
100/0	360	120	550	6	550	6

Table A- 4 Injection molding conditions of Type V specimens for ternary (PEI/PBT)/PTFE blends tensile tests.

(PEI/PBT)/PTFE blend (wt%)	Cylinder temperature (°C)	Mold temperature (°C)	Pressure (bar)	Holding time (s)	Post-pressure (bar)	Holding time (s)
50/50/5	270	120	450	6	450	2
50/50/10	270	120	450	6	450	2
50/50/15	270	120	450	6	450	2
60/40/5	280	120	450	6	450	2
60/40/10	280	120	450	6	450	2
60/40/15	280	120	450	6	450	2
70/30/5	285	120	500	6	450	2
70/30/10	285	120	500	6	450	2
70/30/15	285	120	500	6	450	2
80/20/5	295	120	550	6	450	2
80/20/10	295	120	550	6	450	2
80/20/15	295	120	550	6	450	2

References

1. Utracki, L. A. Characterization methods for high temperature polymer blends. in *High Temperature Polymer Blends* 14–69 (Elsevier, 2014).
2. Barlow, J. W. & Paul, D. R. Polymer blends and alloys—a review of selected considerations. *Polym. Eng. Sci.* **21**, 985–996 (1981).
3. Everaert, V., Aerts, L. & Groeninckx, G. Phase morphology development in immiscible PP/(PS/PPE) blends influence of the melt-viscosity ratio and blend composition. *Polymer* **40**, 6627–6644 (1999).
4. Favis, B. D. & Therrien, D. Factors influencing structure formation and phase size in an immiscible polymer blend of polycarbonate and polypropylene prepared by twin-screw extrusion. *Polymer* **32,** 1474–1481 (1991).
5. Favis, B. D. The effect of processing parameters on the morphology of an immiscible binary blend. *J. Appl. Polym. Sci.* **39**, 285–300 (1990).
6. Favis, B. D. & Chalifoux, J.-P. The effect of viscosity ratio on the morphology of polypropylene/polycarbonate blends during processing. *Polym. Eng. Sci.* **27**, 1591–1600 (1987).
7. Favis, B. D., Lavallee, C. & Derdouri, A. Preparation of composite dispersed phase morphologies in incompatible and compatible blends during melt processing. *J. Mater. Sci.* **27**, 4211–4218 (1992).
8. Filipe, S., Cidade, M. T., Wilhelm, M. & Maia, J. M. Evolution of morphological and rheological properties along the extruder length for blends of a commercial liquid crystalline polymer and polypropylene. *Polymer* **45**, 2367–2380 (2004).

9. Fortelný, I., Minkova, L. I., Kotek, J., Lapčíková, M. & Michálková, D. Morphology and mechanical properties of polypropylene/polystyrene blends compatibilized with styrene-butadiene block copolymers. *Polym. Eng. Sci.* **52**, 191–204 (2012).

10. Gonzalez-Nunez, R., Favis, B. D., Carreau, P. J. & Lavallee, C. Factors influencing the formation of elongated morphologies in immiscible polymer blends during melt processing. *Polym. Eng. Sci.* **33**, 851–859 (1993).

11. Jannasch, P., Hassander, H. & Wesslén, B. On the Macro- and microphase separation of compatibilizers in immiscible polymer blends. *J. Polym. Sci. Part B Polym. Phys.* **34**, 1289–1299 (1996).

12. Lee, J. K. & Han, C. D. Evolution of polymer blend morphology during compounding in a twin-screw extruder. *Polymer* **41**, 1799–1815 (2000).

13. Lee, J. K. & Han, C. D. Evolution of polymer blend morphology during compounding in an internal mixer. *Polymer* **40**, 6277–6296 (1999).

14. Li, H. & Sundararaj, U. Morphology Development of Polymer Blends in Extruder: The Effects of Compatibilization and Rotation Rate. *Macromol. Chem. Phys.* **210**, 852–863 (2009).

15. Li, Y., Hu, S. & Sheng, J. Evolution of phase dimensions and interfacial morphology of polypropylene/polystyrene compatibilized blends during mixing. *Eur. Polym. J.* **43**, 561–572 (2007).

16. Macosko, C. W. Morphology development and control in inmiscible polymer blends. *Macromol. Symp.* **149**, 171–184 (2000).

17. N. Tokita. Analysis of morphology formation in elastomer blends. *Rubber Chem. Technol.* **50**, 292–300 (1977).

18. Ravati, S. & Favis, B. D. Morphological states for a ternary polymer blend demonstrating complete wetting. *Polymer* **51**, 4547–4561 (2010).

19. Reignier, J. & Favis, B. D. Control of the Subinclusion Microstructure in HDPE/PS/PMMA Ternary Blends. *Macromolecules* **33**, 6998–7008 (2000).
20. Scott, C. E. & Macosko, C. W. Morphology development during the initial stages of polymer-polymer blending. *Polymer* **36**, 461–470 (1995).
21. Tyagi, S. & Ghosh, A. K. Morphology development during blending of immiscible polymers in screw extruders. *Polym. Eng. Sci.* **42**, 1309–1321 (2002).
22. Van Puyvelde, P., Velankar, S., Mewis, J., Moldenaers, P. & Leuven, K. U. Effect of Marangoni stresses on the deformation and coalescence in compatibilized immiscible polymer blends. *Polym. Eng. Sci.* **42**, 1956–1964 (2002).
23. Utracki, L. A. *Polymer blends handbook*. **1**, (Kluwer, 2002).
24. M. Jaffe, P. Chen, E.-W. Choe, T.-S. Chung & S. Makhija. High performance polymer blends. in *High performance polymers* 297–327 (Springer-Verlag, 1994).
25. Erjun Zhou, Junzi Cong, Kazuhito Hashimoto & Keisuke Tajima. Control of Miscibility and Aggregation Via the Material Design and Coating Process for High-Performance Polymer Blend Solar Cells. *Adv. Mater.* **25**, 6991–6996 (2013).
26. Bajaj, P. Fire-retardant materials. *Bull. Mater. Sci.* **15**, 67–76 (1992).
28. Bajaj, P., Agrawal, A. K., Dhand, A., Kasturia, N. & Hansraj. Flame retardation of acrylic fibers: an overview. *J. Macromol. Sci. Part C Polym. Rev.* **40**, 309–337 (2000).
29. Kahn, S. A., Woods, J. & Rae, L. Line of duty firefighter fatalities: An evolving trend over time. *J. Burn Care Res.* **36**, 218–224 (2015).
30. A. R. Horrocks. Technical fibers for heat and flame protection. in *Handbook of technical textiles: Technical textiles applications* **2**, (Woodhead Publishing Series in textiles, 2016).
31. DeMeuse, M. *High temperature polymer blends*. (Woodhead Publishing, 2014).
32. *SFPE handbook of fire protection engineering*. (National Fire Protection Association ; Society of Fire Protection Engineers, 2002).

33. Hergenrother, P. M. The Use, Design, Synthesis, and Properties of High Performance/High Temperature Polymers: An Overview. *High Perform. Polym.* **15**, 3–45 (2003).
34. Mark, J. E. *Polymer data handbook.* (Oxford University Press, 2008).
35. Jiang, W., Sundarram, S. S., Wong, D., Koo, J. H. & Li, W. Polyetherimide nanocomposite foams as an ablative for thermal protection applications. *Compos. Part B Eng.* **58**, 559–565 (2014).
36. Scarlet, R. *et al.* Study on the solubility of polyetherimide for nanostructural electrospinning. *Rev. Chim. Buchar.* **63**, 688–692 (2012).
37. Amancio-Filho, S. T., Roeder, J., Nunes, S. P., dos Santos, J. F. & Beckmann, F. Thermal degradation of polyetherimide joined by friction riveting (FricRiveting). Part I: Influence of rotation speed. *Polym. Degrad. Stab.* **93**, 1529–1538 (2008).
38. Carroccio, S., Puglisi, C. & Montaudo, G. Thermal degradation mechanisms of polyetherimide investigated by direct pyrolysis mass spectrometry. *Macromol. Chem. Phys.* **200**, 2345–2355 (1999).
39. Mittal, K. L. *Polyimides. Synthesis, Characterization, and Applications*. **1**, (Springer US, 1984).
40. Woo, E. M. & Yau, S. N. Peculiar glass transition behavior and miscibility in a binary mixture comprising amorphous poly (ether imide) with semicrystalline poly (butylene terephthalate). *Macromolecules* **30**, 3626–3631 (1997).
41. Vallejo, F. J., Eguiazábal, J. I. & Nazábal, J. Solid state features and mechanical properties of PEI/PBT blends. *J. Appl. Polym. Sci.* **80**, 885–892 (2001).
42. Chen, H.-L. *et al.* Phase behaviour of amorphous and semicrystalline blends of poly(butylene terephthalate) and poly(ether imide). *Polymer* **38**, 2747–2752 (1997).
43. Jang, J. & Sim, K. Crystallization behavior in poly (ether imide)/poly (butylene terephthalate) blends using a spectroscopic method. *Polym. Test.* **17**, 507–521 (1998).

44. Osswald, T., Baur, E., Brinkmann, S., Oberbach, K. & Schmachtenberg, E. *International Plastics Handbook: The Resource for Plastics Engineers*. (Hanser, 2006).

45. DeMeuse, M. T. High temperature polymer blends: an overview of the literature. *Polym. Adv. Technol.* **6**, 76–82 (1995).

46. Wang, Y., Xiao, Y., Zhang, Q., Gao, X.-L. & Fu, Q. The morphology and mechanical properties of dynamic packing injection molded PP/PS blends. *Polymer* **44**, 1469–1480 (2003).

47. *Micro- and nanostructured multiphase polymer blend systems: phase morphology and interfaces*. (Taylor & Francis, 2006).

48. Harrats, C. *Multiphase polymer- based materials: an atlas of phase morphology at the nano and micro scale*. (Taylor & Francis, 2009).

49. Wang, D., Li, Y., Xie, X.-M. & Guo, B.-H. Compatibilization and morphology development of immiscible ternary polymer blends. *Polymer* **52**, 191–200 (2011).

50. Favis, B. D. Factors influencing the morphology of immiscible polymer blends in melt processing. in *Polymer blends. Volume 1: Formulation* **1**, (John Wiley & Sons, Inc., 2000).

51. Macosko, C. W. Morphology development and control in immiscible polymer blends. in *Macromolecular symposia* **149**, 171–184 (Wiley-vch, 2000).

52. Favis, B. D. & Willis, J. M. Phase size/composition dependence in immiscible blends: Experimental and theoretical considerations. *J. Polym. Sci. Part B Polym. Phys.* **28**, 2259–2269 (1990).

53. Ryan, A. J. Polymer science: Designer polymer blends. *Nat. Mater.* **1**, 8–10 (2002).

54. Shi, Z. & Utracki, L. Development of polymer blend morphology during compounding in a twin-screw extruder. Part II: Theoretical derivations. *Polym. Eng. Sci.* **32**, 1834–1845 (2004).

55. Potente, H., Bastian, M., Gehring, A., Stephan, M. & Pötschke, P. Experimental investigation of the morphology development of polyblends in corotating twin-screw extruders. *J. Appl. Polym. Sci.* **76**, 708–721 (2000).

56. Polaskova, M. *et al.* Extrusion of polyethylene/polypropylene blends with microfibrillar-phase morphology. *Polym. Compos.* **31**, 1427–1433 (2009).

57. Cowie, J. M. G. & Arrighi, V. Polymers in solution. in *Polymers: Chemistry and Physics of Modern Materials* (Taylor & Francis, 2007).

58. Nyamweya, N. & Hoag, S. W. Assessment of polymer-polymer interactions in blends of HPMC and film forming polymers by modulated temperature differential scanning calorimetry. *Pharm. Res.* **17**, 625–631 (2000).

59. Painter, P., Graf, J. F. & Coleman, M. M. Effect of hydrogen bonding on the enthalpy of mixing and the composition dependence of the glass transition temperature in polymer blends. *Macromolecules* **24**, 5630–5638 (1991).

60. Scott, C. E. & Macosko, C. W. Processing and morphology of polystyrene/ethylene-propylene rubber reactive and nonreactive blends. *Polym. Eng. Sci.* **35**, 1938–1948 (1995).

61. Taghizadeh, A. Novel polymer blends with thermoplastic starch. (École Polytechnique de Montréal, 2012).

62. Wu, S. Interfacial and surface tensions of polymer melts and liquids. in *Polymer Interface and Adhesion* 67–132 (Marcel Dekker, Inc., 1982).

63. Demarquette, N. R., Catelli de Souza, A. M., Palmer, G. & Macaubas, P. H. P. 2003_Demarquette_Comparison of five experimental methods.pdf. *Polym. Eng. Sci.* **43**, 670–683 (2003).

64. Valera, T. S., Morita, A. T. & Demarquette, N. R. Study of Morphologies of PMMA/PP/PS Ternary Blends. *Macromolecules* **39**, 2663–2675 (2006).

65. Palierne, J. F. Linear rheology of viscoelastic emulsions with interfacial tension. *Rheol. Acta* **29**, 204–214 (1990).

66. Jacobs, U., Fahrländer, M., Winterhalter, J. & Friedrich, C. Analysis of Palierne's emulsion model in the case of viscoelastic interfacial properties. *J. Rheol.* **43**, 1495 (1999).

67. Grace, H. P. Dispersion phenomena in high viscosity immiscible fluid systems and application of the static mixers as dispersion devices in such systems. *Chem. Eng. Commun.* **14**, 225–277 (1982).

68. Ho, R. M., Wu, C. H. & Su, A. C. Morphology of plastic/rubber blends. *Polym. Eng. Sci.* **30**, 511–518 (1990).

69. Jordhamo, G. M., Manson, J. A. & Sperling, L. H. Phase continuity and inversion in polymer blends and simultaneous interpenetrating networks. *Polym. Eng. Sci.* **26**, 517–524 (1986).

70. Miles, I. S. & Zurek, A. Preparation, structure, and properties of two-phase co-continuous polymer blends. *Polym. Eng. Sci.* **28**, 796–805 (1988).

71. Utracki, L. A. On the viscosity-concentration dependence of immiscible polymer blends. *J. Rheol.* **35**, 1615–1637 (1991).

72. Paul, D. R. & Barlow, J. W. Polymer Blends. *J. Macromol. Sci. Part C* **18**, 109–168 (1980).

73. Chen, T. H. & Su, A. C. Morphology of poly (p-phenylene sulfide) polyethylene blends. *Polymer* **34**, 4826–4831 (1993).

74. Metelkin, V. I. & Blekht, V. S. Formation of a continuous phase in heterogenous mixtures of polymers. *Kolloid Zh* **46**, 476 (1984).

75. Prochazka, F., Dima, R., Majesté, J.-C. & Carrot, C. Phase inversion and co-continuity domain in immiscible polyethylene/polystyrene blends. *E-Polym.* **3**, 512–522 (2003).

76. Hobbs, S. Y., Dekkers, M. E. J. & Watkins, V. H. Effect of interfacial forces on polymer blend morphologies. *Polymer* **29**, 1598–1602

77. Guo, H. F., Packirisamy, S., Gvozdic, N. V. & Meier, D. J. Prediction and manipulation of the phase morphologies of multiphase polymer blends: 1. Ternary systems. *Polymer* **38**, 785–794 (1997).

78. Guo, H. F., Gvozdic, N. V. & Meier, D. J. Prediction and manipulation of the phase morphologies of multiphase polymer blends: II. Quaternary systems. *Polymer* **38**, 4915–4923 (1997).

79. Macaúbas, P. H. & Demarquette, N. R. Interfacial tension, morphology and linear viscoelasticity behavior of PP/PS blends. *Polímeros* **9**, 71–77 (1999).

80. Reignier, J., Favis, B. D. & Heuzey, M.-C. Factors influencing encapsulation behavior in composite droplet-type polymer blends. *Polymer* **44**, 49–59 (2003).

81. Shokoohi, S. & Arefazar, A. A review on ternary immiscible polymer blends: morphology and effective parameters. *Polym. Adv. Technol.* **20**, 433–447 (2009).

82. Guo, H.-F., Gvozdic, N. V. & Meier, D. J. Prediction and manipulation of the phase morphologies of multiphase polymer blends: II. Quaternary systems. *Polymer* **38**, 4915–4923 (1997).

83. Valera, T. S., Morita, A. T. & Demarquette, N. Study of Morphologies of PMMA-PP-PS Ternary Blends. *Macromolecules* **39**, 2663–2675 (2006).

84. de Freitas, C. A., Valera, T. S., De Souza, A. M. C. & Demarquette, N. R. Morphology of Compatibilized Ternary Blends. *Macromol. Symp.* **247**, 260–270 (2007).

85. Vásquez, M. & Láinez, M. Á. Análisis interfacial en el desarrollo de mezclas poliméricas multicomponentes: aproximación teórica. *Rev. Colomb. Mater.* 71–77 (2014).

86. Torza, S. & Mason, S. G. Three-phase interactions in shear and electrical fields. *J. Colloid Interface Sci.* **33**, 67–83 (1970).

87. Nemirovski, N., Siegmann, A. & Narkis, M. Morphology of ternary immiscible polymer blends. *J. Macromol. Sci. Part B* **34**, 459–475 (1995).

88. DeBolt, M. A. & Robertson, R. E. Morphology of compatibilized ternary blends of polypropylene, nylon 66, and polystyrene. *Polym. Eng. Sci.* **46**, 385–398 (2006).

89. Ravati, S. & Favis, B. D. Morphological states for a ternary polymer blend demonstrating complete wetting. *Polymer* **51**, 4547–4561 (2010).

90. Javidi, Z., Tarashi, Z., Rostami, A. & Nazockdast, H. Role of nanosilica localization on morphology development of HDPE/PS/PMMA immiscible ternary blends. *Express Polym. Lett.* **11**, 362–373 (2017).

91. de Freitas, C. A., Valera, T. S., Catelli de Souza, A. M. & Demarquette, N. R. Morphology of Compatibilized Ternary Blends. *Macromol. Symp.* **247**, 260–270 (2007).

92. Li, L.-P., Yin, B. & Yang, M.-B. Morphology prediction and the effect of core-shell structure on the rheological behavior of PP/EPDM/HDPE ternary blends. *Polym. Eng. Sci.* **51**, 2425–2433 (2011).

93. Alves, T. S., Silva Neto, J. E., Silva, S. M. L., Carvalho, L. H. & Canedo, E. L. Process simulation of laboratory internal mixers. *Polym. Test.* **50**, 94–100 (2016).

94. Ramiro, J., Eguiazábal, J. I. & Nazábal, J. Synergistic mechanical behaviour and improved processability of poly(ether imide) by blending with poly(trimethylene terephthalate): IMPROVED PROCESSABILITY OF POLY(ETHER IMIDE). *Polym. Adv. Technol.* **14**, 129–136 (2003).

95. Wu, X., Wei, H., Zhu, J. & Fang, X. Study on Thermal Properties and Crystallization Behavior of Blends of Poly(phenylene sulfide)/Poly(ether imide). *Polym.-Plast. Technol. Eng.* **49**, 1506–1514 (2010).

96. Zabaleta, A., González, I., Eguiazábal, J. I. & Nazabal, J. Rubber toughening of poly(ether imide) by modification with poly(butylene terephthalate). *Eur. Polym. J.* **45**, 466–473 (2009).

97. Sultan, A. S., Al-Ahmed, A. & Javaid Zaidi, S. M. Reduced viscosity, rheology and morphological properties of sulfonated poly (ether ether ketone): Polyetherimide blends. *Eur. Polym. J.* **47**, 2295–2302 (2011).

98. Runt, J. *et al.* Poly (butylene terephthalate)–polyarylate blends. *Polym. Adv. Technol.* **5**, 333–338 (1994).

99. Bastida, S., Eguiazábal, J. I. & Nazábal, J. Phase behaviour, morphology and properties of poly (ether imide)/polyarylate blends. *Polymer* **37**, 2317–2322 (1996).

100. Runt, J. P., Zhang, X., Miley, D. M., Gallagher, K. P. & Zhang, A. Phase behavior of poly (butylene terephthalate)/polyarylate blends. *Macromolecules* **25**, 3902–3905 (1992).

101. Choi, K.-Y., Lee, S.-G., Lee, J. H. & Liu, J. Morphology and dynamic mechanical properties of nylon 66/poly (ether imide) blends. *Polym. Eng. Sci.* **35**, 1643–1651 (1995).

102. Martinez, J. M., Eguiazabal, J. I. & Nazabal, J. Miscibility level and properties of poly(ether imide)/poly(ethylene terephthalate) blends. *J. Appl. Polym. Sci.* **62**, 385–391 (1996).

103. Mehta, R. H., Madsen, D. A. & Kalika, D. S. Microporous membranes based on poly (ether ether ketone) via thermally-induced phase separation. *J. Membr. Sci.* **107**, 93–106 (1995).

104. Bristow, J. F. & Kalika, D. S. Investigation of semicrystalline morphology in poly (ether ether ketone)/poly (ether imide) blends by dielectric relaxation spectroscopy. *Polymer* **38**, 287–295 (1997).

105. Woo, E. M. & Yau, S. N. Two-stage crystallization kinetics modeling of a miscible blend system containing crystallizable poly (butylene terephthalate). *Polym. Eng. Sci.* **38**, 583–589 (1998).

106. Woo, E. M. & Lee, L.-T. A Novel Quaternary Blend System of Poly (ethy1ene terephthalate), Poly (trimethy1ene terephthalate), Poly (butylene terephthalate), and Poly (ether imide). *Polym. Bull.* **50**, 33–38 (2003).

107. Font, J., Muntasell, J. & Cesari, E. Binary mixtures of semicrystalline/noncrystalline polymers formed by ball milling. *Mater. Res. Bull.* **34**, 2221–2230 (1999).

108. Ren, J. Tribological properties of Xytrex® polymers of 3P comportation. in *International SAMPE Technical Conference* (2006).

109. Mu, L. *et al.* Self-Lubricating Polytetrafluoroethylene/Polyimide Blends Reinforced with Zinc Oxide Nanoparticles. *J. Nanomater.* **2015**, 1–8 (2015).

110. Chen, B., Wang, J. & Yan, F. Microstructure of PTFE-Based Polymer Blends and Their Tribological Behaviors Under Aqueous Environment. *Tribol. Lett.* **45**, 387–395 (2012).

111. Bijwe, J., Sen, S. & Ghosh, A. Influence of PTFE content in PEEK–PTFE blends on mechanical properties and tribo-performance in various wear modes. *Wear* **258**, 1536–1542 (2005).

112. Bijwe, J., Tewari, U. S. & Vasudevan, P. Friction and wear studies of an internally lubricated polyetherimide composite. *Lubr. Sci.* **6**, 179–202 (1989).

113. Zhang, J., Demas, N. G., Polycarpou, A. A. & Economy, J. A new family of low wear, low coefficient of friction polymer blend based on polytetrafluoroethylene and an aromatic thermosetting polyester. *Polym. Adv. Technol.* **19**, 1105–1112 (2008).

114. Hussain, M., Ko, Y. H. & Choa, Y. H. Significant Enhancement of Mechanical and Thermal Properties of Thermoplastic Polyester Elastomer by Polymer Blending and Nanoinclusion. *J. Nanomater.* **2016**, 1–9 (2016).

115. Anbinder, P. S., Peruzzo, P. J., de Siervo, A. & Amalvy, J. I. Surface, thermal, and mechanical properties of composites and nanocomposites of polyurethane/PTFE nanoparticles. *J. Nanoparticle Res.* **16**, (2014).

116. Palabiyik, M. & Bahadur, S. Tribological studies of polyamide 6 and high-density polyethylene blends filled with PTFE and copper oxide and reinforced with short glass fibers. *Wear* **253**, 369–376 (2002).

117. Huang, A., Peng, X. & Turng, L.-S. In-situ fibrillated polytetrafluoroethylene (PTFE) in thermoplastic polyurethane (TPU) via melt blending: Effect on rheological behavior, mechanical properties, and microcellular foamability. *Polymer* **134**, 263–274 (2018).

118. Ali, M. A. B. M., Nobukawa, S. & Yamaguchi, M. Morphology development of polytetrafluoroethylene in a polypropylene melt (IUPAC Technical Report). *Pure Appl. Chem.* **83**, (2011).

119. Md Ali, M. A. B., Okamoto, K., Yamaguchi, M., Kasai, T. & Koshirai, A. Rheological properties for polypropylene modified by polytetrafluoroethylene. *J. Polym. Sci. Part B Polym. Phys.* **47**, 2008–2014 (2009).

120. Ma, Y. *et al.* Tribological properties of PTFE/PEI and graphite/PEI blends. *Chem. J. Chin. Univ.* **35**, 2720–2724 (2014).

121. Yeager, C., Carreno, C. & Rogge, D. Chemical resistance of advanced thermoplastic composites in automotive fluids. in *SAE Technical Papers* (1990).

122. Danila, D., Gerorgescu, C., Pirvu, C. & Deleanu, L. Influence of adding materials in PBT upon tribological characteristics. in *Society of Plastics Engineers - EUROTECH 2013* 353–359 (2013).

123. Musteata, A. E., Stanila, V., Deleanu, L., Bria, V. & Georgescu, C. INFLUENCE OF PTFE CONCENTRATION IN PBT ON MECHANICAL PROPERTIES. *Mech. Test. Diagn.* **6**, 5 (2016).

124. Bajaj, P. Heat and flame protection. in *Handbook of technical textiles* (Woodhead Publishing Limited, 2000).

125. Horrocks, A. R., Kandola, B. K., Davies, P. J., Zhang, S. & Padbury, S. A. Developments in flame retardant textiles – a review. *Polym. Degrad. Stab.* **88**, 3–12 (2005).

126. Alger, M. S. M. High-temperature and fire-resistant polymers. in *Specialty Polymers* 38–64 (Springer, 1987).

127. Horrocks, A. R. Flame retardant challenges for textiles and fibres: New chemistry versus innovatory solutions. *Polym. Degrad. Stab.* **96**, 377–392 (2011).

128. Hull, T. R. & Stec, A. A. Polymers and fire. (2009).

129. Laoutid, F., Bonnaud, L., Alexandre, M., Lopez-Cuesta, J.-M. & Dubois, P. New prospects in flame retardant polymer materials: From fundamentals to nanocomposites. *Mater. Sci. Eng. R Rep.* **63**, 100–125 (2009).

130. Sato, H., Kondo, K., Tsuge, S., Ohtani, H. & Sato, N. Mechanisms of thermal degradation of a polyester flame-retarded with antimony oxide/brominated polycarbonate studied by temperature-programmed analytical pyrolysis. *Polym. Degrad. Stab.* **62**, 41–48 (1998).

131. Montezin, F., Lopez-Cuesta, J.-M., Crespy, A. & Georlette, P. Flame retardant and mechanical properties of a compolymer PP/PE containing brominated compounds/antimony trioxid blends and magnesium hydrixide or talc. *Fire Mater.* **21**, 245–252 (1997).

132. Morgan, A. B. & Gilman, J. W. An overview of flame retardancy of polymeric materials: application, technology, and future directions: AN OVERVIEW OF FLAME RETARDANCY OF POLYMERIC MATERIALS. *Fire Mater.* **37**, 259–279 (2013).

133. Köppl, T. *et al.* Influence of polymeric flame retardants based on phosphorus-containing polyesters on morphology and material characteristics of poly(butylene terephthalate). *J. Appl. Polym. Sci.* **128**, 3315–3324 (2013).

134. *BS 2782 - Part 7: Method 730B: 1994. Plastics — Polymers/resins in the liquid state or as emulsions or dispersions — Determination of viscosity using a rotational viscometer with defined shear state*. (1994).

135. Orman, R. G. & Holland, D. Thermal phase transitions in antimony (III) oxides. *J. Solid State Chem.* **180**, 2587–2596 (2007).

136. Orman, R. G. Phase transitions in antimony oxides and related glasses. (University of Warwick, 2005).

137. Elias, L., Fenouillot, F., Majeste, J. C. & Cassagnau, P. Morphology and rheology of immiscible polymer blends filled with silica nanoparticles. *Polymer* **48**, 6029–6040 (2007).

138. Huang, Y., Jiang, S., Li, G. & Chen, D. Effect of fillers on the phase stability of binary polymer blends: A dynamic shear rheology study. *Acta Mater.* **53**, 5117–5124 (2005).

139. Shepard, K. B. *et al.* Viscoelastic behavior of poly(ether imide) incorporated with multiwalled carbon nanotubes. *J. Polym. Sci. Part B Polym. Phys.* **50**, 1504–1514 (2012).

140. Goodrich, J. E. & Porter, R. S. A rheological interpretation of torque-rheometer data. *Polym. Eng. Sci.* **7**, 45–51 (1967).

141. *Polymer Blends Handbook*. (Springer Netherlands, 2014). doi:10.1007/978-94-007-6064-6

142. Kalika, D. S. Viscoelastic characterizatiion of polymer blends. in *Polymer blends. Volume 1: Formulation* **1**, (John Wiley & Sons, Inc., 2000).

143. Huang, J., Lu, X., Zhang, G. & Qu, J. Study on the rheological, thermal and mechanical properties of thermoplastic polyurethane/poly (butylene terephthalate) blends. *Polym. Test.* **36**, 69–74 (2014).

144. Utracki, L. A. & Schlund, B. Linear low density polyethylenes and their blends: Part 4 shear flow of LLDPE blends with LLDPE and LDPE. *Polym. Eng. Sci.* **27**, 1512–1522 (1987).

145. Utracki, L. A. Viscoelastic behavior of polymer blends. *Polym. Eng. Sci.* **28**, 1401–1404 (1988).

146. Utracki, L. A. & Favis, B. D. Polymer alloys and blends. in *Handbook of Polymer Science and Technology. Volume 4: Composites and specialty applications* **4**, 121–202 (Marcel Dekker, Inc., 1989).

147. Utracki, L. A. On the viscosity-concentration dependence of immiscible polymer blends. *J. Rheol.* **35**, 1615–1637 (1991).

148. Utracki, L. A. Melt flow of polymer blends. *Polym. Eng. Sci.* **23**, 602–609 (1983).

149. Collyer, A. A. The morphology and rheology of liquid crystal polymer blends. in *Rheology and processing of liquid crystal polymers* 185–214 (Springer science and business media, B. V., 1996).

150. Blaine, R. L. Thermal applications notes: Polymers heats of fusion.

151. Wunderlich, B. Theory of Cold Crystallization of High Polymers. *J. Chem. Phys.* **29**, 1395–1404 (1958).

152. Rzyman, M., Grabda, M., Oleszek-Kudlak, S., Shibata, E. & Nakamura, T. Studies on bromination and evaporation of antimony oxide during thermal treatment of tetrabromobisphenol A (TBBPA). *J. Anal. Appl. Pyrolysis* **88**, 14–21 (2010).

153. Alaee, M., Arias, P., Sjödin, A. & Bergam, A. An overview of commercially used brominated flame retardants, their applications, their use patterns in different countries/regions and possible modes of release. *Environ. Int.* **29**, 683–689 (2003).

154. Steinmann, S., Gronski, W. & Friedrich, C. Cocontinuous polymer blends: influence of viscosity and elasticity ratios of the constituent polymers on phase inversion. *Polymer* **42**, 6619–6629 (2001).

155. Shimizu, R. N. & Demarquette, N. R. Evaluation of surface energy of solid polymers using different models. *J. Appl. Polym. Sci.* **76**, 1831–1845 (2000).

156. Kaba, M., Raklaoui, N., Guimon, M. F. & Mas, A. Improvement of the water selectivity of ULTEM poly(ether imide) pervaporation films by an allylamine-plasma-polymerized layer. *J. Appl. Polym. Sci.* **5**, 2088–2096 (2005).

157. Volpe, C. D., Migliaresi, C. & Mari, G. Surface tension analysis of pbt and pet fibres based leukodepletion filters. in *Surface Modification of Polymeric Biomaterials* (Springer US, 1997). doi:10.1007/978-1-4899-1953-3

158. Guerrica-Echevarrıa, G., Eguiazabal, J. I. & Nazabal, J. Interfacial tension as a parameter to characterize the miscibility level of polymer blends. *Polym. Test.* **19**, 849–854 (2000).

159. Hobbs, S. Y. The effect of rubber particle size on the impact properties of high impact polystyrene (HIPS) blends. *Polym. Eng. Sci.* **26**, 74–81 (1986).

160. Pagnoulle, C. & Jérôme, R. Particle-in-particle morphology for the dispersed phase formed in reactive compatibilization of SAN/EPDM blends. *Polymer* **42**, 1893–1906 (2001).

161. Si, Q. B., Zhou, C., Yang, H. D. & Zhang, H. X. Toughening of polyvinylchloride by core–shell rubber particles: Influence of the internal structure of core–shell particles. *Eur. Polym. J.* **43**, 3060–3067 (2007).

162. Vanoene, H. Modes of dispersion of viscoelastic fluids in flow. *J. Colloid Interface Sci.* **40**, 448–467 (1972).

163. Berger, W., Kammer, H. W. & Kummerlöwe, C. Melt rheology and morphology of polymer blends. *Macromol. Chem. Phys.* **8**, 101–108 (1984).

164. Hudson, S. D., Davis, D. D. & Lovinger, A. J. Semicrystalline morphology of poly (aryl ether ether ketone)/poly (ether imide) blends. *Macromolecules* **25**, 1759–1765 (1992).

165. Hsiao, B. S. & Sauer, B. B. Glass transition, crystallization, and morphology relationships in miscible poly (aryl ether ketones) and poly (ether imide) blends. *J. Polym. Sci. Part B Polym. Phys.* **31**, 901–915 (1993).

166. Pötschke, P. & Paul, D. R. Formation of Co-continuous Structures in Melt-Mixed Immiscible Polymer Blends. *J. Macromol. Sci. Part C Polym. Rev.* **43**, 87–141 (2003).

167. Nair, S. V., Oommen, Z. & Thomas, S. Phase morphology development and melt rheological behavior in nylon 6/polystyrene blends. *J. Appl. Polym. Sci.* **86**, 3537–3555 (2002).

168. Joseph, S. *et al.* Polystyrene/polybutadiene blends: An analysis of the phase-inversion region and cophase continuity and a comparison with theoretical predictions. *J. Appl. Polym. Sci.* **89**, 1007–1016 (2003).

169. Bourry, D. & Favis, B. D. Cocontinuity and phase inversion in HDPE/PS blends: influence of interfacial modification and elasticity. *J. Polym. Sci. Part B Polym. Phys.* **36**, 1889–1899 (1998).

170. Mekhilef, N. & Verhoogt, H. Phase inversion and dual-phase continuity in polymer blends: theoretical predictions and experimental results. *Polymer* **37**, 4069–4077 (1996).

171. Bahrami, R., Löbling, T. I., Schmalz, H., Müller, A. H. E. & Altstädt, V. Synergistic effects of Janus particles and triblock terpolymers on toughness of immiscible polymer blends. *Polymer* **109**, 229–237 (2017).

172. Phillin, I., Pimbert, S., Feller, J.-F. & Levesque, G. Crystallization kinetics of poly(butylene terephthalate) (PBT): Influence of additives and free carboxylic acid chain ends. *Polym. Eng. Sci.* **41**, 178–191 (2001).

173. Leclair, A. & Favis, B. D. The role of interfacial contact in immiscible binary polymer blends and its influence on mechanical properties. *Polymer* **37**, 4723–4728 (1996).

174. DeBolt, M. A. & Robertson, R. E. Morphology of compatibilized ternary blends of polypropylene, nylon 66, and polystyrene. *Polym. Eng. Sci.* **46**, 385–398 (2006).

175. Wang, D., Li, Y., Xie, X.-M. & Guo, B.-H. Compatibilization and morphology development of immiscible ternary polymer blends. *Polymer* **52**, 191–200 (2011).

176. Hu, G.-H., Cartier, H. & Plummer, C. Reactive Extrusion: Toward Nanoblends. *Macromolecules* **32**, 4713–4718 (1999).

177. Yang, C. Y., Hide, F., Heeger, A. J. & Cao, Y. Nanostructured polymer blends: novel materials with enhanced optical and electronic properties. *Synth. Met.* **84**, 895–896 (1997).

178. Sundararaj, U. & Macosko, C. W. Drop breakup and coalescence in polymer blends: the effects of concentration and compatibilization. *Macromolecules* **28**, 2647–2657 (1995).

179. Cimmino, S. *et al.* Ternary nylon-6/rubber/modified rubber blends: effect of the mixing procedure on morphology, mechanical and impact properties. *Polymer* **27**, 1874–1884 (1986).

180. Olabisi, O. Interpretations of polymer-polymer miscibility. *J. Chem. Educ.* **58**, 944 (1981).

181. Marwat, Z. K. & Baloch, M. K. Investigating Miscibility of Polymers and Its Impact on the Morphology, Thermal, and Mechanical Properties of Polymer Blends. *Int. J. Thermophys.* **36**, 2755–2768 (2015).

182. Campoy, I., Gómez, M. A. & Marco, C. Thermogravimetric analysis of blends based on nylon 6 and a thermotropic liquid crystal copolyester. *J. Therm. Anal.* **52**, 705–715 (1998).

183. Dodson, B. & McNeill, I. C. Degradation of polymer mixtures. VI. Blends of poly (vinyl chloride) with polystyrene. *J. Polym. Sci. Polym. Chem. Ed.* **14**, 353–364 (1976).

184. Naffakh, M., Ellis, G., Gómez, M. A. & Marco, C. Thermal decomposition of technological polymer blends 1. Poly(aryl ether ether ketone) with a thermotropic liquid crystalline polymer. *Polym. Degrad. Stab.* **66**, 405–413 (1999).

185. Tai, C. M., Li, R. K. & Ng, C. N. Impact behaviour of polypropylene/polyethylene blends. *Polym. Test.* **19**, 143–154 (2000).

186. Veenstra, H. *et al.* On the mechanical properties of co-continuous polymer blends: experimental and modelling. *Polymer* **41**, 1817–1826 (2000).

187. Willemse, R. C., Speijer, A., Langeraar, A. E. & Posthuma de Boer, A. Tensile moduli of co-continuos polymer blends. *Polymer* **40**, 6645–6650 (1999).

188. McNeill, I. C., Gorman, J. G. & Basan, S. Thermal degradation of blends of PVC with poly (tetramethylene sebacate). *Polym. Degrad. Stab.* **33**, 263–276 (1991).

189. Kolařk, J. Simultaneous prediction of the modulus, tensile strength and gas permeability of binary polymer blends. *Eur. Polym. J.* **34**, 585–590 (1998).

190. Tchomakov, K. P., Favis, B. D., Huneault, M. A., Champagne, M. F. & Tofan, F. Mechanical properties and morphology of ternary PP/EPDM/PE blends. *Can. J. Chem. Eng.* **83**, 300–309 (2005).

191. Schwarz, M. C., Barlow, J. W. & Paul, D. R. Mechanical properties of HDPE/(PEC/PS)/SEBS blends. *J. Appl. Polym. Sci.* **35**, 2053–2067 (1988).

192. Joseph, E. A., Lorenz, M. D., Barlow, J. W. & Paul, D. R. Mechanical properties of miscible polycarbonate-copolyester blends. *Polymer* **23**, 112–122 (1982).

193. Murff, S. R., Barlow, J. W. & Paul, D. R. Thermal and mechanical behavior of polycarbonate–poly (ethylene terephthalate) blends. *J. Appl. Polym. Sci.* **29**, 3231–3240 (1984).

194. Li, N. *et al.* Influence of antimony oxide on flammability of polypropylene/intumescent flame retardant system. *Polym. Degrad. Stab.* **97**, 1737–1744 (2012).

195. Sallet, D., Mailhos-Lefievre, V. & Martel, B. Flame retardancy of polyamide 11 with a decabromodiphenyl-antimony trioxide mixture. A bromine-antimony-nitrogen synergism. *Polym. Degrad. Stab.* **30**, 29–39 (1990).

196. Ray, I., Roy, S. & Khastgir, D. Interaction between ethylene vinyl acetate copolymer and polyethylene. *Polym. Bull.* **30**, 685–689 (1993).

197. Khemani, K. C. A novel approach for studying the thermal degradation, and for estimating the rate of acetaldehyde generation by the chain scission mechanism in ethylene glycol based polyesters and copolyesters. *Polym. Degrad. Stab.* **67**, 91–99 (2000).

198. Kinoshita, R., Teramoto, Y. & Yoshida, H. TG-DTA/FT-IR method for analyzing thermal decomposition mechanism of polyesters. *J. Therm. Anal.* **40**, 605–611 (1993).

199. Montaudo, G. Primary thermal degradation mechanisms of PET and PBT.

200. Perng, L. H. Thermal degradation mechanism of poly(ether imide) by stepwise Py–GC/MS. *J. Appl. Polym. Sci.* **79**, 1151–1161 (2000).

201. Sonnier, R., Viretto, A., Taguet, A. & Lopez-Cuesta, J.-M. Influence of the morphology on the fire behavior of a polycarbonate/poly(butylene terephthalate) blend. *J. Appl. Polym. Sci.* **125**, 3148–3158 (2012).

202. Półka, M., Gałaj, J. & Karpovič, Z. Investigation into the influence of flame retardant additives on some fire properties of polyester materials applying small-scale testing techniques. *J. Civ. Eng. Manag.* **19**, 561–572 (2013).

203. McCrum, N. G. *Anelastic and dielectric effects in polymeric solids*. (Dover publications, 1991).

204. Starkweather, H. W. J. The effect of heating rate on the melting of polytetrafluoroethylene. *J. Polym. Sci. Part B Polym. Phys.* **23**, 1177–1185 (1985).

205. Ginzburg, B. M. Influence of sublimation of destruction products on the pattern of DSC thermograms of polymeric materials. *Polym. Sci. Ser. A* **54**, 248–254 (2012).

206. Case, L. C. Viscosity of polytetrafluoroethylene above the melting point. *J. Appl. Polym. Sci.* **3**, 254–254 (1960).

207. Gupta, A. K. & Srinivasan, K. R. Melt rheology and morphology of PP/SEBS/PC ternary blend. *J. Appl. Polym. Sci.* **47**, 167–184 (1993).

208. Reignier, J. & Favis, B. D. Control of the Subinclusion Microstructure in HDPE/PS/PMMA Ternary Blends. *Macromolecules* **33**, 6998–7008 (2000).

209. Owens, D. K. & Wendt, R. C. Estimation of the surface free energy of polymers. *J. Appl. Polym. Sci.* **13**, 1741–1747 (1969).

210. DuPont Fluoropolymers, P. Teflon PTFE Fluoropolymer Resin: Properties Handbook. (1996).

211. Kaushiva, B. D., Wilkes, G. L., Comeaux, C. & Socha, L. Structure–property relationships of poly(tetrafluoroethylene)–poly(tetrafluoroethylene-co-vinylidene fluoride-co-hexafluoropropylene) blends. *Polymer* **42**, 4619–4633 (2001).

212. Ritchie, R. O. The conflicts between strength and toughness. *Nat. Mater.* **10**, 817–822 (2011).